Phil. Trans. R. Soc. Lond. A **303**, 1–104 (1981) [1]
Printed in Great Britain

SPHERICAL HARMONIC ANALYSIS OF GEOMAGNETIC TIDES, 1964–1965

By D. E. WINCH
Department of Applied Mathematics F07,
University of Sydney, Sydney, New South Wales, 2006 *Australia*

(*Communicated by P. H. Roberts, F.R.S. – Received* 7 *March* 1980 –
Revised 7 *October* 1980)

CONTENTS

The mathematical forms chosen for analyses of S_q and L by seventeen different authors are reviewed. On the basis of the review and on consideration of the ionospheric dynamo theory and the Hough function structure of wind velocities in the upper atmosphere, a mathematical model is chosen that includes two more terms than the recent analysis by Malin (1973). Hourly mean values from 130 magnetic observatories for the I.Q.S.Ys (International Quiet Solar Years) 1964 and 1965 were prepared in machine-readable form and analysed. The solar and lunar transient magnetic variations were evaluated, together with the lunar elliptic magnetic tide and the seasonal change at one and two cycles per year for all magnetic tides. Spherical harmonic analyses were made of the phase-law tides and the smaller partial tides. Altogether 94 different spherical harmonic analyses were completed for a total of ten different magnetic tides. Two of the ten tides are the solar and lunar magnetic tides usually denoted S and L respectively. The results are tabulated in a form that distinguishes between eastward- and westward-moving terms, which is suitable for the evaluation of phase angle differences and amplitude ratios between internal and external parts. Malin's ocean dynamo calculation has been applied to the lunar and lunar elliptic magnetic tides. The spherical harmonic coefficients are compared in some detail with those of Malin (1973) for years of high sunspot activity. The magnetic tidal potential associated with a given atmospheric tidal mode is derived theoretically and used to obtain an estimate of the Hough function components of the solar and lunar semi-diurnal atmospheric tides at ionospheric levels from the corresponding magnetic tidal potential.

 [Published 22 October 1981

1. Introduction

When the electrically conducting layers of the upper atmosphere move, they cut the lines of force of the Earth's main magnetic field. Electromotive forces are induced and, as a result, electrical currents flow. The varying magnetic fields associated with such currents are referred to as the transient daily magnetic variations. Those that arise from movements of the upper atmosphere caused by the thermal heating and tidal influence of the Sun are called solar daily magnetic variations and denoted by S. On magnetically quiet days the solar daily magnetic variations are denoted by S_q. Transient magnetic variations arising from the tidal influence of the Moon on the upper atmosphere are called lunar magnetic tides and denoted by L. To simplify the description, both S and L will be referred to as magnetic tides (cf. Chapman & Malin 1970).

It is appropriate to review the available analyses of S and L. It will be seen that although every analysis contains coefficients of spherical harmonics P_2^1, P_3^2, P_4^3, P_5^4 for the 1, 2, 3, 4 c/d (cycles per day) terms respectively, authors differ considerably in the selection of other spherical harmonic terms. There is also variety in the methods of analysis, the choice of data and motivation for the analysis.

The first global analysis of any magnetic tide was that of the solar magnetic tide by Schuster (1889). Using the assumption of local time dependence and antisymmetry about the equator, he analysed data from four magnetic observatories and noted that the hypothesis of external origin gave a model that best fitted the observations. Schuster then used the theory of induction in spherical conductors given by Lamb in an Appendix to the same paper and concluded that no uniformly conducting Earth could give agreement between the different results for the different harmonics. Schuster noted Lamb's suggestion that if the upper layers of the Earth were less conducting than the deeper interior, then the results might be in agreement. He surmised that 'insulators lose their insulating powers at high temperatures' and that therefore such a distribution was physically possible. Schuster represented the magnetic potential of the external part of the magnetic tide by means of a current function, defined by Maxwell (1881). Current function representations have been used in virtually all subsequent analyses of magnetic tides.

Schuster's analysis gave numerical coefficients for the following spherical harmonic functions for the four daily harmonics of the solar magnetic tide:

diurnal	$P_2^1, P_4^1, P_6^1,$	semi-diurnal	$P_3^2, P_5^2, P_7^2,$
ter-diurnal	$P_4^3, P_6^3, P_8^3,$	quater-diurnal	$P_5^4, P_7^4, P_9^4,$
diurnal seasonal differences		$P_1^1, P_3^1, P_5^1,$	
semi-diurnal seasonal differences		$P_2^2, P_4^2, P_6^2.$	

Schuster's first memoir of 1889 provided the foundation for the analysis of magnetic tides together with models of electrical conductivity of the Earth's interior. His second memoir appeared in 1908, and although it contained no new analysis of magnetic data, it set down the fundamental dynamo theory of magnetic tides, with the use of two scalar potentials R, S, to represent the induced electric field. Assuming the upper atmospheric conducting layer to be uniformly electrically conducting, he showed that a term P_n^m in the scalar potential for the wind velocity field (or barometric pressure) would give rise to magnetic tides P_{n+1}^m and P_{n-1}^m only, and for the diurnal magnetic solar tides he surmised that terms of the form P_1^1 and P_3^1 were required

in the representation of the diurnal pressure wave (or wind velocity). He also showed that if the upper atmosphere were uniformly conducting and the Earth's dipole axis inclined to the geographic axis, then a term P_n^m in the pressure potential would give terms of the form P_{n-1}^{m-1}, P_{n+1}^{m-1}, P_{n+1}^{m+1}, P_{n-1}^{m+1}, in the potential of the magnetic tide. Such terms will, because of the variation in the superscript m, no longer depend purely upon local time. He showed that non-local time diurnal terms could dominate in the westerly force magnetic variations at the equator. Inclination of the dipole axis was put forward by McNish (1937) to explain the original observations of enhanced magnetic tides in the region of the magnetic equator, a phenomenon now explained in terms of the equatorial electrojet.

TABLE 1.1. MAGNETIC TIDAL POTENTIAL TERMS RESULTING FROM WIND VELOCITY POTENTIALS P_1^1 AND P_2^2

wind velocity pressure potential...	P_1^1	P_2^2	ionospheric conductivity and magnetic field type
magnetic tidal potential	P_2^1	P_3^2	uniform conductivity, axial dipole
	P_2^0	P_3^1, P_3^3, P_1^1	uniform conductivity, inclined dipole
	$P_1^0, P_1^1,$ P_3^0, P_3^1, P_3^2	$P_2^1, P_2^2,$ P_4^1, P_4^2, P_4^3	conductivity $a_0+a_1 \cos \chi$, axial dipole

If t is the Universal Time (U.T.), and ϕ is the east longitude of an observatory, then $t^* = t+\phi$ is the local time at the observatory. Terms arise in the magnetic tidal potential of the form $mt \pm n\phi$, where m, n, are integers. Only those terms of the form $m(t+\phi)$ will be described as local time terms. All others will be referred to as non-local time terms.

Schuster (1908) dealt with the theoretical analysis of the seasonal change of magnetic tides by assuming that the electrical conductivity of the upper atmosphere varied as $a_0+a_1 \cos \chi$, where χ is the geocentric solar zenith angle, and found that a term P_n^m in the barometric pressure (or wind velocity) gave rise to terms in the magnetic tidal potential of the form

$$P_{n+2}^{m+1}, P_n^{m+1}, P_{n+2}^{m-1}, P_n^{m-1}, P_{n-2}^{m+1}, P_{n-2}^{m-1}.$$

The diurnal and semi-diurnal terms, P_1^1 and P_2^2 respectively, in the wind velocity give rise to terms in the magnetic tidal potential, and these are collected in table 1.1.

Chapman (1919) made the next major contribution to the study of magnetic tides with spherical harmonic analyses of both solar and lunar magnetic tides, for four daily harmonics of each. His spherical harmonic coefficients, as derived, can be summarized as follows for both solar and lunar magnetic tides:

diurnal	P_2^1,	semi-diurnal	P_3^2,
ter-diurnal	P_4^3,	quater-diurnal	P_5^4,
diurnal seasonal differences			P_1^1, P_3^1,
semi-diurnal seasonal differences			P_2^2, P_4^2,
ter-diurnal seasonal differences			P_3^3, P_5^3.

Chapman's seasonal analyses are for three seasons of four months each, known as Lloyd's seasons. Malin (1974) reanalysed Chapman's data and included a correction.

Fritsche (1902, 1905) analysed solar magnetic tides at 27 stations, rejecting results from nine

high latitude observatories to include only those results that varied with local time. He presented the first results of separation of the magnetic tidal fields into internal and external parts. His analysis of the solar magnetic tide determined the following local time terms:

diurnal P_2^1, semi-diurnal P_3^2, ter-diurnal P_4^3,
quater-diurnal P_5^4, seasonal diurnal P_1^1, P_3^1,
seasonal semi-diurnal P_2^2, P_4^2, seasonal ter-diurnal P_3^3,
seasonal quater-diurnal P_5^4.

Walker (1913) used data from nine observatories in an analysis of the solar tide, for annual terms only. His analysis of the diurnal and semi-diurnal terms includes non-local time spherical harmonic coefficients arising from the inclination of the dipole axis to the geographic axis, as indicated in the theory of Schuster (1908):

diurnal P_2^1 and P_2^0, P_2^2, P_1^1,
semi-diurnal P_3^2 and P_3^1, P_3^3, P_1^1.

Walker commented that the inclusion of the non-local time terms (or Schuster terms) went a considerable way towards meeting the difficulties of 'coordinating the data'.

Van Bemmelen (1912, 1913) analysed data from 15 observatories, analysing both solar and lunar magnetic tides for the semi-diurnal term. Using the method of Schuster, he represented the potentials in terms of the spherical harmonics P_2^2, P_3^2, P_4^2, P_5^2, P_6^2, P_7^2. His paper was the first spherical harmonic analysis of lunar magnetic tides to appear. The 1912 paper showed (incorrectly) that the internal induced lunar field was greater than the external inducing field, but this error was corrected in the 1913 paper.

Steiner (1914) reanalysed the data used by Fritsche, subdivided into summer and winter half-years. The following terms were used:

diurnal $P_1^1, P_2^1, P_3^1, P_4^1$, semi-diurnal P_2^2, P_3^2, P_4^2,
ter-diurnal P_3^3, P_4^3, quater-diurnal P_4^4.

Owing partly to the normalization used, the coefficient of P_4^1 in the diurnal term was found to be large.

Van Vleuten (1917*a*, *b*) followed the analysis of Steiner, using the same theoretical form for the potential, but concluded that a substantial part of the magnetic variation field was not derived from a potential. Chapman (1919) pointed out that the physical implication, involving Earth-to-air electric currents was very improbable.

The analysis of the solar magnetic tide by McNish (1937) was the first to include data from what would now be called an equatorial electrojet station: Huancayo, Peru. The data were for five observatories, for equinoctial months only, and the first three daily harmonics were analysed as follows:

diurnal $P_1^1, P_2^1, P_3^1, P_4^1$, semi-diurnal $P_2^2, P_3^2, P_4^2, P_5^2$,
ter-diurnal $P_3^3, P_4^3, P_5^3, P_6^3$.

McNish's analysis differs from earlier analyses in that the equator-symmetric P_1^1, P_3^1 terms are included in the analysis of the diurnal Fourier coefficients. Earlier analyses based on a small number of Northern Hemisphere results assumed that northern summer and southern summer results would be identical, and evaluated P_1^1 and P_3^1 only for the seasonal semi-differences, e.g.

one half of the difference between summer and winter Fourier coefficients. McNish commented that the last two spherical harmonic coefficients for each harmonic were relatively small, but the awkward scaling used for the spherical harmonic functions has misled him. In fact, the terms P_4^1, P_5^2, P_6^3 in his analysis, although smaller than the corresponding principal local time terms P_2^1, P_3^2, P_4^3, respectively, are, nevertheless, appreciable, and the analysis of such terms forms an important part of the present paper.

Benkova (1940) analysed data from 46 of the Second Polar Year (1932–1933) observatories. The assumption of dependence upon local time only was used, and the following coefficients calculated:

diurnal	$P_1^1, P_2^1, P_3^1, P_4^1, P_5^1,$
semi-diurnal	$P_2^2, P_3^2, P_4^2, P_5^2.$

Benkova's analysis was the first to make use of Schmidt normalized spherical harmonics and it is clear for the first time from published coefficients that the P_4^1 and P_5^2 local time terms are appreciable when compared with the principal local time terms P_2^1 and P_3^2 respectively.

Hasegawa & Ota (1950*a*) also analysed the Second Polar Year data. They used the local time assumption, and analysed the first three daily harmonics. Results were given for Schmidt normalized spherical harmonic functions as follows:

diurnal	$P_1^1, P_2^1, P_3^1, P_4^1, P_5^1, P_6^1,$
semi-diurnal	$P_2^2, P_3^2, P_4^2, P_5^2, P_6^2, P_7^2,$
ter-diurnal	$P_4^3, P_6^3.$

For the diurnal term at least, the term P_4^1 stands out in the list after the principal terms P_1^1 and P_2^1. Hasegawa & Ota (1950*b*) presented S_q overhead current systems at two-hourly intervals based on the results of their analysis.

Maeda (1953) also analysed data for the Second Polar Year and set about the evaluation of those terms that did not vary strictly with local time, as Schuster (1908) and Chapman (1919) had indicated would occur, owing to the non-uniform conductivity of the upper atmosphere and also the inclination of the Earth's dipole axis to the geographic axis. Maeda (1953) evaluated numerical coefficients for the following spherical harmonic functions:

diurnal	$P_0^0, P_1^0, P_1^1, P_2^0, P_2^1, P_2^2, P_3^0, P_3^1, P_3^2, P_3^3,$
	$P_4^0, P_4^1, P_4^2, P_4^3, P_5^0, P_5^1, P_5^2, P_5^3,$
	$P_6^0, P_6^1, P_6^2, P_6^3, P_7^2,$

and evaluated similar spherical harmonic coefficients for the semi- and ter-diurnal terms. Assuming a uniform upper atmospheric electrical conductivity, and a wind velocity having potential terms P_1^1, P_2^2 and P_3^3, Maeda (1953) evaluated the following terms in the resulting magnetic tide by using Schuster's dynamo theory:

diurnal	$P_0^0, P_2^0, P_2^1, P_2^2,$
semi-diurnal	$P_1^0, P_1^1, P_3^0, P_3^1, P_3^2, P_3^3,$
ter-diurnal	$P_2^1, P_2^2, P_4^1, P_4^2, P_4^3.$

He then expressed the opinion that not only the velocity potentials P_1^1, P_2^2, P_3^3 but also P_2^1, P_3^2, P_4^3, P_3^2, P_4^2, 'play a fair role in the S_q field'.

Matsushita & Maeda (1965*a*) analysed the S_q field using data from 69 observatories for the

I.G.Y. subdivided into Lloyd's seasons and three zones of longitude. They computed coefficients of the following spherical harmonic functions:

diurnal	$P_1^1, P_2^1, P_3^1, P_4^1, P_5^1, P_6^1, P_7^1, P_8^1,$
semi-diurnal	$P_2^2, P_3^2, P_4^2, P_5^2, P_6^2, P_7^2,$
ter-diurnal	$P_3^3, P_4^3, P_5^3, P_6^3,$
quater-diurnal	$P_4^4, P_5^4.$

All terms are dependent upon local time only. Not all coefficients were published, but the principal annual and seasonal terms were given together with the corresponding results previously published by other authors.

Matsushita & Maeda (1965*b*) and Matsushita (1966) analysed the lunar magnetic tide using data from 37 stations for various epochs. The stations were divided into three zones of longitude as in their analysis of the solar magnetic tide. Only the lunar semi-diurnal magnetic tide was considered and the following local time terms evaluated:

semi-diurnal $P_2^2, P_3^2, P_4^2, P_5^2, P_6^2, P_7^2, P_8^2, P_9^2, P_{10}^2, P_{11}^2.$

From the results for seasonal subdivisions of data, the authors concluded that the seasonal change in the lunar magnetic tide was only slightly larger than for the solar magnetic tide. Their conclusion is not in agreement with the earlier result of Chapman (1919) or with that of Gupta & Malin (1972), or indeed, with the conclusion of the present paper.

Yaramenko (1978) computed the solar magnetic tide from 33 observatories for the I.G.Y. years, with particular reference to low latitude and equatorial observatories. To represent equatorial electrojet effects in magnetic tides he included higher-order spherical harmonics, thus:

diurnal	$P_1^1, P_2^1, P_3^1, P_4^1, P_{15}^1, P_{16}^1, P_{17}^1, P_{24}^1, P_{26}^1,$
semi-diurnal	$P_2^2, P_3^2, P_4^2, P_5^2, P_{14}^2, P_{15}^2, P_{16}^2, P_{23}^2, P_{25}^2,$
ter-diurnal	$P_3^3, P_4^3, P_5^3, P_{15}^3, P_{16}^3, P_{17}^3, P_{24}^2, P_{26}^3,$
quater-diurnal	$P_4^4, P_5^4, P_{14}^4, P_{15}^4, P_{16}^4, P_{21}^4, P_{25}^4.$

Numerical coefficients were not given explicitly, but curves showing synthesized values were plotted against observed values of the Fourier coefficients.

Price & Wilkins (1963) also reanalysed the Second Polar Year data. They used a surface integral method relying upon the absence of 'curl' in the solar magnetic tide at the surface of the Earth. Equivalently, they assumed that the Earth-to-air electric currents could be ignored, or that the solar magnetic tide is purely poloidal with no toroidal component. The method of Price & Wilkins does not produce spherical harmonic coefficients, indeed the method was devised to avoid their use, but it does give current functions for both internal and external fields at four-hour intervals for each of the three Lloyd's seasons. Berdichevskiy & Faynberg (1972, 1974), showed that the assumption of the negligibility of the toroidal component of the solar magnetic tide was justified.

Parkinson (1971) analysed data from the I.G.Y. for the solar magnetic tide S_q only, using four seasonal subdivisions. The number of observatories in each seasonal subdivision varied from 42 to 54. Parkinson assumed that the S_q field is zero at local midnight and included in his analysis spherical harmonic coefficients to represent the time-independent difference between the midnight value and that given by the sum of the first four harmonics at midnight. The general effect of this calculation was to reduce the magnitude of the S_q current system in

the night-time hemisphere to a realistically small value. A similar calculation was made by Malin & Gupta (1977). Parkinson (1971) also made an attempt to estimate the terms that did not vary with local time by allowing spherical harmonic coefficients, normally averaged with respect to longitude, to be expressed in the form $a+c\cos\phi+d\sin\phi$. Terms evaluated were

constant	$P_0^0, P_1^0, P_2^0, P_3^0, P_4^0, P_5^0, P_6^0,$
diurnal	$P_1^1, P_2^1, P_3^1, P_4^1, P_5^1,$
semi-diurnal	$P_2^2, P_3^2, P_4^2, P_5^2,$
ter-diurnal	$P_3^3, P_4^3, P_5^3, P_6^3.$

The quater-diurnal (4 c/d) harmonics were not analysed.

Malin (1973) analysed the solar and lunar magnetic tides using data from 100 observatories for the interval 1957.5 to 1960.0. The data were not subdivided into seasons. The semi-diurnal Fourier coefficients for the lunar magnetic tide were recalculated to allow for the dynamo action of the oceans, which are in tidal movement. Malin's analysis included calculations of non-local time terms more directly than Parkinson (1971) but not as extensively as Maeda (1953). The exact choice of spherical harmonic coefficients to be included was based on considerations of the non-local time field on the theory of the method of least squares, which requires that statistically insignificant terms be excluded. The same coefficients were determined for both the solar and lunar magnetic tides:

diurnal	$P_1^0, P_1^1, P_2^0, P_2^1, P_2^2, P_3^0, P_3^1, P_3^2, P_3^3, P_4^1, P_4^2,$
semi-diurnal	$P_1^1, P_2^1, P_2^2, P_3^1, P_3^2, P_3^3, P_4^1, P_4^2, P_4^3, P_4^4,$
ter-diurnal	$P_2^2, P_3^2, P_3^3, P_4^2, P_4^3, P_4^4, P_5^3,$
quater-diurnal	$P_3^3, P_4^3, P_4^4, P_5^3, P_5^4, P_5^5, P_6^4.$

The same mathematical model has been used in the present analysis of solar and lunar magnetic tides and their seasonal changes, except that a P_5^2 term has been added to the semi-diurnal terms and P_6^3 to the ter-diurnal terms.

Suzuki & Maeda (1978) presented equivalent current systems of the solar magnetic variations for December 1964, using data from 68 observatories. Only three terms were used in the calculations, namely P_2^1, P_3^2, P_4^3, with spherical harmonics analyses being made at two-hour intervals. Numerical values of the spherical harmonic coefficients were not given. Maeda & Suzuki (1967) and Suzuki (1973) gave spherical harmonic coefficients for the S_q field for the I.G.Y., with particular reference to the effects of the equatorial electrojet. Their results could be compared directly with the analysis of Matsushita & Maeda (1965*a*). The following coefficients were evaluated:

diurnal	$P_n^1, \quad n = 1, 2, \ldots, 10,$
semi-diurnal	$P_n^2, \quad n = 2, 3, \ldots, 11,$
ter-diurnal	$P_n^3, \quad n = 3, 4, \ldots, 12,$
quater-diurnal	$P_n^4, \quad n = 4, 5, \ldots, 13,$

and given separately for subdivisions of Lloyd's seasons. Suzuki (1979) analysed S_q at two-hour intervals for December 1964, using data from 60 observatories. Local time terms only were calculated, $m = 1$, $n = 1, 2, \ldots, 8$ for diurnal terms etc.

In all of the analyses mentioned the principal terms for the annual average solar and lunar magnetic tides have been P_2^1, P_3^2, P_4^3, P_5^4, for the diurnal, and semi-, ter- and quater-diurnal terms respectively. Some authors have also included the terms P_4^1, P_5^2, P_6^3, P_7^4, and, a suitable

normalization for the spherical harmonic functions having been chosen, such terms are appreciable when compared with the corresponding coefficients P_2^1, P_3^2, P_4^3, P_5^4, respectively. It will be shown that the terms P_4^1, P_5^2, P_6^3, P_7^4, are associated with the Hough function structure of winds in the upper atmosphere. It is indeed remarkable that the magnitudes of such Hough function terms have not been commented upon by the authors who calculated them.

It is the purpose of the present paper to analyse the most recent and most extensive tabulation of hourly mean magnetic values available, i.e. those recorded during the I.Q.S.Y. years 1964 and 1965. The analysis will include the non-local time terms arising from geographic and auroral zone effects, and also the Hough function terms referred to above. The analysis will be of the solar magnetic tide, the principal lunar magnetic tide, and the lunar magnetic elliptic tide, and will include harmonic analyses of the annual and semi-annual change of the magnetic tides. Spherical harmonic coefficients are given for phase-law tides and partial tides (to use the nomenclature introduced by Schneider (1963)). Equivalent overhead current systems are given for all computed magnetic tides, with the exception of long-period terms.

2. The Chapman–Miller method

The analysis of lunar magnetic tides is usually done by a 'fixed-age' method, such as the Chapman–Miller method (Chapman & Miller 1940) or some variation (see, for example, Winch 1970). The 'fixed solar hour' method of Schlapp & Weekes (1973) is also of value. The basis of the Chapman–Miller fixed-age method is that every Greenwich day is assigned an integer character number between one and twelve based on the rate of change of a specific combination of astronomical parameters. Appropriate combinations are described in equations (1)–(4). For the analysis of the principal lunar magnetic tide the character numbers are assigned in such a way that a particular number will recur on the average, every half synodic month of approximately 14.7653 days. One year of hourly mean values is required for the estimation of magnetic tides free of any contribution from seasonal change and it is a standard practice to exclude the five days in each calendar month nominated as International Disturbed Days. Magnetic storms and magnetic activity on International Disturbed Days add approximately 50 nT noise to the data from which one is hoping to estimate a lunar magnetic tide of amplitude only 1 or 2 nT. The exclusion of only five days per calendar month is modest compared with the rejection of almost two-thirds of the data in the analysis of solar and lunar tides in atmospheric pressure. Chapman (1951) found that it was only by rejection of days with large tropospheric variations that the comparatively small lunar pressure tide could be detected.

Lunar magnetic tides are estimated from magnetic hourly mean values which contain a large solar daily magnetic variation having a very substantial day-to-day variability. Consequently the reliable estimation of both solar and lunar magnetic tides requires the analysis of many more hourly mean values than are contained in, say, half a synodic month. The analysis of magnetic hourly mean values as if they were sea-level changes is not useful because the mathematical form of magnetic tides is much more complex than that of the ocean tides.

Twelve groups of 25 hourly mean values are formed in the Chapman–Miller method, and they provide a 12×25 array suitable for a double Fourier analysis. The 25th value in the array is the first value of the following day and is required for the elimination of the non-cyclic variation associated with the slow recovery of the magnetic field intensity from its diminished level after a magnetic storm. The Chapman–Miller method then requires that linear combi-

nations be formed amongst the Fourier coefficients in a matrix multiplication type of procedure. The matrix is denoted D_{mpS}, and incorrect values given for its elements by more than one author (including Chapman & Miller 1940) have added unnecessary difficulties to a relatively simple calculation. The application of the D_{mpS} matrix gives a new set of Fourier coefficients differing but little from those computed from the original 12×25 array. Hence the results would not be seriously affected if the D_{mpS} array were to be replaced by a unit matrix, i.e. if the D_{mpS} calculation were not made. The present work includes the analysis of partial tides, and a generalized complex form of the D_{mpS} matrix, denoted $E_{mm'S}$ (Winch 1970), has been used throughout. However, from what has been written above it should be clear that the $E_{mm'S}$ calculation is an added refinement rather than an essential part.

To check the relevance of the Chapman–Miller method, Schlapp & Malin (1976) examined the width of tidal lines in the geomagnetic spectrum and found them to be sufficiently narrow for the Chapman–Miller method to be suitable for the analysis of lunar magnetic tides. Another point in favour of the Chapman–Miller method is that it needs no special modification to deal with missing observations. Days with, say, three or more missing hourly mean values are simply excluded from the analysis.

The magnetic tides exhibit a very pronounced dependence upon season, being generally much larger in local summer months than in local winter months. The seasonal dependence of magnetic tides is often treated by subdividing the data into four seasons of three months or into the so-called Lloyd's seasons consisting of three seasons of four months each. Spherical harmonic coefficients for the potential of the magnetic tide are computed for each seasonal subdivision. The subdivision into seasons is straightforward, but as Stening & Winch (1979) point out, is too coarse to represent the sharp changes at some observatories. Seasonal subdivisions also provide spherical harmonic coefficients at only four distinct frequencies. It is possible to obtain spherical harmonic coefficients at the sixteen different 'sum and difference' seasonal frequencies by treating the seasonal change of a magnetic tide as just another magnetic tide, with frequencies differing from the four standard frequencies by (plus or minus) one or two cycles per year. By this means an electromagnetic response function for the Earth can be obtained at more frequencies.

The calculations for the seasonal magnetic tides are made by a minor variation of the Chapman–Miller method. For example, the 1 c/a (cycle per year) seasonal change of the principal lunar magnetic tide is computed by using 15.3873 days and 14.1916 days for character number repetitions, 14.7653 days having been used for the principal lunar magnetic tide. The same type of modification makes it possible to analyse the elliptic magnetic tides associated with the atmospheric tide N_2, the principal elliptic tide to M_2, the principal lunar semi-diurnal tide. The same technique is used to analyse the seasonal changes of the elliptic magnetic tides.

Observatory hourly mean values are all tabulated in Universal Time (U.T.), with mean values centred midway between the hours for convenience in derivation from magnetograms, the first tabulated hourly mean value being between 0 h and 1 h U.T. It is convenient therefore to derive, in degrees, the east longitude of the mean Moon, mean Sun and mean perigee of the Moon, denoted s, h, p, respectively, by using the following formulae of Bartels (1957):

$$s = 270.43659 + 481267.891\ T + 0.00198\ T^2, \tag{1}$$

$$h = 279.69668 + 36000.7689\ T + 0.00030\ T^2, \tag{2}$$

$$p = 334.32956 + 4069.03403\ T - 0.01032\ T^2, \tag{3}$$

where T is the time measured in Julian centuries of 36525 mean solar days elapsed from 1899, December 30.5, at which instant $T = 0$. The Universal Time t is given in degrees by

$$t = 180 + 13\,149\,000\ T \pmod{360}. \tag{4}$$

The *Explanatory supplement to the astronomical ephemeris* (1961) gives formulae corresponding to equations (1)–(3) based on Ephemeris Time. The seasonal parameter h is zero at the vernal equinox, on about 21 March, each year. The angle $s-h$, being a measure of the angle subtended at the Earth between the mean Moon and Sun, is a measure of lunar phase, while the expression $t-s+h$ is a measure of time elapsing between successive crossings of the meridian at a place by the Moon. The expression $t-s+h$ is therefore sometimes called lunar time and denoted by τ.

Rates of change obtained from linear terms of equations (1)–(3) will be denoted by w, i.e.

$$w(2s-4h) = \mathrm{d}(2s-4h)/\mathrm{d}t,$$

or, with only linear dependence upon time,

$$2s-4h = wt + \text{const.} \tag{5}$$

The following rates of change will be required in the subsequent sections:

$$\begin{aligned}
\frac{\mathrm{d}}{\mathrm{d}t}(2s-4h) &= \frac{1}{16.0641}\,\mathrm{day}^{-1} = 720.493\,\mathrm{nHz}, & \frac{\mathrm{d}}{\mathrm{d}t}(3s-3h-p) &= \frac{1}{9.8736}\,\mathrm{day}^{-1} = 1172.22\,\mathrm{nHz},\\
\frac{\mathrm{d}}{\mathrm{d}t}(2s-3h) &= \frac{1}{15.3873}\,\mathrm{day}^{-1} = 752.184\,\mathrm{nHz}, & \frac{\mathrm{d}}{\mathrm{d}t}(3s-2h-p) &= \frac{1}{9.6137}\,\mathrm{day}^{-1} = 1203.91\,\mathrm{nHz},\\
\frac{\mathrm{d}}{\mathrm{d}t}(2s-2h) &= \frac{1}{14.7653}\,\mathrm{day}^{-1} = 783.870\,\mathrm{nHz}, & \frac{\mathrm{d}}{\mathrm{d}t}(3s-h-p) &= \frac{1}{9.3672}\,\mathrm{day}^{-1} = 1235.60\,\mathrm{nHz},\\
\frac{\mathrm{d}}{\mathrm{d}t}(2s-h) &= \frac{1}{14.1916}\,\mathrm{day}^{-1} = 815.558\,\mathrm{nHz}, & \frac{\mathrm{d}}{\mathrm{d}t}(h) &= \frac{1}{365.2422}\,\mathrm{day}^{-1} = 31.6888\,\mathrm{nHz},\\
\frac{\mathrm{d}}{\mathrm{d}t}(2s) &= \frac{1}{13.6608}\,\mathrm{day}^{-1} = 847.247\,\mathrm{nHz}, & \frac{\mathrm{d}}{\mathrm{d}t}(2h) &= \frac{1}{182.6211}\,\mathrm{day}^{-1} = 63.3775\,\mathrm{nHz}.
\end{aligned}$$

Note that the rates of change of the parameters $2s$ and $3s-h-p$ have periods close to the second and third harmonics, respectively, of the 27-day recurrence tendency in magnetic activity.

The basis of the Chapman–Miller method for the analysis of lunar magnetic tides is the assigning of a character number to each day, traditionally values of $2s-2h$ only being used. From the list of the rates of change, the character numbers from one to twelve will recur, on average, every 14.7653 days. Much use has been made of these character numbers, and three catalogues of them are available: Bartels & Fanselau (1938), Bartels *et al.* (1954), Sugiura & Fanselau (1966). It is so simple to compute the character numbers as required for any combination of s, h, p for any particular day that the catalogues are useful only for checking results. The considerable variation of magnetic tides with season requires that only *complete* years of hourly mean values should be analysed. If the number of mean solar days elapsed from the epoch of equations (1)–(3) has been evaluated for the first day of a given year, it is simple to work through the year day by day, by adding one to the day count and dividing by 36525 to obtain the elapsed time in Julian centuries.

The mathematical form chosen for magnetic tides depends upon the forms chosen for the representations of atmospheric tides and of ionospheric electrical conductivity. The time-dependence of electrical conductivity of the ionosphere K is governed by the geocentric zenith distance of the Sun, denoted χ. Thus,

$$\cos\chi = \sin\delta\cos\theta - \cos\delta\sin\theta\cos t^*,$$

where θ is the colatitude of the sub-solar point, δ is the Sun's declination and t^* is the local solar time measured from local midnight. The following models for K have been proposed:

$K = K_0(1+\cos\chi)$ (Schuster 1908),

$K = K_0(1+3\cos\chi+2.25\cos^2\chi)$ (Chapman 1913, 1919),

$K = K_0(1+2.45\cos\chi+2.25\cos^2\chi)$ (Chakrabarty & Pratap 1954),

$K = K_0(1+0.9\cos\chi)^{-1}$ (Ashour & Price 1948),

$K = K_0(1+2.00\cos\chi+1.46\cos^2\chi)$ (Maeda 1956),

together with models valid for $\theta = 0$, $\delta = 0$, given by Maeda (1952, 1955), Hasegawa (1950), Hasegawa & Maeda (1951), and Matsushita (1969). For the present analysis, the time-dependence of electrical conductivity in the upper atmosphere is represented by

$$K = K_0 \sum_{n=0}^{4} a_n \sin(nt^* + \alpha_n), \tag{7}$$

where t^* and α_n are the local time and phase angle in angular measure. The amplitudes a_n will be functions of colatitude, east longitude and season. Four harmonics are required in equation (7) to enable the Fourier series to cope with the 'step-function' nature of ionospheric conductivity, which increases rapidly at sunrise and diminishes rapidly at sunset.

Forbes & Lindzen (1976) use the formula

$$K = 0.4114 + 0.5428\cos t^* + 0.1368\cos 2t^* - 0.0788\cos 3t^* - 0.0414\cos 4t^*$$

as an approximation to the day–night shape factor in local time t^* variation of E-region ionization, following a $\cos^{\frac{1}{2}}\chi$ dependence on the solar zenith angle.

We shall be concerned with only four terms in the lunar tide generating potential. They are given in Darwin's notation by Doodson (1921) as

$$\mathrm{M}_2 \equiv 0.90812\, G_2 \cos(2t - 2s + 2h), \tag{8a}$$

$$\mathrm{O}_1 \equiv 0.37689\, G_1 \sin(t - 2s + h), \tag{8b}$$

$$\mathrm{N}_2 \equiv 0.17387\, G_2 \cos(2t - 3s + 2h + p), \tag{8c}$$

$$\mathrm{Q}_1 \equiv 0.07216\, G_1 \sin(t - 3s + h + p), \tag{8d}$$

where the geographical amplitude factors G_1 and G_2 are given by

$$G_1 = G\sin 2\theta = \tfrac{2}{3}\sqrt{3}\, G P_2^1, \quad G_2 = G\sin^2\theta = \tfrac{2}{3}\sqrt{3}\, G P_2^2,$$

where θ is the geographic colatitude, and G is a constant. The geographical constant G_1, associated with the tides O_1 and Q_1, is zero when $\theta = \frac{1}{2}\pi$, i.e. at the equator.

The time-dependence of M_2 is essentially lunar semi-diurnal but it can also be regarded as semi-diurnal in a solar day but with a slowly varying phase angle $2s - 2h$. It is from such an

analysis that the Chapman–Miller method of assigning daily character numbers based on $2s-2h$ has been derived. No matter how the tide is considered, however, the period of the tide is still one half of a *lunar* day. The magnetic tide associated with M_2 will be denoted $L(M_2)$ and its time-dependence is given by the product of equations (7) and (8*a*):

$$L(M_2) = \sum_{n=-2}^{6} A_n \sin(nt-2s+2h+a_n). \tag{9}$$

Similarly, the magnetic tides associated with the tide O_1 will be denoted by $L(O_1)$, and have time-dependence given by

$$L(O_1) = \sum_{n=-3}^{5} B_n \sin(nt-2s+h+b_n). \tag{10}$$

The expression for upper atmosphere electrical conductivity varies with season, i.e. with the parameter h, and hence it is to be expected that the seasonal change of $L(M_2)$ will have annual component sum and difference frequencies expressible as

$$\sum_{n=-2}^{6} C_n \sin(nt-2s+3h+c_n), \tag{11}$$

and

$$\sum_{n=-2}^{6} D_n \sin(nt-2s+h+\mathrm{d}_n). \tag{12}$$

However, the expression in equation (12) for a seasonal change component of $L(M_2)$ has the same mathematical form as the magnetic tide denoted $L(O_1)$. To avoid the misleading nomenclature $L(M_2)$, $L(O_1)$, it seems preferable, after Winch & Cunningham (1972), to write

$$L(2s-3h) = \sum_{n} E_n \sin(nt-2s+3h+e_n), \tag{13}$$

$$L(2s-2h) = \sum_{n} F_n \sin(nt-2s+2h+f_n), \tag{14}$$

$$L(2s-h) = \sum_{n} G_n \sin(nt-2s+h+g_n), \tag{15}$$

in which the magnetic tides are labelled according to the character numbers used in their calculation, rather than according to an atmospheric tide with which it is not exclusively associated. The magnetic tide calculation based on h, $2h$, gives the 1, 2 c/a seasonal change of the solar daily variation S. The results will therefore be denoted $S(h)$ and $S(2h)$.

The summands $n = 1, 2, 3, 4$ in equations (13)–(15) are the standard 'phase-law' terms. The term $n = 0$ is a long-period term, while terms corresponding to negative values of n are denoted, after Schneider (1963), as partial tides. Such tides were considered theoretically by Chapman (1919), but never evaluated, on the ground that, compared with phase-law-tides, their phase changed rapidly throughout a lunar month. The partial tides are not entirely without interest, and a modification to the Chapman–Miller method for their calculation has been given by Winch (1970) and applied by Rao & Sastri (1971, 1972). For mathematical and computational convenience, the range of summation in the equations (13)–(15) representing magnetic tides, is taken to be $-4 \leqslant n \leqslant +4$.

It is not appropriate to subdivide the seasonal change $S(h)$ and $S(2h)$ of the solar magnetic

tide S into phase law and partial tides. Instead, the following notation will be used:

$$S^+(h) = \sum_{n=1}^{4} A_n^+ \sin(nt+h+\epsilon_n^+),$$

$$S^-(h) = \sum_{n=1}^{4} A_n^- \sin(nt-h+\epsilon_n^-),$$

$$S^+(2h) = \sum_{n=1}^{4} A_{2n}^+ \sin(nt+2h+\epsilon_{2n}^+),$$

$$S^-(2h) = \sum_{n=1}^{4} A_{2n}^- \sin(nt-2h+\epsilon_{2n}^-).$$

When computed from relatively short 'runs' of data, such as the two years used in the present analysis, the partial tides may contain a significant component arising from quasi-periodicities in the ionospheric electrical conductivity, associated with the 27-day recurrence tendency of magnetic activity, the point being that the 27-day period of the recurrence tendency of magnetic activity is not far removed from the 28.28-day period of the lunar month.

With the use of the expression w of equation (5), phase-law tides have the form

$$\sum_{n=1}^{4} H_n \{\sin(n-w)t+h_n\}, \tag{16}$$

while the partial tides can be expressed in the form

$$\sum_{n=1}^{4} J_n \{\sin(n+w)t+j_n\}. \tag{17}$$

The four terms that make up each lunar magnetic tide, unlike the terms of a Fourier series, have periods that *are not* integer submultiples of some constant period. It is this fact that allows four sine-terms to represent adequately a quantity depending both on local time and on a combination of astronomical parameters that varies slowly.

Of the lunar magnetic tides described, it is standard practice to evaluate only $L(2s-2h)$ for various seasons and/or lunar distances (see, for example, Chapman 1915, 1918; Arora & Rao 1975). In the present work, the seasonal and lunar distance effects are dealt with by calculating lunar magnetic tides for a range of character numbers, in particular,

(*a*) lunar semi-diurnal tides and seasonal changes:

$$L(2s-4h),\ L(2s-3h),\ L(2s-2h),\ L(2s-h),\ L(2s);$$

(*b*) lunar elliptic tides and seasonal changes:

$$L(3s-3h-p),\ L(3s-2h-p),\ L(3s-h-p);$$

(*c*) solar seasonal magnetic variations:

$$S(h),\ S(2h).$$

Long-period tides and the solar magnetic tide S are obtained as by-products of the calculations.

TABLE 3.1. MAGNETIC OBSERVATORIES AND THREE-CHARACTER MNEMONICS, LISTED IN DESCENDING ORDER OF GEOGRAPHIC LATITUDE

observatory		lat.	long. E	observatory		lat.	long. E
Alert	ALE	82.50	297.50	Toledo	TOL	39.88	355.95
Heiss Island	HIS	80.62	58.05	Fredericksburg	FRD	38.20	282.63
Cape Chelyuksin	CCS	77.72	104.28	Ashkabad	ASH	37.95	58.10
Thule- Qanaq	THL	77.48	290.83	Almeria	ALM	36.85	357.53
Mould Bay	MBC	76.20	240.60	San Fernando	SFS	36.47	353.80
Resolute Bay	RES	74.70	265.10	Kakioka	KAK	36.23	140.18
Dixon Island	DIK	73.55	80.57	Tehran	TEH	35.73	51.38
Tixie Bay	TIK	71.58	129.00	Simosato	SSO	33.57	135.93
Barrow	BRW	71.30	203.25	Dallas	DAL	32.98	263.25
Tromso	TRO	69.67	18.95	Tucson	TUC	32.25	249.17
Godhavn	GDH	69.23	306.48	Kanoya	KNY	31.42	130.88
Murmansk	MRM	68.25	33.08	Misallat	MLT	29.52	30.90
Kiruna	KIR	67.83	20.42	Tenerife	SZT	28.48	343.72
Sodankyla	SOD	67.37	26.63	Havana	HVN	22.97	277.85
Cape Wellen	CWE	66.17	190.17	Honolulu	HON	21.32	202.00
College	CMO	64.87	212.17	Teoloyucan	TEO	19.75	260.82
Baker Lake	BLC	64.33	263.97	Alibag	ABG	18.63	72.87
Leirvogur	LRV	64.18	338.30	San Juan	SJG	18.12	293.85
Dombas	DOB	62.07	9.12	Hyderabad	HYB	17.42	78.55
Yakutsk	YAK	62.02	129.67	Mbour	MBO	14.40	343.03
Nurmijarvi	NUR	60.52	24.65	Muntinlupa	MUT	14.37	121.02
Lerwick	LER	60.13	358.82	Guam	GUA	13.58	144.87
Leningrad	LNN	59.95	30.70	Annamalainagar	ANN	11.37	79.68
Lovo	LOV	59.35	17.83	Addis Ababa	AAE	9.03	38.77
Fort Churchill	FCC	58.80	265.90	Trivandrum	TRD	8.48	76.95
Sitka	SIT	57.07	224.67	Freetown	FTN	8.47	346.78
Sverdlovsk	SVD	56.73	61.07	Koror	KOR	7.33	134.50
Rude Skov	RSV	55.85	12.45	Paramaribo	PAB	5.82	304.78
Kazan	KZN	55.83	48.85	Fuquene	FUQ	5.47	286.27
Moscow	MOS	55.48	37.32	Bangui	BNG	4.43	18.57
Eskdailemuir	ESK	55.32	356.80	Moca	MFD	3.35	8.67
Meanook	MEA	54.62	246.67	Tatuoca	TTB	−1.20	311.48
Minsk	MNK	54.10	26.52	Nairobi	NAI	−1.32	36.82
Stonyhurst	STO	53.85	357.53	Lwiro	LWI	−2.30	28.80
Wingst	WNG	53.75	9.07	Tanggerang	TNG	−6.17	106.63
Witteveen	WIT	52.82	6.67	Luanda	LUA	−8.92	13.17
Irkutsk-Patrony	IRK	52.17	104.45	Port Moresby	PMG	−9.42	147.15
Swider	SWI	52.12	21.25	Huancayo	HUA	−12.05	284.67
Niemegk	NGK	52.07	12.68	Apia	API	−13.80	188.22
Valentia	VAL	51.93	349.75	Arequipa	ARE	−16.47	288.52
Hartland	HAD	51.00	355.52	Tananarive	TAN	−18.92	47.55
Kiev	KIV	50.72	30.30	Tsumeb	TSU	−19.20	17.58
Dourbes	DOU	50.10	4.60	La Quiaca	LQA	−22.10	294.40
Pruhonice	PRU	49.98	14.55	Pilar	PIL	−31.67	296.12
Lvov	LVV	49.90	23.75	Gnangara	GNA	−31.78	115.95
Victoria	VIC	48.50	236.60	Hermanus	HER	−34.42	19.20
Wien-Kobenzl	WIK	48.27	16.32	Toolangi	TOO	−37.53	145.47
Furstenfeldbruck	FUR	48.17	11.28	Amberley	AML	−43.15	172.72
Chambon-la-Foret	CLF	48.02	2.27	Trelew	TRW	−43.20	294.70
Hurbanovo	HRB	47.87	18.18	Port aux Francais	PAF	−49.35	70.22
Yuzhno-Sakhalinsk	YSS	46.95	142.72	Macquarie Island	MCQ	−54.50	158.95
Tihany	THY	46.90	17.90	Argentine Islands	AIA	−65.25	295.73
Odessa-Stepanovka	ODE	46.78	30.88	Wilkes	WIL	−66.28	111.53
Surlari	SUA	44.68	26.25	Mirny	MIR	−66.55	93.00
Roburent	ROB	44.30	7.88	Dumont Durville	DRV	−66.67	140.00
Memambetsu	MMB	43.90	144.20	Mawson	MAW	−67.60	62.88
Agincourt	AGN	43.78	280.73	Roi Baudouin	RBD	−70.43	24.30
Vladivostok	VLA	43.68	132.17	Sanae	SNA	−70.47	357.52
Panagjurischte	PAG	42.52	24.18	Novolazarevskaya	NVL	−70.77	11.82
Logrono	LGR	42.45	357.50	Eights	EGS	−75.23	282.83
L'Aquila	AQU	42.38	13.32	Halley Bay	HBA	−75.52	333.38
Tbilisi	TIF	42.08	44.70	Scott Base	SBA	−77.85	166.78
Tashkent	TKT	41.42	69.20	Vostok	VOS	−78.45	106.87
Ebro	EBR	40.82	0.50	Byrd Station	BYR	−80.00	240.50
Coimbra	COI	40.22	351.58	South Pole	SPA	−89.98	0.00

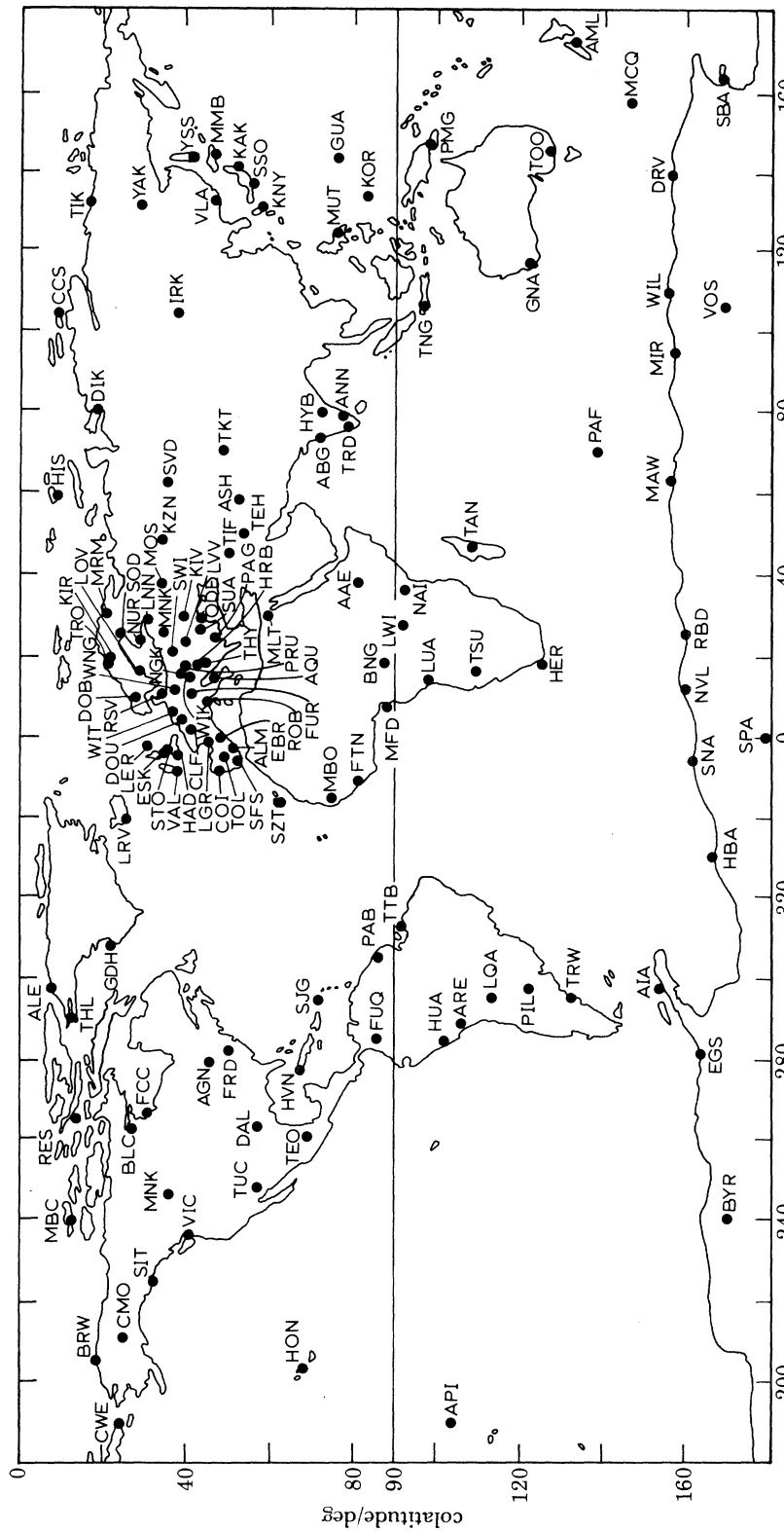

FIGURE 3.1. Magnetic observatories with hourly mean values available for 1964–65 and used in the present analysis.

3. Analysis of observatory data

The number and distribution of magnetic observatories have improved steadily since Schuster's (1889) first analysis of data from five observatories and, indeed, since Malin's (1973) recent analysis of data from 100 observatories. The availability of magnetic data has also improved, particularly with the establishment of the World Data Centres. In fact, without the active cooperation of World Data Center A in Boulder, Colorado, the analysis to be given here would still be in the early stages of data collection.

The present analysis of geomagnetic hourly mean values for 1964 and 1965 is based on data provided from 130 magnetic observatories, 34 in the Southern Hemisphere and 96 in the Northern Hemisphere. Malin's (1973) analysis used 100 observatories, 23 in the Southern Hemisphere and 77 in the Northern Hemisphere. Each observatory has been assigned a three-character mnemonic (*I.A.G.A. News* 1977), and those used are listed, along with the geographic latitude and east longitude, in table 3.1. The distribution of observatories is shown in figure 3.1 and it is interesting to note that the cluster of observatories in Europe is now being balanced, to some extent, by a cluster of observatories in Antarctica.

The magnetic data available for analysis consist of 79064, 78953, 83536 days of hourly mean values for declination D, horizontal intensity H and vertical intensity Z respectively. There were also 6047 and 6107 days of hourly mean values for the northward component X and eastward component Y, respectively. Of the 130 observatories, 129 provided hourly mean values for the three components or elements of the magnetic field, and one observatory, San Fernando, provided hourly mean values for declination and horizontal intensity only. Approximately one third of the data were available in machine-readable form on magnetic tape from World Data Center A, while the remaining two thirds were prepared on punch cards from observatory yearbooks and from microfilm provided by World Data Center A. Funds were provided by the Australian Research Grants Committee. Two cards were required for the 24 three-digit numbers that constitute one day of data, and approximately 350000 cards were prepared and checked by double punching. This work was done at the University of New England, Armidale, New South Wales, and took just over two years to complete.

The hourly mean magnetic values are published in monthly tables, consisting of rows of three-digit numbers, together with a constant larger main field base value which is to be added to each hourly mean value to give the magnetic field component correct to five significant figures. The data, after being edited and corrected, were adjusted by the addition or subtraction of a constant, so that the monthly base value was constant for the entire interval 1964–1965. This procedure was intended to minimize the difficulties in computing long-period magnetic tides, those corresponding to the summand $n = 0$ in equations (13)–(15).

Gaps in the data consisting of only one or two missing values were filled by linear interpolation, while three or more missing values were indicated by a string of nines, one missing value in the string being indicated by the figure 9999. Publication errors noted by punch card operators (for example, 31 days in September, no values for the interval 11 h–12 h), and those noted by the author while listing and editing the cards, were checked against magnetograms by World Data Center A, or by correspondence with the observatory, and corrected. The cards were transferred to magnetic tape, one magnetic tape being for D- and X-values, one for H- and Y-values, and a third tape for Z-values. This grouping presents no difficulties although the grouping D, Y and H, X would have been more appropriate. The hourly mean

values were then checked by computing all first differences, and checking all those greater than 200 tabulated units with the published value or against magnetograms. Results were then corrected, after correspondence, where necessary, with World Data Center A. Many large first differences were found to be associated with magnetic storms, and no correction was needed. All hourly mean values are published in columns in U.T. and for the calculation the first value of the next day was added to each row of 24 hourly mean values. This 25th value is required in the analysis for the elimination of non-cyclic variation. In practice, in lunar magnetic tide calculations, the non-cyclic variation, corresponding to the slow recovery of the magnetic field from a magnetic storm, is virtually negligible, but its removal has the theoretical property that the elements of the matrix D_{mpS} used in magnetic tide analysis, have only real values. This simplifies the resultant numerical work.

For the mathematical process of representation of the scalar potential of magnetic tides as a linear combination of solid spherical harmonics, Fourier coefficients are required for the tides in the components X, Y, Z. Nine observatories published results for the elements X, Y, Z directly, while 120 published results for D, H, Z, and San Fernando published D, H only. The equations

$$X = H\cos D, \quad Y = H\sin D$$

provide the following formulae for relations between small variations in X, Y, and H, D:

$$\left.\begin{aligned} \Delta X &= \Delta H\cos D - H\,\Delta D\sin D,\\ \Delta Y &= \Delta H\sin D + H\,\Delta D\cos D.\end{aligned}\right\} \tag{18}$$

For the analysis of magnetic tides from two years of hourly mean values, it is possible that the evaluation of hourly mean values for X and Y at every observatory would introduce rounding errors detrimental to the estimation of lunar magnetic tides, which are of the order of the least significant tabulated figure. The H and D Fourier coefficients have been regarded as small variations ΔH and ΔD, and equation (18) used, together with main field values of H and D averaged over the years 1964 and 1965, to obtain the corresponding values of ΔX and ΔY. The analysis of I.G.Y. data by Malin (1973) uses hourly mean values already expressed in terms of components X, Y, Z.

Magnetic tapes containing the hourly mean values for 1964 and 1965 have been prepared in standard format, having the 25th hourly value place taken by the daily average, and are available from World Data Center A, Boulder, Colorado, on request.

The five International Disturbed Days per month have been excluded from the analysis, but auroral or high latitude observatories and equatorial observatories have been included. The mathematical model chosen, i.e. the spherical harmonic coefficients chosen to represent each daily harmonic, allows the possibility of representing terms that do not vary strictly with local time, such terms being likely to arise from auroral observatories. It was considered desirable to have a global representation of the magnetic tide rather than one valid only for certain latitudes. It was also considered desirable to have an analysis that conformed closely to the recent substantial analysis of solar and magnetic tides by Malin (1973) for the I.G.Y. years, which also did not exclude high latitude observatories. Numerical experiments analysing S, $S(h)$ and $S(2h)$ with the 1964–1965 hourly mean values showed that the results were varied only slightly by excluding certain groups of observatories, the equatorial and auroral groups in particular. For these reasons, auroral and equatorial observatories were not excluded.

The Chapman–Miller method of analysis concludes with certain adjustments to amplitudes and phase angles of computed parameters and, consequently, the output from the analysis of observatory data for D, H, Z is in the form

$$\left.\begin{aligned}\Delta D &= \sum_m a_{Dm} \sin (mt+\epsilon_{Dm}),\\ \Delta H &= \sum_m a_{Hm} \sin (mt+\epsilon_{Hm}),\\ \Delta Z &= \sum_m a_{Zm} \sin (mt+\epsilon_{Zm}),\end{aligned}\right\} \tag{19}$$

where $m = n-w$ for phase-law tides, $m = w$ for long-period tides, and $m = n+w$ for partial tides, w being defined as in equation (5). By means of the formulae

$$A_{Dm} = a_{Dm} \sin \epsilon_{Dm}, \quad B_{Dm} = a_{Dm} \cos \epsilon_{Dm},$$

the Chapman–Miller output of equation (19) may be expressed in the form

$$\left.\begin{aligned}\Delta D &= \sum_m (A_{Dm} \cos mt + B_{Dm} \sin mt),\\ \Delta H &= \sum_m (A_{Hm} \cos mt + B_{Hm} \sin mt),\\ \Delta Z &= \sum_m (A_{Zm} \cos mt + B_{Zm} \sin mt).\end{aligned}\right\} \tag{20}$$

The coefficients A_{Dm}, A_{Hm}, and B_{Dm}, B_{Hm}, are converted into coefficients A_{Xm}, A_{Ym}, and B_{Xm}, B_{Ym}, with the conversion formulae given in equation (18). Hence the Fourier coefficients for magnetic tides at all observatories are obtained in the form

$$\left.\begin{aligned}\Delta X &= \sum_m (A_{Xm} \cos mt + B_{Xm} \sin mt),\\ \Delta Y &= \sum_m (A_{Ym} \cos mt + B_{Ym} \sin mt),\\ \Delta Z &= \sum_m (A_{Zm} \cos mt + B_{Zm} \sin mt).\end{aligned}\right\} \tag{21}$$

Malin's (1973) analysis of $L(2s-2h)$ phase-law tides and the solar daily variation S_q for 100 observatories evaluated only 1600 Fourier coefficients A_{Xm}, B_{Xm}, etc., which can readily be tabulated and published. For the present analysis, however, there are 94 Fourier coefficients obtained at each of 130 observatories, and the publication of 12220 Fourier coefficients, although desirable, would be an unnecessary extravagance. The coefficients are available on magnetic tape and a copy will be provided on request. To give some idea of typical results of a Chapman–Miller analysis (in lieu of pages of Fourier coefficients), the results of the analysis of magnetic tides in the northward component X, at Fürstenfeldbruck, near Munich, have been given in figures 3.2–3.4.

Magnetic tides at a particular observatory are functions of time and of astronomical parameters varying slowly with time. Such a two-variable interpretation is the very basis of the Chapman–Miller method of analysis, and can be used as in figures 3.2–3.4 to represent the results of the calculation at a particular observatory. As in the Chapman–Miller calculation, the astronomical parameters are shown as character numbers $0(\equiv 12)$, 1, 2, ..., 12, corresponding to 360° in angular measure. The phase-law tides for $L(2s-2h)$, say, have terms with arguments $nt-(2s-2h)$, or equivalently $nt-wt$ or mt. Thus there are four harmonics $n = 1, 2, 3, 4$ for dependence on time, but only *one* fundamental harmonic for dependence on the astronomical parameters.

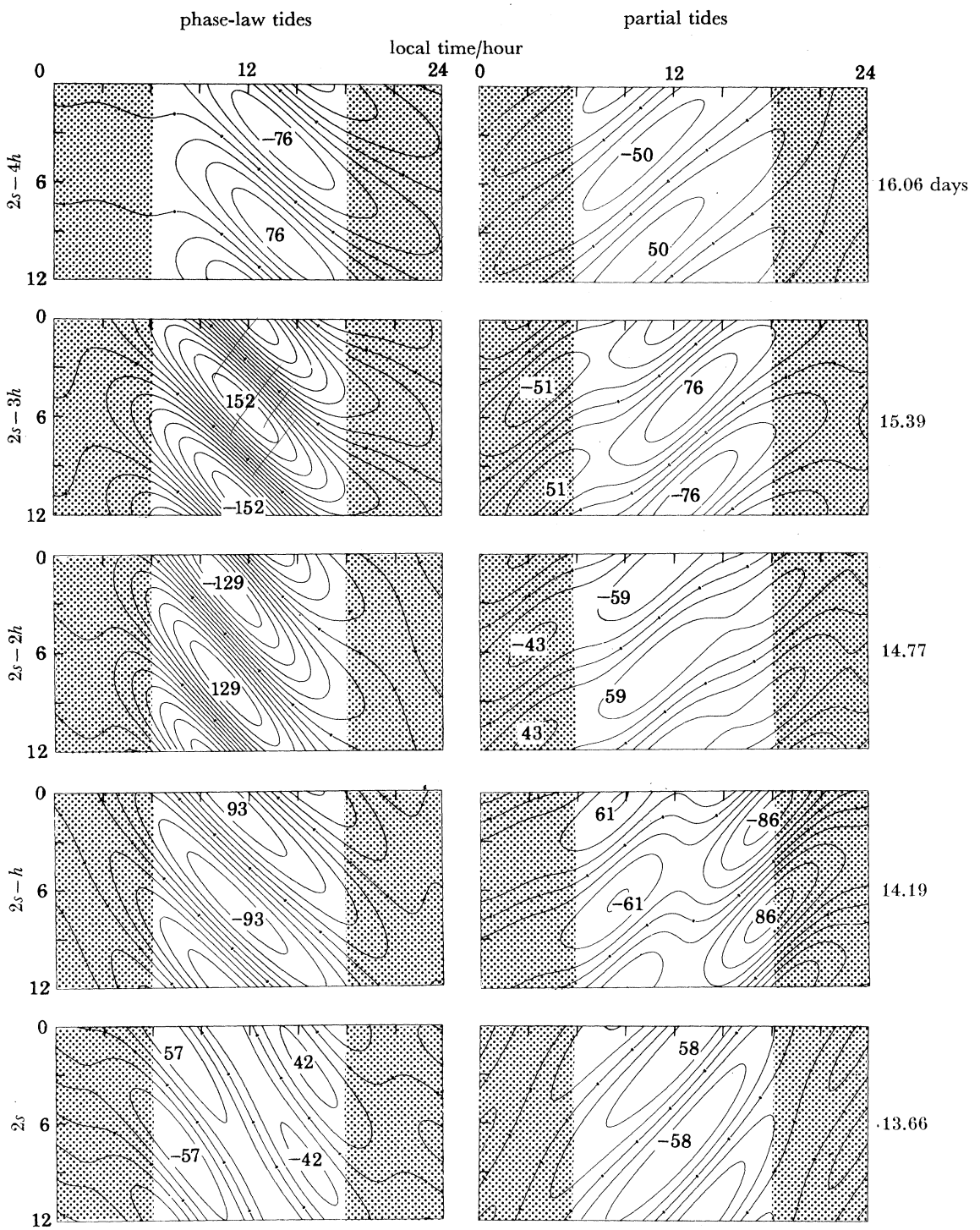

FIGURE 3.2. Fürstenfeldbruck, horizontal component north, lunar semi-diurnal magnetic tides.
Phase-law tides: $L(2s-2h)/10^{-2}\,\mathrm{nT} = \Sigma_{n=1}^{4} a_{Xn} \sin(nt-2s+2h+\alpha_{Xn})$.
Partial tides: $L(2s-2h)/10^{-2}\,\mathrm{nT} = \Sigma_{n=1}^{4} b_{Xn} \sin(nt+2s-2h+\beta_{Xn})$.

In figures 3.2–3.4 contours have been plotted for magnetic tides at intervals of 0.2 nT, while extrema are given in 0.01 nT. Contours for the annual change of S, contoured as $S^{\pm}(h)$ and $S^{\pm}(2h)$, are given at intervals of 0.05 nT, while extrema are given in 0.01 nT. The figures show clearly that the magnetic tides are larger during the day when the ionospheric electrical conductivity is greatest, and vary sinusoidally with respect to the astronomical parameters indicated. The partial tides are generally smaller than the corresponding phase-law tides. They are also generally smaller during the night than during the day but the difference is not as clear-cut as for the phase-law tides. This could be due to the presence of second and third harmonics of the 27-day recurrence tendency in magnetic activity giving long-period variations in ionospheric electrical conductivity, contributing equally to both phase-law and partial magnetic tides.

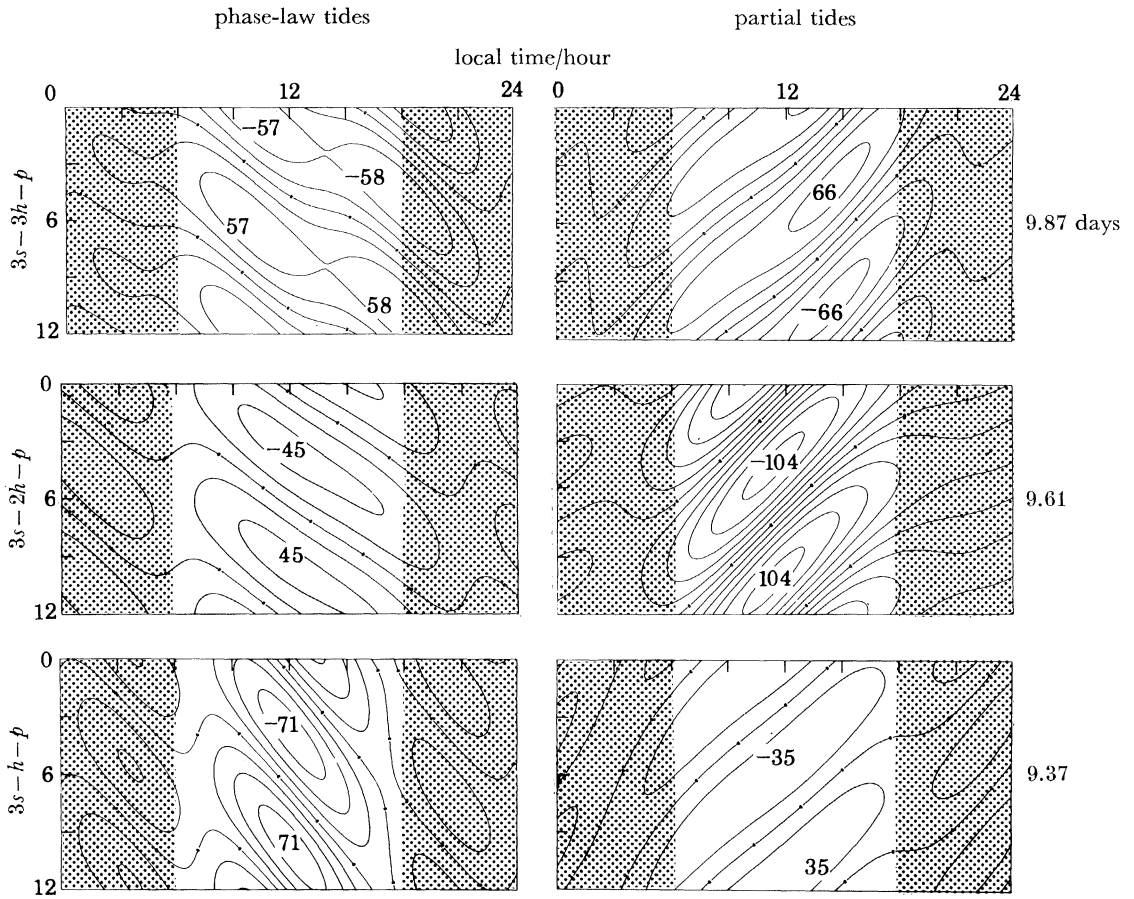

FIGURE 3.3. Fürstenfeldbruck, horizontal component north, elliptic lunar magnetic tides.
Phase-law tides: $L(3s-2h-p)/10^{-2}\,\mathrm{nT} = \Sigma_{n=1}^{4} c_{Xn} \sin(nt-3s+2h+p+\gamma_{Xn})$.
Partial tides: $L(3s-2h-p)/10^{-2}\,\mathrm{nT} = \Sigma_{n=1}^{4} d_{Xn} \sin(nt+3s-2h-p+\delta_{Xn})$.

The partial tide for $L(3s-2h-p)$ is larger than the corresponding phase-law tide, and it is difficult to see such a large partial tide arising through a tidal dynamo mechanism associated with the N_2 tide. A large $L(3s-2h-p)$ partial tide is not confined to Fürstenfeldbruck and, globally, it will be shown that $L(3s-2h-p)$ phase-law tides are about equal to the corresponding partial tides. The effect may be associated with the seven to ten day periodicity found by Shiraki (1974) and Kitamura (1979) in the position of the S_q current focus. Matsushita

(1975) associated movements in the S_q current focus with the direction of the Interplanetary Magnetic Field (I.M.F.), and hence the $L(3s-2h-p)$ partial tide could possibly be of magnetospheric rather than ionospheric origin.

When the Moon is at perigee $s-p = 0$, it is at its point of closest approach to the Earth, and the parameter $3s-2h-p$ reduces to $2s-2h$. The similar forms of the contours for phase-law tides $L(2s-2h)$ and $L(3s-2h-p)$ at Fürstenfeldbruck indicate that when the phase-law tides $L(2s-2h)$ are evaluated for only those days for which the Moon is at or near perigee, the extremum value will be increased from 1.20 to 1.97 nT.

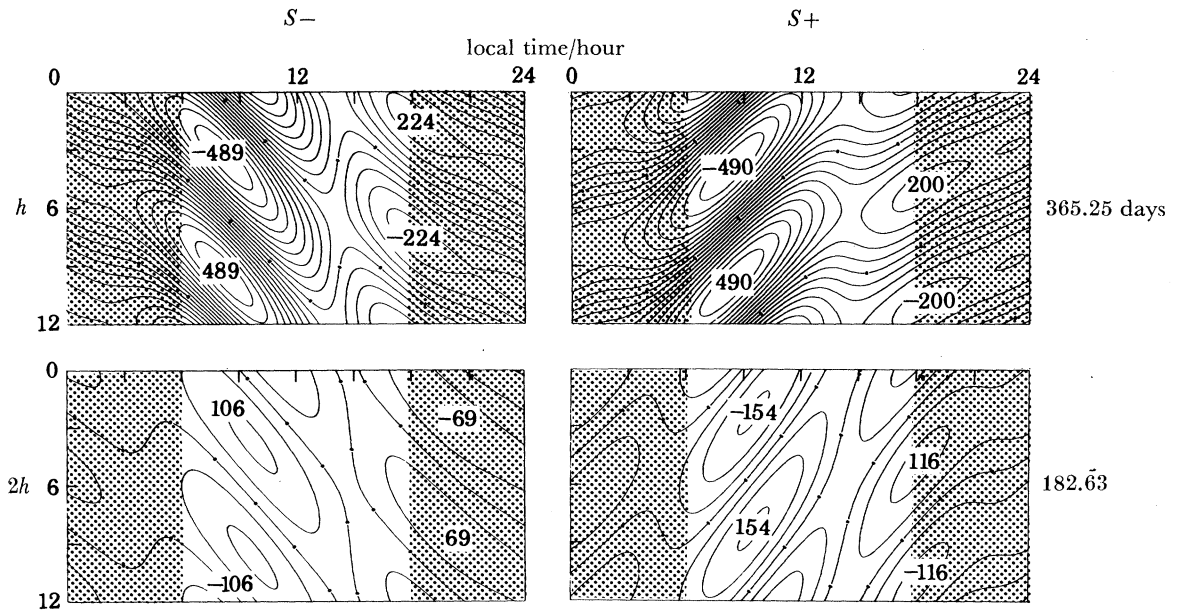

FIGURE 3.4. Fürstenfeldbruck, horizontal component north, annual change of the solar magnetic tide S:
$S^-(h)/10^{-2}\,\mathrm{nT} = \Sigma_{n=1}^{4} e_{Xn} \sin(nt-h+\epsilon_{Xn})$; $S^+(h)/10^{-2}\,\mathrm{nT} = \Sigma_{n=1}^{4} f_{Xn} \sin(nt+h+\phi_{Xn})$;
$S^-(2h)/10^{-2}\,\mathrm{nT} = \Sigma_{n=1}^{4} g_{Xn} \sin(nt-2h+\psi_{Xn})$; $S^+(2h)/10^{-2}\,\mathrm{nT} = \Sigma_{n=1}^{4} h_{Xn} \sin(nt+2h+\chi_{Xn})$.

The dominance of $L(2s-3h)$ over both $L(2s-2h)$ and $L(2s-h)$ provides a simple representation of the complex seasonal change in this component. For example, during mid-January when $h \approx 295°$, corresponding to character number 10, contributions to the lunar magnetic tide at character numbers $2s-2h = 9$, $2s-3h = 11$, $2s-h = 7$ at local noon amount to $129-152-93 = -116$ units (0.01 nT). In mid-July, when $h \approx 115°$, corresponding to character number 4, contributions to the lunar magnetic tide at character numbers $2s-2h = 9$, $2s-3h = 5$, $2s-h = 1$ at local noon amount to $129+152+93 = 374$ units. Thus $L(2s-2h)$ in X estimated at different seasons shows an apparent phase change. With the larger value for X in local summer rather than local winter, the Fürstenfeldbruck observatory is not included amongst those mid-latitude and equatorial observatories that show a global enhancement of lunar magnetic tides in January, as noted by Schlapp & Malin (1979).

From the ionospheric dynamo theory it follows that the magnetic tide $L(2s-h)$ must contain a part deriving from the atmospheric tide O_1. In Doodson's tide-producing potential the amplitude of O_1 is only one-third that of M_2, but, on considering that $L(2s-h)$ contains a contribution from the seasonal change of $L(2s-2h)$ and yet is small, it would seem that either the two components tend to annihilate each other or that both components are in fact small,

i.e. $L(2s-h)$ as a seasonal part of $L(2s-2h)$ is small and as a dynamo tide from O_1 is also small, i.e. the dynamo mechanism is not as efficient for the O_1 diurnal atmospheric tide as it is for the M_2 semi-diurnal atmospheric tide.

The seasonal change of the solar magnetic tide S at Fürstenfeldbruck is given by $S(h)$ and $S(2h)$, corresponding to the annual and semi-annual changes respectively. Both $S(h)$ and $S(2h)$ have large midnight values, which further complicates the problem of the appropriate baseline to be chosen for the analysis of the solar magnetic tide. It would seem that the analyses of Parkinson (1971) and Malin & Gupta (1977) for differences between the mean value and the midnight value of the Fourier series for S could also be repeated for $S(h)$ and $S(2h)$.

The equality of the maxima and minima of $S^+(h)$ and $S^-(h)$ indicates that the origin of these tides is not a dynamo mechanism involving an atmospheric tide such as K_1 of the form $\sin(t+h)$, but rather the annual variation of ionospheric electrical conductivity applied to the expression for the solar magnetic tide S. The occurrence of terms of the form $\sin h$, $\sin 2h$ in conductivity, with $\sin t$ in wind velocity, could give terms $\sin(t\pm h)$, $\sin(t\pm 2h)$.

The contours for $S(h)$ show principal extrema just after mean sunrise at approximately 09h, and smaller extrema just after mean sunset, with a similar pattern for $S(2h)$. This pattern is also found globally, and appears to be associated with the step-function dependence of ionospheric conductivity on sunlight and the variation of sunset and sunrise times throughout the year Thus, the change of the solar magnetic tide with respect to season, as recorded on a magnetogram, will be greatest at 09h and 18h.

The inequalities between the extrema for $S^+(2h)$ and $S^-(2h)$ in the semi-annual change of S indicate the possibility of dynamo action in the ionosphere as their origin. Among the possible mechanisms are the following.

(*a*) The atmospheric tide K_2 of the form $\sin(2t+2h)$, or the semi-annual component of thermally driven winds, interacts with the yearly average electrical conductivity.

(*b*) The tide K_1 of the form $\sin(t+h)$, or the annual component of thermally driven winds, interacts with the annually varying component of electrical conductivity.

(*c*) The yearly mean thermally driven wind interacts with the semi-annual component of electrical conductivity.

Time-dependence of tides in (*a*) and (*b*) would lead to larger $S^+(2h)$ tides than $S^-(2h)$ tides, as actually found. The semi-annual variation of S, namely $S(2h)$ is found to be much smaller than the annual variation $S(h)$, and the possibility of confusion of $S(h)$ and $S(2h)$ at individual observatories is discussed in §5.

4. Spherical harmonic analysis

Spherical harmonic analyses of the sets of Fourier coefficients A_{Xm}, A_{Ym}, A_{Zm} and B_{Xm}, B_{Ym}, B_{Zm}, where m indicates the number of cycles per day, obtained from the observatory data as in equation (21), give scalar potentials A_m and B_m,

$$A_{Xm} = \frac{1}{R}\frac{\partial A_m}{\partial \theta}, \quad A_{Ym} = -\frac{1}{R}\frac{1}{\sin\theta}\frac{\partial A_m}{\partial \phi}, \quad A_{Zm} = \frac{\partial A_m}{\partial r},$$

$$B_{Xm} = \frac{1}{R}\frac{\partial B_m}{\partial \theta}, \quad B_{Ym} = -\frac{1}{R}\frac{1}{\sin\theta}\frac{\partial B_m}{\partial \phi}, \quad B_{Zm} = \frac{\partial B_m}{\partial r},$$

where R is the radius of the Earth. A_m and B_m can be represented as sums of solid spherical harmonics:

$$\left.\begin{aligned} A_m &= R\sum_{j,k}\left\{\left(\frac{R}{r}\right)^{j+1}(A'^k_{jmi}\cos k\phi + A''^k_{jmi}\sin k\phi)\right. \\ &\qquad \left. + \left(\frac{r}{R}\right)^{j}(A'^k_{jme}\cos k\phi + A''^k_{jme}\sin k\phi)\right\} P^k_j(\cos\theta), \\ B_m &= \sum_{j,k}\left\{\left(\frac{R}{r}\right)^{j+1}(B'^k_{jmi}\cos k\phi + B''^k_{jmi}\sin k\phi)\right. \\ &\qquad \left. + \left(\frac{r}{R}\right)^{j}(B'^k_{jme}\cos k\phi + B''^k_{jme}\sin k\phi)\right\} P^k_j(\cos\theta), \end{aligned}\right\} \tag{22}$$

where P^k_j is an associated Legendre function, Schmidt quasi-normalized as is standard practice (see, for example, Chapman & Bartels 1940, ch. 17, §4). (See table 4.1.) The subscripts i and e are used to denote internal and external components, respectively.

The magnetic tidal potential corresponding to the mathematical coefficients A_m, B_m above, is simply $A_m\cos mt + B_m\sin mt$, and if this term is denoted V_m, i.e. if

$$V_m = A_m\cos mt + B_m\sin mt,$$

then the term V_m will have internal and external parts, denoted V_{mi}, V_{me}, respectively, i.e.

$$V_m = V_{mi} + V_{me}.$$

The solid spherical harmonic forms for V_{mi}, V_{me} are given by:

$$V_{mi} = R\sum_{j,k}\left(\frac{R}{r}\right)^{j+1}\{(A'^k_{jmi}\cos k\phi + A''^k_{jmi}\sin k\phi)\cos mt + (B'^k_{jmi}\cos k\phi + B''^k_{jmi}\sin k\phi)\sin mt\}\, P^k_j(\cos\theta), \tag{23}$$

$$V_{me} = R\sum_{j,k}\left(\frac{r}{R}\right)^{j}\{(A'^k_{jme}\cos k\phi + A''^k_{jme}\sin k\phi)\cos mt + (B'^k_{jme}\cos k\phi + B''^k_{jme}\sin k\phi)\sin mt\}\, P^k_j(\cos\theta). \tag{24}$$

By using trigonometrical product formulae, the expression for V_{mi} can be written:

$$V_{mi} = \tfrac{1}{2}R\sum_{j,k}\left(\frac{R}{r}\right)^{j+1}\{(A'^k_{jmi} - B''^k_{jmi})\cos(k\phi+mt) + (A''^k_{jmi} + B'^k_{jmi})\sin(k\phi+mt) + (A'^k_{jmi} + B''^k_{jmi})\cos(k\phi-mt) + (A''^k_{jmi} - B'^k_{jmi})\sin(k\phi-mt)\}\, P^k_j(\cos\theta),$$

and in terms of amplitudes and phase angles:

$$V_{mi} = R\sum_{j,k}\left(\frac{R}{r}\right)^{j+1}\{A^k_{jmi}\cos(k\phi+mt+\alpha^k_{jmi}) + B^k_{jmi}\cos(k\phi-mt+\beta^k_{jmi})\}\, P^k_j(\cos\theta). \tag{25}$$

Similarly for the external component V_{me}:

$$V_{me} = \tfrac{1}{2}R\sum_{j,k}\left(\frac{r}{R}\right)^{j}\{(A'^k_{jme} - B''^k_{jme})\cos(k\phi+mt) + (A''^k_{jme} + B'^k_{jme})\sin(k\phi+mt) + (A'^k_{jme} + B''^k_{jme})\cos(k\phi-mt) + (A''^k_{jme} - B'^k_{jme})\sin(k\phi-mt)\}\, P^k_j(\cos\theta),$$

and in terms of amplitudes and phase angles:

$$V_{me} = R\sum_{j,k}\left(\frac{r}{R}\right)^{j}\{A^k_{jme}\cos(k\phi+mt+\alpha^k_{jme}) + B^k_{jme}\cos(k\phi-mt+\beta^k_{jme})\}\, P^k_j(\cos\theta). \tag{26}$$

The arguments of the various terms in equations (25), (26) must be interpreted as follows:

(*a*) phase-law tides, $k\phi - mt = k\phi - nt + wt$, $k\phi + mt = k\phi + nt - wt$;
(*b*) long-period tides, $k\phi - mt = k\phi - wt$, $k\phi + mt = k\phi + wt$;
(*c*) partial tides, $k\phi - mt = k\phi - nt - wt$, $k\phi + mt = k\phi + nt + wt$;

where wt is to be replaced by the appropriate tidal parameters.

Cosines are used in equations (25), (26) to follow the convention introduced by Chapman (1919).

Arguments of the form $k\phi + mt$, where ϕ is east longitude and t is Universal Time, correspond to westward-moving phenomena, while $k\phi - mt$ is the argument for an eastward-moving effect. The magnetic tides depend indirectly on the Sun, which moves westward, and consequently terms with argument $k\phi + mt$, namely A^k_{jme}, A^k_{jmi}, will dominate those terms with arguments $k\phi - mt$, i.e. B^k_{jme}, B^k_{jmi}. The distinction between eastward and westward movements is important and there is a definite advantage in having the eastward–westward forms of equations (25), (26) as representations for magnetic tides in place of the strictly trigonometric forms given in equations (23), (24). Unfortunately, many authors give only four local time terms P^n_{n+1} in the eastward–westward form of equations (25), (26), and leave many coefficients in the relatively useless form of equations (23), (24).

The phase-law component of the lunar semi-diurnal magnetic tide is given in equation (14) as

$$L(2s - 2h) = \sum_{n=1}^{4} l_n \sin (nt^* - 2s + 2h + \lambda_n), \tag{27}$$

where t^* is local time. Malin (1969, 1970, 1977), Sastri & Rao (1971) and Schlapp (1977) considered the contribution to the magnetic tide from an ocean dynamo in addition to the ionospheric dynamo used to derive equation (17). In the ionospheric dynamo, the time-dependence of the atmospheric tidal movements and ionospheric conductivity lead to the form given in equation (27). For the ocean dynamo, however, the time-dependence of the ocean's tidal movement is that of M_2. The ocean has an electrical conductivity that is independent of local time and is sufficient to allow small electrical currents to flow in response to the e.m.fs generated by dynamo action. The mathematical form of the ocean dynamo magnetic tide will be, after Malin (1970)

$$L_0(2s - 2h) = l_0 \sin (2t^* - 2s + 2h + \lambda_0),$$

and since it consists of only one harmonic, will in general, be non-zero at local midnight $t^* = 0$, having the form

$$l_0 \sin (-2s + 2h + \lambda_0).$$

The corresponding form of the lunar magnetic tide as calculated, by using the model equation (27) above, at local midnight is

$$\sum_{n=1}^{4} l_n \sin (-2s + 2h + \lambda_n),$$

and, consequently, if the ionospheric dynamo with negligible electrical conductivity at local midnight can generate a magnetic tide, then for all values of the parameters $2s - 2h$ the last two expressions are equal:

$$\text{when} \quad 2s - 2h = 0, \quad l_0 \sin \lambda_0 = \sum_{n=1}^{4} l_n \sin \lambda_n,$$

$$\text{when} \quad 2s - 2h = \tfrac{1}{2}\pi, \quad l_0 \cos \lambda_0 = \sum_{n=1}^{4} l_n \cos \lambda_n.$$

A lunar semi-diurnal magnetic tide of purely ionospheric origin can now be constructed:

$$L_{\mathrm{I}}(2s-2h) = \sum_{n=1}^{4} l_{n\mathrm{I}} \sin\,(nt-2s+2h+\lambda_{n\mathrm{I}}),$$

where

$$l_{1\mathrm{I}} = l_1, \quad \lambda_{1\mathrm{I}} = \lambda_1,$$

$$l_{3\mathrm{I}} = l_3, \quad \lambda_{3\mathrm{I}} = \lambda_3,$$

$$l_{4\mathrm{I}} = l_4, \quad \lambda_{4\mathrm{I}} = \lambda_4,$$

$$l_{2\mathrm{I}} \cos\lambda_{2\mathrm{I}} = l_2 \cos\lambda_2 - l_0 \cos\lambda_0 = -l_1 \cos\lambda_1 - l_3 \cos\lambda_3 - l_4 \cos\lambda_4,$$

$$l_{2\mathrm{I}} \sin\lambda_{2\mathrm{I}} = l_2 \sin\lambda_2 - l_0 \sin\lambda_0 = -l_1 \sin\lambda_1 - l_3 \sin\lambda_3 - l_4 \sin\lambda_4.$$

Similarly, because the oceans will also have a tidal component associated with N_2, it is possible to repeat the above calculations with the results of $L(3s-2h-p)$ to derive a lunar magnetic tide $L_{\mathrm{I}}(3s-2h-p)$ also of purely ionospheric origin.

To test the validity and relevance of the assumptions used in the calculation of the ocean effect, it was repeated with results of $L(2s-3h)$, for which it is expected that there is no significant ocean tide, diurnal or semi-diurnal, associated with the parameter $2s-3h$.

Observations of components of the Earth's magnetic field are in fact observations of magnetic induction $\boldsymbol{B}$, whose SI units are teslas (T), the equivalent of 10^4 gauss. Hourly mean values of the Earth's magnetic field are published in nanoteslas, which are about equal to the order of the observational accuracy. The nanotesla, formerly called a gamma, is equivalent to 10^{-5} gauss. Analysis of the hourly mean values leads to an 'external' potential V_{me} given by

$$V_{me} = R \sum_{j,k} \left(\frac{r}{R}\right)^j \{A^k_{jme} \cos\,(k\phi + mt + \alpha^k_{jme})\}\, P^k_j, \tag{28}$$

the mathematical form of which has been chosen so that the units of the evaluated amplitudes A^k_{jme} are those of the observations, i.e. nanoteslas.

A convenient way of presenting the results of the analysis is by means of an equivalent overhead current system flowing in a sphere of radius a. It is essentially a toroidal current system producing the observed poloidal magnetic tide. The current system can be derived from a scalar quantity $\mathscr{R}$ called the current function, originally introduced by Maxwell (1881):

$$\mathscr{R} = -\frac{10R}{4\pi} \sum_{j,k} \left(\frac{a}{R}\right)^j \frac{2j+1}{j+1} \{A^k_{jme} \cos\,(k\phi + mt + \alpha^k_{jme})\}\, P^k_j. \tag{29}$$

When the Earth's radius R is in centimetres and the amplitude A^k_{jme} in gauss, $\mathscr{R}$ is in amperes. Similarly, if R is expressed in kilometres and A^k_{jme} in nanoteslas, then $\mathscr{R}$ is again in amperes. It is a standard procedure to express the current function $\mathscr{R}$ in kiloamperes. For calculation $R = 6371$ km, $a = 6486$ km, and A^k_{jme} is in nanoteslas.

Current function contours provide an effective means of illustrating the geographical form of the external component of the magnetic tide and they have been much used for the solar daily variation S and the lunar magnetic tide $L(2s-2h)$. Attempts have been made to observe the ionospheric current systems directly (Burrows & Hall 1964; Davis *et al.* 1956, 1966). In the present analysis as well as in those of Maeda (1953), Parkinson (1971) and Malin (1973), all of which include non-local time terms, the current functions will vary when 'viewed from the Sun' as the Earth rotates about its axis. Accordingly, the current functions presented in figures 8.1–8.12 include maps of the world.

Current function diagrams are given for 21 magnetic tides, for two different epochs U.T. = 0 h and U.T. = 12 h; and for tidal parameter combinations of 0° and 270°, corresponding to character numbers 12 and 9, respectively. These epochs have been chosen because the coefficients required for each involve either A' and A'', or B' and B'', which, as noted above, are computed separately from either A or B Fourier coefficients from each observatory.

Phase-law tide current functions

Consider the external component of the lunar magnetic tide $L(2s-2h)$, phase-law terms, given by

$$R \sum_{j,k,n} \left(\frac{r}{R}\right)^j \{(A'^k_{jne} \cos k\phi + A''^k_{jne} \sin k\phi) \cos (nt-2s+2h) + (B'^k_{jne} \cos k\phi + B''^k_{jne} \sin k\phi) \sin (nt-2s+2h)\} P^k_j(\cos\theta). \quad (30)$$

When U.T. $t = 0$ h, and $2s-2h = 0°$, corresponding to a $2s-2h$ character number of either zero or 12, and to a lunar phase $s-h = 0°$ or 180°, i.e. new Moon or full Moon, the external potential of phase-law terms in $L(2s-2h)$ becomes

$$R \sum_{j,k} \left(\frac{r}{R}\right)^j \{(A'^k_{j1e}+A'^k_{j2e}+A'^k_{j3e}+A'^k_{j4e}) \cos k\phi + (A''^k_{j1e}+A''^k_{j2e}+A''^k_{j3e}+A''^k_{j4e}) \sin k\phi\} P^k_j(\cos\theta), \quad (31)$$

requiring only coefficients A' and A'', derived from the A_m Fourier coefficients for each observatory.

When U.T. $t = 0$ h, and $2s-2h = 270°$, the $2s-2h$ character number is 9, corresponding to a lunar phase $s-h = 135°$ or 315°, or to a waxing half-Moon or waning half-Moon, respectively. The external potential of $L(2s-2h)$ becomes

$$R \sum_{j,k} \left(\frac{r}{R}\right)^j \{(B'^k_{j1e}+B'^k_{j2e}+B'^k_{j3e}+B'^k_{j4e}) \cos k\phi + (B''^k_{j1e}+B''^k_{j2e}+B''^k_{j3e}+B''^k_{j4e}) \sin k\phi\} P^k_j(\cos\theta), \quad (32)$$

requiring only the coefficients B' and B'', derived from the B_m Fourier coefficients for each observatory. The descriptions of lunar phases indicate the difficulties involved in referring to magnetic tides in anything other than expressions such as $2s-2h$ in angular measure.

To illustrate the non-local time character of the magnetic potentials, a second time t had to be selected, and $t = 12$ h was chosen. The times $t = 6$ h and 18 h, would also show very clearly the non-local time effects; Malin's (1973) diagrams, for example, show an increase in intensity of the S overhead current systems at $t = 6$ h, 18 h. To keep the diagrams to a manageable number, current function contours $t = 0$ h, 12 h only are given. When U.T. $t = 12$ h, and $2s-2h = 0°$, the external part of phase-law tides $L(2s-2h)$ becomes

$$R \sum_{j,k} \left(\frac{r}{R}\right)^j \{(-A'^k_{j1e}+A'^k_{j2e}-A'^k_{j3e}+A'^k_{j4e}) \cos k\phi + (-A''^k_{j1e}+A''^k_{j2e}-A''^k_{j3e}+A''^k_{j4e}) \sin k\phi\} P^k_j(\cos\theta), \quad (33)$$

which uses coefficients A', A'' only, computed from A_m Fourier coefficients.

When U.T. $t = 12$ h, and $2s-2h = 270°$, the external potential of phase-law tides of $L(2s-2h)$ becomes

$$R \sum_{j,k} \left(\frac{r}{R}\right)^j \{(-B'^k_{j1e}+B'^k_{j2e}-B'^k_{j3e}+B'^k_{j4e}) \cos k\phi + (-B''^k_{j1e}+B''^k_{j2e}-B''^k_{j3e}+B''^k_{j4e}) \sin k\phi\} P^k_j(\cos\theta). \quad (34)$$

which uses coefficients B', B'' only, computed from B_m Fourier coefficients.

Partial tide current functions

For the partial tides of $L(2s-2h)$, different combinations of computed coefficients are required for different epochs. Thus the external potential of partial tides of $L(2s-2h)$ has the form

$$R \sum_{j,k,n} \left(\frac{r}{R}\right)^j \{(A'^k_{jne} \cos k\phi + A''^k_{jne} \sin k\phi) \cos (nt+2s-2h) + (B'^k_{jne} \cos k\phi + B''^k_{jne} \sin k\phi) \sin (nt+2s-2h)\} P^k_j(\cos\theta), \quad (35)$$

where the coefficients A', A'', B', B'' of equation (35) are as given in tables for partial tides of $L(2s-2h)$.

When U.T. $t = 0$ h, and $2s-2h = 0°$, the external potential of partial tides of the lunar magnetic tide $L(2s-2h)$ becomes

$$R \sum_{j,k} \left(\frac{r}{R}\right)^j \{(A'^k_{j1e}+A'^k_{j2e}+A'^k_{j3e}+A'^k_{j4e}) \cos k\phi + (A''^k_{j1e}+A''^k_{j2e}+A''^k_{j3e}+A''^k_{j4e}) \sin k\phi\} P^k_j(\cos\theta). \quad (36)$$

When U.T. $t = 0$ h, and $2s-2h = 270°$, the external potential of the partial tides of the lunar magnetic tide $L(2s-2h)$ becomes

$$R \sum_{j,k} \left(\frac{r}{R}\right)^j \{(-B'^k_{j1e}-B'^k_{j2e}-B'^k_{j3e}-B'^k_{j4e}) \cos k\phi + (-B''^k_{j1e}-B''^k_{j2e}-B''^k_{j3e}-B''^k_{j4e}) \sin k\phi\} P^k_j(\cos\theta). \quad (37)$$

When U.T. $t = 12$ h, and $2s-2h = 0°$ this external potential of the partial tides of the lunar magnetic tide $L(2s-2h)$ becomes

$$R \sum_{j,k} \left(\frac{r}{R}\right)^j \{(-A'^k_{j1e}+A'^k_{j2e}-A'^k_{j3e}+A'^k_{j4e}) \cos k\phi + (-A''^k_{j1e}+A''^k_{j2e}-A''^k_{j3e}+A''^k_{j4e}) \sin k\phi\} P^k_j(\cos\theta). \quad (38)$$

When U.T. $t = 12$ h, and $2s-2h = 270°$, the external potential of the partial tides of the lunar magnetic tide $L(2s-2h)$ becomes

$$R \sum_{j,k} \left(\frac{r}{R}\right)^j \{(B'^k_{j1e}-B'^k_{j2e}+B'^k_{j3e}-B'^k_{j4e}) \cos k\phi + (B''^k_{j1e}-B''^k_{j2e}+B''^k_{j3e}-B''^k_{j4e}) \sin k\phi\} P^k_j(\cos\theta). \quad (39)$$

Solar magnetic variation current functions

For the solar magnetic tide, the situation is slightly different, in that there are no astronomical parameters other than U.T. to be concerned with. The external part of the potential for S has the form

$$R \sum_{j,k,n} \left(\frac{r}{R}\right)^j \{(A'^k_{jne} \cos k\phi + A''^k_{jne} \sin k\phi) \cos nt + (B'^k_{jne} \cos k\phi + B''^k_{jne} \sin k\phi) \sin nt\} P^k_j(\cos\theta). \quad (40)$$

Evaluation of the external potential at $t = 0$ h gives:

$$R \sum_{j,k} \left(\frac{r}{R}\right)^j \{(A'^k_{j1e}+A'^k_{j2e}+A'^k_{j3e}+A'^k_{j4e}) \cos k\phi + (A''^k_{j1e}+A''^k_{j2e}+A''^k_{j3e}+A''^k_{j4e}) \sin k\phi\} P^k_j(\cos\theta), \quad (41)$$

involving only A' and A'' terms computed from A_m Fourier coefficients for the solar magnetic tide S.

Evaluation of the external potential at U.T. $t = 12$ h gives

$$R \sum_{j,k} \left(\frac{r}{R}\right)^j \{(-A'^k_{j1e} + A'^k_{j2e} - A'^k_{j3e} + A'^k_{j4e}) \cos k\phi + (-A''^k_{j1e} + A''^k_{j2e} - A''^k_{j3e} + A''^k_{j4e}) \sin k\phi\} P^k_j(\cos\theta), \quad (42)$$

again involving only A' and A'', as computed from A_m Fourier coefficients and, consequently, neither the $t = 0$ h nor $t = 12$ h contoured current functions of S have made use of the results from the analysis of B_m Fourier coefficients. In fact, there is no single instant at which the external potential of S involves only B' and B'' computed from B_m Fourier coefficients.

TABLE 4.1. SCHMIDT QUASI-NORMALIZED ASSOCIATED LEGENDRE FUNCTIONS OF THE FIRST KIND $P^m_n(\cos\theta)$

$P^0_1 = \cos\theta$, $P^1_1 = \sin\theta$, $P^0_2 = \frac{1}{2}(3\cos^2\theta - 1)$
$P^1_2 = \sqrt{3}\sin\theta\cos\theta$, $P^2_2 = \frac{1}{2}\sqrt{3}\sin^2\theta$, $P^0_3 = \frac{1}{2}(5\cos^3\theta - 3\cos\theta)$
$P^1_3 = \frac{1}{4}\sqrt{6}\sin\theta(5\cos^2\theta - 1)$, $P^2_3 = \frac{1}{2}\sqrt{15}\sin^2\theta\cos\theta$
$P^3_3 = \frac{1}{4}\sqrt{10}\sin^3\theta$, $P^0_4 = \frac{1}{8}(35\cos^4\theta - 30\cos^2\theta + 3)$
$P^1_4 = \frac{1}{4}\sqrt{10}\sin\theta(7\cos^3\theta - 3\cos\theta)$, $P^2_4 = \frac{1}{4}\sqrt{5}\sin^2\theta(7\cos^2\theta - 1)$
$P^3_4 = \frac{1}{4}\sqrt{70}\sin^3\theta\cos\theta$, $P^4_4 = \frac{1}{8}\sqrt{35}\sin^4\theta$
$P^0_5 = \frac{1}{8}(63\cos^5\theta - 70\cos^3\theta + 15\cos\theta)$
$P^1_5 = \frac{1}{8}\sqrt{15}\sin\theta(21\cos^4\theta - 14\cos^2\theta + 1)$
$P^2_5 = \frac{1}{4}\sqrt{105}\sin^2\theta(3\cos^3\theta - 4\cos\theta)$, $P^3_5 = \frac{1}{16}\sqrt{70}\sin^3\theta(9\cos^2\theta - 1)$
$P^4_5 = \frac{3}{8}\sqrt{35}\sin^4\theta\cos\theta$, $P^5_5 = \frac{3}{16}\sqrt{14}\sin^5\theta$
$P^0_6 = \frac{1}{16}(231\cos^6\theta - 315\cos^4\theta + 105\cos^2\theta - 5)$
$P^1_6 = \frac{1}{8}\sin\theta(33\cos^5\theta - 30\cos^3\theta + 5\cos\theta)$
$P^2_6 = \frac{1}{32}\sqrt{210}\sin^2\theta(33\cos^4\theta - 18\cos^2\theta + 1)$
$P^3_6 = \frac{1}{16}\sqrt{210}\sin^3\theta(11\cos^3\theta - 3\cos\theta)$
$P^4_6 = \frac{3}{16}\sqrt{7}\sin^4\theta(11\cos^2\theta - 1)$, $P^5_6 = \frac{3}{16}\sqrt{154}\sin^5\theta\cos\theta$
$P^6_6 = \frac{1}{32}\sqrt{462}\sin^6\theta$.

5. DISCUSSION OF RESULTS

Current function contours for the lunar magnetic tide $L(2s-2h)$ are given in figures 8.1*a* and 8.4*a*. Contours in figure 8.1*a* are based on spherical harmonic coefficients in which the $n = 2$ semi-diurnal terms have been derived from the $n = 1, 3, 4$, terms by using the ocean dynamo calculation of Malin (1970). It will be seen that the pattern of figure 5.1*a* is closer to the four-cell pattern commonly associated with the lunar magnetic tide (see, for example, Matsushita 1966), and it appears that there is a smaller current intensity at midnight in the contours freed of the ocean dynamo contribution.

From table 8.4 the dominant semi-diurnal local time terms in $L(2s-2h)$, including contributions from the ocean dynamo, are

$$280\cos(2t^* - 2s + 2h + 240°)P^2_3 + 69\cos(2t^* - 2s + 2h + 79°)P^2_5, \quad (43)$$

where amplitudes are in pT and $t^* = t + \phi$ is the local time. The corresponding terms given in table 8.1, evaluated from the 1, 3, 4 c/d terms, by using the ocean dynamo calculation of Malin (1970), are

$$254\cos(2t^* - 2s + 2h + 261°)P^2_3 + 108\cos(2t^* - 2s + 2h + 79°)P^2_5. \quad (44)$$

The difference of phase angles between the ocean-dynamo-free terms of equation (44) is much closer to 180° than the phase difference for the same terms in equation (43). Note also that the phase of the P_3^2 term in equation (44) is closer to 270° than the phase of the same term in equation (43). The Hough function representation of wind velocity requires the phases of the P_3^2 and P_5^2 coefficients either to be the same or to differ by 180°. The time dependence of the P_3^2 term may be written as $\cos(2\tau + 261°)$ where $\tau = t^* - s + h$ is the local lunar time and will have extrema at $\tau = 50°, 140°, 230°, 320°$, when the observatory is midway between high tide and low tide, and when the ionospheric wind speeds are likely to be greater than at other times.

Expressions corresponding to equations (43), (44) for the lunar elliptic tide $L(3s-2h-p)$ are given in tables 8.8 and 8.1 respectively:

$$61 \cos(2t^* - 3s + 2h + p + 250°) P_3^2 + 17 \cos(2t^* - 3s + 2h + p + 97°) P_5^2, \tag{45}$$

which includes a contribution from the dynamo effect of the N_2 ocean tide, and

$$84 \cos(2t^* - 3s + 2h + p + 284°) P_3^2 + 17 \cos(2t^* - 3s + 2h + p + 109°) P_5^2 \tag{46}$$

with the ocean dynamo contribution removed. Again the phase angle difference in the ocean-dynamo-free terms of equation (46) is closer to 180° than the phase angle difference given by the terms of equation (45) that include an ocean dynamo contribution. The phase angle of the P_3^2 term in equation (46) is closer to 270°. These results show the validity and the importance of applying Malin's ocean dynamo calculation to magnetic tidal results to obtain more useful, physically significant results.

The ocean dynamo effect calculation described above was repeated with results for the seasonal variation $L(2s-3h)$ of the lunar magnetic tide $L(2s-2h)$. Semi-diurnal Fourier coefficients for $L(2s-3h)$ were computed by using the remaining three pairs of Fourier coefficients, on the assumption that the magnetic field should be zero at local midnight. Spherical harmonic coefficients computed from such semi-diurnal coefficients were virtually identical with those from the original semi-diurnal coefficients, thereby providing further evidence of the value of Malin's ocean dynamo calculation and of the validity of the assumptions involved. The diurnal term of the lunar magnetic tide $L(2s-h)$ could possibly contain an ocean dynamo component from the O_1-tide. However, the ocean dynamo calculation was not applied to $L(2s-h)$.

Principal lunar magnetic tide $L(2s-2h)$

The principal external phase-law terms for $L(2s-2h)$ for 1964–65 (quiet Sun) are given in table 8.1, and the corresponding results of Malin (1973) for 1957–60 (active Sun) are given in table 8.14. For comparison the principal terms P_{n+1}^n from both analyses are collected in table 5.1, together with the corresponding local time terms P_{n+3}^n. Both sets of terms are westward moving and antisymmetric about the equator. The terms P_{n+1}^n are well known from the point of view of the ionospheric dynamo theory, while the terms P_{n+3}^n have their origin in the Hough-function structure of atmospheric tides.

The only dynamo theory available that gives theoretical expressions for the 1, 2, 3, 4, c/d local time terms P_2^1, P_3^2, P_4^3, P_5^4, by using a semi-diurnal wind velocity potential P_2^2 and a time-dependent ionospheric conductivity, is that of Chapman (1913). The theory uses conductivity κ in the form

$$\kappa = 1 + 3\cos\chi + 2.25\cos^2\chi = (1 + \tfrac{3}{2}\cos\chi)^2$$

which has the property that the conductivity is never negative. Baker & Martyn (1952) showed that the analysis included equatorial observatories provided that the conductivity was taken to be the height-integrated Cowling conductivity σ_3.

Current theories of wind systems in the upper atmosphere refer to modes of oscillation rather than to individual terms with potential, say, P_2^2. The modal structure comes about when the Coriolis force term is included in the equations of motion for the oscillations of the atmosphere. It is found that eigenfunctions can be determined given by a linear combination of spherical harmonics P_n^m, P_{n+2}^m, P_{n+4}^m, ... Such eigenfunctions are often referred to as Hough functions, after Hough (1898) who first derived them.

TABLE 5.1. PRINCIPAL LOCAL TIME PHASE-LAW TERMS FOR THE LUNAR MAGNETIC TIDE $L(2s-2h)$

	1964–65	1957–60
terms of the form P_{n+1}^n	$174\cos(t^*-2s+2h+86°)P_2^1$	$338\cos(t^*-2s+2h+94°)P_2^1$
	$254\cos(2t^*-2s+2h+261°)P_3^2$	$497\cos(2t^*-2s+2h+273°)P_3^2$
	$134\cos(3t^*-2s+2h+93°)P_4^3$	$189\cos(3t^*-2s+2h+101°)P_4^3$
	$42\cos(4t^*-2s+2h+272°)P_5^4$	$39\cos(4t^*-2s+2h+266°)P_5^4$
terms of the form P_{n+3}^n	$117\cos(t^*-2s+2h+245°)P_4^1$	$151\cos(t^*-2s+2h+270°)P_4^1$
	$180\cos(2t^*-2s+2h+79°)P_5^2$	not calculated
	$61\cos(3t^*-2s+2h+314°)P_6^3$	not calculated

The dominant lunar semi-diurnal wind velocity mode in the ionospheric E region is considered to be the (2, 2) mode (see, for example, Tarpley 1970*a*, *b*). In §6 of the present work this mode is denoted $M_2(2, 2)$, where the prefix M_2 indicates in Darwin's tidal notation the appropriate lunar semi-diurnal gravitational tide. Represented as a sum of Schmidt normalized functions

$$M_2(2, 2) = P_2^2 - 0.374\,713\,P_4^2 + \ldots .$$

It will be seen that P_2^2 is the dominant spherical harmonic in the (2, 2) mode, and hence the dynamo theory of Chapman (1913) is still relevant.

A simplified form of the ionospheric dynamo theory, with the assumption of an axial geomagnetic dipole and uniform ionospheric electrical conductivity, indicates that the magnetic tide associated with the (2, 2) mode will have a potential proportional to $-P_3^2 + 0.1518\,P_5^2$. Thus the P_3^2 lunar semi-diurnal tide expressed as a cosine as in table 5.1 is expected to have a phase of 270°, and similarly the P_5^2 term is expected to be 180° out of phase with P_3^2. From table 5.1, it is found that the phase of the P_3^2 term is 261°, and that the phase angle difference between the P_3^2 and P_5^2 terms is 178°. The amplitude ratio for the terms, $P_5^2/P_3^2 = 108/254 = 0.425$, differs from the ratio 0.1518 indicated by the theory, but as shown in §6, the presence of other tidal modes, in particular the (2, 4) mode, can be inferred and used to give the precise amplitude ratio.

To examine the relevance of the theory of Chapman (1913) for the interpretation of the results of the present analysis, a constant k was taken as a coefficient of proportionality, and in terms of Schmidt-normalized spherical harmonics, the ratios of the four principal local time terms were obtained as shown in table 5.2. With a value 4.142 for the constant k, it will be seen from table 5.2 that Chapman's dynamo theory provides an adequate representation of the principal local time lunar magnetic tides as observed. A minor improvement could be effected by using the expression $1 + 2.7\cos\chi + 2.25\cos^2\chi$ for the ionospheric conductivity. This expression also has the property of never being negative.

It has been noted that the principal local time terms of the form P^n_{n+1} are antisymmetric about the equator. The antisymmetry arises from a combination of the wind velocity potential P^2_2 which is symmetric about the equator and the antisymmetric nature of the vertical components of the Earth's main magnetic field with a potential of the form P^0_1.

TABLE 5.2. APPLICATION OF CHAPMAN'S (1913) DYNAMO THEORY

	P^1_2	P^2_3	P^3_4	P^4_5
theory (Chapman 1913)	$44k$	$51k$	$33k$	$9k$
present results, table 5.1	174	254	134	42
calculated with $k = 4.142$	194	224	145	41

TABLE 5.3. AMPLITUDE RATIOS AND PHASE ANGLE DIFFERENCES FOR PRINCIPAL LUNAR LOCAL TIME TERMS FOR ACTIVE SUN YEARS AGAINST QUIET SUN YEARS

	P^1_2	P^2_3	P^3_4	P^4_5
amplitude ratios (± 0.1)	1.9	2.0	1.4	0.9
phase angle differences/deg	8	12	8	-6

In the absence of a coefficient of P^2_5 for the I.G.Y. years it is not possible to determine the combination of wind velocity modes (2, 2) and (2, 4) for years of high sunspot number for comparison with the known combination for low sunspot number. However, given the weakness of the (2, 4) mode as a generator of magnetic tides and the dominance of the P^2_3 lunar magnetic tide generated principally by the P^2_2 term in the wind velocity potential, it will be assumed for the purpose of the argument that the lunar semi-diurnal wind velocity mode is principally the (2, 2) mode in years of either low or high sunspot number. If the magnitude of the (2, 2) mode were to be increased in years of high sunspot number, then all local time terms P^1_2, P^2_3, P^3_4, P^4_5 in the magnetic tidal potential would increase in the same ratio. It is clear from table 5.3 that they have not all increased in the same ratio. Indeed, one term, P^4_5, remains virtually unchanged in amplitude. It must be concluded, therefore, that there is no change in the intensity of the atmospheric lunar semi-diurnal wind mode (2, 2) through the sunspot cycle.

The lunar atmospheric tide is generated in the lower, denser layers of the atmosphere and propagated upwards with increasing amplitude through the higher layers. It is very sensitive to the rate of decrease of temperature in the mesosphere (corresponding to the ionospheric D region). Belmont *et al.* (1974) have proposed that particle precipitation associated with magnetic activity would produce atomic oxygen by dissociation of O_2. Thus an increase in ozone concentration would occur in the mesosphere leading to higher temperatures, stronger winds and changes in the temperature profile because of increased solar u.v. absorption. The proposal could lead to a variation in lunar atmospheric tides with increasing magnetic activity. However, Callis *et al.* (1979) reported that ozone over selected North American stations increased at a rate of 4–8 % per decade during the 1960s and noted other increases at other stations around the globe. Thus, only a slight increase in ozone concentration has been found, and, given the mechanism of Belmont *et al.* (1974), it would seem reasonable to expect only a slight variation in the intensity of lunar atmospheric tidal winds with increasing magnetic activity. This has already been inferred from the response of the principal local time terms of $L(2s-2h)$ to increased sunspot number.

To derive the different amplitude ratios for the principal local time lunar magnetic tides, the following models of height-integrated ionospheric conductivity are required:

$$\kappa = 1 + 2.7 \cos \chi + 2.25 \cos^2 \chi, \quad \text{low sunspot number,}$$

$$\kappa = 2 + 4.2 \cos \chi + 2.25 \cos^2 \chi, \quad \text{high sunspot number.}$$

A consequence of the different models would be that the relative variation of the lunar magnetic tide with respect to season would be less in years of high sunspot number than in years of low sunspot number.

The phase angle differences in the principal local time terms from years of high sunspot number to years of low sunspot number represent an advance of phase with respect to increasing sunspot number. Given the uncertainty in the level at which the lunar ionospheric dynamo operates, it is difficult to propose a suitable mechanism. It could, for example, be the result of the lack of symmetry with respect to local noon of the recombination rate of electrons and ions at the ionospheric lunar dynamo level, varying with sunspot number.

Chapman's (1919) work included the dynamo theory of magnetic tides and gave theoretical results for what are called partial magnetic tides in the present paper. Chapman (1919) did not evaluate the partial tides directly from the limited observational data available, but, by means of the dynamo theory, showed that the partial tides should be small and that the diurnal partial tides would be the largest of the four daily harmonics. The results given in table 8.4 confirm these predictions. From figures 8.1 and 8.4 the $L(2s-2h)$ lunar magnetic partial tides are seen to be much smaller than the corresponding phase-law tides. They vary considerably from one lunar phase to another. They are largest during daylight. The net current circulation of the partial tides current systems is generally less than one third of the corresponding phase-law system. The separation into internal and external parts of the partial tides has, however, for the more significant terms, been accurate enough to permit the use of the results in induction studies.

The lunar magnetic tide $L(2s-2h)$ includes phase-law and partial tides that are diurnal, zonal and dependent upon U.T. Such terms are listed in table 5.4. The partial tide listed in table 5.4 has the largest amplitude of any of the partial tides listed in table 8.1 for $L(2s-2h)$. The combination of the largest zonal U.T. phase-law and partial tides for 1964–65 in table 5.4 is given by

$$190 \cos (t - 2s + 2h + 152°) P_2^0 + 200 \cos (t + 2s - 2h + 167°) P_1^0,$$

which, to a good approximation, is equal to

$$(190 P_2^0 + 200 P_1^0) \cos (2s - 2h) \cos (t + 160°).$$

The U.T. component indicates an association with the motion of the Earth's magnetic axis about the geographic axis. The factor $\cos (t + 160°)$ is maximized when $t = 200°$ (equivalently U.T. 13.33 h), when the Sun is 20 °W of Greenwich and some 50 °E of the meridian on which the Earth's geomagnetic dipole axis (or the most southerly point of the zone of maximum auroral frequency) lies. The $\cos (2s - 2h)$ term is more likely to be associated with the second 'harmonic' of the 27-day recurrence tendency in sunspot than it is with any effect associated with lunar phase $2s - 2h$. The initial factor $190 P_2^0 + 200 P_1^0$ is greater in northern than in southern latitudes and is greatest at the North Pole.

In addition to the P^n_{n+1} equator-antisymmetric local time terms, the phase-law tides of $L(2s-2h)$ also include some smaller equator-symmetric sectorial terms P^n_n, listed in table 5.5. The sectorial terms, both phase-law and partial, come into phase at local noon, $t^* = 180°$, when the equivalent overhead current system for these terms will have a single focus on the equator, directly beneath the Sun. Sectorial magnetic tides may arise through the interaction of a P^0_1 or $\cos\theta$ component of ionospheric conductivity with the electric fields that give rise to the principal local time terms P^n_{n+1} when the ionospheric conductivity is constant. The combination of sectorial phase-law and partial tides can arise only through a long period $2s-2h$ modulation of the P^0_1 component of ionospheric conductivity, associated more with the second 'harmonic' of the 27-day recurrence tendency in magnetic activity than with the semi-synodic month $2s-2h$.

TABLE 5.4. DIURNAL, ZONAL, U.T.-DEPENDENT TERMS IN $L(2s-2h)$

	1964–65	1957–60
phase-law tides	$91\cos(t-2s+2h+300°)P^0_1$	—
	$190\cos(t-2s+2h+152°)P^0_2$	$132\cos(t-2s+2h+191°)P^0_2$
	—	$102\cos(t-2s+2h+347°)P^0_3$
	$72\cos(t-2s+2h+3°)P^0_4$	—
partial tides	$200\cos(t+2s-2h+167°)P^0_1$	not calculated

TABLE 5.5. SECTORIAL LOCAL TIME PHASE-LAW TERMS IN $L(2s-2h)$

	1964–65	1957–60
phase-law tides	$33\cos(t^*-2s+2h+157°)P^1_1$	$91\cos(t^*-2s+2h+159°)P^1_1$
	$69\cos(2t^*-2s+2h+297°)P^2_2$	$103\cos(2t^*-2s+2h+338°)P^2_2$
	$48\cos(3t^*-2s+2h+120°)P^3_3$	$45\cos(3t^*-2s+2h+112°)P^3_3$
	$9\cos(4t^*-2s+2h+330°)P^4_4$	—
partial tides	$49\cos(t^*+2s-2h+185°)P^1_1$	not calculated
	$46\cos(2t^*+2s-2h+53°)P^2_2$	not calculated
	$25\cos(3t^*+2s-2h+271°)P^3_3$	not calculated
	$15\cos(4t^*+2s-2h+142°)P^4_4$	not calculated

The principal lunar magnetic tide $L(2s-2h)$ includes very significant *non-local* time terms P^n_n, westward moving, sectorial and symmetric about the equator, as listed in table 5.6. With $2\nu = 2s-2h$, $t^* = t+\phi$, $t \equiv$ U.T., the time dependence of the sectorial non-local time terms may be written

$$nt^*-2\nu-t, \quad n = 2, 3, 4, 5, \quad \text{and} \quad nt^*-2\nu+t, \quad n = 1, 2, 3,$$

indicating a U.T. modulation of a local time lunar magnetic tide. The amplitude of the P^1_1 term, being 219 pT, is almost equal to the amplitude of the principal local time term P^2_3, at 254 pT. The sectorial form and symmetry about the equator of the P^n_n non-local time terms cause considerable distortion of the current systems associated with the principal local time terms P^n_{n+1} that are anti-symmetric about the equator.

Although the non-local time terms of table 5.6 show a U.T. variation, they also contain a strong dependence upon local time, because the sectorial terms come into phase in two separate groups at local noon, $t^* = 180°$, as indicated in table 5.7. The two separate groups of terms come into phase at U.T. $t = 98°$ and 278°, corresponding to U.T. 06h30, and 18h30 respectively. At these times the Sun is over the Indian Ocean and over the eastern Pacific Ocean respectively.

The non-local time terms show no consistent increase in amplitude from years of low to years of high sunspot number. The first group of four in table 5.6 shows phase angles retarded by approximately 60°, while the second group of three shows phase angles retarded by approximately 30°. The phase angle differences are much greater than those for the principal local time terms, indicating that they arise through secondary effects, e.g. the influence of land topography and ocean distribution on either the mesospheric temperature profile or wind systems (Chapman & Lindzen 1970, p. 157; Beer 1974, p. 237), or the induction of current systems in the highly conducting oceans.

The partial tides for $L(2s-2h)$ also include significant local time and non-local time terms, as given in table 5.8. Other partial tides given in tables 5.4 and 5.5 are associated with magnetic disturbance rather than any lunar effect.

TABLE 5.6. WESTWARD-MOVING, EQUATOR-SYMMETRIC, NON-LOCAL TIME TERMS IN $L(2s-2h)$

	1964–65	1957–60
of the form P_n^n	$99\cos(2\phi+t-2s+2h+181°)P_2^2$	$120\cos(2\phi+t-2s+2h+127°)P_2^2$
	$159\cos(3\phi+2t-2s+2h+3°)P_3^3$	$132\cos(3\phi+2t-2s+2h+300°)P_3^3$
	$108\cos(4\phi+3t-2s+2h+203°)P_4^4$	$54\cos(4\phi+3t-2s+2h+119°)P_4^4$
	$27\cos(5\phi+4t-2s+2h+32°)P_5^5$	$20\cos(5\phi+4t-2s+2h+316°)P_5^5$
	$219\cos(\phi+2t-2s+2h+167°)P_1^1$	$123\cos(\phi+2t-2s+2h+135°)P_1^1$
	$147\cos(2\phi+3t-2s+2h+345°)P_2^2$	$144\cos(2\phi+3t-2s+2h+303°)P_2^2$
	$35\cos(3\phi+4t-2s+2h+146°)P_3^3$	$24\cos(3\phi+4t-2s+2h+111°)P_3^3$
of the form P_{n+2}^n	$153\cos(\phi+2t-2s+2h+332°)P_3^1$	$198\cos(\phi+2t-2s+2h+40°)P_3^1$

TABLE 5.7. NON-LOCAL TIME TERMS IN $L(2s-2h)$ AT LOCAL NOON

	1964–65	1957–60
of the form P_n^n	$99\cos(-t-2s+2h+181°)P_2^2$	$120\cos(-t-2s+2h+127°)P_2^2$
	$159\cos(-t-2s+2h+183°)P_3^3$	$132\cos(-t-2s+2h+120°)P_3^3$
	$108\cos(-t-2s+2h+203°)P_4^4$	$54\cos(-t-2s+2h+119°)P_4^4$
	$27\cos(-t-2s+2h+212°)P_5^5$	$20\cos(-t-2s+2h+136°)P_5^5$
	$219\cos(t-2s+2h+347°)P_1^1$	$123\cos(t-2s+2h+315°)P_1^1$
	$147\cos(t-2s+2h+345°)P_2^2$	$144\cos(t-2s+2h+303°)P_2^2$
	$35\cos(t-2s+2h+326°)P_3^3$	$24\cos(t-2s+2h+291°)P_3^3$

TABLE 5.8. SIGNIFICANT PARTIAL TIDES IN $L(2s-2h)$

local time terms	$45\cos(t^*+2s-2h+251°)P_2^1$	
	$73\cos(t^*+2s-2h+132°)P_4^1$	
non-local time terms	$61\cos(\phi+2t+2s-2h+184°)P_1^1$	(westward-moving)
	$22\cos(2\phi+3t+2s-2h+13°)P_2^2$	(westward-moving)
	$62\cos(\phi-t+2s-2h+233°)P_2^1$	(eastward-moving)

The solar magnetic tide S

The principal external terms for the solar magnetic tide for 1964–65 are given in table 8.10, and the corresponding results given by Malin (1973) for 1957–60 are given in table 8.14. For comparison the principal terms are collected together in table 5.9. As with the lunar magnetic tide the principal local time terms are of the form P_{n+1}^n and are antisymmetric about the equator. They are accompanied by local time terms of the form P_{n+3}^n which are also antisymmetric about the equator and which have their origin in the Hough-function structure of atmospheric tides.

The phase angles of the principal terms in the solar and lunar magnetic tides give an indication of their thermal and gravitational origins respectively. The modulus of the principal solar term, $\cos(t^*+19°)P_2^1$, is greatest when $t^* = 161°$ or 341°, the day-time value occurring about one hour before local noon ($t^* = 180°$). The four principal local-time solar magnetic tidal terms will be in phase at approximately $t^* = 180°$. The times of maxima and minima refer to the time when the overhead current system focus crosses the local meridian. The principal lunar term, $\cos(2\tau+261°)P_3^2$, has extrema at local lunar times $\tau = 50°, 140°, 230°, 329°$, occurring when the local meridian is midway between the maxima and minima of the M_2 tide-producing potential. The lunar term can be compared with the tide $0.93\cos(2\tau+202°)$ km found by Appleton & Weekes (1939) in the movement of the height of the lower boundary of the E region.

TABLE 5.9. PRINCIPAL LOCAL TIME TERMS OF EXTERNAL ORIGIN FOR THE SOLAR MAGNETIC TIDE S

	1964–65	1957–60
terms of the form P^n_{n+1}	$6146\cos(t^*+19°)P_2^1$	$12213\cos(t^*+7°)P_2^1$
	$2922\cos(2t^*+197°)P_3^2$	$5953\cos(2t^*+182°)P_3^2$
	$1168\cos(3t^*+33°)P_4^3$	$2144\cos(3t^*+16°)P_4^3$
	$238\cos(4t^*+215°)P_5^4$	$420\cos(4t^*+209°)P_5^4$
terms of the form P^n_{n+3}	$1100\cos(t^*+161°)P_4^1$	$2928\cos(t^*+160°)P_4^1$
	$281\cos(2t^*+47°)P_5^2$	not calculated
	$67\cos(3t^*+224°)P_6^3$	not calculated

TABLE 5.10. AMPLITUDE RATIOS FOR PRINCIPAL LOCAL TIME TERMS OF SOLAR AND LUNAR MAGNETIC TIDES

solar S/lunar $L(2s-2h)$	P_2^1	P_3^2	P_4^3	P_5^4
low sunspot number	35 ± 2	11.5 ± 0.5	8.7 ± 0.3	5.7 ± 0.4
high sunspot number	36 ± 2	12.0 ± 0.5	11.3 ± 0.5	10.8 ± 0.9

TABLE 5.11. AMPLITUDE RATIOS AND PHASE ANGLE DIFFERENCES FOR THE SOLAR MAGNETIC TIDE FOR ACTIVE SUN YEARS AGAINST QUIET SUN YEARS

solar magnetic tide S	P_2^1	P_3^2	P_4^3	P_5^4
amplitude ratios (±0.5)	1.99	2.04	1.84	1.76
phase angle differences/deg	−12	−15	−17	−6

The dominance of the diurnal P_2^1 local time term in the solar magnetic tide and the semi-diurnal P_3^2 local lunar time term in the lunar magnetic tide gives the basic current system configurations shown in figures 8.1 and 8.10. Both systems are antisymmetric about the equator; the P_2^1 solar term gives single foci in both the Northern and Southern Hemispheres, while the P_3^2 lunar term gives pairs of foci in both the Northern and Southern Hemispheres.

Amplitude ratios of the principal local time terms of the solar and lunar magnetic tides are given in table 5.10. The amplitude ratios show that the diurnal term P_2^1 in the solar magnetic tide S is three times as great as would be expected if the solar atmospheric tide were of the form P_2^2 only, or in terms of present day theory, an atmospheric tidal mode of the form (2, 2). Chapman's (1913) dynamo theory shows that a P_1^1 atmospheric tidal potential gives rise to a magnetic tide of the form P_2^1 with only minor contributions to the terms P_3^2 and P_4^3. It is clear therefore that the wind velocity producing the solar magnetic tide has a scalar potential consisting of a combination of terms P_1^1 and P_2^2.

Amplitude ratios and phase angle differences for the solar magnetic tide for active Sun years against quiet Sun years are given in table 5.11. The different response of the amplitude of the P_5^4 local time term in lunar and solar magnetic tides to the sunspot cycle, together with the phase angle advance of the local time terms of the lunar magnetic tide and the retardation of phase of the corresponding solar local time terms, and the different variation of solar and lunar magnetic tides with respect to season (yet to be discussed), has led to the conclusion that solar and lunar magnetic tides are produced at different levels in the ionosphere (see, for example, Gupta & Malin 1972; Malin *et al.* 1975).

Chapman & Bartels (1940, p. 762) noted that if the solar and lunar ionospheric wind velocities were in the same ratio to one another at all heights, then their magnetic effects would be in the same ratio, and the solar and lunar magnetic tides would be produced in the same conducting layer. They concluded that the differences between the solar and lunar magnetic tides implied that there were important variations in the relative magnitudes of the solar and lunar ionospheric winds at different heights. The height-dependent structure of atmospheric tides inferred by Chapman & Bartels is associated with the modal structure of wind velocity. The theory of atmospheric tides (see, for example, Chapman & Lindzen 1970) indicates that the variation with height of the different modes depends upon the variation of temperature with height, particularly in the mesosphere (i.e. the D region). For the modes that generate magnetic tides, Kato (1966*a*, *b*) and Lindzen (1966) suggested a diurnal negative mode denoted (1, −2) for the solar magnetic daily variation, while Stening (1969) and Tarpley (1970*a*, *b*) found that the (1, −2) mode produced a solar magnetic tide very similar to the observed magnetic tide. It will be shown in §6, however, that a further mode, the (1, 1) mode, is required to give the phase angle differences of 180° observed between the local time terms P_2^1 and P_4^1 in the solar magnetic tide.

The different modal structure of the solar and lunar semi-diurnal tides is indicated in the present analysis by the ratio of the local time terms P_5^2/P_3^2. The ratio is $281/2922 = 0.096$ for the solar magnetic tide and $108/254 = 0.425$ for the lunar magnetic tide. This considerable difference is discussed further in terms of (2, 2) and (2, 4) modes in §6. In the absence of coefficients for P_5^2 for solar and lunar semi-diurnal magnetic tides in the analysis of Malin (1973), it is not possible to determine if the modal combination of tides (2, 2) and (2, 4) changes with respect to sunspot activity or increases in some direct proportion. It is therefore essential that the coefficient of the local time, semi-diurnal magnetic tide P_5^2 term for both solar and lunar magnetic tides be determined.

Because the P_5^4 diurnal local time term for the solar magnetic tide increases by a factor of 1.76 throughout the sunspot cycle, it cannot be inferred, with the assumption that the (2, 2) mode remains the dominant wind velocity mode, that the thermally generated ionospheric wind velocities producing the solar magnetic tide remain invariant. In fact they could increase by up to a factor of 1.76 throughout the sunspot cycle. Matsushita (1967) considered the rates of increase of solar and lunar magnetic tides with respect to the electron density N_e, and sunspot number S:

$$N_e = 1.24 \times 10^{-4} (4.38 \times 10^{-3} S + 3.04)^2,$$

and concluded that the wind velocities increased by a factor of 1.4. Given such an increase, the electrical conductivity of the relevant ionospheric dynamo layer need not increase by a factor of 2.0 as required for the lunar magnetic tides, but only by a factor of approximately 1.6. Thus it would appear that the conductivity of the solar dynamo region is less sensitive to

changes in sunspot number than the lunar dynamo region. The opposite conclusion is obtained if it is assumed that the solar *and* lunar ionospheric winds are independent of sunspot number (see, for example, Malin 1971).

The following models of height-integrated ionospheric conductivity are required for use in Chapman's dynamo theory to produce the observed solar and lunar magnetic tides:

$$\text{low sunspot number,} \quad \kappa = 1.0 + 2.7\cos\chi + 2.25\cos^2\chi \quad \text{(solar, lunar),}$$

$$\text{high sunspot number,} \quad \kappa = 1.6 + 4.2\cos\chi + 3.60\cos^2\chi \quad \text{(solar),}$$

$$\kappa = 2.0 + 4.2\cos\chi + 2.25\cos^2\chi \quad \text{(lunar).}$$

Depending upon the value chosen for the amplification factor for ionospheric solar winds, somewhere between 1.00 and 1.76, the conductivity model to be used for the solar magnetic tide at high sunspot number could vary from $1.0 + 2.7\cos\chi + 2.25\cos^2\chi$ to $1.8 + 4.9\cos\chi + 3.96\cos^2\chi$.

TABLE 5.12. EQUATOR-SYMMETRIC LOCAL TIME TERMS IN THE SOLAR MAGNETIC TIDE

	1964–65	1957–60
terms of the form P^n_{n+1}	$1019\cos(t^*+81°)P^1_1$	$1359\cos(t^*+55°)P^1_1$
	$1102\cos(2t^*+268°)P^2_2$	$1307\cos(2t^*+254°)P^2_2$
	$457\cos(3t^*+104°)P^3_3$	$521\cos(3t^*+93°)P^3_3$
	$174\cos(4t^*+302°)P^4_4$	$171\cos(4t^*+267°)P^4_4$
terms of the form P^n_{n+2}	$454\cos(t^*+202°)P^1_3$	$1071\cos(t^*+171°)P^1_3$
	$371\cos(2t^*+256°)P^2_4$	$696\cos(2t^*+347°)P^2_4$
	$201\cos(3t^*+69°)P^3_5$	$146\cos(3t^*+119°)P^3_5$
	$102\cos(4t^*+258°)P^4_6$	$143\cos(4t^*+276°)P^4_6$

TABLE 5.13. RESPONSE OF EQUATOR-SYMMETRIC LOCAL TIME TERMS IN THE SOLAR MAGNETIC TIDE TO INCREASED SUNSPOT NUMBER

solar magnetic tide S	P^1_1	P^2_2	P^3_3	P^4_4
amplitude ratios (± 0.3)	1.4	1.2	1.2	1.0
phase angle differences/deg	−23	−14	−11	−35

The solar magnetic tide includes a group of local time terms that are symmetric about the equator. Some are sectorial of the form P^n_n, and there is a corresponding group of terms of the form P^n_{n+2}, as listed in table 5.12. These terms differ from the corresponding terms in the lunar magnetic tide $L(2s-2h)$ by the presence of the P^n_{n+2} terms, an amplification factor of only 1.3 with respect to sunspot number for the larger terms P^1_1 and P^2_2, and the retardation of phase with increasing sunspot number. The corresponding terms in $L(2s-2h)$ show a greater amplification and a phase angle advance with increasing sunspot number.

The occurrence of equator-symmetric local time terms in pairs P^n_n and P^n_{n+2} in the solar magnetic tide, points strongly to a dynamo origin with atmospheric wind velocity potential of the form $\cos t^* P^1_2$ and $\cos 2t^* P^2_3$, or in terms of modes $(1, -1)$ and $(2, 3)$. The $(2, 3)$ mode has been considered by Schieldge *et al.* (1973). The response of the terms to increase in sunspot number is summarized in table 5.13. The constancy of the P^4_4 term indicates that the responsible dominant mode of the semi-diurnal wind system remains invariant throughout the sunspot cycle. It also follows that the $\cos^2\chi$ term in any model for ionospheric conductivity in the region in which this term is produced, remains constant.

The equator-symmetric local time terms in S are responsible for the difference in magnitude and skewing of the equivalent overhead current foci, shown in figure 8.10. Because the equator-symmetric terms depend upon local time t^*, they cannot arise through the interaction of the principal local time terms with fixed geographic features such as the oceans, or the topographic features of the land distribution such as mountain ranges.

The day-to-day variability of S_q (the solar magnetic tide S observed on magnetically quiet days) has been associated with changes in position of the overhead current foci (Hasegawa 1960; Matsushita 1960), and also with the skewing of the current system foci (Brown & Williams 1969; Brown 1975). Hasegawa (1960) indicated that, with regard to the day-to-day changes of the S_q field, the presence of the symmetrical terms P_1^1, P_3^1, P_2^2 in the magnetic tidal potential was 'conspicuous', and that the corresponding wind system was a wind circulation across the equator. The wind system considered here, with potentials of the form P_2^1, P_3^2, consists of a movement southward across the equator during the morning, northward in the afternoon, with easterly motion in northern mid-latitudes and westerly motion in southern mid-latitudes during daylight. In terms of modes, the diurnal modes are (1, −1), (1, −3), and the semi-diurnal modes are (2, 3) and (2, 5).

The combination of two dominant local time equator-symmetric terms

$$1019 \cos (t^* + 81°) P_1^1 + 1102 \cos (2t^* + 268°) P_2^2$$

has extrema occurring at local times $t^* = 130°$, 240°, corresponding to 09 h 00 and 16 h 00 respectively. At these times the foci of the equivalent overhead current system for the two terms will cross the observatory's meridian. If day-to-day variability of S_q is associated with the equator-symmetric local time terms, then day-to-day variability can be expected to be greatest at these times.

The solar magnetic tide also contains a substantial, zonal, diurnal U.T.-dependent term $979 \cos (t + 106°) P_2^0$ during I.Q.S.Y. years and $3443 \cos (t + 85°) P_2^0$ during I.G.Y. years. The threefold increase of amplitude with sunspot number is greater than the twofold increase already noted for the principal local time terms. The 1964–65 term is greatest at U.T. $t = 254°$ (17 h), when the Sun is 74 °W of Greenwich, virtually on the meridian containing the Earth's geomagnetic dipole axis. The zonal form and the U.T. dependence indicate that the origin of the term is in the modulation of current systems associated with magnetic disturbance due to the non-alignment of the geographic and geomagnetic axes, i.e. the zonal U.T. term occurring in the solar magnetic tide does not derive from the ionospheric dynamo mechanism that gives the principal local time terms. Zonal, diurnal, U.T.-dependent terms in S are listed in table 5.14.

TABLE 5.14. DIURNAL, ZONAL, U.T.-DEPENDENT TERMS IN S

1964–65	1957–60
$1405 \cos (t + 12°) P_1^0$	$1904 \cos (t + 288°) P_1^0$
$979 \cos (t + 106°) P_2^0$	$3443 \cos (t + 85°) P_2^0$
—	$2154 \cos (t + 277°) P_3^0$

The solar magnetic tide also includes very significant non-local time terms which are westward moving and symmetric about the equator. The terms are given in table 5.15. One group is sectorial and a smaller group is of the form P_{n+2}^n; both groups are symmetric about the equator. The amplitudes, apart from the P_4^4 term, show a marked increase with sunspot number,

whereas the corresponding non-local time terms in $L(2s-2h)$ show, if anything, a slight decrease (see table 5.6). The amplitudes of the sectorial non-local time terms in the solar magnetic tide are only about one tenth of the principal local time terms P^n_{n+1}, and hence do not distort the equivalent overhead current systems. From tables 5.1 and 5.6, the corresponding sectorial non-local time terms in the lunar magnetic tide are almost equal to the principal local time terms and hence the equivalent overhead current system is distorted considerably. The phase angles of both the solar and lunar non-local time terms are retarded with increasing sunspot number.

TABLE 5.15. WESTWARD-MOVING, EQUATOR-SYMMETRIC, NON-LOCAL TIME TERMS IN S

	1964–65	1957–60
of the form P^n_n	$784\cos(2\phi+t+95°)P^2_2$	$2939\cos(2\phi+t+65°)P^2_2$
	$397\cos(3\phi+2t+288°)P^3_3$	$1050\cos(3\phi+2t+238°)P^3_3$
	$209\cos(4\phi+3t+125°)P^4_4$	$166\cos(4\phi+3t+45°)P^4_4$
	$1414\cos(\phi+2t+99°)P^1_1$	$2499\cos(\phi+2t+58°)P^1_1$
	$214\cos(2\phi+3t+220°)P^2_2$	$700\cos(2\phi+3t+196°)P^2_2$
	—	$182\cos(3\phi+4t+12°)P^3_3$
of the form P^n_{n+2}	$394\cos(\phi+2t+249°)P^1_3$	$999\cos(\phi+2t+301°)P^1_3$
	$120\cos(2\phi+3t+81°)P^2_4$	$326\cos(2\phi+3t+43°)P^2_4$

TABLE 5.16. NON-LOCAL TIME TERMS IN S AT LOCAL NOON

	1964–65	1957–60
of the form P^n_n	$784\cos(-t+95°)P^2_2$	$2939\cos(-t+65°)P^2_2$
	$397\cos(-t+108°)P^3_3$	$1050\cos(-t+58°)P^3_3$
	$209\cos(-t+125°)P^4_4$	$166\cos(-t+45°)P^4_4$
	$1414\cos(t+279°)P^1_1$	$2499\cos(t+238°)P^1_1$
	$214\cos(t+220°)P^2_2$	$700\cos(t+196°)P^2_2$
	not significant	$182\cos(t+192°)P^3_3$

In terms of local time t^*, the time dependence of the non-local time terms can be written as

$$nt^*-t,\quad n=2,3,4,\quad \text{and}\quad nt^*+t,\quad n=1,2,3,$$

indicating a U.T. modulation of a local time solar magnetic tide. The solar non-local time terms have similar phase angles at local noon, $t^*=180°$, as shown in table 5.1. The two groups of terms indicated in table 5.16 come into phase at about U.T. $t=90°$ and 270°, i.e. at about the same U.T. as the corresponding $L(2s-2h)$ terms. The different amplitudes of the solar and lunar non-local time terms relative to the corresponding local time terms indicate different causes and exclude, for example, the direct influence of the high electrical conductivity of the oceans on the induced current systems (see, for example, Rikitake 1961, Roden 1964). The solar non-local time terms may be associated with the variation in atmospheric water vapour in the upper atmosphere over land and ocean areas, and the combination of P^1_1 and P^1_3 non-local time terms suggests a U.T. modulation of the dynamo mechanism associated with a combination of (1, 1) and (1, −2) modes of wind velocity. The lunar non-local time terms may be associated with a U.T.-dependent variation in the transmissivity of the mesosphere to the lunar atmospheric tide.

The dominantly sectorial nature of the non-local time terms in both the solar and lunar magnetic tides indicates the great value of the separation of groups of observatories into longitudinal sectors (see, for example, Matsushita & Maeda 1965*a*, *b*).

Annual variation of the lunar magnetic tide

The lunar magnetic tides $L(2s-3h)$ and $L(2s-h)$ represent the seasonal variation of the principal lunar magnetic tide $L(2s-2h)$ that proceeds at the rate of 1 c/y. The numerical results are given in tables 8.3 and 8.5, and the equivalent overhead current system contours are given in figures 8.3 and 8.5. The contours show the strongly sectorial nature of the phase-law tides for both $L(2s-3h)$ and $L(2s-h)$, with current foci for $L(2s-3h)$ being greater than those for $L(2s-h)$. Comparison of figures 8.1 and 8.3, shows that the current foci for $L(2s-3h)$ are almost equal to those for the principal lunar magnetic tide $L(2s-2h)$. The partial tides for both $L(2s-3h)$ and $L(2s-h)$ are much smaller than the corresponding phase-law tides, with the equivalent overhead current system of the $L(2s-h)$ partial tide showing very pronounced U.T. dependence.

TABLE 5.17. PRINCIPAL LOCAL TIME PHASE-LAW TERMS FOR $L(2s-3h)$ AND $L(2s-h)$; SEASONAL CHANGE OF THE LUNAR MAGNETIC TIDE $L(2s-2h)$

	$L(2s-3h)$	$L(2s-h)$
terms of the form P_n^n	$218\cos(t^*-2s+3h+317°)P_1^1$	$212\cos(t^*-2s+h+226°)P_1^1$
	$268\cos(2t^*-2s+3h+148°)P_2^2$	$151\cos(2t^*-2s+h+26°)P_2^2$
	$122\cos(3t^*-2s+3h+334°)P_3^3$	$78\cos(3t^*-2s+h+226°)P_3^3$
	$11\cos(4t^*-2s+3h+148°)P_4^4$	—
terms of the form P_{n+2}^n	$62\cos(t^*-2s+3h+85°)P_3^1$	$43\cos(t^*-2s+h+250°)P_3^1$
	$67\cos(2t^*-2s+3h+162°)P_4^2$	$54\cos(2t^*-2s+h+30°)P_4^2$
	$41\cos(3t^*-2s+3h+333°)P_5^3$	$26\cos(3t^*-2s+h+205°)P_5^3$
	$10\cos(4t^*-2s+3h+190°)P_6^4$	$9\cos(4t^*-2s+h+19°)P_6^4$

Results for $L(2s-3h)$ and $L(2s-h)$ for the I.G.Y. years are not available, and hence the results required in the following discussion are collected together, as in table 5.17. The principal local time terms in both $L(2s-3h)$ and $L(2s-h)$ are sectorial, of the form P_n^n, and they are accompanied by terms of the form P_{n+2}^2. Both terms P_n^n and P_{n+2}^n are symmetric about the equator. The pairs of terms P_{n+1}^n and P_{n+3}^n occurring in the principal solar and lunar magnetic tides are derived from pairs of terms P_2^2 and P_4^2 in the wind velocity potential associated with the Hough-function modal structure of upper atmosphere winds. However, the same pairs of terms P_n^n and P_{n+2}^n occurring in the seasonal change $L(2s-3h)$ and $L(2s-h)$ of the principal lunar magnetic tide derive from just one term P_2^2 in the tidal potential and therefore cannot be used to evaluate combinations of modes for the upper atmosphere wind systems.

For $L(2s-h)$ the terms P_n^n, P_{n+2}^n could both derive from an ionospheric dynamo involving the wind velocity potential P_2^1 associated with the diurnal atmospheric tide O_1. It is not possible to separate the lunar dynamo effect of the atmospheric tide O_1 from the seasonal variation of the principal lunar magnetic tide $L(2s-2h)$.

With $2s-2h$ denoted by 2ν, the principal diurnal local time terms in $L(2s-3h)$ and $L(2s-h)$ can be added to give

$$\begin{aligned}
&218\cos(t^*-2\nu+h+317°)P_1^1+212\cos(t^*-2\nu-h+226°)P_1^1\\
&\quad=6\cos(t^*-2\nu+2°)P_1^1, && \text{when } h=45°, \text{ about 8 May},\\
&\quad=430\cos(t^*-2\nu+92°)P_1^1, && \text{when } h=135°, \text{ about 7 August},\\
&\quad=6\cos(t^*-2\nu+182°)P_1^1, && \text{when } h=225°, \text{ about 6 November},\\
&\quad=430\cos(t^*-2\nu+272°)P_1^1, && \text{when } h=315°, \text{ about 6 February}.
\end{aligned}$$

Comparison with the diurnal term in $L(2s-2h)$, namely $174\cos(t^*-2\nu+86°)P_2^1$, shows the considerable variation of the diurnal term for $L(2s-2h)$ if evaluated for specific seasons. If the amplitude only is considered of the combination of the diurnal local time term in $L(2s-2h)$ and the four seasonal contributions listed, then the annual variation might be incorrectly interpreted as a semi-annual variation with maxima in early August and early February. Stening & Winch (1979) and Campbell (1980) have 'rectified' the annual variation by just this means, and described it as semi-annual. If the phase angle of the combination of terms is not included, either explicitly or in a vectorgram, then the relatively small semi-annual variation in the lunar magnetic tides may be grossly overestimated.

With $2s-2h$ still denoted by 2ν, the principal semi-diurnal local time terms have the form

$$\begin{aligned}
&268\cos(2t^*-2\nu+h+148°)P_2^2+151\cos(2t^*-2\nu-h+26°)P_2^2\\
&\quad=117\cos(2t^*-2\nu+177°)P_2^2, \quad \text{when } h=29°, \text{ about 22 April.}\\
&\quad=419\cos(2t^*-2\nu+267°)P_2^2, \quad \text{when } h=119°, \text{ about 21 July,}\\
&\quad=117\cos(2t^*-2\nu+357°)P_2^2, \quad \text{when } h=209°, \text{ about 21 October,}\\
&\quad=419\cos(2t^*-2\nu+87°)P_2^2, \quad \text{when } h=299°, \text{ about 20 January.}
\end{aligned}$$

These terms are to be compared with the semi-diurnal term in $L(2s-2h)$, given by $254\times\cos(2t^*-2\nu+261°)P_3^2$, showing that the variation with season of this semi-diurnal term is quite large.

Sectorial terms P_n^n in the magnetic potential give no variation in the X component of the magnetic field at the equator, while tesseral terms P_{n+1}^n give no variation in the Y and Z components of the magnetic field at the equator. Consequently, at equatorial observatories, variations in the X component are associated with the tesseral terms P_{n+1}^n in $L(2s-2h)$ and will show little or no seasonal variation, while lunar variations in the Y and Z components are associated with the sectorial terms P_n^n in $L(2s-3h)$ and $L(2s-h)$, and as such will have an almost zero annual average.

It has been shown that combinations of diurnal and semi-diurnal terms from $L(2s-3h)$, $L(2s-2h)$ and $L(2s-h)$ lead to large lunar magnetic tides in northern summer in late July and early August. Such magnetic tides are larger than might be expected to arise purely from seasonal variations in ionospheric conductivity which would tend to give northern summer extrema in late June. A possible mechanism appears to be seasonal variation in the transmissivity of the mesosphere to the lunar atmospheric tide, proposed by Geller (1970).

The seasonal variation of the solar and lunar magnetic tides is traditionally discussed in terms of solstitial or equinoctial semi-differences, e.g. results based on the summer–winter semi-difference or spring–autumn semi-difference, for Northern-Hemisphere seasons. By using the following values for h in relation to season,

$$\begin{aligned}
&h=0°, \quad \text{northern spring,} \quad h=90°, \quad \text{northern summer,}\\
&h=180°, \quad \text{northern autumn,} \quad h=270°, \quad \text{northern winter,}
\end{aligned}$$

it is possible to derive the appropriate semi-differences. The local time coefficients of P_1^1 and P_2^2 in $L(2s-3h)$ and $L(2s-h)$ give the following expression for the spring–autumn semi-difference:

$$301\cos(t^*-2s+2h+272°)P_1^1+371\cos(2t^*-2s+2h+78°)P_2^2;$$

and for the summer–winter semi-difference:

$$307\cos(t^*-2s+2h+91°)P_1^1+400\cos(2t^*-2s+2h+259°)P_2^2.$$

The result given by Chapman (1919) for the summer–winter semi-difference is

$$419 \cos (t^* - 2s + 2h + 72°) P_1^1 + 512 \cos (2t^* - 2s + 2h + 257°) P_2^2,$$

so that the different descriptions are seen to be in good agreement.

Another group of local time terms, antisymmetric about the equator, appears in both the phase-law and partial tides of $L(2s-3h)$ and $L(2s-h)$. Significant terms of the form P_{n+1}^n and P_{n+3}^n occur, but only those of the form P_{n+1}^n are given in table 5.18. The dominant term in this particular group is a partial tide, $101 \cos (t^* + 2s - h + 298°) P_2^1$. The presence of significant partial tides indicates that this group of terms is not associated with seasonal or annual changes of the lunar magnetic tide $L(2s-2h)$, but rather with long-period variations in ionospheric conductivity corresponding roughly to the second 'harmonic' of the 27-day sunspot recurrence tendency. If the long-period variation in ionospheric conductivity has P_1^0 or $\cos\theta$ dependence,

TABLE 5.18. EQUATOR-ANTISYMMETRIC LOCAL TIME TERMS IN $L(2s-3h)$ AND $L(2s-h)$

	$L(2s-3h)$	$L(2s-h)$
	terms of the form P_{n+1}^n	
phase-law	—	$41 \cos (t^* - 2s + h + 319°) P_2^1$
	$35 \cos (2t^* - 2s + 3h + 29°) P_3^2$	$73 \cos (2t^* - 2s + h + 218°) P_3^2$
	$16 \cos (3t^* - 2s + 3h + 238°) P_4^3$	$61 \cos (3t^* - 2s + h + 45°) P_4^3$
	—	$32 \cos (4t^* - 2s + h + 224°) P_5^4$
partial	$44 \cos (t^* + 2s - 3h + 230°) P_2^1$	$101 \cos (t^* + 2s - h + 298°) P_2^1$
	$42 \cos (2t^* + 2s - 3h + 177°) P_3^2$	$28 \cos (2t^* + 2s - h + 263°) P_3^2$
	$15 \cos (3t^* + 2s - 3h + 37°) P_4^3$	$22 \cos (3t^* + 2s - h + 33°) P_4^3$
	$8 \cos (47^* + 2s - 3h + 282°) P_5^4$	$14 \cos (4t^* + 2s - h + 219°) P_5^4$

TABLE 5.19. ZONAL PHASE-LAW AND PARTIAL TIDES IN $L(2s-3h)$, $L(2s-h)$

	$L(2s-3h)$	$L(2s-h)$
phase-law	$216 \cos (t - 2s + 3h + 153°) P_1^0$	$162 \cos (t - 2s + h + 92°) P_1^0$
	$132 \cos (t - 2s + 3h + 209°) P_2^0$	—
	$41 \cos (t - 2s + 3h + 340°) P_4^0$	$50 \cos (t - 2s + h + 298°) P_4^0$
partial	—	$112 \cos (t + 2s - h + 18°) P_2^0$
	$47 \cos (t + 2s - 3h + 207°) P_4^0$	$55 \cos (t + 2s - h + 307°) P_4^0$

then the equator-antisymmetric group of terms could be generated by interaction with the electric fields that produce the equator-symmetric local time terms P_n^n in the solar magnetic tide when the ionospheric conductivity is constant. From equation (6) the periods associated with $2s-3h$ and $2s-h$ are 15.4 and 14.2 days, respectively, which places them on the longer-period side of the 13.5-day period forming the second 'harmonic' of the 27-day sunspot recurrence tendency. Similar equator-antisymmetric local time terms, P_{n+1}^n and P_{n+3}^n, occur in the seasonal change of the elliptic magnetic tide, with amplitudes about the same as the corresponding terms in $L(2s-3h)$ and $L(2s-h)$. This adds support to the theory and indicates that the source is not the seasonal variation of ionospheric conductivity.

The lunar magnetic tides $L(2s-3h)$ and $L(2s-h)$ contain zonal, U.T.-dependent phase-law and partial tides, listed in table 5.19. The amplitudes of these terms are roughly half the amplitudes of the principal local time terms of $L(2s-2h)$ in table 5.1, and about equal to the amplitudes of the zonal U.T.-dependent terms of $L(2s-2h)$ in table 5.4. The zonal U.T.-dependence of such terms indicates an origin in the daily variation of a zonal overhead current

system associated with magnetic disturbance brought about by the diurnal motion of the geomagnetic axis about the geographic axis. The parameters $2s-3h$ and $2s-h$ indicates a further modulation near the second 'harmonic' of the 27-day recurrence tendency, with periods of 15.4 and 14.2 days.

Sectorial, westward-moving non-local time terms in $L(2s-3h)$ and $L(2s-h)$ are given in table 5.20. At local noon when $t^* = 180°$, each group is seen to have about the same phase angle. The $L(2s-3h)$ group and the $L(2s-h)$ group come into phase at $h = 116°$ and 296° corresponding to about 20 July and 18 January respectively. At $h = 116°$ the combination becomes

$$314 \cos(\phi+2t-2\nu+171°)P_1^1+134\cos(\phi+2t-2\nu+172°)P_2^2,$$

to be compared with the principal local time terms written as

$$174\cos(2\phi+2t-2\nu+86°)P_2^1+254\cos(2\phi+2t-2\nu+261°)P_3^2.$$

Clearly, the principal lunar magnetic tide $L(2s-2h)$ will be greatly modified by the presence of the sectorial, westward-moving, non-local time terms in $L(2s-3h)$ and $L(2s-h)$. In the absence of corresponding terms for the I.G.Y. years, no definite conclusion can be drawn as to the origin of these terms, but a U.T.-variation of the transmissivity of the mesosphere to the lunar atmospheric tide over ocean areas could be considered.

TABLE 5.20. SECTORIAL, WESTWARD-MOVING, NON-LOCAL TIME PHASE-LAW TIDES IN $L(2s-3h)$ and $L(2s-h)$

$L(2s-3h)$	$L(2s-h)$
$203\cos(\phi+2t-2s+3h+235°)P_1^1$	$111\cos(\phi+2t-2s+h+106°)P_1^1$
$77\cos(2\phi+3t-2s+3h+56°)P_2^2$	$57\cos(2\phi+3t-2s+h+277°)P_2^2$
$17\cos(3\phi+4t-2s+3h+266°)P_3^3$	$25\cos(3\phi+4t-2s+h+109°)P_3^3$
terms evaluated at local noon $t^* = t+\phi = 180°$	
$203\cos(t-2\nu+h+55°)P_1^1$	$111\cos(t-2\nu-h+286°)P_1^1$
$77\cos(t-2\nu+h+56°)P_2^2$	$57\cos(t-2\nu-h+277°)P_2^2$
$17\cos(t-2\nu+h+86°)P_3^3$	$25\cos(t-2\nu-h+239°)P_3^3$

TABLE 5.21. SECTORIAL, LOCAL TIME PARTIAL TIDES IN $L(2s-3h)$ AND $L(2s-h)$

$L(2s-3h)$	$L(2s-h)$
—	$144\cos(t^*+2s-h+191°)P_1^1$
$37\cos(2t^*+2s-3h+80°)P_2^2$	$42\cos(2t^*+2s-h+97°)P_2^2$
$24\cos(3t^*+2s-3h+262°)P_3^3$	—
$11\cos(4t^*+2s-3h+152°)P_4^4$	—

Apart from the partial tides given in tables 5.18, 5.19, both $L(2s-3h)$ and $L(2s-h)$ contain a group of sectorial, local-time partial tides, and these are listed in table 5.21. The amplitudes of these terms are much smaller than the corresponding phase-law terms given in table 5.17 (being the principal terms in both $L(2s-3h)$ and $L(2s-h)$).

Semi-annual variation of the lunar magnetic tide

The semi-annual variation of the principal lunar magnetic tide $L(2s-2h)$ is given by two magnetic tides $L(2s-4h)$ and $L(2s)$. The numerical results are given in tables 8.2, 8.6, and the equivalent overhead current function contours in figures 8.2, 8.6. The contours show that

the phase-law tides are greater during daylight, with phase-law tides for $L(2s)$ being greater than those of $L(2s-4h)$. Contours for $L(2s-4h)$ phase-law tides show an interesting transition from sectorial to zonal form at different values of $2s-4h$. Partial tides for both $L(2s-4h)$ and $L(2s)$ have smaller current foci than the corresponding phase-law tides.

The dominant terms in $L(2s-4h)$ and $L(2s)$ are not local time terms, but the zonal, diurnal, U.T.-dependent terms listed in table 5.22. The external potential $rP_1^0 = r\cos\theta = z$ corresponds to the potential of a uniform magnetic field parallel to the z-axis. The equivalent current system is either a ring current in the Earth's equatorial plane flowing well above the ionosphere, or a P_1^0 equivalent overhead current system flowing at a level either in or above the ionosphere.

TABLE 5.22. ZONAL, DIURNAL, U.T.-DEPENDENT TERMS IN PHASE-LAW AND PARTIAL TIDES OF $L(2s-4h)$ AND $L(2s)$

	$L(2s-4h)$	$L(2s)$
phase-law	$309\cos(t-2s+4h+285°)P_1^0$	$86\cos(t-2s+149°)P_1^0$
partial	$67\cos(t+2s-4h+117°)P_1^0$	$113\cos(t+2s+166°)P_1^0$

TABLE 5.23. LOCAL TIME PHASE-LAW AND PARTIAL TIDES IN $L(2s-4h)$ AND $L(2s)$

	$L(2s-4h)$	$L(2s)$
	equator-symmetric sectorial terms, P_n^n	
phase-law	$42\cos(t^*-2s+4h+224°)P_1^1$	$127\cos(t^*-2s+62°)P_1^1$
	$59\cos(2t^*-2s+4h+165°)P_2^2$	$136\cos(2t^*-2s+259°)P_2^2$
	$31\cos(3t^*-2s+4h+17°)P_3^3$	$88\cos(3t^*-2s+87°)P_3^3$
	$7\cos(4t^*-2s+4h+194°)P_4^4$	$22\cos(4t^*-2s+295°)P_4^4$
partial	$84\cos(t^*+2s-4h+190°)P_1^1$	$140\cos(t^*+2s+333°)P_1^1$
	$27\cos(2t^*+2s-4h+325°)P_2^2$	$71\cos(2t^*+2s+249°)P_2^2$
	$13\cos(3t^*+2s-4h+131°)P_3^3$	$42\cos(3t^*+2s+85°)P_3^3$
	$8\cos(4t^*+2s-4h+251°)P_4^4$	$8\cos(4t^*+2s+312°)P_4^4$
	equator-antisymmetric tesseral terms P_{n+1}^n	
phase-law	$55\cos(t^*-2s+4h+260°)P_2^1$	$87\cos(t^*-2s+32°)P_2^1$
	$23\cos(2t^*-2s+4h+60°)P_3^2$	$34\cos(2t^*-2s+238°)P_3^2$
	—	$31\cos(3t^*-2s+78°)P_4^3$
	$9\cos(4t^*-2s+4h+233°)P_5^4$	$16\cos(4t^*-2s+261°)P_5^4$
partial	$86\cos(t^*+2s-4h+178°)P_2^1$	$121\cos(t^*+2s+286°)P_2^1$
	$33\cos(2t^*+2s-4h+162°)P_3^2$	$14\cos(2t^*+2s+326°)P_3^2$
	—	$12\cos(3t^*+2s+63°)P_4^3$

Both systems are associated with magnetic disturbance, and the diurnal U.T.-variation of the terms of table 5.22 indicates a possible origin in the modulation of such steady current systems by the movement of the geomagnetic axis about the geographic axis. The presence of phase-law and partial tides with parameters $2s-4h$ and $2s$ indicates further long-period modulation at 16.1 and 13.7 days, associated with the second 'harmonic' of the 27-day recurrence tendency in sunspot number and magnetic activity.

The magnetic tides dealt with so far have included local time terms of the form P_n^n and P_{n+1}^n, with one group being considerably greater than the other. In the magnetic tides $L(2s-4h)$ and $L(2s)$, both groups are present, but with approximately the same amplitudes. The largest terms in each group are the partial tides, P_1^1 in the P_n^n group and P_2^1 in the P_{n+1}^n group.

From equation (6) the periods associated with $2s-4h$ and $2s$ are 16.0641 and 13.6608 days, respectively. If the long-period modulation of ionospheric conductivity at about the second 'harmonic' of the 27-day recurrence tendency is equator-antisymmetric, for example P_1^0 in form, then it is suggested that the P_n^n local time terms in $L(2s-4h)$ and $L(2s)$ arise through the interaction of the long-period modulation of ionospheric conductivity with the electric fields that produce the principal local time terms P_{n+1}^n in the solar magnetic tide when the ionospheric conductivity is constant. The P_n^n phase-law and partial tides given in table 5.23 are comparable in magnitude with the P_n^n phase-law and partial tides in $L(2s-2h)$ given in table 5.5.

The semi-annual variation in ionospheric conductivity is associated with the $\cos^2\chi$ term, and is therefore symmetric about the equator. It is suggested that the P_{n+1}^n local time terms in $L(2s-4h)$ and $L(2s)$ in table 5.23 arise through interaction of the semi-annual variation in ionospheric conductivity with the electric fields that produce the principal local time terms P_{n+1}^n in the lunar magnetic tide $L(2s-2h)$ when the ionospheric conductivity is constant.

It will now be shown that at certain lunar phases at three-monthly intervals, the contributions from the diurnal local time phase-law and partial tide terms in $L(2s-4h)$ and $L(2s)$ will dominate the diurnal local time term in the principal lunar magnetic tide $L(2s-2h)$.

The diurnal, local time, phase-law P_n^n terms in $L(2s-4h)$ and $L(2s)$, with $2\nu = 2s-2h$, are

$$\begin{aligned} &42\cos(t^*-2\nu+2h+224^\circ)P_1^1+127\cos(t^*-2\nu-2h+62^\circ)P_1^1 \\ &\quad=169\cos(t^*-2\nu+324^\circ)P_1^1 \quad \text{when} \quad h=50^\circ,\ 230^\circ, \\ &\quad=169\cos(t^*-2\nu+144^\circ)P_1^1 \quad \text{when} \quad h=140^\circ,\ 320^\circ. \end{aligned}$$

The corresponding partial tides in $L(2s-4h)$ and $L(2s)$ are

$$\begin{aligned} &84\cos(t^*+2\nu-2h+190^\circ)P_1^1+140\cos(t^*+2\nu+2h+333^\circ)P_1^1 \\ &\quad=224\cos(t^*+2\nu+72^\circ)P_1^1 \quad \text{when} \quad h=54^\circ,\ 234^\circ. \\ &\quad=224\cos(t^*+2\nu+252^\circ)P_1^1 \quad \text{when} \quad h=144^\circ,\ 324^\circ, \end{aligned}$$

and it is of interest that the epochs at which the partial tides come into phase are almost identical with the epochs for the corresponding phase-law tides. When $h = 144^\circ$ or 324°, about 15 August or 15 February respectively, the phase-law and partial tide diurnal terms come into phase at certain lunar ages:

$$\begin{aligned} &169\cos(t^*-2\nu+144^\circ)P_1^1+224\cos(t^*+2\nu+252^\circ)P_1^1 \\ &\quad=393\cos(t^*+18^\circ)P_1^1 \quad \text{when} \quad \nu=63^\circ,\ 243^\circ, \\ &\quad=393\cos(t^*+198^\circ)P_1^1 \quad \text{when} \quad \nu=153^\circ,\ 333^\circ. \end{aligned}$$

Similar expressions, differing in phase by 180°, are obtained when $h = 54^\circ$ or 234°, about 15 May and 15 November.

The diurnal, local time, phase-law P_{n+1}^n terms in $L(2s-4h)$ and $L(2s)$ are

$$\begin{aligned} &55\cos(t^*-2\nu+2h+260^\circ)P_2^1+87\cos(t^*-2\nu-2h+32^\circ)P_2^1 \\ &\quad=142\cos(t^*-2\nu+326^\circ)P_2^1 \quad \text{when} \quad h=33^\circ,\ 213^\circ, \\ &\quad=142\cos(t^*-2\nu+146^\circ)P_2^1 \quad \text{when} \quad h=123^\circ,\ 303^\circ, \end{aligned}$$

which can be compared with the principal diurnal term in $L(2s-2h)$, namely

$$174\cos(t^*-2\nu+86^\circ)P_2^1.$$

The diurnal, local time, partial tide P^n_{n+1} terms in $L(2s-4h)$ and $L(2s)$ are

$$\begin{aligned} &86\cos(t^*+2\nu-2h+178^\circ)P^1_2+121\cos(t^*+2\nu+2h+286^\circ)P^1_2 \\ &\quad=207\cos(t^*+2\nu+52^\circ)P^1_2 \quad \text{when} \quad h=63^\circ, 243^\circ, \\ &\quad=207\cos(t^*+2\nu+232^\circ)P^1_2 \quad \text{when} \quad h=153^\circ, 333^\circ, \end{aligned}$$

and the partial tides come into phase some 30°, i.e. about one month, after the phase-law tides. At an intermediate value of h, then, i.e. when $h = 138^\circ$ or 318°, corresponding to about 9 August or 9 February, respectively, the phase-law and partial tides have the form

$$\begin{aligned} &124\cos(t^*-2\nu+138^\circ)P^1_2+180\cos(t^*+2\nu+226^\circ)P^1_2 \\ &\quad=304\cos(t^*+2^\circ)P^1_2 \quad \text{when} \quad \nu=68^\circ, 248^\circ, \\ &\quad=304\cos(t^*+182^\circ)P^1_2 \quad \text{when} \quad \nu=158^\circ, 338^\circ. \end{aligned}$$

At $\nu = 68^\circ$ or 248°, the principal local time diurnal term in $L(2s-2h)$ becomes $174\times\cos(t^*+320^\circ)P^1_2$, with phase only 40° behind that of the $L(2s-4h)$ and $L(2s)$ combination just given. The influence of $L(2s-4h)$ and $L(2s)$ is therefore shown to be significant at certain combinations of season and lunar phase.

TABLE 5.24. WESTWARD-MOVING, SECTORIAL NON-LOCAL TIME TERMS IN $L(2s-4h)$ AND $L(2s)$

	$L(2s-4h)$	$L(2s)$
phase-law	$65\cos(2\phi+t-2s+4h+134^\circ)P^2_2$	$51\cos(2\phi+t-2s+213^\circ)P^2_2$
	$65\cos(3\phi+2t-2s+4h+329^\circ)P^3_3$	$63\cos(3\phi+2t-2s+21^\circ)P^3_3$
	$38\cos(4\phi+3t-2s+4h+178^\circ)P^4_4$	$33\cos(4\phi+3t-2s+175^\circ)P^4_4$
partial	$112\cos(\phi+2t+2s-4h+87^\circ)P^1_1$	$83\cos(\phi+2t+2s+299^\circ)P^1_1$

The magnetic tides $L(2s-4h)$ and $L(2s)$ also include a group of non-local time, westward-moving, sectorial terms, listed in table 5.24. It is of interest that this same type of term has appeared in all magnetic tides examined so far, e.g. $L(2s-2h)$, S, $L(2s-3h)$, $L(2s-4h)$, $L(2s)$. It is also of interest that they all have the property that they come into phase at local noon $t^* = t+\phi = 180^\circ$.

Seasonal change of the solar magnetic tide

The seasonal change of the solar magnetic tide S is denoted by $S(h)$, and the results presented here in table 8.11 have been obtained by using the same computer program as used for the various lunar magnetic tides, with lunar parameters replaced by h. The nomenclature 'phase-law' and 'partial' tide, as applied to the lunar magnetic tides, is not appropriate for the seasonal change of the solar magnetic tide, and hence terms with arguments $k\phi+nt+h+\alpha$ have been denoted $S^+(h)$, those with arguments $k\phi+nt-h+\alpha$ denoted $S^-(h)$. The dominant terms in $S^-(h)$, $S^+(h)$, are equator-symmetric local time terms, being either sectorial P^n_n or of the form P^n_{n+2}; they are listed in table 5.25.

According to Chapman's (1919) dynamo theory, the local time terms P^n_n, P^n_{n+2} in the seasonal variation of the solar magnetic tide arise through the seasonal modulation of ionospheric conductivity, as indicated by the $\cos\chi$ term, interacting with the P^1_1 and P^2_2 wind velocity potentials, or equivalently with the (1, −2) and (2, 2) wind velocity modes. The inequalities in the amplitudes of the corresponding $S^-(h)$ and $S^+(h)$ terms can be attributed to the dynamo

effect of the atmospheric tides K_1 and P_1 with potentials $\sin(t^*+h)P_2^1$ and $\sin(t^*-h)P_2^1$ respectively.

The principal diurnal local time terms in the seasonal variation of S have the form

$$\begin{aligned} 2535\cos(t^*-h+117^\circ)P_1^1 &+ 2894\cos(t^*+h+276^\circ)P_1^1 \\ &= 359\cos(t^*+286^\circ)P_1^1 \quad \text{when} \quad h = 10^\circ, \text{ about 2 April}, \\ &= 5429\cos(t^*+16^\circ)P_1^1 \quad \text{when} \quad h = 100^\circ, \text{ about 2 July}, \\ &= 359\cos(t^*+106^\circ)P_1^1 \quad \text{when} \quad h = 190^\circ, \text{ about 2 October}, \\ &= 5429\cos(t^*+196^\circ)P_1^1 \quad \text{when} \quad h = 280^\circ, \text{ about 1 January}. \end{aligned}$$

Comparison of these expressions with the yearly average solar diurnal magnetic tide given by $6146\cos(t^*+19^\circ)P_2^1$ shows that the greatest amplitudes for the diurnal component of the solar magnetic tide in Northern-Hemisphere observatories will occur when $h = 100^\circ$, on about 2 July. Greatest amplitudes for the corresponding lunar magnetic tidal terms occur about a month later when $h = 135^\circ$ on 7 August.

TABLE 5.25. LOCAL TIME TERMS IN THE SEASONAL CHANGE OF THE SOLAR MAGNETIC TIDE

	$S^-(h)$	$S^+(h)$
sectorial terms P_n^n	$2535\cos(t^*-h+117^\circ)P_1^1$	$2894\cos(t^*+h+276^\circ)P_1^1$
	$923\cos(2t^*-h+11^\circ)P_2^2$	$1325\cos(2t^*+h+147^\circ)P_2^2$
	$543\cos(3t^*-h+224^\circ)P_3^3$	$711\cos(3t^*+h+354^\circ)P_3^3$
	$248\cos(4t^*-h+95^\circ)P_4^4$	$206\cos(4t^*+h+214^\circ)P_4^4$
equator-symmetric terms P_{n+2}^n	$907\cos(t^*-h+74^\circ)P_3^1$	$585\cos(t^*+h+260^\circ)P_3^1$
	$383\cos(2t^*-h+269^\circ)P_4^2$	$309\cos(2t^*+h+107^\circ)P_4^2$

It should be noted that if the amplitude and phase angle of the solar diurnal magnetic tide are determined at any observatory for different seasons, consideration of the amplitude only would be equivalent to rectification of the seasonal change, which might then be incorrectly interpreted as a semi-annual variation.

The principal semi-diurnal local time terms in $S^-(h)$, $S^+(h)$ have the form

$$\begin{aligned} 923\cos(2t^*-h+11^\circ)P_2^2 &+ 1325\cos(2t^*+h+147^\circ)P_2^2 \\ &= 402\cos(2t^*+169^\circ)P_2^2 \quad \text{when} \quad h = 22^\circ, \text{ about 15 April}, \\ &= 2248\cos(2t^*+259^\circ)P_2^2 \quad \text{when} \quad h = 112^\circ, \text{ about 15 July}, \\ &= 402\cos(2t^*+349^\circ)P_2^2 \quad \text{when} \quad h = 202^\circ, \text{ about 15 October}, \\ &= 2248\cos(2t^*+79^\circ)P_2^2 \quad \text{when} \quad h = 292^\circ, \text{ about 15 January}. \end{aligned}$$

These terms are to be compared with the yearly average solar semi-diurnal term $2922\times\cos(2t^*+197^\circ)P_3^2$. In contrast to the corresponding lunar magnetic tides, the solar yearly average diurnal term is greater than the seasonal terms.

Largest values for seasonal contributions of the solar daily variation diurnal and semi-diurnal terms occur at $h = 100^\circ$, 112°, respectively, corresponding to 2 and 15 July. Seasonal contributions to the lunar magnetic tides by diurnal and semi-diurnal terms have maxima at $h = 135^\circ$, 119°, respectively, corresponding to 7 August and 21 July. The later dates for the lunar variation extrema indicate a dependence upon atmospheric temperature rather than directly upon solar zenith angle χ.

Chapman (1919) and Chapman *et al.* (1971) drew attention to the fact that the relative seasonal change in the lunar magnetic tide is approximately three times the relative seasonal change in the solar magnetic tide. The same result can be seen in the present work. By considering the diurnal terms only, the seasonal change of the solar magnetic tide is

$$6146\cos(t^*+19°)P_2^1+\{2535\cos(t^*-h+117°)+2894\cos(t^*+h+276°)\}P_1^1,$$

and of the lunar magnetic tide

$$174\cos(t^*-2\nu+86°)P_2^1+\{218\cos(t^*-2\nu+h+317°)+212\cos(t^*-2\nu-h+226°)\}P_1^1$$

TABLE 5.26. EQUATOR-ANTISYMMETRIC LOCAL TIME TERMS IN THE SEASONAL CHANGE OF S

	$S^-(h)$	$S^+(h)$
terms of the form P^n_{n+1}	$274\cos(t^*-h+267°)P_2^1$	$328\cos(t^*+h+25°)P_2^1$
	—	$113\cos(2t^*+h+150°)P_3^2$
	$82\cos(3t^*-h+338°)P_4^3$	$41\cos(3t^*+h+55°)P_4^3$
	$110\cos(4t^*-h+174°)P_5^4$	$91\cos(4t^*+h+311°)P_5^4$
terms of the form P^n_{n+3}	$103\cos(t^*-h+298°)P_4^1$	$124\cos(t^*+h+127°)P_4^1$
	$77\cos(2t^*-h+300°)P_5^2$	$66\cos(2t^*+h+150°)P_5^2$
	$68\cos(3t^*-h+102°)P_6^3$	$41\cos(3t^*+h+254°)P_6^3$

These diurnal expressions confirm that the seasonal variation of the lunar magnetic tide is greater than that of the solar magnetic tide. The semi-diurnal terms also give the same result. It follows, therefore, that the wind systems producing the solar and lunar magnetic tides do not have the same ratio to one another at all heights at all times throughout the year. This serves to emphasize the different origins, thermal and gravitational, respectively, of the wind systems producing the solar and lunar magnetic tides. The variation with season of the lunar magnetic tide is so great that the equator-symmetric seasonal terms in the winter hemisphere overwhelm the equator-antisymmetric annual average terms. This has been interpreted as a failure of the lunar tidal dynamo in the winter hemisphere (see, for example, Stening & Winch 1979).

The seasonal change of the solar magnetic tide includes equator-antisymmetric local time terms of the form P^n_{n+1} and P^n_{n+3}, listed in table 5.27. It is very likely that these terms arise through the seasonal change of ionospheric conductivity, antisymmetric about the equator, interacting with electric fields produced by wind velocity modes giving the sectorial terms P^n_n in the solar magnetic tide when the ionospheric conductivity is constant. That the P_2^1 (diurnal) terms come into phase when $h = 121°$, $301°$, about 24 July and 22 January respectively, supports the association with the seasonal change of ionospheric conductivity.

Non-local time sectorial terms occur only in the $S^+(h)$ group, and are associated with the dynamo action of the atmospheric tide K_1. The terms are as follows:

$$294\cos(2\phi+t+h+147°)P_2^2+214\cos(3\phi+2t+h+161°)P_3^3$$
$$+163\cos(4\phi+3t+h+161°)P_4^4+67\cos(5\phi+4t+h+352°)P_5^5.$$

As with other terms of this type, they come into phase at local noon, $t+\phi = 180°$. Associated with this group of non-local time sectorial terms in $S^+(h)$ are zonal, diurnal, U.T.-dependent terms:

$$314\cos(t+h+153°)P_2^0+222\cos(t+h+257°)P_3^0.$$

Similar zonal terms occur in $S^-(h)$:

$$278 \cos (t-h+224°) P_1^0 + 328 \cos (t-h+16°) P_2^0.$$

It is unlikely that the $S^-(h)$ zonal terms with their apparent dependence upon sidereal time, $t-h$ in the present notation, derive from the rotation of the Earth in an interplanetary magnetic field.

Semi-annual variation of the solar magnetic tide

The semi-annual variation of the solar magnetic tide is given by $S(2h)$. Terms corresponding to phase-law and partial tides are denoted $S^-(2h)$ and $S^+(2h)$ respectively. Results are given in table 8.12, and the equivalent overhead current system in figure 8.12. It will be seen from figure 8.12 that the intensities of the current foci are only about one tenth of those of the solar magnetic tide, and from comparison with figure 8.1 are equal in intensity to those of the principal lunar magnetic tide $L(2s-2h)$. Hence the semi-annual variation of the solar magnetic tide is relatively small.

TABLE 5.27. EQUATOR-SYMMETRIC LOCAL TIME TERMS IN THE SEMI-ANNUAL CHANGE OF THE SOLAR MAGNETIC TIDE

	$S^-(2h)$	$S^+(2h)$
sectorial terms P_n^n	—	$358 \cos (t^*+2h+94°) P_1^1$
	$154 \cos (2t^*-2h+3°) P_2^2$	$446 \cos (2t^*+2h+296°) P_2^2$
	$38 \cos (3t^*-2h+195°) P_3^3$	$192 \cos (3t^*+2h+116°) P_3^3$
	$49 \cos (4t^*-2h+62°) P_4^4$	$58 \cos (4t^*+2h+312°) P_4^4$
terms of the form P_{n+2}^n	$81 \cos (t^*-2h+55°) P_3^1$	$106 \cos (t^*+2h+271°) P_3^1$
	$76 \cos (2t^*-2h+339°) P_4^2$	$76 \cos (2t^*+2h+302°) P_4^2$
	$47 \cos (3t^*-2h+117°) P_5^3$	$68 \cos (3t^*+2h+64°) P_5^3$

In spite of its relative smallness, much has been written on the semi-annual variation of S. Pogrebnoy (1969) considered seasonal variations in the neutral wind régime in the upper atmosphere as the most likely source of the semi-annual variation in S_q. Bhargava (1972*a*, *b*, *c*) considered the semi-annual variation of S_q to arise from two components, modulation of the field by disturbance, and a small but significant component of ionospheric origin. Boller & Stolov (1970) proposed that the semi-annual variation of magnetic activity was due to a Kelvin–Helmholtz instability along the flanks of the magnetosphere. Sawyer (1974) considered the semi-annual variation in the interplanetary field polarity pattern. Kolesnik (1976) argued that semi-annual variations in the ionosphere and upper atmosphere were associated with semi-annual variations of $n(0)$-concentration at the base of the thermosphere, which he showed to be sufficient to produce corresponding variations in the ionized components. Wagner (1968*a*) considered the effect of increasing sunspot number on the semi-annual variation of S_q.

The dominant local time terms are symmetric about the equator and of the form P_n^n and P_{n+2}^n. They are listed in table 5.27. The P_2^2 and P_3^3 terms come into phase at $h = 17°$ and 20°, respectively, indicating an origin in the semi-annual variation of ionospheric conductivity associated with a semi-annual wave in magnetic activity, whose maximum value, according to Chree (1912), occurs between 10 to 36 days after the vernal equinox, i.e. between $h = 10°$ and $h = 36°$, approximately.

There is also a group of local time terms, antisymmetric about the equator, of the form P_{n+1}^n and P_{n+3}^n, listed in table 5.28. As with the corresponding terms in the semi-annual variation

of the lunar magnetic tide, it is suggested that these equator-antisymmetric terms arise from the equator-symmetric semi-annual variation in ionospheric conductivity associated with the $\cos^2 \chi$ term interacting with the electric fields that produce the principal local time terms P^n_{n+1} in the solar magnetic tide when the ionospheric conductivity is constant. The equator-antisymmetric form P^n_{n+1} of these local time terms, and the comparability of their amplitudes with those of the corresponding terms in the principal lunar magnetic tide $L(2s-2h)$ suggests another possible dynamo mechanism. From the dependence on season h, such terms could originate from wind velocities associated with the K_2 tide in the atmosphere, with potential $\cos(2t^*+2h)P^2_2$.

TABLE 5.28. EQUATOR-ANTISYMMETRIC LOCAL TIME TERMS IN THE SEMI-ANNUAL CHANGE OF THE SOLAR MAGNETIC TIDE

	$S^-(2h)$	$S^+(2h)$
terms of the form P^n_{n+1}	$164\cos(t^*-2h+45°)P^1_2$	$273\cos(t^*+2h+345°)P^1_2$
	$122\cos(2t^*-2h+155°)P^2_3$	$363\cos(2t^*+2h+150°)P^2_3$
	$91\cos(3t^*-2h+40°)P^3_4$	$190\cos(3t^*+2h+4°)P^3_4$
	$88\cos(4t^*-2h+255°)P^4_5$	$117\cos(4t^*+2h+211°)P^4_5$
terms of the form P^n_{n+3}	$203\cos(t^*-2h+154°)P^1_4$	$243\cos(t^*+2h+166°)P^1_4$
	$82\cos(2t^*-2h+110°)P^2_5$	$144\cos(2t^*+2h+59°)P^2_5$

TABLE 5.29. SECTORIAL NON-LOCAL TIME TERMS IN $S^-(2h)$, $S^+(2h)$

$S^-(2h)$	$S^+(2h)$
—	$100\cos(2\phi+t+2h+197°)P^2_2$
$72\cos(3\phi+2t-2h+125°)P^3_3$	$114\cos(3\phi+2t+2h+34°)P^3_3$
$42\cos(4\phi+3t-2h+301°)P^4_4$	$77\cos(4\phi+3t+2h+210°)P^4_4$
$59\cos(5\phi+4t-2h+154°)P^5_5$	$39\cos(5\phi+4t+2h+68°)P^5_5$

TABLE 5.30. ZONAL, DIURNAL, U.T.-DEPENDENT TERMS IN $S^-(2h)$, $S^+(2h)$

$S^-(2h)$	$S^+(2h)$
$114\cos(t-2h+225°)P^0_1$	$208\cos(t+2h+354°)P^0_1$
$81\cos(t-2h+52°)P^0_3$	$129\cos(t+2h+91°)P^0_3$
$113\cos(t-2h+231°)P^0_4$	$147\cos(t+2h+208°)P^0_4$

There is also a group of sectorial non-local time terms, listed in table 5.29. As with other terms of this type in other magnetic tides, the two groups of terms $S^-(2h)$ and $S^+(2h)$ come into phase at local noon. The P^3_3 terms in $S^-(2h)$ and $S^+(2h)$ come into phase when h = 23°, 113°, 203°, and 293°, which indicates a connection with the semi-annual wave in magnetic activity.

A group of zonal, diurnal U.T.-dependent terms is listed in table 5.30. By analogy with corresponding terms in the semi-annual variation of the principal lunar magnetic tide, i.e. in $L(2s-4h)$ and $L(2s)$, it is suggested that these terms arise through a diurnal modulation of zonal current systems associated with the semi-annual variation in magnetic activity. The diurnal modulation comes from the motion of the geomagnetic axis and the auroral zones about the geographic axis.

The lunar elliptic magnetic tide $L(3s-2h-p)$

The semi-diurnal external phase-law terms for the lunar elliptic magnetic tide $L(3s-2h-p)$ have been corrected for any contribution from the direct dynamo action of the ocean tide N_2, and the results given in table 8.1. The original semi-diurnal results, both phase-law and partial tides, are given in table 8.8. Corresponding contours for equivalent overhead current functions are given in figures 8.1, 8.8. The principal local time terms in the lunar elliptic magnetic tide are antisymmetric about the equator, of the form P^n_{n+1} with accompanying terms P^n_{n+3}. Results are not available for the I.G.Y. years, and because of the interest in comparing the lunar and lunar elliptic magnetic tides, the external part of the principal local time terms for $L(2s-2h)$ and $L(3s-2h-p)$ are collected together in table 5.31.

TABLE 5.31. PRINCIPAL LOCAL TIME TERMS IN THE LUNAR AND LUNAR ELLIPTIC MAGNETIC TIDES

	$L(2s-2h)$	$L(3s-2h-p)$
of the form P^n_{n+1}	$174\cos(t^*-2s+2h+86°)P^1_2$	$93\cos(t^*-3s+2h+p+93°)P^1_2$
	$254\cos(2t^*-2s+2h+261°)P^2_3$	$84\cos(2t^*-3s+2h+p+284°)P^2_3$
	$134\cos(3t^*-2s+2h+93°)P^3_4$	$26\cos(3t^*-3s+2h+p+89°)P^3_4$
of the form P^n_{n+3}	$117\cos(t^*-2s+2h+245°)P^1_4$	$33\cos(t^*-3s+2h+p+274°)P^1_4$
	$108\cos(2t^*-2s+2h+79°)P^2_5$	$17\cos(2t^*-3s+2h+p+109°)P^2_5$

The ratio of the tides M_2 and N_2 in Doodson's tide-generating potential is $0.17387/0.90812 = 0.19$, and it is clear from table 5.31 that the ratios of the corresponding diurnal and semi-diurnal magnetic tides in $L(3s-2h-p)$ and $L(2s-2h)$ are greater than this. Because the tides M_2 and N_2 appear in the tide-generating potential with the same phase, it is of interest that, with the exception of P^3_4, the phase angles of the elliptic magnetic tide are in advance of the principal lunar magnetic tide.

From table 5.31 it is clear that in both lunar and lunar elliptic magnetic tides the amplitude of the P^2_3 external local time term is greater than that of the corresponding P^2_5 term. Also the phase-angle differences between the P^2_3 and P^2_5 terms are close to 180° for both $L(2s-2h)$ and $L(3s-2h-p)$. These results indicate that the wind velocity producing the principal local time terms in both $L(2s-2h)$ and $L(3s-2h-p)$ is predominantly of the (2, 2) mode. The different oscillation eigenvalues (or equivalent depths) for this mode are 7.07 km and 6.67 km for M_2 and N_2 respectively. The different eigenvalues give different rates of upward propagation through the atmosphere, which gives rise to the phase-angle advance of the elliptic magnetic tide over the principal lunar magnetic tide. The amplitude ratios P^2_5/P^2_3 for $L(2s-2h)$ and $L(3s-2h-p)$ are 0.43 and 0.20 respectively. It will be shown in §6 that this indicates that a different combination of the modes (2, 2) and (2, 4) is required for $L(2s-2h)$ and $L(3s-2h-p)$ wind systems.

It can also be seen from table 5.31 that the amplitude of the diurnal term for $L(3s-2h-p)$ is greater than that of the semi-diurnal term. The reverse is true for $L(2s-2h)$. On the basis of Chapman's dynamo theory, a model for ionospheric conductivity is required for $L(3s-2h-p)$ that has a very strong diurnal term. Alternatively, a diurnal wind component could be postulated, but this seems unlikely given the semi-diurnal nature of the N_2 gravitational tide.

Chapman (1915, 1918) studied the lunar magnetic tide and its changes with lunar distance. His results, and the more recent results of Arora & Rao (1975), can be summarized by noting that the amplitude of the lunar magnetic tide increases from apogee to perigee by an amount comparable with, though perhaps less than, the increase in the tidal force of the Moon, and that over the same time there is a phase angle advance through about 20° or 25°. Precisely these results are contained in the semi-diurnal local time phase-law terms P_3^2 for $L(2s-2h)$ and $L(3s-2h-p)$:

$$254\cos(2t^*-2s+2h+261°)P_3^2+84\cos(2t^*-3s+2h+p+284°)P_3^2. \tag{47}$$

The Moon is at perigee, its point of closest approach when $s-p=0$, when the east longitude of the mean Moon and the perigee of the mean Moon are equal. At perigee then, $3s-2h-p=2s-2h$, and the lunar semi-diurnal magnetic tide evaluated on such a day, by using equation (47), would have the form

$$\begin{aligned}254\cos(2t^*-2s+2h+261°)P_3^2+84\cos(2t^*-2s+2h+284°)P_3^2\\ =333\cos(2t^*-2s+2h+267°)P_3^2.\end{aligned} \tag{48}$$

Similarly at apogee, the point on the Moon's orbit furthest from the Earth, $s-h=180°$, and the lunar semi-diurnal magnetic tide, evaluated by using equation (47), would be

$$\begin{aligned}254\cos(2t^*-2s+2h+261°)P_3^2-84\cos(2t^*-2s+2h+284°)P_3^2\\ =179\cos(2t^*-2s+2h+250°)P_3^2.\end{aligned} \tag{49}$$

It will be seen from equations (48), (49) that the phase of the P_3^2 lunar semi-diurnal magnetic tide advances by 17° from apogee to perigee and that there is a corresponding increase in amplitude given by $333/179=1.86$. The phase angle advance is associated with the different equivalent depths of the fundamental (2, 2) modes of atmospheric oscillations for the tides M_2 and N_2, and should not be confused with a similar phase angle advance resulting from subdivision of data into four lunar-distance groups PER, REC, APO, NEA, (perigee, receding, apogee, nearing). By using the numbers given in equation (8*a*, *c*) for the amplitudes of M_2 and N_2, the apparent increase in tidal potential from apogee to perigee is given by

$$(0.908\,12+0.173\,87)/(0.908\,12-0.173\,87)=1.47,$$

which is smaller than the ratio 1.86, as already noted by Chapman.

The lunar elliptic magnetic tide includes a diurnal, zonal U.T.-dependent, phase-law term $77\cos(t-3s+2h+p+47°)P_1^0$, and a similar partial tide term $114\cos(t+3s-2h-p+68°)P_2^0$. The partial tide has the second largest amplitude of all the $L(3s-2h-p)$ partial tides. The corresponding $L(2s-2h)$ partial tide has the largest amplitude of all the $L(2s-2h)$ partial tides. The origin of these terms is a U.T.-modulation of the zonal current systems associated with magnetic disturbance by the diurnal motion of the geomagnetic axis and the auroral zones about the geographic axis. For $L(2s-2h)$ the magnetic disturbance current systems are associated with the second 'harmonic' of the 27-day recurrence tendency of sunspots and magnetic activity, and for $L(3s-2h-p)$ the third 'harmonic' of the same tendency. Sectorial local time terms P_n^n in $L(3s-2h-p)$ are given in table 5.32, along with the corresponding terms in $L(2s-2h)$ for comparison. The $L(3s-2h-p)$ terms come into phase at local noon as do the $L(2s-2h)$ terms. The presence of substantial partial tides indicates that some mechanism is

required other than that for the principal local time terms P^n_{n+1}. It is suggested that a long-period $3s-2h-p$ modulation of the P^0_1 component of ionospheric conductivity, associated with the third 'harmonic' of the 27-day recurrence tendency, interacts with the electric fields that produce the principal local time terms (with constant ionospheric conductivity). That the $L(3s-2h-p)$ sectorial local time terms are greater than those of $L(2s-2h)$ may be a consequence of the 'period' of $3s-2h-p$ being closer, at 9.6 days, to the third harmonic of the 27-day recurrence tendency than the 'period' of $2s-2h$, at 14.6 days, is to the second harmonic of the same 27-day recurrence tendency.

TABLE 5.32. EQUATOR-SYMMETRIC SECTORIAL LOCAL TIME TERMS IN $L(3s-2h-p)$

	$L(2s-2h)$	$L(3s-2h-p)$
phase-law	$33\cos(t^*-2s+2h+157°)P^1_1$	$91\cos(t^*-3s+2h+p+37°)P^1_1$
	$69\cos(2t^*-2s+2h+297°)P^2_2$	$98\cos(2t^*-3s+2h+p+214°)P^2_2$
	$48\cos(3t^*-2s+2h+120°)P^3_3$	$26\cos(3t^*-3s+2h+p+80°)P^3_3$
	$9\cos(4t^*-2s+2h+330°)P^4_4$	$19\cos(4t^*-3s+2h+p+333°)P^4_4$
partial	$49\cos(t^*+2s-2h+185°)P^1_1$	—
	$46\cos(2t^*+2s-2h+53°)P^2_2$	$75\cos(2t^*+3s-2h-p+306°)P^2_2$
	$25\cos(3t^*+2s-2h+271°)P^3_3$	$32\cos(3t^*+3s-2h-p+166°)P^3_3$
	$15\cos(4t^*+2s-2h+142°)P^4_4$	$11\cos(4t^*+3s-2h-p+9°)P^4_4$

TABLE 5.33. WESTWARD-MOVING, SECTORIAL NON-LOCAL TIME TERMS IN $L(3s-2h-p)$

phase-law	partial
$24\cos(2\phi+t-3s+2h+p+86°)P^2_2$	$27\cos(2\phi+t+3s-2h-p+112°)P^2_2$
$37\cos(3\phi+2t-3s+2h+p+317°)P^3_3$	—
$23\cos(4\phi+3t-3s+2h+p+226°)P^4_4$	$11\cos(4\phi+3t+3s-2h-p+5°)P^4_4$
$12\cos(5\phi+4t-3s+2h+p+51°)P^5_5$	—
$90\cos(\phi+2t-3s+2h+p+173°)P^1_1$	$120\cos(\phi+2t+3s-2h-p+60°)P^1_1$
$47\cos(2\phi+3t-3s+2h+p+26°)P^2_2$	$56\cos(2\phi+3t+3s-2h-p+235°)P^2_2$
$19\cos(3\phi+4t-3s+2h+p+203°)P^3_3$	$10\cos(3\phi+4t+3s-2h-p+352°)P^3_3$

The $L(3s-2h-p)$ phase-law and partial tides include non-local time terms, sectorial, westward-moving and symmetric about the equator. These terms are collected in table 5.33, and similar terms have been found in all the magnetic tides examined so far. The $L(3s-2h-p)$ group do not come into phase at local noon as strongly as do the same terms in $L(2s-2h)$, and comparison of phase angles of corresponding terms in tables 5.6 and 5.33 for $L(2s-2h)$ and $L(3s-2h-p)$ respectively shows no simple consistent relation such as that noted for the local time terms, both sectorial P^n_n and tesseral P^n_{n+1}, which show a phase lead and phase lag respectively.

The lunar elliptic magnetic tide $L(3s-2h-p)$ contains zonal, U.T.-dependent phase-law and partial tides, listed in table 5.34. The amplitudes of these terms are about half those of the corresponding zonal terms in the principal lunar magnetic tide $L(2s-2h)$ given in table 5.4. The zonal, U.T.-dependence indicates an origin in the daily variation of a zonal overhead current system that is associated with the diurnal motion of the geomagnetic axis and auroral zones about the geographic axis. The parameter $3s-2h-p$ in both phase-law and partial tides indicates a further modulation near the third 'harmonic' of the 27-day recurrence tendency, with a period of 9.61 days.

The partial tides for $L(3s-2h-p)$ are different from those of other magnetic tides in that certain terms in the spherical harmonic representation are greater than the corresponding terms for the phase-law tides. Indeed, at some observatories, e.g. Fürstenfeldbruck as in §3, the $L(3s-2h-p)$ partial tides are greater than the corresponding phase-law tides, although this is not true at all observatories. Partial tides about equal to the corresponding phase-law tides cannot be produced by dynamo action involving an atmospheric tide, N_2 for $L(3s-2h-p)$, and are more likely to be produced by a long-period variation, e.g. the third harmonic of the 27-day recurrence tendency, interacting with the electric fields that, with an ionosphere of constant conductivity, give rise to the principal local time magnetic tides P^n_{n+1}.

TABLE 5.34. ZONAL, DIURNAL, U.T.-DEPENDENT TERMS IN $L(3s-2h-p)$

phase-law	partial
$77\cos(t-3s+2h+p+47°)P^0_1$	$67\cos(t+3s-2h-p+3°)P^0_1$
$36\cos(t-3s+2h+p+195°)P^0_2$	$114\cos(t+3s-2h-p+68°)P^0_2$
$27\cos(t-3s+2h+p+332°)P^0_3$	$32\cos(t+3s-2h-p+27°)P^0_3$
$25\cos(t-3s+2h+p+78°)P^0_4$	$20\cos(t+3s-2h-p+211°)P^0_4$

TABLE 5.35. PRINCIPAL LOCAL TIME PHASE-LAW TERMS FOR $L(3s-3h-p)$ AND $L(3s-h-p)$; SEASONAL CHANGE OF THE LUNAR ELLIPTIC MAGNETIC TIDE $L(3s-2h-p)$

	$L(3s-3h-p)$	$L(3s-h-p)$
terms of the form P^n_n	$123\cos(t^*-3s+3h+p+319°)P^1_1$	$70\cos(t^*-3s+h+p+175°)P^1_1$
	$97\cos(2t^*-3s+3h+p+143°)P^2_2$	$46\cos(2t^*-3s+h+p+68°)P^2_2$
	$52\cos(3t^*-3s+3h+p+315°)P^3_3$	$26\cos(3t^*-3s+h+p+240°)P^3_3$
	$17\cos(4t^*-3s+3h+p+103°)P^4_4$	$19\cos(4t^*-3s+h+p+34°)P^4_4$
terms of the form P^n_{n+2}	$21\cos(t^*-3s+3h+p+67°)P^1_3$	$34\cos(t^*-3s+h+p+74°)P^1_3$
	$26\cos(2y^*-3s+3h+p+218°)P^2_4$	—

Seasonal variation of the lunar elliptic magnetic tide

The magnetic tides $L(3s-3h-p)$ and $L(3s-h-p)$ contain the seasonal variation of the lunar elliptic magnetic tide which proceeds at the rate of 1 c/a. Spherical harmonic coefficients are given in tables 8.7, 8.9, with contours of the equivalent overhead current system given in figures 8.7, 8.9. The principal local time phase-law terms, of the form P^n_n, are collected in table 5.35.

The amplitudes of terms listed in table 5.35, other than P^4_4, are about one half to one third of the corresponding terms in the seasonal variation of the principal lunar magnetic tide, $L(2s-3h)$ and $L(2s-h)$ listed in table 5.17. The phase angles of $L(2s-3h)$ and $L(3s-3h-p)$ show good agreement, although the phase angles of $L(2s-h)$ and $L(3s-h-p)$ are more disparate. The disparity may be associated with the dynamo contributions of the atmospheric tides O_1 to $L(2s-2h)$ and Q_1 to $L(3s-h-p)$, but may also indicate a lower level of mesospheric control over the seasonal change of $L(3s-2h-p)$ than over $L(2s-2h)$. The principal diurnal terms P^1_1 of $L(3s-3h-p)$ and $L(3s-h-p)$ come into phase when $h = 108°$ and $208°$ (about the 10 July and 9 January), which is closer to the corresponding results for the solar magnetic tides $S^-(h)$ and $S^+(h)$, $h = 100°$ and $280°$, than to that for the lunar magnetic tides $L(2s-3h)$ and $L(2s-h)$, for which $h = 135°$ and $315°$.

The seasonal variation of the diurnal and semi-diurnal local time lunar elliptic tidal terms is given by

(*a*) diurnal,

$$93\cos(t^*-3s+2h+p+93°)P_2^1+123\cos(t^*-3s+3h+p+319°)P_1^1 +70\cos(t^*-3s+h+p+175°)P_1^1,$$

(*b*) semi-diurnal,

$$84\cos(2t^*-3s+2h+p+284°)P_3^2 +97\cos(2t^*-3s+3h+p+143°)P_2^2+46\cos(2t^*-3s+h+p+68°)P_2^2.$$

Thus the seasonal change of the lunar elliptic magnetic tide is relatively as great as that of the principal lunar magnetic tide $L(2s-2h)$, and the description of the phenomenon as a failure of the dynamo in the winter hemisphere is still appropriate.

TABLE 5.36. EQUATOR-ANTISYMMETRIC LOCAL TIME TERMS IN $L(3s-3h-p)$ AND $L(3s-h-p)$

	$L(3s-3h-p)$	$L(3s-h-p)$
phase-law	$51\cos(t^*-3s+3h+p+287°)P_2^1$	$111\cos(t^*-3s+h+p+104°)P_2^1$
	—	$53\cos(2t^*-3s+h+p+278°)P_3^2$
	—	$42\cos(3t^*-3s+h+p+108°)P_4^3$
	$8\cos(4t^*-3s+3h+p+1°)P_5^4$	$22\cos(4t^*-3s+h+p+338°)P_5^4$
partial	$51\cos(t^*+3s-3h-p+150°)P_2^1$	$76\cos(t^*+3s-h-p+188°)P_2^1$
	$18\cos(2t^*+3s-3h-p+90°)P_3^2$	$19\cos(2t^*+3s-h-p+213°)P_3^2$
	—	$15\cos(3t^*+3s-h-p+341°)P_4^3$
	$10\cos(4t^*+3s-3h-p+81°)P_5^4$	$10\cos(4t^*+3s-h-p+138°)P_5^4$

TABLE 5.37. ZONAL PHASE-LAW AND PARTIAL TIDES IN $L(3s-3h-p)$ AND $L(3s-h-p)$

	$L(3s-3h-p)$	$L(3s-h-p)$
phase-law	$57\cos(t-3s+3h+p+251°)P_1^0$	$183\cos(t-3s+h+p+288°)P_1^0$
	$68\cos(t-3s+3h+p+293°)P_2^0$	—
	$28\cos(t-3s+3h+p+285°)P_4^0$	—
partial	$243\cos(t+3s-3h-p+97°)P_1^0$	$109\cos(t+3s-h-p+303°)P_1^0$
	$53\cos(t+3s-3h-p+262°)P_2^0$	$29\cos(t+3s-h-p+81°)P_2^0$
	$32\cos(t+3s-3h-p+137°)P_3^0$	$36\cos(t+3s-h-p+283°)P_3^0$
	$29\cos(t+3s-3h-p+177°)P_4^0$	$23\cos(t+3s-h-p+36°)P_4^0$

A group of local time terms, antisymmetric about the equator, appears in phase-law and partial tides for $L(3s-3h-p)$ and $L(3s-h-p)$, and the relevant terms are collected in table 5.36. These tides are of the same order of magnitude as the local time equator-antisymmetric terms in $L(2s-3h)$ and $L(2s-h)$, and are given in table 5.18. For such terms it was postulated that a periodicity in a P_1^0 component of ionospheric conductivity associated with the *second* harmonic of the 27-day sunspot recurrence tendency interacted with the electric fields producing the equator-symmetric local time P_n^n terms in the solar magnetic tide. It is now postulated that the *third* harmonic of the 27-day sunspot recurrence tendency in the same theory gives rise to the terms of table 5.36.

$L(3s-3h-p)$ and $L(3s-h-p)$ contain zonal, U.T.-dependent phase-law and partial tides, listed in table 5.37. The amplitudes are roughly equal to the amplitudes of the zonal U.T.-dependent terms in $L(2s-3h)$ and $L(2s-h)$, listed in table 5.19. It is suggested that these terms are associated with the diurnal motion of the geomagnetic axis and the auroral zones

about the geographic axis, modulating zonal current systems associated with the third harmonic of the 27-day recurrence tendency. The parameters $3s-3h-p$ and $3s-h-p$ have periods 9.9 and 9.4 days respectively.

TABLE 5.38. SECTORIAL, WESTWARD-MOVING, NON-LOCAL TIME PHASE-LAW TIDES IN $L(3s-3h-p)$ AND $L(3s-h-p)$

$L(3s-3h-p)$	$L(3s-h-p)$
$62\cos(\phi+2t-3s+3h+p+283°)P_1^1$	$52\cos(\phi+2t-3s+h+p+42°)P_1^1$
$33\cos(2\phi+3t-3s+3h+p+157°)P_2^2$	$22\cos(2\phi+3t-3s+h+p+225°)P_2^2$
—	$12\cos(3\phi+4t-3s+h+p+19°)P_3^3$
terms evaluated at local noon $t^*=t+\phi=180°$	
$62\cos(t-3s+3h+p+103°)P_1^1$	$52\cos(t-3s+h+p+222°)P_1^1$
$33\cos(t-3s+3h+p+157°)P_2^2$	$22\cos(t-3s+h+p+225°)P_2^2$
—	$12\cos(t-3s+h+p+199°)P_3^3$

TABLE 5.39. SECTORIAL, LOCAL TIME PARTIAL TIDES IN $L(3s-3h-p)$ AND $L(3s-h-p)$

$L(3s-3h-p)$	$L(3s-h-p)$
$88\cos(t^*+3s-3h+p+45°)P_1^1$	$68\cos(t^*+3s-h-p+209°)P_1^1$
$60\cos(2t^*+3s-3h-p+223°)P_2^2$	$34\cos(2t^*+3s-h-p+347°)P_2^2$
$23\cos(3t^*+3s-3h-p+3°)P_3^3$	$21\cos(3t^*+3s-h-p+214°)P_3^3$

A group of sectorial, westward-moving non-local time phase-law terms are given in table 5.38. The groups for $L(3s-3h-p)$ and $L(3s-h-p)$ are seen to have about the same phase-angle at local noon, although the coincidence of phase angles in the two groups is not as pronounced as it is for the seasonal tides $L(2s-3h)$ and $L(2s-h)$ in table 5.20. The semi-diurnal P_1^1 terms come into phase when $h=60°$ or 240° (about 23 May or 22 November respectively), about two months earlier than the corresponding terms in $L(2s-3h)$ and $L(2s-h)$. At $h=60°$, the P_1^1 and P_2^2 terms,

$$114\cos(\phi+2t-3s+2h+p+343°)P_1^1+53\cos(2\phi+3t-3s+2h+p+204°)P_2^2,$$

are to be compared with the principal local time terms from $L(3s-2h-p)$, from table 5.31, written in the form

$$93\cos(\phi+t-3s+2h+p+93°)P_2^1+84\cos(2\phi+2t-3s+2h+p+284°)P_3^2.$$

Hence the elliptic magnetic tide will be greatly modified by the sectorial, westward-moving, non-local time terms in $L(3s-3h-p)$ and $L(3s-h-p)$, especially in equatorial regions where the sectorial functions and their gradients are greatest.

Finally, as with $L(2s-3h)$ and $L(2s-h)$, there is a group of sectorial, local time partial tides; they are listed in table 5.39. They are of the same order of magnitude as the corresponding tides in $L(2s-3h)$ and $L(2s-h)$ given in table 5.21, but smaller than the corresponding phase-law terms (the principal terms) in $L(3s-3h-p)$ and $L(3s-h-p)$ listed in table 5.35.

Long-period tides

Spherical harmonic coefficients for internal and external components of long-period tides are given in table 8.13. It will be seen from this table that the long-period tides based on lunar parameters are all dominantly of a zonal P_1^0 type. Given the relation between the 'periods' of

the lunar parameters, as in equation (6), e.g. $2s-2h$ and $3s-2h-p$, with the second and third 'harmonics' of the 27-day recurrence tendency in sunspots and magnetic activity, such long-period magnetic fields appear to originate in ring current systems about the Earth, in which the current flow oscillates with the relevant period. From the list of external components of long-period tides given in table 5.40, it is apparent that the phase angles tend to be near either 0° or 180°. Analysing the data used in the present paper, for periods of from 4 to 30 days, Anderssen *et al.* (1979) found that the phase is essentially constant with a mean value of 165°. The increase in amplitude as the period approaches either 13.5 or 9.0 days is quite noticeable in table 5.40. As already indicated, such periodicities correspond to the second and third harmonics of the 27-day recurrence tendency, or could be associated with the long-period tides noted by Shiraki (1974) and Kitamura (1979).

TABLE 5.40. LONG-PERIOD TIDES

$597\cos(2s-4h+331°)P_1^0$	16.06 days
$387\cos(2s-3h+9°)P_1^0$	15.39 days
$652\cos(2s-2h+189°)P_1^0$	14.77 days
$905\cos(2s-h+164°)P_1^0$	14.19 days
$1135\cos(2s+164°)P_1^0$	13.66 days
$325\cos(3s-3h-p+27°)P_1^0$	9.87 days
$176\cos(3s-2h-p+330°)P_1^0$	9.61 days
$854\cos(3s-h-p+24°)P_1^0$	9.37 days

TABLE 5.41. ANNUAL AND SEMI-ANNUAL LONG-PERIOD TIDES

	internal	external
annual	$4417\cos(h+174°)P_1^0$	$653\cos(h+309°)P_1^0$
	$3969\cos(h+356°)P_2^0$	$2007\cos(h+68°)P_2^0$
semi-annual	$1694\cos(2h+251°)P_1^0$	$1732\cos(2h+301°)P_1^0$
	$1808\cos(2h+58°)P_2^0$	$1290\cos(2h+82°)P_2^0$

The long-period tides, other than the annual and semi-annual tides, have internal coefficients smaller than external coefficients, consistent with the hypothesis of an external ring current origin. However, for the annual and semi-annual long-period tides, the internal term exceeds the external term (see table 5.41). All the magnetic tides of the present paper, including all long-period tides, have been computed by using *all* hourly mean values, whereas in studies of the annual and semi-annual tides specifically, e.g. Lewis *et al.* (1955), Malin & Mete Isikara (1976), only the hourly mean values for local midnight are used. By this means any contribution from the annual variation of the solar magnetic tide S or S_q is minimized. It is also a practice to exclude observatories in high latitudes, because, as Malin & Mete Isikara (1976) noted, Fourier coefficients for the annual long-period tide in high latitudes fluctuate erratically. By using the data of the present paper, numerical experiments excluding certain groups of observatories from the spherical harmonic analysis of long-period tides obtained from all-day data yielded different numerical values for the annual and semi-annual spherical harmonic coefficients but did not alter the dominance of internal terms over external terms.

Given the value of long-period terms for induction studies and electromagnetic modelling of the Earth's interior, it is disappointing to find that an analysis of the most widely distributed data available should show that the annual and semi-annual long-period terms are of internal

origin. There is however, definite value in having an entire collection of coefficients for magnetic tides computed by the same method from the same data, and for this reason the results for the annual and semi-annual tides have not been excluded. In seeking possible physical causes, one is led to consider that poor baseline control at certain observatories might be responsible. Baseline errors give long-period Fourier coefficients with large standard deviations, and such coefficients are not given much weight in numerical analysis by the method of least squares. All equations of condition have been weighted so that the Fourier coefficients have a standard deviation of unity. Errors in baseline control would affect all the long-period results and not just the annual and semi-annual magnetic tides alone.

The zonal nature of the spherical harmonic coefficients for the annual and semi-annual long-period tides precludes their origin in the oceans which are sectorial in nature. There are however, the possibilities of annual and semi-annual variations in Earth currents of deep origin (Roberts & Lowes 1961), or movement of the magnetic variometer pier due to permafrost action, or a change of magnetic moment of rock in regions near the observatory with temperature (Rodgers 1980).

6. Ionospheric dynamo theory and Hough functions

The purpose of this section is to show the very simple relation between the theory of Hough functions as developed by Longuet-Higgins (1968) and the observed magnetic tides.

When an electric field $\boldsymbol{E}$ is applied to an ionized gas in the presence of a magnetic field $\boldsymbol{B}$, as in the ionosphere, the resulting electric current density $\boldsymbol{J}$ depends upon the relative orientation of the electric and magnetic fields. In general, $\boldsymbol{E}$ may be resolved into components $\boldsymbol{E}_0$ and $\boldsymbol{E}_1$, parallel and perpendicular to $\boldsymbol{B}$, respectively, and if $\boldsymbol{b}$ is a unit vector parallel to $\boldsymbol{B}$, then the current density $\boldsymbol{J}$ is given by Baker & Martyn (1953) as

$$\boldsymbol{J} = \sigma_0 \boldsymbol{E}_0 + \sigma_1 \boldsymbol{E}_1 + \sigma_2 (\boldsymbol{b} \times \boldsymbol{E}), \tag{50}$$

where

$$\boldsymbol{E}_0 = (\boldsymbol{E} \cdot \boldsymbol{b})\, \boldsymbol{b}$$

and

$$\boldsymbol{E}_1 = \boldsymbol{E} - (\boldsymbol{E} \cdot \boldsymbol{b})\, \boldsymbol{b}.$$

The parameter σ_0 is the longitudinal or parallel conductivity, while σ_1, σ_2 are Pedersen and Hall conductivities, respectively. Typical noon values 120 km above the equator at the equinox during conditions of average solar activity are given by Forbes & Lindzen (1976) as

$$\sigma_0 = 1.0, \quad \sigma_1 = 0.0004, \quad \sigma_2 = 0.006 \text{ A V}^{-1}\text{m}^{-1}, \tag{51}$$

which vary with magnetic inclination and local time.

At the higher altitude of the F-region, σ_0 becomes still larger than σ_1 or σ_2, and hence any $\boldsymbol{E}$ parallel to $\boldsymbol{B}$ is neutralized by the rapid movement of electrons. In the F-region, therefore, the lines of magnetic force are lines of constant electric potential.

Let $\boldsymbol{J}$ and $\boldsymbol{E}$ have spherical polar components given by

$$\left.\begin{aligned} \boldsymbol{J} &= J_r \boldsymbol{e}_r + J_\theta \boldsymbol{e}_\theta + J_\phi \boldsymbol{e}_\phi, \\ \boldsymbol{E} &= E_r \boldsymbol{e}_r + E_\theta \boldsymbol{e}_\theta + E_\phi \boldsymbol{e}_\phi, \end{aligned}\right\} \tag{52}$$

where $\boldsymbol{e}_r$, $\boldsymbol{e}_\theta$, $\boldsymbol{e}_\phi$ are unit vectors in the direction of r, θ, ϕ increasing, i.e. upwards, southwards and eastwards, respectively.

The radial component of current J_r is found from equation (50) to be

$$\begin{aligned} J_r = {} & (E_r/B^2)\{(\sigma_0-\sigma_1)B_r^2+\sigma_1 B^2\} \\ & +(E_\theta/B^2)\{(\sigma_0-\sigma_1)B_\theta B_r-\sigma_2 BB_\phi\} \\ & +(E_\phi/B^2)\{(\sigma_0-\sigma_1)B_\phi B_r+\sigma_2 BB_\theta\}. \end{aligned} \tag{53}$$

For ionospheric current systems flowing in the E-region, the currents are regarded as flowing in a spherical shell, and J_r is assumed to be zero. This assumption gives E_r as a function of E_θ and E_ϕ. Hence it can be shown that

$$J_\theta = \sigma_{\theta\theta}E_\theta+\sigma_{\theta\phi}E_\phi, \quad J_\phi = \sigma_{\phi\theta}E_\theta+\sigma_{\phi\phi}E_\phi, \tag{54}$$

where

$$\left.\begin{aligned} \sigma_{\theta\theta} &= \frac{\sigma_0\sigma_1 B^2-(\sigma_0\sigma_1-\sigma_1^2-\sigma_2^2)B_\phi^2}{\sigma_0 B_r^2+\sigma_1(B_\theta^2+B_\phi^2)}, \\ \sigma_{\theta\phi} &= \frac{(\sigma_0\sigma_1-\sigma_1^2-\sigma_2^2)B_\theta B_\phi-\sigma_2\sigma_0 BB_r}{\sigma_0 B_r^2+\sigma_1(B_\theta^2+B_\phi^2)}, \\ \sigma_{\phi\theta} &= \frac{(\sigma_0\sigma_1-\sigma_1^2-\sigma_2^2)B_\theta B_\phi+\sigma_2\sigma_0 BB_r}{\sigma_0 B_r^2+\sigma_1(B_\theta^2+B_\phi^2)}, \\ \sigma_{\phi\phi} &= \frac{\sigma_0\sigma_1 B^2-(\sigma_0\sigma_1-\sigma_1^2-\sigma_2^2)B_\theta^2}{\sigma_0 B_r^2+\sigma_1(B_\theta^2+B_\phi^2)}, \end{aligned}\right\} \tag{55}$$

from which it will be clear that $\sigma_{\theta\phi} = -\sigma_{\phi\theta}$ only when $B_\theta = 0$ or $B_\phi = 0$.

The assumption that $J_r = 0$ does not apply in the auroral region, particularly during magnetic disturbances. The present analysis, although including auroral observations, has excluded disturbed days, and only partly represents effects originating in the narrow auroral region (or the electrojet region). Dynamo theories including vertical, or field-aligned, currents linking the ionosphere and magnetosphere have been developed by Maeda & Murata (1965), Fukushima (1968), Price (1969), van Sabben (1970, 1971), Matsushita (1971), Mishin *et al.* (1971) and Stening (1977*b*). A series of papers on S_q dynamo theory dealing with several developments have been given by Wagner (1968*b*, *c*, 1971) and Möhlmann (1971–1977).

We now assume that the Earth's main magnetic field is that of an axial dipole with potential $P_1^0(\cos\theta)$, where θ now represents the geomagnetic colatitude. Let a, R be the radii of the ionosphere and Earth respectively. Thus $R/a = 6371/6486 = 0.9823$. At the level of the ionosphere, the geomagnetic main field components are given by

$$B_r = 2(R/a)^3 G\cos\theta, \quad B_\theta = (R/a)^3 G\sin\theta, \quad B_\phi = 0. \tag{56}$$

The tensor components of conductivity reduce to

$$\left.\begin{aligned} \sigma_{\theta\theta} &= \frac{\sigma_0\sigma_1(1+3\cos^2\theta)}{4\sigma_0\cos^2\theta+\sigma_1\sin^2\theta}, \\ \sigma_{\theta\phi} &= \frac{\sigma_2\sigma_0\cos\theta(1+3\cos^2\theta)^{\frac{1}{2}}}{4\sigma_0\cos^2\theta+\sigma_1\sin^2\theta}, \\ \sigma_{\phi\theta} &= -\sigma_{\theta\phi}, \\ \sigma_{\phi\phi} &= \frac{4\sigma_0\sigma_1\cos^2\theta+(\sigma_1^2+\sigma_2^2)\sin^2\theta}{4\sigma_0\cos^2\theta+\sigma_1\sin^2\theta}. \end{aligned}\right\} \tag{57}$$

With the numerical values given for σ_0, σ_1, σ_2 in equation (51), in the ionospheric E-region,

$$\sigma_{\theta\theta} \approx \sigma_1, \quad \sigma_{\theta\phi} \approx \sigma_2, \quad \sigma_{\phi\phi} \approx \sigma_1. \tag{58}$$

The relation between current and electric field can be expressed as

$$J_\theta = \sigma_1 E_\theta + \sigma_2 E_\phi, \quad J_\phi = -\sigma_2 E_\theta + \sigma_1 E_\phi. \tag{59}$$

A local time factor (see, for example, Forbes & Lindzen 1976), must be applied to each component of conductivity. Equation (59) integrated throughout the ionosphere may be written

$$J_\theta = C_1 E_\theta + C_2 E_\phi, \quad J_\phi = -C_2 E_\theta + C_1 E_\phi. \tag{60}$$

Integrating equation (59) to a height of 150 km from the base of the ionosphere, Ferris & Price (1964) give the following:

$$C_1 = 0.854 \times 10^{-8}, \quad C_2 = 1.455 \times 10^{-8} \text{ e.m.u. cm.}$$

Swift (1972) examined the validity of such formulae. In the ionospheric E-region, an electric field $\boldsymbol{E}$ arises by dynamo action from movements of electrically conducting material with velocity $\boldsymbol{v}$ through the geomagnetic main field where

$$\boldsymbol{E} = \boldsymbol{v} \times \boldsymbol{B}. \tag{61}$$

The resulting currents, with density $\boldsymbol{J}$, flow without the continuing accumulation of charge at any point and, hence, the region being assumed to have constant electrical permittivity ϵ,

$$\nabla \cdot \boldsymbol{E} = 0, \tag{62}$$

i.e. the electric field is solenoidal. Such vector fields can be represented as a sum of poloidal $\boldsymbol{S}_n^m$ and toroidal $\boldsymbol{T}_n^m$ fields:

$$\left.\begin{aligned} E_r &= \sum_{n,m} \frac{n(n+1)}{r^2} S_n^m(r)\, Y_n^m(\theta\phi), \\ E_\theta &= \sum_{n,m} \left\{ \frac{1}{r^2} \frac{\mathrm{d}S_n^m}{\mathrm{d}r} \frac{\partial Y_n^m}{\partial \theta} + \frac{1}{r} \frac{T_n^m(r)}{\sin\theta} \frac{\partial Y_n^m}{\partial \phi} \right\}, \\ E_\phi &= \sum_{n,m} \left(\frac{1}{r^2} \frac{\mathrm{d}S_n^m}{\mathrm{d}r} \frac{\partial Y_n^m}{\partial \phi} - \frac{1}{r} T_n^m \frac{\partial Y_n^m}{\partial \theta} \right) \end{aligned}\right\} \tag{63}$$

(see, for example, Bullard & Gellman 1954), with $Y_n^m(\theta\phi) = P_n^m(\cos\theta)\, \mathrm{e}^{\mathrm{i}m\phi}$.

Poloidal and toroidal functions are orthogonal over the surface of a sphere, so that equation (63) provides a suitable representation of the field.

The meridional and azimuthal components of the dynamo electric field can be written more briefly as

$$E_\theta = \frac{1}{a} \frac{\partial S}{\partial \theta} + \frac{1}{a \sin\theta} \frac{\partial T}{\partial \phi}, \quad E_\phi = \frac{1}{a \sin\theta} \frac{\partial S}{\partial \phi} - \frac{1}{a} \frac{\partial T}{\partial \theta}. \tag{64}$$

The poloidal field $\boldsymbol{S}$ as indicated in equation (63) has a radial component, and is therefore unable to drive a steady current system in the ionospheric conducting shell; it does give rise to an electrostatic field. The toroidal electric field $\boldsymbol{T}$ with no radial component is able to drive the ionospheric current system that gives rise to the time-varying magnetic fields observed at the surface of the Earth as magnetic tides.

Let the spherical polar components of the velocity $\boldsymbol{v}$ and magnetic field $\boldsymbol{B}$ be given by (w, u, v) and (B_r, B_θ, B_ϕ), respectively. The spherical polar components of the dynamo electric field are then given by

$$\left.\begin{aligned}(\boldsymbol{v}\times\boldsymbol{B})_r &= uB_\phi - vB_\theta,\\ (\boldsymbol{v}\times\boldsymbol{B})_\theta &= vB_r - wB_\phi,\\ (\boldsymbol{v}\times\boldsymbol{B})_\phi &= wB_\theta - uB_r.\end{aligned}\right\} \tag{65}$$

The spherical polar components of the geomagnetic main field are given by $\boldsymbol{B} = -\nabla U$, i.e.

$$B_r = -\frac{\partial U}{\partial r},\quad B_\theta = -\frac{1}{r}\frac{\partial U}{\partial \theta},\quad B_\phi = -\frac{1}{r\sin\theta}\frac{\partial U}{\partial \phi}, \tag{66}$$

where the scalar potential

$$U = R\sum_{n,m}\left(\frac{R}{r}\right)^{n+1} G_n^m Y_n^m(\theta\phi), \tag{67}$$

and the G_n^m are known complex constants. We shall use only

$$U = \frac{R^3}{r^2} G_1^0 Y_1^0 = \frac{R^3}{r^2} G_1^0 \cos\theta, \tag{68}$$

which is the potential of an axial dipole.

In common with the theory of atmospheric tides (Siebert 1961; Jones 1970, 1973) we assume that the vertical component of velocity w is small when compared to the horizontal components u, v. In a sphere of radius $r = a$, the θ, ϕ components of the dynamo electric field give, by using equations (61), (64)–(66),

$$\left.\begin{aligned}-v\frac{\partial U}{\partial r} &= \frac{1}{a}\left(\frac{\partial S}{\partial\theta} + \frac{1}{\sin\theta}\frac{\partial T}{\partial\phi}\right),\\ u\frac{\partial U}{\partial r} &= \frac{1}{a}\left(\frac{1}{\sin\theta}\frac{\partial S}{\partial\phi} - \frac{\partial T}{\partial\theta}\right).\end{aligned}\right\} \tag{69}$$

The θ, ϕ components of the electric fields driving the current system $\boldsymbol{J}$ are given (with $r = a$) by

$$E_\theta = \frac{1}{a\sin\theta}\frac{\partial T}{\partial\phi},\quad E_\phi = -\frac{1}{a}\frac{\partial T}{\partial\theta}. \tag{70}$$

The magnetic tides are represented by a scalar current function $\mathscr{R}$, as a toroidal current system flowing in a thin shell of radius $r = a$:

$$J_\theta = \frac{1}{a\sin\theta}\frac{\partial\mathscr{R}}{\partial\phi},\quad J_\phi = -\frac{1}{a}\frac{\partial\mathscr{R}}{\partial\theta}. \tag{71}$$

It follows directly from equations (60), (69)–(71) that

$$\left.\begin{aligned}\frac{1}{\sin\theta}\frac{\partial\mathscr{R}}{\partial\phi} &= -C_1\left(av\frac{\partial U}{\partial r} + \frac{\partial S}{\partial\theta}\right) + C_2\left(au\frac{\partial U}{\partial r} - \frac{1}{\sin\theta}\frac{\partial S}{\partial\phi}\right),\\ -\frac{\partial\mathscr{R}}{\partial\theta} &= C_2\left(av\frac{\partial U}{\partial r} + \frac{\partial S}{\partial\theta}\right) + C_1\left(au\frac{\partial U}{\partial r} - \frac{1}{\sin\theta}\frac{\partial S}{\partial\phi}\right).\end{aligned}\right\} \tag{72}$$

Equation (72) can be 'solved' to obtain

$$\left.\begin{aligned}av\frac{\partial U}{\partial r} + \frac{\partial S}{\partial\theta} &= \frac{-1}{C_1^2+C_2^2}\left(\frac{C_1}{\sin\theta}\frac{\partial\mathscr{R}}{\partial\phi} + C_2\frac{\partial\mathscr{R}}{\partial\theta}\right),\\ au\frac{\partial U}{\partial r} - \frac{1}{\sin\theta}\frac{\partial S}{\partial\phi} &= \frac{1}{C_1^2+C_2^2}\left(\frac{C_2}{\sin\theta}\frac{\partial\mathscr{R}}{\partial\phi} - C_1\frac{\partial\mathscr{R}}{\partial\theta}\right).\end{aligned}\right\} \tag{73}$$

Eliminating the function S from equation (73) we obtain

$$a\frac{\partial}{\partial\phi}\left(v\frac{\partial U}{\partial r}\right)+a\frac{\partial}{\partial\theta}\left(u\sin\theta\frac{\partial U}{\partial r}\right)=-C_3\left\{\frac{\partial}{\partial\theta}\left(\sin\theta\frac{\partial\mathscr{R}}{\partial\theta}\right)+\frac{1}{\sin\theta}\frac{\partial^2\mathscr{R}}{\partial\phi^2}\right\}$$
$$-\sin\theta\left\{\frac{\partial C_3}{\partial\theta}\frac{\partial\mathscr{R}}{\partial\theta}+\frac{1}{\sin^2\theta}\frac{\partial C_3}{\partial\phi}\frac{\partial\mathscr{R}}{\partial\phi}\right\}, \tag{74}$$

where
$$C_3=C_1/(C_1^2+C_2^2) \tag{75}$$

is a form of the Cowling conductivity σ_3 based on height-integrated values of σ_1, σ_2.

The current function $\mathscr{R}$ is independent of r, and consequently

$$\frac{\partial C_3}{\partial\theta}\frac{\partial\mathscr{R}}{\partial\theta}+\frac{1}{\sin^2\theta}\frac{\partial C_3}{\partial\phi}\frac{\partial\mathscr{R}}{\partial\phi}=\nabla C_3\cdot\nabla\mathscr{R}. \tag{76}$$

Daily variations in the conductivity C_3 produce 1, 3, and 4 c/d magnetic tides from a semi-diurnal wind velocity and an axial geomagnetic dipole. Constant conductivity C_3 with a semi-diurnal wind velocity, with Chapman's (1919) dynamo theory, gives a good estimate of the semi-diurnal magnetic tide. Consider C_3 as a constant in equation (74), then equation (67) reduces to

$$a\frac{\partial}{\partial\phi}\left(v\frac{\partial U}{\partial r}\right)+a\frac{\partial}{\partial\theta}\left(u\sin\theta\frac{\partial U}{\partial r}\right)=-C_3\left\{\frac{\partial}{\partial\theta}\left(\sin\theta\frac{\partial\mathscr{R}}{\partial\theta}\right)+\frac{1}{\sin\theta}\frac{\partial^2\mathscr{R}}{\partial\phi^2}\right\}. \tag{77}$$

If an external magnetic tidal potential, V, with coefficients V_n^m in nanotesla, and R in kilometres,

$$V=R\sum_{n,m}\left(\frac{r}{R}\right)^n V_n^m Y_n^m(\theta\phi), \tag{78}$$

is produced by a steady surface distribution of current over a sphere of radius $r=a$ (the ionosphere), then the corresponding current function $\mathscr{R}$ for the toroidal current system, with a poloidal magnetic field equivalent to the observed magnetic tide, is given in amperes by Chapman & Bartels (1962, ch. 17, §18)

$$\mathscr{R}=\sum_{n,m}\mathscr{R}_n^m Y_n^m(\theta\phi), \tag{79}$$

where
$$\mathscr{R}_n^m=-\frac{10R}{4\pi}\left(\frac{a}{R}\right)^n\frac{2n+1}{n+1}V_n^m.$$

Here $R=6371$ km, $a/R=6486/6371$ (cf. equation (29)). Substitution of equation (79) into equation (77) gives

$$a\frac{\partial}{\partial\phi}\left(v\frac{\partial U}{\partial r}\right)+a\frac{\partial}{\partial\theta}\left(u\sin\theta\frac{\partial U}{\partial r}\right)=\frac{10C_3R}{4\pi}\sum_{n,m}n(2n+1)\left(\frac{a}{R}\right)^n V_n^m Y_n^m\sin\theta. \tag{80}$$

Consider now only the axial dipole term in the geomagnetic potential

$$U=-(R^3/r^2)\,G\cos\theta,\quad G=|G_1^0|,$$

which gives, at ionospheric levels $r=a$,

$$\frac{\partial U}{\partial r}=2\left(\frac{R}{a}\right)^3 G\cos\theta,\quad \frac{1}{a}\frac{\partial U}{\partial\theta}=\left(\frac{R}{a}\right)^3 G\sin\theta.$$

The dynamo equation (80) now becomes

$$\frac{1}{\sin\theta}\left\{\frac{\partial}{\partial\theta}(u\sin\theta\cos\theta)+\frac{\partial}{\partial\phi}(v\cos\theta)\right\}=\frac{5C_3}{4\pi G}\sum_{n,m}n(2n+1)\left(\frac{a}{R}\right)^{n+2}V_n^m Y_n^m(\theta\phi). \tag{81}$$

The equations of motion for atmospheric tides are linearized Eulerian equations of hydrodynamics for small oscillations of the atmosphere about a configuration of static equilibrium on a rotating Earth, namely

$$\frac{\partial u}{\partial t} - 2\Omega v \cos\theta = -\frac{1}{a}\frac{\partial F}{\partial \theta}, \tag{82}$$

$$\frac{\partial v}{\partial t} + 2\Omega u \cos\theta = -\frac{1}{a \sin\theta}\frac{\partial F}{\partial \phi}. \tag{83}$$

The function F represents the scalar potential of conservative forces

$$F = \delta p/\rho + V.$$

Assuming $e^{i\sigma t}$ time-dependence for the functions u, v, F, and $e^{im\phi}$ dependence upon longitude, the equations of motion become

$$i\sigma u - 2\Omega v \cos\theta = -(1/a)\,\partial F/\partial\theta, \tag{84}$$

$$i\sigma v + 2\Omega u \cos\theta = -(im/a \sin\theta)F. \tag{85}$$

The geophysical relevance of these equations is discussed by Stewartson & Walton (1976). Solving for u, v, we obtain

$$u = \frac{i\sigma}{4a\Omega^2(f^2 - \cos^2\theta)}\left(\frac{\partial}{\partial\theta} + \frac{m}{f}\cot\theta\right)F, \tag{86}$$

$$v = \frac{-\sigma}{4a\Omega^2(f^2 - \cos^2\theta)}\left(\frac{\cos\theta}{f}\frac{\partial}{\partial\theta} + \frac{m}{\sin\theta}\right)F, \tag{87}$$

where $f = \sigma/2\Omega$.

After Love (1913), Price & Cocks (1969) and Longuet-Higgins (1968), functions Φ and Ψ are introduced analogous to the velocity potential and stream function:

$$u = \frac{\partial\Phi}{\partial\theta} + \frac{1}{\sin\theta}\frac{\partial\Psi}{\partial\phi}, \quad v = \frac{1}{\sin\theta}\frac{\partial\Phi}{\partial\phi} - \frac{\partial\Psi}{\partial\theta}. \tag{88}$$

With this representation we find that

$$\frac{1}{\sin\theta}\left[\frac{\partial v}{\partial\phi} + \frac{\partial}{\partial\theta}(u \sin\theta)\right] = \nabla^2\Phi, \tag{89}$$

$$\frac{1}{\sin\theta}\left[\frac{\partial u}{\partial\phi} - \frac{\partial}{\partial\theta}(v \sin\theta)\right] = \nabla^2\Psi, \tag{90}$$

where the operator ∇^2 represents the horizontal Laplacian operator given by

$$\nabla^2 = \frac{1}{\sin\theta}\frac{\partial}{\partial\theta}\left(\sin\theta\frac{\partial}{\partial\theta}\right) + \frac{1}{\sin^2\theta}\frac{\partial^2}{\partial\phi^2}.$$

Using equations (86), (87) for u, v, we find that

$$\frac{1}{\sin\theta}\left[\frac{\partial v}{\partial\phi} + \frac{\partial}{\partial\theta}(u \sin\theta)\right] = \frac{i\sigma}{4a\Omega^2}\mathscr{L}F, \tag{91}$$

where the operator $\mathscr{L}$ is defined by

$$\mathscr{L}F = \frac{1}{\sin\theta}\frac{\partial}{\partial\theta}\left(\frac{\sin\theta}{f^2 - \cos^2\theta}\frac{\partial F}{\partial\theta}\right) - \frac{1}{f^2 - \cos^2\theta}\left[\frac{mf^2 + \cos^2\theta}{f f^2 - \cos^2\theta} + \frac{m^2}{\sin^2\theta}\right]F. \tag{92}$$

From equations (89), (91) it follows that

$$\nabla^2\Phi = (\mathrm{i}\sigma/4a\Omega^2)\,\mathscr{L}F. \tag{93}$$

We require eigenfunctions of the operator $\mathscr{L}$, denoted Θ^σ, i.e.

$$\mathscr{L}\Theta^\sigma = -(4a^2\Omega^2/gh^\sigma)\,\Theta^\sigma. \tag{94}$$

For a specific value of σ, such eigenfunctions form an orthogonal set. The eigenvalue $4a^2\Omega^2/gh^\sigma$ is chosen to correspond to the theory of the oscillations of a shallow ocean of depth h on a rotating sphere of radius a.

The displacement of the shallow ocean may be denoted ζ when $g\zeta$ corresponds to the function F used for the scalar potential of conservative forces in the theory of atmospheric tides. The equations of motion for the shallow ocean are otherwise identical with those of the oscillating atmosphere. The equation of continuity for the shallow ocean has the form

$$\frac{\partial\zeta}{\partial t} = \frac{h}{\sin\theta}\left[\frac{\partial v}{\partial\phi} + \frac{\partial}{\partial\theta}(u\sin\theta)\right],$$

which by equation (89) gives

$$\nabla^2\Phi = (\mathrm{i}\sigma/h)\,\zeta. \tag{95}$$

From equations (93,) (94) it follows that for atmospheric oscillations

$$\nabla^2\Phi = -(\mathrm{i}a\sigma/gh^\sigma)\,\Theta^\sigma, \tag{96}$$

and consequently from equation (96)

$$(\mathrm{i}/2a\Omega)\,\nabla^2\Theta^\sigma = -(gh^\sigma/2a^2\Omega\sigma)\,\nabla^4\Phi. \tag{97}$$

Now from

$$\frac{1}{\sin\theta}\left[\frac{\partial}{\partial\phi}(84) - \frac{\partial}{\partial\theta}\{(85)\sin\theta\}\right]$$

and

$$\frac{1}{\sin\theta}\left[\frac{\partial}{\partial\phi}(85) + \frac{\partial}{\partial\theta}\{(84)\sin\theta\}\right],$$

making use of equations (89), (90) and with the substitution

$$f = \sigma/2\Omega, \quad \partial/\partial\phi = \mathrm{i}m,$$

we obtain

$$(f\nabla^2 + m)\,\mathrm{i}\Psi - (\cos\theta\nabla^2 - \sin\theta\,\partial/\partial\theta)\,\Phi = 0 \tag{98}$$

$$(f\nabla^2 + m)\,\Phi - (\cos\theta\nabla^2 - \sin\theta\,\partial/\partial\theta)\,\mathrm{i}\Psi = (\mathrm{i}/2\Omega a)\,\nabla^2 F. \tag{99}$$

When the function F is an eigenfunction of Hough's equation (94), derived from the equations of motion, $F = \Theta^\sigma$, and

$$\begin{aligned}(\mathrm{i}/2\Omega a)\,\nabla^2 F &= (\mathrm{i}/2\Omega a)\,\nabla^2\Theta^\sigma,\\ &= -(gh^\sigma/2a^2\Omega\sigma)\,\nabla^4\Phi,\end{aligned} \tag{100}$$

by equation (97).

When a parameter ϵ is introduced such that

$$1/\epsilon = gh^\sigma/4a^2\Omega^2$$

and

$$1/\epsilon f = gh^\sigma/2a^2\Omega\sigma, \tag{101}$$

equation (99) becomes

$$\{f\nabla^2 + m + (1/\epsilon f)\,\nabla^4\}\,\Phi - (\cos\theta\nabla^2 - \sin\theta\,\partial/\partial\theta)\,\mathrm{i}\Psi = 0. \tag{102}$$

Let Φ and Ψ be represented by sums of spherical harmonics:

$$\Phi = \sum_{n=m}^{\infty} A_n^m P_n^m(\mu)\, e^{i(m\phi+\sigma t)}, \tag{103}$$

$$\Psi = \sum_{n=m}^{\infty} iB_n^m P_n^m(\mu)\, e^{i(m\phi+\sigma t)}, \tag{104}$$

where $\mu = \cos\theta$ and $\nabla^2 P_n^m = -n(n+1)P_n^m$.

The functions $\nabla^2\Phi$, being proportional to the displacement ζ of a shallow ocean, as in equation (95), are the Hough functions

$$\nabla^2\Phi = \sum_{n=m}^{\infty} -n(n+1)A_n^m P_n^m(\mu)\, e^{i(m\phi+\sigma t)}, \tag{105}$$

and the exact form of these functions will depend upon the choice of normalization.

If the Earth's main magnetic field is represented by an axial dipole, it will now be shown that the geomagnetic tide resulting from a Hough function, $\{n(n+1)A_n^m\}$, will have a potential $\{V_n^m\}$, that can be derived directly from the function Ψ, namely $\{B_n^m\}$, and that the sets of coefficients $\{A_n^m\}$, $\{B_n^m\}$ are linearly related.

From the equations of motion, equations (84), (85), it follows that

$$\begin{aligned}
&\frac{1}{\sin\theta}\left\{\frac{\partial}{\partial\theta}(u\sin\theta\cos\theta)+\frac{\partial}{\partial\phi}(v\cos\theta)\right\}\\
&\quad=\frac{-i\sigma}{2\Omega\sin\theta}\left\{\frac{\partial}{\partial\theta}(v\sin\theta)-\frac{\partial u}{\partial\phi}\right\}\quad\text{(Maeda } et\ al.\ 1979)\\
&\quad=\frac{i\sigma}{2\Omega}\nabla^2\Psi,\quad\text{by equation (90),}\\
&\quad=\frac{\sigma}{2\Omega}\sum_{n=m}^{\infty} n(n+1)B_n^m P_n^m e^{i(m\phi+\sigma t)},\quad\text{by equation (104),}\\
&\quad=\frac{5C_3}{4\pi G}\sum_{n=m}^{\infty} n(2n+1)\left(\frac{a}{R}\right)^{n+2} V_n^m P_n^m e^{i(m\phi+\sigma t)},\quad\text{by equation (81).}
\end{aligned}$$

Therefore, of the Φ and Ψ components of wind velocity, only the Ψ component produces a magnetic tide. The following theory will show that associated with any eigenfunction Ψ is a uniquely determined eigenfunction Φ. Thus, by including the equation of motion in the theory of the ionospheric dynamo, the non-uniqueness in deriving the wind velocity from the magnetic tide (Price 1968) is resolved. By the orthogonality of the associated Legendre functions, it follows from the last equation that

$$V_n^m = \frac{4\pi G}{5C_3}\frac{\sigma}{2\Omega}\frac{n+1}{2n+1}\left(\frac{R}{a}\right)^{n+2} B_n^m, \tag{106}$$

as required, i.e. the magnetic tides associated with the Hough function $\nabla^2\Phi$ are proportional to $\nabla^2\Psi$, where Φ and Ψ are used in the representation of the wind velocity vector as in equation (88).

Eigenfunction calculations were made as described by Longuet-Higgins (1968), and the notation used to refer to the various eigenvectors is that of Flattery (1967). The method of Longuet-Higgins uses f as the required eigenvalue, and starts by estimating a value of the parameter $1/\epsilon f$, which remains constant for the calculation.

To provide a brief description of Hough-function calculations, it will be convenient to introduce an unnormalized associated Legendre function $P_{n,m}$, where

$$P_{n,m} = \frac{1}{2^n n!}(1-\mu^2)^{\frac{1}{2}m}\left(\frac{\mathrm{d}}{\mathrm{d}\mu}\right)^{n+m}(\mu^2-1)^n \tag{107}$$

and

$$\Phi = \sum_{n=m}^{\infty} A_{n,m} P_{n,m} \mathrm{e}^{\mathrm{i}(m\phi+\sigma t)}, \quad \Psi = \sum_{n=m}^{\infty} \mathrm{i}B_{n,m} P_{n,m} \mathrm{e}^{\mathrm{i}(m\phi+\sigma t)}. \tag{108}$$

Recurrence relations are given by

$$\nabla^2 P_{n,m} = -n(n+1) P_{n,m}, \tag{109}$$

$$\cos\theta P_{n,m} = \frac{n+m}{2n+1} P_{n-1,m} + \frac{n-m+1}{2n+1} P_{n+1,m}, \tag{110}$$

$$\cos\theta \nabla^2 P_{n,m} - \sin\theta \frac{\mathrm{d}P_{n,m}}{\mathrm{d}\theta} = -\frac{(n-1)(n+1)(n+m)}{2n+1} P_{n-1,m} - \frac{n(n+2)(n-m+1)}{2n+1} P_{n+1,m}. \tag{111}$$

Equations (102), (98) become respectively

$$\left\{-n(n+1)f + m + \frac{1}{\epsilon f} n^2(n+1)^2\right\} A_{n,m} + \left\{\frac{n(n+2)(n+m+1)}{2n+3} B_{n+1,m} + \frac{(n-1)(n+1)(n-m)}{2n-1} B_{n-1,m}\right\} = 0, \tag{112}$$

$$\{n(n+1)f - m\} B_{n,m} - \left\{\frac{n(n+2)(n+m+1)}{2n+3} A_{n+1,m} + \frac{(n-1)(n+1)(n-m)}{2n-1} A_{n-1,m}\right\} = 0, \tag{113}$$

which can be written

$$\left.\begin{aligned} K_{n,m} A_{n,m} + p_{n+1,m} B_{n+1,m} + q_{n-1,m} B_{n-1,m} &= 0, \\ L_{n,m} B_{n,m} - p_{n+1,m} A_{n+1,m} - q_{n-1,m} A_{n-1,m} &= 0, \end{aligned}\right\} \tag{114}$$

$$\begin{aligned} K_{n,m} &= f - m/n(n+1) - (1/\epsilon f) n(n+1), \\ L_{n,m} &= f - m/n(n+1), \\ p_{n+1,m} &= (n+2)(n+m+1)/(n+1)(2n+3), \\ q_{n-1,m} &= (n-1)(n-m)/(2n-1)(2n+1). \end{aligned}$$

The equations form two groups, the first consisting of terms symmetric about the equator,

$$\begin{bmatrix} K_{n,m} & p_{m+1,m} & 0 & 0 & \cdots \\ q_{m,m} & L_{m+1,m} & p_{m+2,m} & 0 & \cdots \\ 0 & q_{m+1,m} & K_{m+2,m} & p_{m+3,m} & \cdots \\ 0 & 0 & q_{m+2,m} & L_{m+3,m} & \cdots \\ \cdot & \cdot & \cdot & \cdot & \cdots \\ \cdot & \cdot & \cdot & \cdot & \cdots \\ \cdot & \cdot & \cdot & \cdot & \cdots \end{bmatrix} \begin{bmatrix} A_{m,m} \\ B_{m+1,m} \\ A_{m+2,m} \\ B_{m+3,m} \\ \cdot \\ \cdot \\ \cdot \end{bmatrix} = \begin{bmatrix} 0 \\ 0 \\ 0 \\ 0 \\ \cdot \\ \cdot \\ \cdot \end{bmatrix}, \tag{115}$$

and the second containing only terms that are antisymmetric about the equator.

For a given tidal frequency σ (or f), an infinite number of eigenvectors is obtained, with eigenvalues in the form of equivalent depths h^σ, which for convenience are arranged in descending order of magnitude.

In terms of Schmidt quasinormalized functions, it will be clear that sets of coefficients

$$\begin{bmatrix} A_m^m \\ A_{m+2}^m \\ A_{m+4}^m \\ \cdot \\ \cdot \\ \cdot \end{bmatrix}, \quad \begin{bmatrix} B_{m+1}^m \\ B_{m+3}^m \\ B_{m+5}^m \\ \cdot \\ \cdot \\ \cdot \end{bmatrix}$$

are obtained simultaneously in the Longuet-Higgins formulation of the eigenfunction calculation.

The series $\{A_n^m\}$ leads to the Hough function, representing the Φ component of wind velocity, while the series $\{B_n^m\}$ gives the Ψ component of wind velocity, and, by means of equation (106), the corresponding magnetic tide.

For a given σ (or f), a parameter ϵ, denoted ϵ^σ, is obtained for each eigenvector. The corresponding equivalent depth h^σ is given by equation (106) as

$$h^\sigma = \frac{4a^2\Omega^2}{g}\frac{1}{\epsilon^\sigma}, \quad \text{i.e.} \quad h^\sigma = \frac{1}{0.01135}\frac{1}{\epsilon^\sigma}, \tag{116}$$

where Ω is the rate of the Earth's rotation in radians per second.

Flattery (1967) in his tables 71–72 gives

$$h^\sigma = 0.01135/\epsilon^\sigma \text{ km},$$

which is apparently a misprint, because the tabulated values are correct. Hough-function calculations have also been published by Kato (1966*a*, *b*), Möhlmann (1975), Jones (1970, 1973), Volland (1974), Chen Zhe-Ming (1979).

Associated with each eigenfunction is a vertical structure or variation of velocity and phase with height, dependent upon the variation of temperature with height. Comparison of the vertical structures of the eigenfunctions with the structures expected on the basis of the mechanism of generation, e.g. absorption of u.v. radiation by ozone, restricts the eigenfunctions relevant to the problem. From the work of Stening (1968, 1969, 1977*a*), Tarpley (1970*a*, *b*), Ayamenc (1974), Forbes & Lindzen (1976), Evans (1978), Forbes & Garrett (1979) and Richmond (1979), the most important modes for diurnal solar and lunar magnetic tides are, in the notation of Flattery (1967), (1, −2), (1, 1), and for the semi-diurnal solar and lunar magnetic tides (2, 2) and (2, 4).

For each of the four diurnal local time harmonics computed for the solar and lunar magnetic tides, the results presented include two spherical harmonic coefficients, corresponding to the magnetic tide produced by some combination of Hough functions. By using equation (106) and the known combinations of spherical harmonics in the Hough functions indicated above, it is possible to obtain an estimate of the appropriate combination of Hough functions.

The solar diurnal tide

For the solar diurnal mode $S_1(1, -2)$, the first symmetric diurnal rotational (trapped) mode, the relevant parameters are $f = 0.498634$, equivalent depth $h = -12.2703$ km, with a Hough function in Schmidt quasinormalized functions

$$P_1^1 + 0.749795\, P_3^1 + 0.096703\, P_5^1 + 0.005154\, P_7^1,$$

and, apart from a multiplicative factor $4\pi Gf/5C_3$, the corresponding magnetic tide is

$$-0.345514\, P_2^1 - 0.038109\, P_4^1 - 0.001953\, P_6^1 - 0.000057\, P_8^1.$$

For the solar diurnal mode $S_1(1, 1)$, the symmetric diurnal gravitational (propagating) mode, the relevant parameters are $f = 0.498634$, equivalent depth $h = 0.690886$ km, with a Hough function

$$P_1^1 - 3.448455\, P_3^1 + 4.202936\, P_5^1 - 2.660800\, P_7^1,$$

and corresponding magnetic tide

$$0.020349\, P_2^1 + 0.061159\, P_4^1 - 0.049323\, P_6^1 + 0.020816\, P_8^1.$$

The trapped $(1, -2)$ mode is therefore seen to be a more efficient producer of magnetic tides than the propagating (1, 1) mode. The $(1, -2)$ mode generates principally the P_2^1 magnetic tide, while the (1, 1) mode somewhat inefficiently generates principally the P_4^1 magnetic tide. This supports the work of Stening (1969) and Tarpley (1970*b*) showing that the $(1, -2)$ mode reproduces the S_q system well.

The observed solar diurnal external local time magnetic tide has dominant terms of the form

$$(6146\, P_2^1 - 1100\, P_4^1) \cos(t^* + 19°). \tag{117}$$

Such a magnetic tide would be produced by the following numerical combination of Hough-function modes:

$$\{-19561\, S_1(1, -2) - 30109\, S_1(1, 1)\} \cos(t^* + 19°), \tag{118}$$

which indicates that greater velocities in the dynamo-producing region are associated with the (1, 1) mode rather than the $(1, -2)$ mode. Hines (1966) and Richmond (1971) note that the average diurnal tide in the 90–120 km region appears to be dominated by the (1, 1) mode.

It has been inferred in the present paper, in §5, that the day-to-day variability of S is associated with the equator-symmetric local time terms P_1^1, P_3^1, P_2^2 in the geomagnetic tidal potential. Such terms could not be produced by the $(1, -2)$ or (1, 1) tidal modes (Matsushita 1973), and the modes $(1, -1)$, $(1, -3)$ are implicated, i.e. the day-to-day variability of such modes produces the day-to-day variability of S.

Solar semidiurnal tide

For the $S_2(2, 2)$ mode the relevant parameters are $f = 0.99726956$, equivalent depth $h = 7.85193$ km, with Hough function

$$P_2^2 - 0.339478\, P_4^2 + 0.040984\, P_6^2 - 0.002458\, P_8^2,$$

and, apart from a multiplicative factor $4\pi Gf/5C_3$, the corresponding magnetic tide is

$$-0.031232\, P_3^2 + 0.004263\, P_5^2 - 0.000270\, P_7^2 + 0.000010\, P_9^2.$$

For the $S_2(2, 4)$ mode, $f = 0.99726956$, $h = 2.10979$ km with Hough function

$$P_2^2 + 4.958338\, P_4^2 - 4.060083\, P_6^2 + 1.191571\, P_8^2,$$

and magnetic tide

$$-0.127091\, P_3^2 - 0.034474\, P_5^2 + 0.022321\, P_7^2 - 0.004416\, P_9^2,$$

which show that both the (2, 2) and (2, 4) modes act as efficient generators of the P_3^2 semi-diurnal local time term in the geomagnetic tidal potential, but that only the (2, 2) mode is able to produce the 180° difference between the P_2^2 and P_4^2 terms of the geomagnetic tidal potential.

The observed solar semi-diurnal external magnetic tide has dominant terms of the form

$$2922 \cos (2t^* + 197°) P_3^2 + 281 \cos (2t^* + 47°) P_5^2 \qquad (119)$$

and such a magnetic tide would be approximated by the following numerical combination of tides:

$$\{-84\,305\ S_2(2,2) - 2274\ S_2(2,4)\} \cos (2t^* + 197°) \qquad (120)$$

which shows that the (2, 2) mode is the dominant mode in the dynamo region. This result is in agreement with the results of Tarpley (1970*b*) and Stening (1977*a*). Forbes & Lindzen (1976) using a more general form of the dynamo theory than that of the present paper found that at mid-latitudes the relative contributions of the (2, 2) and (2, 4) modes were roughly equal, but that the (2, 2) mode accounted for almost all of the equatorial magnetic variation.

However, meteor-trail observations and the analysis of chemical-release trails indicate that the period of vertical wavelength of wind patterns are near values expected for the (2, 4) mode. Salah (1974), Salah & Wand (1974), and Salah *et al.* (1975) show that the (2, 4) mode dominates in the mid-latitude E-region thermal structure in the altitude range 100 to 125 km. The data of Ayamenc (1974) show that the (2, 2) mode is the dominant semi-diurnal mode above 130 km, and the (2, 4) mode is dominant below this height. More interestingly, Volland (1971) considers that the S_q current height of 115 km determined by rocket-borne measurements is only a secondary maximum and that the centre of the S_q current system should be between 130 km and 160 km. Forbes & Lindzen (1976) find vertical current densities that support the expectations of Volland (1971).

Finally we note that a comparison of equations (118), (120) shows that the semi-diurnal winds are stronger than the diurnal winds even though, from equations (117), (119), the diurnal component of S is stronger than the semi-diurnal component. This is in agreement with the results of Roper (1966) and White (1960). Möhlmann (1976*b*) notes that the ionospheric quiet time electrostatic potential is due to the dynamo action of the diurnal (1, −2) and (1, 1) modes. Richmond *et al.* (1976) showed electric fields associated with (1, −2) and (2, 4) modes to be in fair agreement with observations.

Lunar semi-diurnal tide

For the $M_2(2, 2)$ mode the relevant parameters are $f = 0.963\,498$, equivalent depth $h = 7.070\,064$ km, with Hough function

$$P_2^2 - 0.374\,713\ P_4^2 + 0.050\,097\ P_5^2 - 0.003\,331\ P_7^2$$

and, apart from a multiplicative factor $4\pi Gf/5C_3$, the corresponding magnetic tide is

$$-0.031\,892\ P_3^2 + 0.004\,842\ P_5^2 - 0.000\,340\ P_7^2 + 0.000\,014\ P_9^2.$$

For the $M_2(2, 4)$ mode, f is as for the (2, 2) mode, equivalent depth $h = 1.848\,642$ km, with Hough function

$$P_2^2 + 4.408\,820\ P_4^2 - 4.194\,317\ P_6^2 + 1.408\,951\ P_8^2,$$

and magnetic tide

$$-0.122\,113\ P_3^2 - 0.026\,941\ P_5^2 + 0.023\,043\ P_7^2 - 0.005\,310\ P_9^2.$$

The observed lunar semi-diurnal external magnetic tide for 1964–65 has dominant terms of the form

$$254 \cos (2t^* - 2s + 2h + 261°) P_3^2 + 108 \cos (2t^* - 2s + 2h + 79°) P_5^2. \qquad (121)$$

Such a magnetic tide would be produced by the following numerical combination of modes:

$$\{-13\,814\ \mathrm{M}_2(2,2)+1528\ \mathrm{M}_2(2,4)\}\cos(2t^*-2s+2h+261°) \tag{122}$$

showing that the (2, 2) mode dominates the (2, 4) mode. The ratio of (2, 4) to (2, 2) modes is greater for the lunar than for the solar semi-diurnal tides. By comparing equations (119), (122), it will be seen that the solar semi-diurnal modes (2, 2), (2, 4) have the same sign, while the lunar semi-diurnal modes have opposite signs. The different combinations of modes also appears as a disparity in the ratio P_5^2/P_3^2 for lunar and solar semi-diurnal local time magnetic tides, being 281/2922 for solar terms and 108/254 for lunar terms, as noted in §5.

By analogy with the behaviour of the solar fundamental semi-diurnal (2, 2) tide which generates higher-order modes (2, 4) and (2, 5) through mode coupling via background winds in the mesosphere, Evans (1978) suggests that the lunar (2, 2) tide may also produce higher-order modes through such coupling. He notes that since the solar (2, 4) and (2, 5) modes appear to dominate in the lower E-region (105–125 km), the ionospheric effects that have been attributed to the lunar (2, 2) tide should be re-examined to see if they can be better explained as consequences of the lunar (2, 4), (2, 5) modes. The results for the lunar semi-diurnal mode given above indicate that the lunar (2, 2) mode is the dominant mode in the generation of lunar semi-diurnal magnetic tides, and consequently if the (2, 4) and (2, 5) modes are generated in the dynamo region through mode coupling via background winds, then they make only a minor contribution to the observed magnetic tides. From these results and from those for the solar semi-diurnal tide, it would appear that the lower E-region is not the dynamo region.

Lunar semi-diurnal elliptic magnetic tide

For the $\mathrm{N}_2(2,2)$ mode, $f = 0.945406$, equivalent depth $h = 6.666701$ km, and the Hough function is

$$P_2^2-0.395710\,P_4^2+0.055995\,P_6^2-0.003944\,P_8^2,$$

with corresponding magnetic tide

$$-0.032227\,P_3^2+0.005192\,P_5^2-0.000387\,P_7^2+0.000017\,P_9^2.$$

For the $\mathrm{N}_2(2,4)$ mode, f is as for the $\mathrm{N}_2(2,2)$ mode, equivalent depth $h = 1.71755$ km, with Hough function

$$P_2^2+4.122096\,P_4^2-4.271794\,P_6^2+1.548171\,P_8^2$$

and magnetic tide

$$-0.119417\,P_3^2-0.022731\,P_5^2+0.023386\,P_7^2-0.005880\,P_9^2.$$

The observed lunar elliptic semi-diurnal local time tide for I.Q.S.Y. years 1964–65 has the form

$$\{84\,P_3^2-17\,P_5^3\}\cos(2t^*-3s+2h+p+284°).$$

Such a magnetic tide is produced by the following numerical combination of modes:

$$\{-2913\ \mathrm{N}_2(2,2)+83\ \mathrm{N}_2(2,4)\}\cos(2t^*-3s+2h+p+284°).$$

The $\mathrm{N}_2(2,2)$ and $\mathrm{N}_2(2,4)$ modes differ in sign, as do the corresponding $\mathrm{M}_2(2,2)$ and $\mathrm{M}_2(2,4)$ modes. The ratio of the $\mathrm{N}_2(2,4)$ and $\mathrm{N}_2(2,2)$ modes is smaller than that for M_2 and is closer to the ratio given by the solar than by the lunar semi-diurnal tides. The ratio of coefficients $P_5^2/P_3^2 = 17/84$ is midway between the ratio for the lunar magnetic tide, namely 108/254 and that for the solar magnetic tides, 281/2922.

7. Summary

Hourly mean values of the Earth's magnetic field from a total of 253 707 element-days from 130 magnetic observatories operating during the I.Q.S.Y. years 1964–65 have been analysed for solar, lunar and lunar elliptic magnetic tides, and their seasonal change. Results for all tides have been expressed in a way that provides a wealth of material for electrical conductivity modelling of the Earth's interior.

The ionospheric dynamo theory of Schuster (1908), Chapman (1919) and Baker & Martyn (1952) is found to be adequate in that the amplitudes of the four principal daily harmonics of the lunar magnetic tide are found to be in reasonable accord with the theory. The wind velocity is assumed to have a scalar potential of the form P_2^2. For the solar magnetic tide S, an additional wind velocity potential of the form P_1^1 is required. By using coefficients of local time semi-diurnal terms P_3^2, P_5^2 and diurnal terms P_1^1, P_3^1, the results are interpreted in terms of the known modal structure of winds in the upper atmosphere.

Any contribution from the direct dynamo action of the ocean has been removed from both lunar and lunar elliptic tides by using the calculation of Malin (1970). The physical relevance of the calculation is indicated by the absence of an ocean dynamo component in the seasonal magnetic tide $L(2s-3h)$.

Equator-symmetric sectorial terms in phase-law and partial tides in $L(2s-2h)$ and $L(3s-2h-p)$ are considered to be associated with harmonics of the 27-day recurrence tendency in magnetic activity. Sectorial local time terms in the solar magnetic tide appear to be associated with the wind velocity modes $(1, -1)$ and $(2, 3)$. Local time sectorial terms are responsible for the difference in intensity of the S_q overhead current foci in the Northern and Southern Hemispheres, and because the terms depend upon local time only, they cannot arise from the influence of geographical or topographical features of the Earth. The day-to-day variability of S is, following the work of Hasegawa (1960), associated with the variability of local time sectorial terms in the S potential.

Comparison of the results for the solar and lunar magnetic tides with the corresponding results derived by Malin (1973) for the I.G.Y. years indicates important differences between the variation of solar and lunar magnetic tides with increasing sunspot number.

The seasonal variation of the lunar magnetic tide is found to be three times greater than that of the solar magnetic tide. Extremum amplitudes of the lunar magnetic tide occur in early August and early February, while extremum amplitudes for solar magnetic tides occur in June and December. There is evidence for a dynamo contribution from the tide K_1 in the seasonal variation of the solar magnetic tide.

The lunar elliptic tide $L(3s-2h-p)$ is such that it gives rise to enhanced values of the principal lunar tide $L(2s-2h)$ at perigee, $s-p = 0$, the closest approach of the Moon to the Earth. There are, however, some differences between the lunar and lunar elliptic tides. The phase of the lunar elliptic tide is in advance of the lunar magnetic tide, and the lunar elliptic tide diurnal term is greater than the semi-diurnal term. The semi-annual variation of S relative to S is much smaller than the semi-annual variation of $L(2s-2h)$ relative to $L(2s-2h)$. It is suggested that some analyses of the semi-annual variation of the lunar magnetic tide have in fact simply 'rectified' the annual or seasonal variation to give it a semi-annual appearance. Dominant terms in the semi-annual variation of the lunar magnetic tide are principally zonal, as if associated with variations of a disturbance ring current about the Earth.

TABLE 8.1 (*a*). SPHERICAL HARMONIC ANALYSIS OF MAGNETIC PHASE-LAW TIDES $L(2s-2h)_{\text{iono.}}$

(Amplitudes in picoteslas; phase angles in degrees.)

n j k / n j k	internal I / I′	α^k_{jmi} / β^k_{jmi}	external II / II′	α^k_{jme} / β^k_{jme}
1 1 0	27 ± 21	322	91 ± 34	300
1 1 1	39 ± 14	233	33 ± 19	157
1 1 1	4 ± 14	241	38 ± 19	63
1 2 0	31 ± 16	186	190 ± 21	152
1 2 1	131 ± 14	88	174 ± 17	86
1 2 1	27 ± 14	237	47 ± 17	319
1 2 2	42 ± 11	163	99 ± 13	181
1 2 2	20 ± 11	32	43 ± 13	51
1 3 0	15 ± 15	236	21 ± 19	270
1 3 1	21 ± 11	229	26 ± 13	340
1 3 1	23 ± 11	62	30 ± 13	269
1 3 2	22 ± 11	272	63 ± 12	225
1 3 2	14 ± 11	190	18 ± 12	131
1 4 0	9 ± 12	44	72 ± 13	3
1 4 1	33 ± 8	309	117 ± 9	245
1 4 1	12 ± 8	311	44 ± 9	50
1 4 2	6 ± 8	162	39 ± 9	53
1 4 2	17 ± 8	333	36 ± 9	305
2 1 1	42 ± 26	48	219 ± 33	167
2 1 1	61 ± 26	233	83 ± 33	119
2 2 1	52 ± 22	231	55 ± 26	37
2 2 1	82 ± 22	53	81 ± 26	238
2 2 2	71 ± 20	89	69 ± 24	297
2 2 2	81 ± 20	6	54 ± 24	198
2 3 1	44 ± 17	39	153 ± 19	332
2 3 1	36 ± 17	184	86 ± 19	77
2 3 2	214 ± 18	291	254 ± 20	261
2 3 2	24 ± 18	146	72 ± 20	332
2 3 3	11 ± 15	282	159 ± 17	3
2 3 3	24 ± 15	57	53 ± 17	235
2 4 1	18 ± 13	54	47 ± 14	132
2 4 1	7 ± 13	187	77 ± 14	182
2 4 2	56 ± 14	140	21 ± 16	267
2 4 2	33 ± 14	246	55 ± 16	158
2 4 3	46 ± 12	22	41 ± 13	68
2 4 3	24 ± 12	233	63 ± 13	33
2 5 2	21 ± 11	122	108 ± 13	79
2 5 2	11 ± 11	32	43 ± 13	308
3 2 2	10 ± 9	336	147 ± 12	345
3 2 2	44 ± 9	207	42 ± 12	74
3 3 2	21 ± 9	41	19 ± 10	169
3 3 2	38 ± 9	12	43 ± 10	192
3 3 3	28 ± 9	241	48 ± 10	120
3 3 3	37 ± 9	237	9 ± 10	69
3 4 2	21 ± 8	168	36 ± 8	154
3 4 2	17 ± 8	200	25 ± 8	279
3 4 3	101 ± 8	114	134 ± 9	93
3 4 3	40 ± 8	71	26 ± 9	303
3 4 4	4 ± 8	74	108 ± 9	203
3 4 4	34 ± 8	21	15 ± 9	208
3 5 2	14 ± 6	306	9 ± 6	4
3 5 2	5 ± 6	42	4 ± 7	103
3 5 3	13 ± 7	269	42 ± 8	140
3 5 3	6 ± 7	220	33 ± 8	128
3 5 4	19 ± 6	214	37 ± 7	1
3 5 4	17 ± 6	192	20 ± 7	46
3 6 3	20 ± 6	359	61 ± 6	314
3 6 3	9 ± 6	198	17 ± 6	311
4 3 3	14 ± 4	183	35 ± 5	146
4 3 3	8 ± 4	127	7 ± 5	66
4 4 3	2 ± 4	272	10 ± 4	192
4 4 3	12 ± 4	280	11 ± 4	272
4 4 4	5 ± 4	72	9 ± 4	330
4 4 4	17 ± 4	332	6 ± 4	196
4 5 3	8 ± 3	333	8 ± 3	273
4 5 3	6 ± 3	88	9 ± 3	89
4 5 4	26 ± 3	291	42 ± 4	272
4 5 4	2 ± 3	178	5 ± 4	293
4 5 5	11 ± 3	44	27 ± 3	32
4 5 5	5 ± 3	349	6 ± 3	253
4 6 4	7 ± 3	22	7 ± 3	323
4 6 4	6 ± 3	199	1 ± 3	276

I, $A^k_{jmi}\cos(k\phi+mt+\alpha^k_{jmi})P^k_j$; II, $A^k_{jme}\cos(k\phi+mt+\alpha^k_{jme})P^k_j$;
I′, $B^k_{jmi}\cos(k\phi-mt+\beta^k_{jmi})P^k_j$; II′, $B^k_{jme}\cos(k\phi-mt+\beta^k_{jme})P^k_j$.

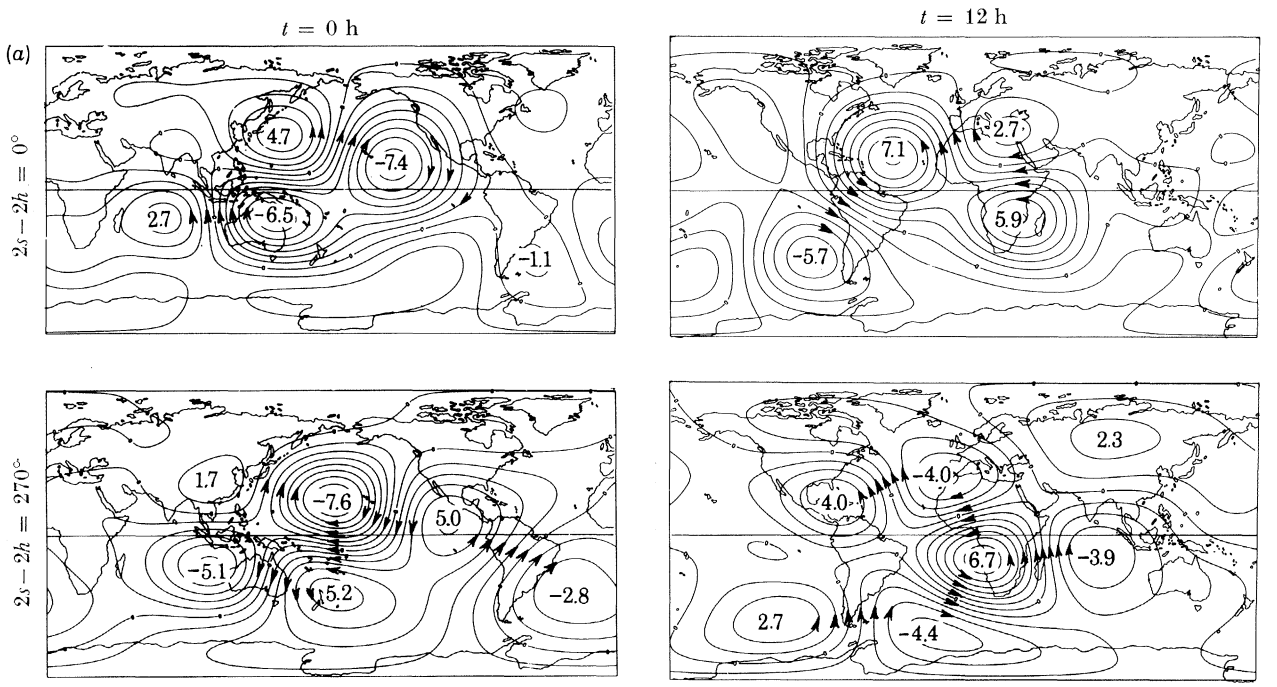

FIGURE 8.1 (*a*). $L(2s-2h)_{\text{iono.}}$ phase-law tide current function; extrema in kiloamperes.

TABLE 8.1 (*b*). SPHERICAL HARMONIC ANALYSIS OF MAGNETIC PHASE-LAW TIDE $L(3s-2h-p)_{\text{iono.}}$

(Amplitudes in picoteslas; phase angles in degrees.)

			internal		external	
n	j	k	I	α^k_{jmi}	II	α^k_{jme}
n	j	k	I′	β^k_{jmi}	II′	β^k_{jme}
1	1	0	31 ± 16	31	77 ± 23	47
1	1	1	47 ± 10	64	91 ± 13	37
1	1	1	27 ± 10	177	16 ± 13	42
1	2	0	19 ± 13	113	36 ± 17	195
1	2	1	28 ± 10	79	93 ± 12	93
1	2	1	14 ± 10	34	36 ± 12	129
1	2	2	16 ± 8	155	24 ± 10	86
1	2	2	15 ± 8	328	16 ± 10	332
1	3	0	12 ± 11	202	27 ± 13	332
1	3	1	21 ± 8	173	7 ± 10	240
1	3	1	15 ± 8	161	20 ± 10	8
1	3	2	4 ± 8	13	23 ± 9	194
1	3	2	6 ± 8	138	2 ± 9	31
1	4	0	11 ± 9	14	25 ± 10	78
1	4	1	26 ± 6	317	33 ± 7	274
1	4	1	19 ± 6	1	8 ± 7	130
1	4	2	6 ± 6	286	18 ± 7	7
1	4	2	5 ± 6	94	20 ± 7	199
2	1	1	19 ± 17	343	90 ± 21	173
2	1	1	29 ± 17	270	15 ± 21	159
2	2	1	26 ± 15	188	60 ± 17	318
2	2	1	4 ± 15	82	35 ± 17	259
2	2	2	42 ± 13	206	98 ± 15	214
2	2	2	32 ± 13	50	5 ± 15	307
2	3	1	17 ± 11	307	30 ± 13	97
2	3	1	22 ± 11	297	40 ± 13	16
2	3	2	49 ± 11	287	84 ± 13	284
2	3	2	18 ± 11	220	28 ± 13	16
2	3	3	15 ± 10	321	37 ± 11	317
2	3	3	16 ± 10	46	29 ± 11	256
2	4	1	17 ± 8	177	37 ± 10	207
2	4	1	16 ± 8	227	34 ± 10	231
2	4	2	1 ± 10	115	17 ± 11	230
2	4	2	25 ± 10	46	15 ± 11	195
2	4	3	6 ± 8	2	6 ± 9	96
2	4	3	24 ± 8	244	16 ± 9	233
2	5	2	11 ± 8	153	17 ± 8	109
2	5	2	15 ± 8	265	9 ± 8	336
3	2	2	5 ± 5	98	47 ± 6	26
3	2	2	10 ± 5	241	15 ± 6	16
3	3	2	5 ± 5	171	23 ± 5	183
3	3	2	7 ± 5	342	13 ± 5	57
3	3	3	8 ± 4	21	26 ± 5	80
3	3	3	11 ± 5	227	6 ± 5	172
3	4	2	6 ± 4	195	18 ± 4	194
3	4	2	11 ± 4	123	11 ± 4	242
3	4	3	20 ± 4	125	26 ± 5	89
3	4	3	10 ± 4	47	9 ± 5	302
3	4	4	6 ± 4	49	23 ± 5	226
3	4	4	13 ± 4	24	1 ± 5	283
3	5	2	3 ± 3	334	14 ± 3	38
3	5	2	7 ± 3	22	15 ± 3	67
3	5	3	9 ± 4	32	2 ± 4	265
3	5	3	6 ± 4	322	10 ± 4	119
3	5	4	13 ± 3	226	4 ± 4	18
3	5	4	13 ± 3	183	9 ± 4	20
3	6	3	3 ± 3	347	7 ± 3	31
3	6	3	3 ± 3	163	2 ± 3	163
4	3	3	4 ± 3	266	19 ± 3	203
4	3	3	6 ± 3	154	3 ± 3	124
4	4	3	2 ± 3	88	3 ± 3	38
4	4	3	6 ± 3	352	3 ± 3	277
4	4	4	7 ± 3	24	19 ± 3	333
4	4	4	5 ± 3	303	4 ± 3	129
4	5	3	11 ± 2	2	20 ± 2	345
4	5	3	4 ± 2	100	7 ± 2	80
4	5	4	4 ± 2	295	5 ± 3	261
4	5	4	3 ± 2	97	6 ± 3	341
4	5	5	4 ± 2	108	12 ± 2	51
4	5	5	3 ± 2	333	1 ± 2	298
4	6	4	4 ± 2	52	6 ± 2	358
4	6	4	3 ± 2	104	4 ± 2	136

I, $A^k_{jmi}\cos(k\phi+mt+\alpha^k_{jmi})P^k_j$; II, $A^k_{jme}\cos(k\phi+mt+\alpha^k_{jme})P^k_j$;
I′, $B^k_{jmi}\cos(k\phi-mt+\beta^k_{jmi})P^k_j$; II′, $B^k_{jme}\cos(k\phi-mt+\beta^k_{jme})P^k_j$.

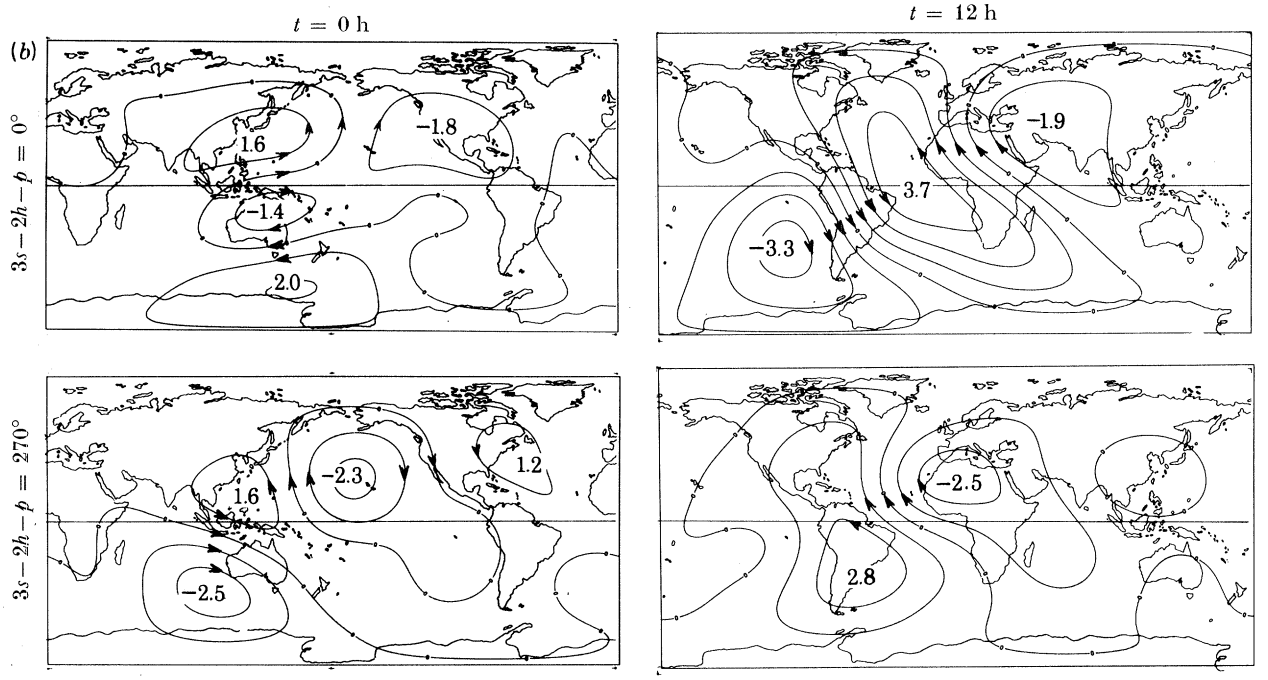

FIGURE 8.1 (*b*). $L(3s-2h-p)_{\text{iono.}}$ phase-law tide current function; extrema in kiloamperes.

TABLE 8.2 (*a*). SPHERICAL HARMONIC ANALYSIS OF $L(2s-4h)$ PHASE-LAW TIDES

(Amplitudes in picoteslas; phase angles in degrees.)

			internal		external	
n	j	k	I	α^k_{jmi}	II	α^k_{jme}
n	j	k	I′	β^k_{jmi}	II′	β^k_{jme}
1	1	0	101 ± 15	308	309 ± 21	285
1	1	1	31 ± 10	276	42 ± 14	224
1	1	1	8 ± 10	321	28 ± 14	72
1	2	0	23 ± 12	269	30 ± 15	265
1	2	1	33 ± 10	215	55 ± 12	230
1	2	1	11 ± 10	75	17 ± 12	256
1	2	2	28 ± 8	160	65 ± 10	134
1	2	2	10 ± 8	127	26 ± 10	249
1	3	0	12 ± 11	242	9 ± 13	235
1	3	1	9 ± 8	152	59 ± 9	154
1	3	1	16 ± 8	231	15 ± 9	335
1	3	2	10 ± 8	116	21 ± 9	185
1	3	2	22 ± 8	249	15 ± 9	306
1	4	0	13 ± 9	64	27 ± 10	273
1	4	1	11 ± 6	212	21 ± 7	219
1	4	1	4 ± 6	348	14 ± 7	259
1	4	2	11 ± 6	334	37 ± 7	317
1	4	2	7 ± 6	74	16 ± 7	159
2	1	1	40 ± 10	316	72 ± 14	257
2	1	1	32 ± 10	254	29 ± 14	79
2	2	1	25 ± 9	172	82 ± 11	57
2	2	1	27 ± 9	41	39 ± 11	307
2	2	2	36 ± 8	152	59 ± 10	165
2	2	2	21 ± 8	67	13 ± 10	81
2	3	1	20 ± 7	58	17 ± 8	261
2	3	1	15 ± 7	262	15 ± 8	358
2	3	2	13 ± 7	355	23 ± 8	60
2	3	2	7 ± 7	218	13 ± 8	6
2	3	3	24 ± 6	0	65 ± 7	329
2	3	3	4 ± 6	69	2 ± 7	344
2	4	1	15 ± 5	296	37 ± 6	73
2	4	1	5 ± 5	243	31 ± 6	236
2	4	2	10 ± 6	72	3 ± 7	307
2	4	2	7 ± 6	245	7 ± 6	150
2	4	3	8 ± 5	341	9 ± 6	53
2	4	3	7 ± 5	246	17 ± 6	164
2	5	2	5 ± 5	61	15 ± 5	37
2	5	2	3 ± 5	115	4 ± 5	70
3	2	2	18 ± 6	102	14 ± 7	69
3	2	2	5 ± 5	238	15 ± 7	115
3	3	2	10 ± 5	31	17 ± 6	76
3	3	2	4 ± 5	348	15 ± 6	314
3	3	3	11 ± 5	5	31 ± 6	17
3	3	3	19 ± 5	236	10 ± 6	339
3	4	2	11 ± 4	125	18 ± 5	119
3	4	2	8 ± 4	29	7 ± 5	52
3	4	3	6 ± 5	301	6 ± 5	277
3	4	3	10 ± 5	82	12 ± 5	38
3	4	4	11 ± 5	235	38 ± 5	178
3	4	4	12 ± 5	100	8 ± 5	131
3	5	2	1 ± 3	190	5 ± 4	324
3	5	2	3 ± 3	225	2 ± 4	311
3	5	3	4 ± 4	237	6 ± 5	0
3	5	3	2 ± 4	328	9 ± 4	233
3	5	4	10 ± 4	133	4 ± 4	176
3	5	4	5 ± 4	269	2 ± 4	2
3	6	3	5 ± 3	188	16 ± 4	135
3	6	3	1 ± 3	342	5 ± 4	98
4	3	3	6 ± 3	136	7 ± 3	220
4	3	3	3 ± 3	324	3 ± 3	243
4	4	3	2 ± 3	298	6 ± 3	2
4	4	3	7 ± 3	138	5 ± 3	125
4	4	4	5 ± 3	232	7 ± 3	194
4	4	4	6 ± 3	198	3 ± 3	312
4	5	3	1 ± 2	263	6 ± 2	312
4	5	3	2 ± 2	311	4 ± 2	273
4	5	4	4 ± 3	209	9 ± 3	233
4	5	4	2 ± 3	212	3 ± 3	285
4	5	5	5 ± 2	52	10 ± 2	9
4	5	5	7 ± 2	14	3 ± 2	286
4	6	4	1 ± 2	158	13 ± 2	218
4	6	4	3 ± 2	348	4 ± 2	318

I, $A^k_{jmi}\cos(k\phi+mt+\alpha^k_{jmi})P^k_j$; II, $A^k_{jme}\cos(k\phi+mt+\alpha^k_{jme})P^k_j$;
I′, $B^k_{jmi}\cos(k\phi-mt+\beta^k_{jmi})P^k_j$; II′, $B^k_{jme}\cos(k\phi-mt+\beta^k_{jme})P^k_j$.

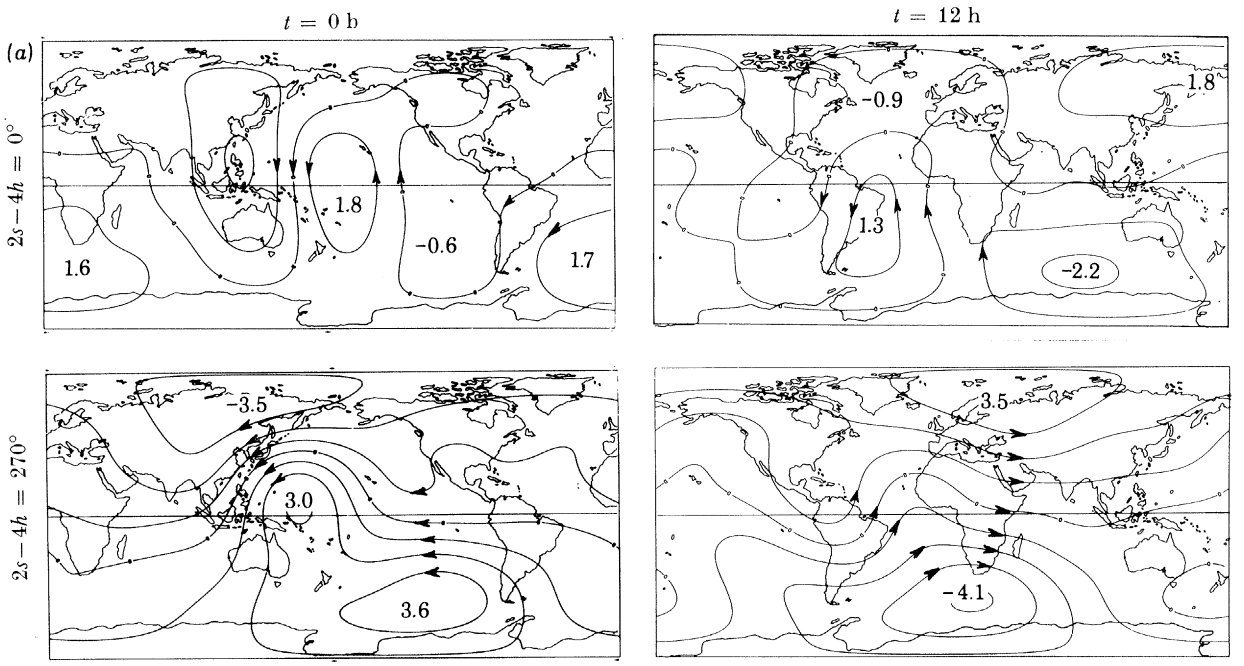

FIGURE 8.2 (*a*). $L(2s-4h)$ phase-law tide current function; extrema in kiloamperes.

TABLE 8.2 (*b*). SPHERICAL HARMONIC ANALYSIS OF $L(2s-4h)$ PARTIAL TIDES

(Amplitudes in picoteslas; phase angles in degrees.)

			internal		external	
			III	$\alpha^k_{jm'i}$	IV	$\alpha^k_{jm'e}$
n	j	k	III′	$\beta^k_{jm'i}$	IV′	$\beta^k_{jm'e}$
1	1	0	24± 15	123	67± 22	117
1	1	1	48± 9	158	84± 13	190
1	1	1	16± 9	67	36± 13	110
1	2	0	19± 12	74	61± 15	45
1	2	1	32± 9	230	86± 11	178
1	2	1	9± 9	43	23± 11	9
1	2	2	20± 7	213	40± 9	260
1	2	2	5± 8	44	24± 9	148
1	3	0	17± 11	360	28± 13	247
1	3	1	10± 8	210	32± 9	237
1	3	1	5± 8	318	13± 9	305
1	3	2	11± 7	2	21± 9	66
1	3	2	10± 7	150	17± 9	15
1	4	0	10± 8	194	22± 9	203
1	4	1	17± 6	150	43± 6	164
1	4	1	15± 6	336	13± 6	286
1	4	2	16± 6	102	16± 7	115
1	4	2	11± 6	294	18± 7	296
2	1	1	37± 9	98	112± 12	87
2	1	1	8± 9	214	14± 12	27
2	2	1	19± 8	241	44± 9	233
2	2	1	9± 8	322	24± 9	293
2	2	2	22± 7	290	27± 9	325
2	2	2	3± 7	319	10± 9	5
2	3	1	6± 6	23	12± 7	209
2	3	1	7± 6	354	5± 7	332
2	3	2	16± 6	137	33± 7	162
2	3	2	11± 6	328	27± 7	277
2	3	3	21± 5	56	22± 6	58
2	3	3	4± 5	215	6± 6	148
2	4	1	16± 4	260	26± 5	267
2	4	1	11± 4	306	30± 5	348
2	4	2	1± 5	54	5± 6	77
2	4	2	14± 5	79	15± 6	102
2	4	3	4± 4	176	15± 5	291
2	4	3	4± 4	205	6± 5	85
2	5	2	4± 4	122	11± 4	100
2	5	2	8± 4	233	8± 4	338
3	2	2	16± 5	280	28± 6	272
3	2	2	10± 5	64	8± 6	42
3	3	2	10± 4	61	5± 5	229
3	3	2	10± 4	313	14± 5	252
3	3	3	5± 4	192	13± 5	131
3	3	3	12± 4	202	2± 5	19
3	4	2	11± 4	206	4± 4	26
3	4	2	2± 4	179	12± 4	34
3	4	3	9± 4	53	9± 5	45
3	4	3	6± 4	42	13± 5	295
3	4	4	2± 4	340	20± 4	278
3	4	4	12± 4	308	3± 4	173
3	5	2	11± 3	37	14± 3	29
3	5	2	1± 3	53	7± 3	321
3	5	3	7± 3	324	6± 4	317
3	5	3	4± 3	30	10± 4	105
3	5	4	7± 3	245	5± 3	105
3	5	4	6± 3	151	5± 3	16
3	6	3	5± 3	125	3± 3	168
3	6	3	4± 3	276	5± 3	283
4	3	3	5± 3	144	9± 3	152
4	3	3	6± 3	90	5± 3	53
4	4	3	1± 3	347	2± 3	313
4	4	3	2± 3	278	3± 3	175
4	4	4	4± 3	307	8± 3	251
4	4	4	3± 3	191	2± 3	263
4	5	3	4± 2	53	5± 2	51
4	5	3	4± 2	57	8± 2	24
4	5	4	4± 2	294	8± 3	269
4	5	4	1± 2	125	5± 3	96
4	5	5	2± 2	235	3± 2	110
4	5	5	9± 2	264	1± 2	264
4	6	4	1± 2	148	3± 2	109
4	6	4	1± 2	201	1± 2	333

III, $A^k_{jm'i}\cos(k\phi+m't+\alpha^k_{jm'i})P^k_j$; IV, $A^k_{jm'e}\cos(k\phi+m't+\alpha^k_{jm'e})P^k_j$;
III′, $B^k_{jm'i}\cos(k\phi-m't+\beta^k_{jm'i})P^k_j$; IV′, $B^k_{jm'e}\cos(k\phi-m't+\beta^k_{jm'e})P^k_j$.

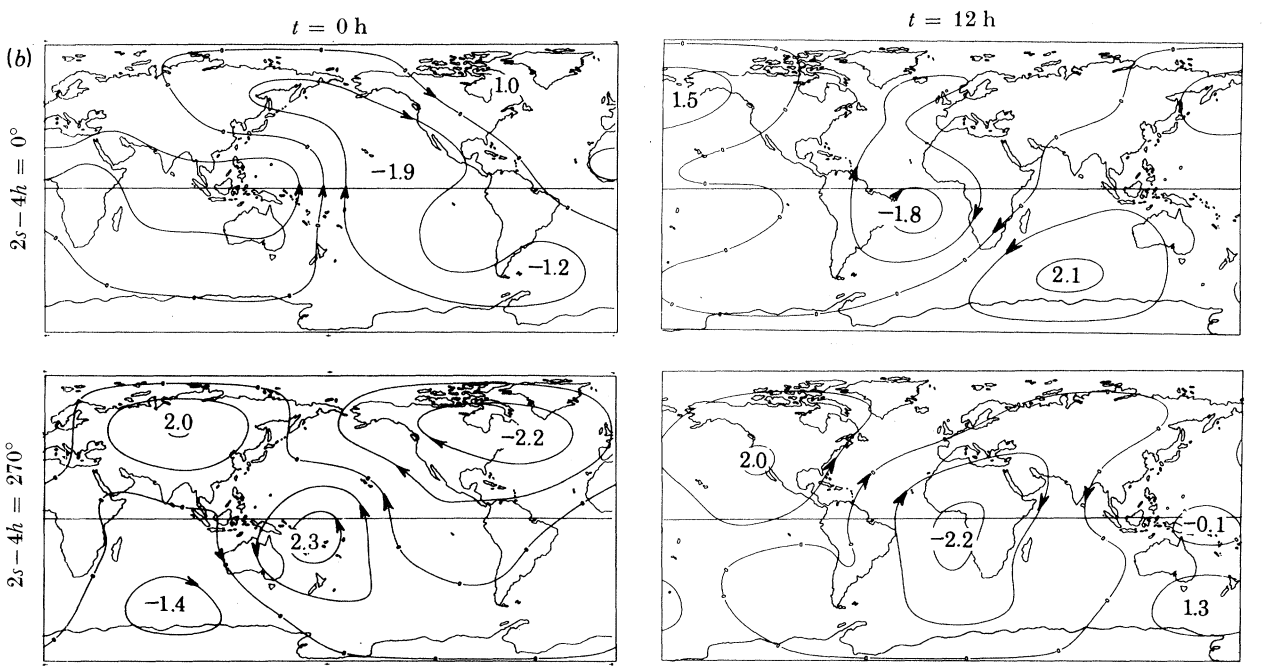

FIGURE 8.2 (*b*). $L(2s-4h)$ partial tide current function; extrema in kiloamperes.

TABLE 8.3 (*a*). SPHERICAL HARMONIC ANALYSIS OF $L(2s-3h)$ PHASE-LAW TIDES

(Amplitudes in picoteslas; phase angles in degrees.)

			internal		external	
n	j	k	I	α^k_{jmi}	II	α^k_{jme}
n	j	k	I′	β^k_{jmi}	II′	β^k_{jme}
1	1	0	101 ± 17	148	216 ± 27	153
1	1	1	77 ± 11	345	218 ± 15	317
1	1	1	7 ± 11	267	49 ± 15	332
1	2	0	44 ± 15	230	132 ± 18	209
1	2	1	15 ± 11	193	24 ± 13	358
1	2	1	7 ± 11	32	33 ± 13	10
1	2	2	2 ± 9	292	16 ± 11	46
1	2	2	24 ± 9	248	34 ± 11	143
1	3	0	8 ± 12	357	22 ± 15	310
1	3	1	18 ± 10	86	62 ± 11	85
1	3	1	20 ± 10	350	30 ± 11	94
1	3	2	19 ± 9	335	11 ± 10	106
1	3	2	29 ± 9	73	29 ± 10	356
1	4	0	27 ± 11	76	41 ± 12	340
1	4	1	12 ± 7	171	19 ± 8	30
1	4	1	10 ± 7	79	38 ± 8	71
1	4	2	6 ± 7	153	2 ± 8	72
1	4	2	7 ± 7	188	40 ± 8	165
2	1	1	99 ± 15	268	203 ± 19	235
2	1	1	25 ± 15	0	16 ± 19	283
2	2	1	4 ± 12	79	93 ± 15	305
2	2	1	37 ± 13	209	40 ± 15	50
2	2	2	112 ± 12	148	268 ± 14	148
2	2	2	17 ± 12	75	34 ± 14	210
2	3	1	17 ± 10	325	48 ± 11	11
2	3	1	40 ± 10	16	30 ± 11	328
2	3	2	8 ± 10	311	35 ± 12	29
2	3	2	15 ± 10	264	21 ± 12	26
2	3	3	16 ± 9	134	26 ± 10	117
2	3	3	19 ± 9	108	23 ± 10	125
2	4	1	6 ± 7	106	20 ± 8	247
2	4	1	20 ± 7	254	23 ± 8	345
2	4	2	27 ± 8	169	67 ± 9	162
2	4	2	1 ± 8	51	2 ± 9	287
2	4	3	21 ± 7	260	23 ± 8	257
2	4	3	7 ± 7	71	7 ± 8	67
2	5	2	13 ± 6	340	26 ± 7	272
2	5	2	14 ± 6	32	9 ± 7	83
3	2	2	29 ± 7	67	77 ± 8	56
3	2	2	10 ± 7	261	27 ± 8	266
3	3	2	11 ± 6	258	21 ± 7	192
3	3	2	7 ± 6	303	14 ± 7	30
3	3	3	55 ± 6	356	122 ± 7	334
3	3	3	5 ± 6	79	19 ± 7	5
3	4	2	7 ± 5	163	7 ± 6	209
3	4	2	3 ± 5	348	19 ± 6	251
3	4	3	20 ± 5	214	16 ± 6	238
3	4	3	3 ± 5	301	12 ± 6	199
3	4	4	2 ± 5	208	23 ± 6	292
3	4	4	11 ± 5	161	8 ± 6	168
3	5	2	2 ± 4	355	15 ± 4	216
3	5	2	3 ± 4	62	17 ± 4	57
3	5	3	25 ± 5	4	41 ± 5	333
3	5	3	13 ± 5	37	14 ± 5	88
3	5	4	3 ± 4	25	25 ± 4	115
3	5	4	5 ± 4	240	6 ± 4	268
3	6	3	5 ± 4	115	19 ± 4	40
3	6	3	11 ± 4	193	4 ± 4	197
4	3	3	7 ± 3	321	17 ± 4	266
4	3	3	6 ± 3	280	6 ± 4	249
4	4	3	5 ± 3	257	2 ± 4	162
4	4	3	4 ± 3	67	7 ± 4	74
4	4	4	7 ± 3	197	11 ± 4	148
4	4	4	8 ± 3	251	7 ± 4	34
4	5	3	4 ± 2	70	5 ± 3	70
4	5	3	4 ± 2	196	6 ± 3	202
4	5	4	10 ± 3	29	3 ± 3	359
4	5	4	12 ± 3	59	3 ± 3	332
4	5	5	5 ± 2	113	9 ± 3	90
4	5	5	1 ± 2	283	5 ± 3	171
4	6	4	9 ± 2	191	10 ± 2	190
4	6	4	4 ± 2	276	3 ± 2	106

I, $A^k_{jmi}\cos(k\phi+mt+\alpha^k_{jmi})P^k_j$; II, $A^k_{jme}\cos(k\phi+mt+\alpha^k_{jme})P^k_j$;
I′, $B^k_{jmi}\cos(k\phi-mt+\beta^k_{jmi})P^k_j$; II′, $B^k_{jme}\cos(k\phi-mt+\beta^k_{jme})P^k_j$.

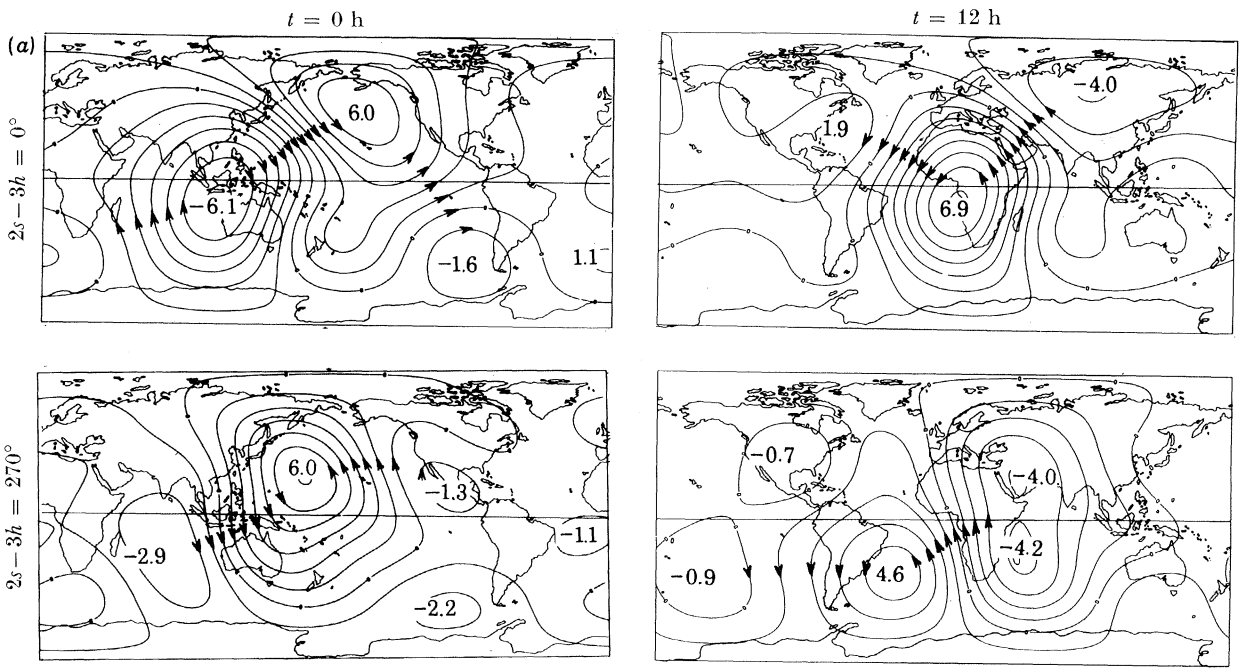

FIGURE 8.3 (*a*). $L(2s-3h)$ phase-law tide current function; extrema in kiloamperes.

TABLE 8.3 (*b*). SPHERICAL HARMONIC ANALYSIS OF $L(2s-3h)$ PARTIAL TIDES

(Amplitudes in picoteslas; phase angles in degrees.)

n j k / n j k	internal III	$\alpha^k_{jm'i}$	external IV	$\alpha^k_{jm'e}$
	internal III′	$\beta^k_{jm'i}$	external IV′	$\beta^k_{jm'e}$
1 1 0	44 ± 14	59	35 ± 21	66
1 1 1	12 ± 9	293	13 ± 12	308
1 1 1	23 ± 9	320	16 ± 12	21
1 2 0	21 ± 12	236	14 ± 15	179
1 2 1	11 ± 9	286	44 ± 11	230
1 2 1	10 ± 9	97	25 ± 11	6
1 2 2	13 ± 8	288	15 ± 9	306
1 2 2	9 ± 8	160	9 ± 9	312
1 3 0	11 ± 10	199	10 ± 12	228
1 3 1	12 ± 8	268	38 ± 9	251
1 3 1	8 ± 8	34	33 ± 9	121
1 3 2	9 ± 7	256	17 ± 8	353
1 3 2	9 ± 7	179	22 ± 8	230
1 4 0	3 ± 8	185	47 ± 9	207
1 4 1	14 ± 6	184	23 ± 6	160
1 4 1	5 ± 6	76	3 ± 6	286
1 4 2	13 ± 5	127	22 ± 6	172
1 4 2	2 ± 5	99	21 ± 6	154
2 1 1	36 ± 8	209	17 ± 11	164
2 1 1	7 ± 8	58	28 ± 11	307
2 2 1	23 ± 7	355	12 ± 8	262
2 2 1	4 ± 7	332	26 ± 8	50
2 2 2	7 ± 6	203	37 ± 8	80
2 2 2	8 ± 6	159	28 ± 8	40
2 3 1	20 ± 5	202	22 ± 6	223
2 3 1	11 ± 5	10	26 ± 6	308
2 3 2	24 ± 6	151	42 ± 7	177
2 3 2	6 ± 6	293	35 ± 7	224
2 3 3	5 ± 5	121	16 ± 6	169
2 3 3	16 ± 5	173	16 ± 6	95
2 4 1	5 ± 4	5	22 ± 4	23
2 4 1	15 ± 4	212	16 ± 4	296
2 4 2	4 ± 5	295	6 ± 5	74
2 4 2	5 ± 5	245	11 ± 5	16
2 4 3	6 ± 4	303	10 ± 4	288
2 4 3	1 ± 4	270	19 ± 4	271
2 5 2	7 ± 4	93	17 ± 4	165
2 5 2	4 ± 4	187	8 ± 4	227
3 2 2	6 ± 5	333	22 ± 6	283
3 2 2	16 ± 3	332	8 ± 6	345
3 3 2	3 ± 4	85	8 ± 5	57
3 3 2	2 ± 4	89	9 ± 5	210
3 3 3	12 ± 4	292	24 ± 5	262
3 3 3	9 ± 4	167	8 ± 5	94
3 4 2	8 ± 4	237	2 ± 4	94
3 4 2	9 ± 4	258	11 ± 4	4
3 4 3	13 ± 4	58	15 ± 5	37
3 4 3	8 ± 4	52	3 ± 5	251
3 4 4	2 ± 4	209	4 ± 4	243
3 4 4	10 ± 4	247	4 ± 4	275
3 5 2	9 ± 3	86	6 ± 3	182
3 5 2	4 ± 3	232	19 ± 3	246
3 5 3	3 ± 4	213	7 ± 4	121
3 5 3	2 ± 4	165	13 ± 4	89
3 5 4	2 ± 3	81	2 ± 3	9
3 5 4	4 ± 3	21	5 ± 3	28
3 6 3	5 ± 3	228	10 ± 3	284
3 6 3	2 ± 3	132	2 ± 3	176
4 3 3	8 ± 3	164	9 ± 3	130
4 3 3	6 ± 3	22	2 ± 3	307
4 4 3	6 ± 3	10	1 ± 3	342
4 4 3	8 ± 3	186	6 ± 3	131
4 4 4	7 ± 3	203	11 ± 3	152
4 4 4	2 ± 3	337	1 ± 3	60
4 5 3	5 ± 2	111	4 ± 2	68
4 5 3	3 ± 2	348	5 ± 2	305
4 5 4	3 ± 2	308	8 ± 3	282
4 5 4	4 ± 2	265	5 ± 3	242
4 5 5	3 ± 2	10	4 ± 2	343
4 5 5	3 ± 2	187	1 ± 2	286
4 6 4	2 ± 2	212	1 ± 2	166
4 6 4	6 ± 2	100	6 ± 2	64

III, $A^k_{jm'i}\cos(k\phi+m't+\alpha^k_{jm'i})P^k_j$; IV, $A^k_{jm'e}\cos(k\phi+m't+\alpha^k_{jm'e})P^k_j$;
III′, $B^k_{jm'i}\cos(k\phi-m't+\beta^k_{jm'i})P^k_j$; IV′, $B^k_{jm'e}\cos(k\phi-m't+\beta^k_{jm'e})P^k_j$.

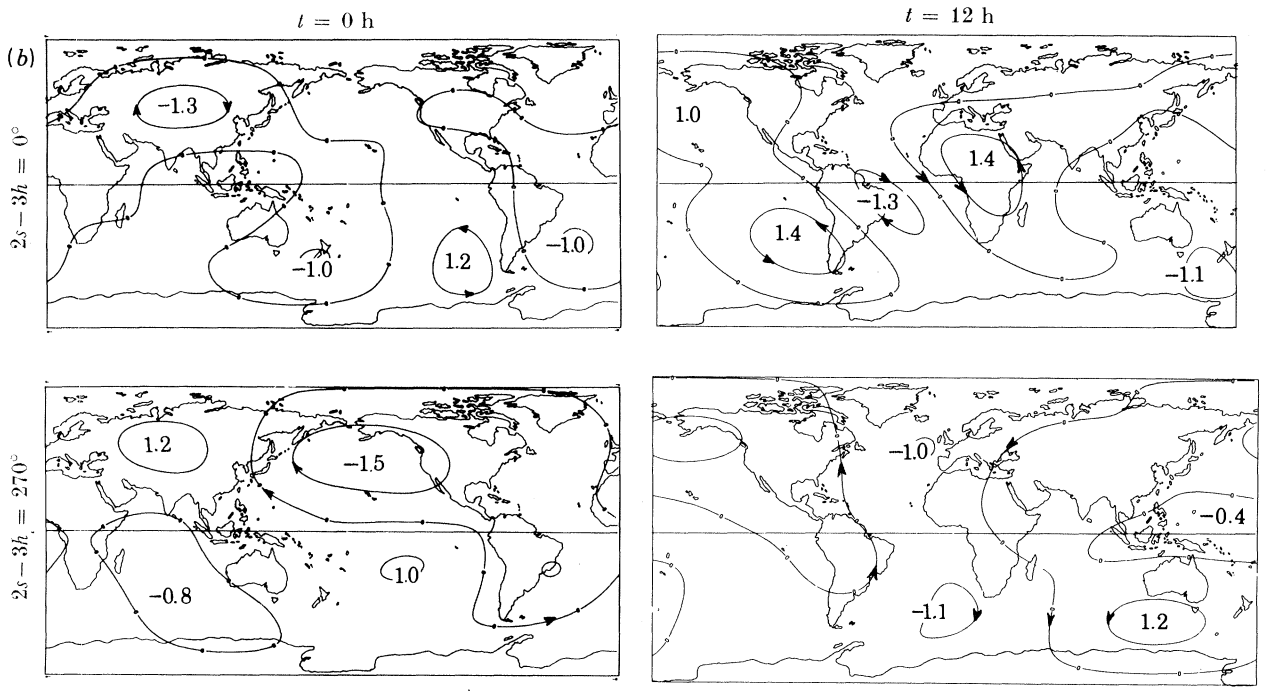

FIGURE 8.3 (*b*). $L(2s-3h)$ partial tide current function; extrema in kiloamperes.

TABLE 8.4 (*a*). SPHERICAL HARMONIC ANALYSIS OF $L(2s-2h)_{\text{iono.+oc.}}$ PHASE-LAW TIDES

(Amplitudes in picoteslas; phase angles in degrees.)

n n	j j	k k	internal I / I′	α^k_{jmi} / β^k_{jmi}	external II / II′	α^k_{jme} / β^k_{jme}
1	1	0	27±21	322	91±34	300
1	1	1	39±14	233	33±19	157
1	1	1	4±14	241	38±19	63
1	2	0	31±16	186	190±21	152
1	2	1	131±14	88	174±17	86
1	2	1	27±14	237	47±17	319
1	2	2	42±11	163	99±13	181
1	2	2	20±11	32	43±13	51
1	3	0	15±15	236	21±19	270
1	3	1	21±11	229	23±13	340
1	3	1	23±11	62	30±13	239
1	3	2	22±11	272	63±12	225
1	3	2	14±11	190	18±12	131
1	4	0	9±12	44	72±13	3
1	4	1	33± 8	309	117± 9	245
1	4	1	12± 8	311	44± 9	50
1	4	2	6± 8	162	39± 9	53
1	4	2	17± 8	333	36± 9	305
2	1	1	88±40	148	482±46	165
2	1	1	165±40	253	123±46	94
2	2	1	78±32	116	92±34	351
2	2	1	60±32	48	40±35	274
2	2	2	58±32	186	170±35	339
2	2	2	47±31	336	29±35	26
2	3	1	34±24	270	88±23	8
2	3	1	37±24	129	5±26	1
2	3	2	227±26	297	280±28	240
2	3	2	49±26	91	38±28	254
2	3	3	29±23	234	165±25	24
2	3	3	37±23	14	46±25	177
2	4	1	48±18	117	51±19	210
2	4	1	70±18	248	100±19	115
2	4	2	42±20	149	48±22	310
2	4	2	59±20	252	36±21	99
2	4	3	58±17	57	34±19	282
2	4	3	21±17	274	67±19	343
2	5	2	23±16	193	69±17	79
2	5	2	56±16	7	29±17	239
3	2	2	10± 9	336	147±12	345
3	2	2	44± 9	207	42±12	74
3	3	2	21± 9	41	19±10	169
3	3	2	38± 9	12	43±10	192
3	3	3	28± 9	241	48±10	120
3	3	3	37± 9	237	9±10	69
3	4	2	21± 8	168	36± 8	154
3	4	2	17± 8	200	25± 8	279
3	4	3	101± 8	114	134± 9	93
3	4	3	40± 8	71	26± 9	303
3	4	4	4± 8	74	108± 9	203
3	4	4	34± 8	21	15± 9	208
3	5	2	14± 6	306	9± 6	4
3	5	2	5± 6	42	4± 7	103
3	5	3	13± 7	269	42± 8	140
3	5	3	6± 7	220	33± 8	128
3	5	4	19± 6	214	37± 7	1
3	5	4	17± 6	192	20± 7	46
3	6	3	20± 6	359	61± 6	314
3	6	3	9± 6	198	17± 6	311
4	3	3	14± 4	183	35± 5	146
4	3	3	8± 4	127	7± 5	66
4	3	4	2± 4	272	10± 4	192
4	4	3	12± 4	280	11± 4	272
4	4	4	5± 4	72	9± 4	330
4	4	4	17± 4	332	6± 4	196
4	5	3	8± 3	333	8± 3	273
4	5	3	6± 3	88	9± 3	89
4	5	4	26± 3	291	42± 4	272
4	5	4	2± 3	178	5± 4	293
4	5	5	11± 3	44	27± 3	32
4	5	5	5± 3	349	6± 3	253
4	6	4	7± 3	22	7± 3	323
4	6	4	6± 3	199	1± 3	276

I, $A^k_{jmi}\cos(k\phi+mt+\alpha^k_{jmi})P^k_j$; II, $A^k_{jme}\cos(k\phi+mt+\alpha^k_{jme})P^k_j$;
I′, $B^k_{jmi}\cos(k\phi-mt+\beta^k_{jmi})P^k_j$; II′, $B^k_{jme}\cos(k\phi-mt+\beta^k_{jme})P^k_j$.

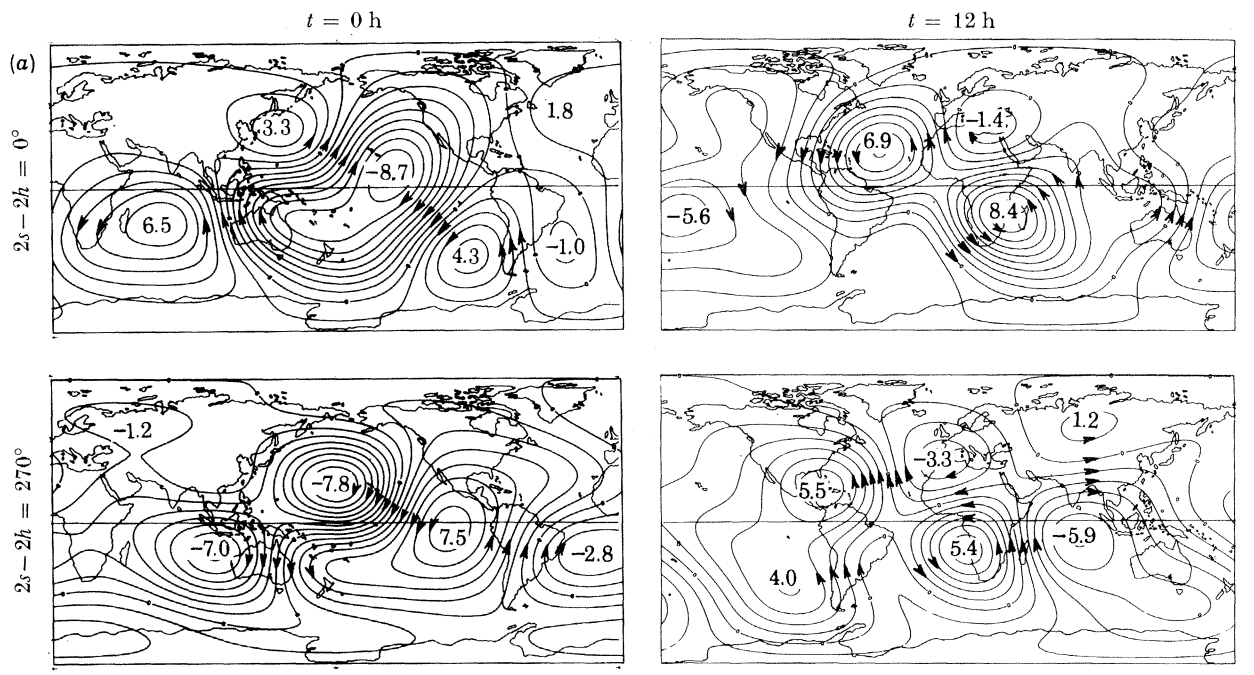

FIGURE 8.4 (*a*). $L(2s-2h)_{\text{iono.+oc.}}$ phase-law tide current function; extrema in kiloamperes.

TABLE 8.4 (*b*). SPHERICAL HARMONIC ANALYSIS OF $L(2s-2h)_{\text{iono.+oc.}}$ PARTIAL TIDES

(Amplitudes in picoteslas; phase angles in degrees.)

			internal		external	
n	j	k	III	$\alpha^k_{jm'i}$	IV	$\alpha^k_{jm'e}$
n	j	k	III′	$\beta^k_{jm'i}$	IV′	$\beta^k_{jm'e}$
1	1	0	70 ± 12	168	200 ± 18	167
1	1	1	34 ± 8	172	49 ± 11	185
1	1	1	13 ± 8	253	5 ± 11	38
1	2	0	38 ± 11	127	30 ± 14	100
1	2	1	32 ± 8	263	45 ± 10	251
1	2	1	13 ± 8	83	62 ± 10	233
1	2	2	16 ± 7	268	21 ± 8	275
1	2	2	5 ± 7	232	15 ± 8	353
1	3	0	23 ± 9	264	27 ± 10	323
1	3	1	9 ± 7	15	8 ± 8	288
1	3	1	5 ± 7	273	43 ± 8	31
1	3	2	27 ± 6	31	36 ± 7	74
1	3	2	10 ± 6	320	8 ± 7	317
1	4	0	22 ± 7	30	30 ± 8	303
1	4	1	20 ± 5	167	73 ± 5	132
1	4	1	10 ± 5	47	26 ± 5	186
1	4	2	20 ± 5	221	42 ± 6	244
1	4	2	11 ± 5	172	7 ± 6	180
2	1	1	23 ± 7	204	61 ± 10	184
2	1	1	14 ± 8	262	22 ± 10	179
2	2	1	14 ± 6	33	18 ± 8	349
2	2	1	1 ± 6	158	8 ± 8	324
2	2	2	30 ± 6	55	46 ± 8	53
2	2	2	5 ± 6	27	6 ± 8	242
2	3	1	8 ± 5	254	32 ± 6	335
2	3	1	6 ± 5	340	9 ± 6	245
2	3	2	3 ± 5	200	3 ± 6	96
2	3	2	6 ± 5	243	7 ± 6	153
2	3	3	9 ± 5	193	6 ± 6	336
2	3	3	3 ± 5	52	9 ± 6	247
2	4	1	5 ± 4	53	19 ± 4	137
2	4	1	12 ± 4	296	25 ± 4	349
2	4	2	7 ± 4	62	25 ± 5	90
2	4	2	8 ± 4	239	16 ± 5	358
2	4	3	8 ± 4	308	13 ± 4	229
2	4	3	9 ± 4	295	11 ± 4	10
2	5	2	5 ± 3	197	11 ± 4	268
2	5	2	6 ± 3	80	18 ± 4	249

			internal		external	
n	j	k	III	$\alpha^k_{jm'i}$	IV	$\alpha^k_{jm'e}$
n	j	k	III′	$\beta^k_{jm'i}$	IV′	$\beta^k_{jm'e}$
2	2	2	14 ± 4	10	22 ± 5	13
3	3	2	8 ± 4	8	18 ± 5	23
3	3	2	7 ± 4	164	10 ± 5	50
3	3	2	2 ± 4	232	10 ± 5	235
3	3	3	3 ± 4	333	25 ± 5	271
3	3	3	3 ± 4	25	17 ± 5	264
3	4	2	4 ± 3	79	6 ± 4	176
3	4	9	3 ± 3	197	2 ± 4	55
3	4	3	3 ± 4	9	20 ± 4	130
3	4	3	7 ± 4	288	7 ± 4	223
3	4	4	3 ± 4	234	8 ± 4	342
3	4	4	8 ± 4	151	7 ± 4	31
3	5	2	4 ± 3	86	8 ± 3	40
3	5	2	5 ± 3	328	6 ± 3	297
3	5	3	4 ± 3	219	10 ± 4	261
3	5	3	5 ± 3	94	3 ± 4	19
3	5	4	2 ± 3	125	9 ± 3	88
3	5	4	2 ± 3	230	13 ± 3	142
3	6	3	4 ± 3	83	12 ± 3	53
3	6	3	4 ± 3	164	3 ± 3	206
4	3	3	4 ± 3	328	2 ± 3	328
4	3	3	9 ± 3	17	3 ± 3	329
4	4	3	2 ± 2	180	9 ± 3	284
4	4	3	2 ± 2	92	7 ± 3	91
4	4	4	8 ± 3	193	15 ± 3	142
4	4	4	6 ± 3	207	4 ± 3	109
4	5	3	3 ± 2	164	8 ± 2	143
4	5	3	2 ± 2	146	3 ± 2	306
4	5	4	7 ± 2	46	11 ± 3	346
4	5	4	2 ± 2	59	4 ± 3	256
4	5	5	2 ± 2	17	10 ± 2	224
4	5	5	2 ± 2	167	3 ± 2	33
4	6	4	3 ± 2	203	1 ± 2	201
4	6	4	2 ± 2	355	3 ± 2	346

III, $A^k_{jm'i}\cos(k\phi+m't+\alpha^k_{jm'i})P^k_j$; IV, $A^k_{jm'e}\cos(k\phi+m't+\alpha^k_{jm'e})P^k_j$;
III′, $B^k_{jm'i}\cos(k\phi-m't+\beta^k_{jm'i})P^k_j$; IV′, $B^k_{jm'e}\cos(k\phi-m't+\beta^k_{jm'e})P^k_j$.

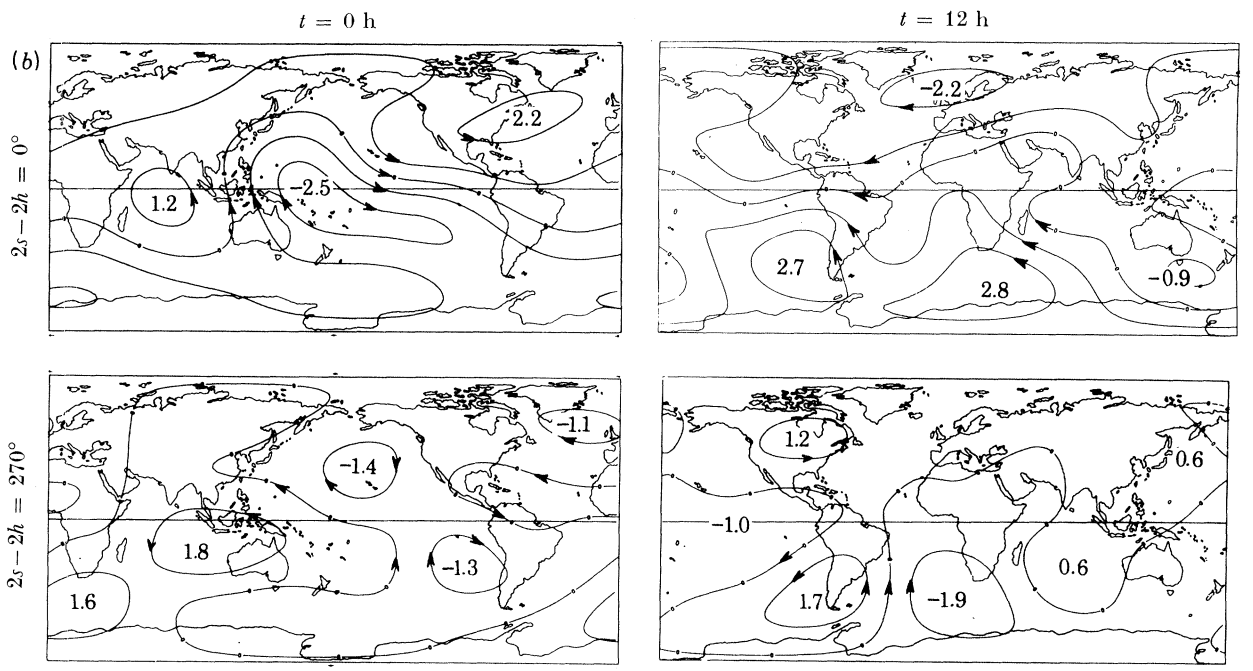

FIGURE 8.4 (*b*). $L(2s-2h)_{\text{iono.+oc.}}$ partial tide current function; extrema in kiloamperes.

TABLE 8.5 (*a*). SPHERICAL HARMONIC ANALYSIS OF $L(2s-h)$ PHASE-LAW TIDES

(Amplitudes in picoteslas; phase angles in degrees.)

n j k	internal I	internal α^k_{jmi}	external II	external α^k_{jme}	n j k	internal I	internal α^k_{jmi}	external II	external α^k_{jme}
n j k	I′	β^k_{jmi}	II′	β^k_{jme}	n j k	I′	β^k_{jmi}	II′	β^k_{jme}
1 1 0	85 ± 24	131	162 ± 35	92	3 2 2	19 ± 7	290	57 ± 9	277
1 1 1	94 ± 15	205	212 ± 21	226	3 2 2	7 ± 7	72	50 ± 9	113
1 1 1	25 ± 15	281	38 ± 21	296	3 3 2	12 ± 6	301	24 ± 8	343
1 2 0	70 ± 21	153	41 ± 24	112	3 3 2	15 ± 6	49	21 ± 8	287
1 2 1	53 ± 15	48	41 ± 18	319	3 3 3	44 ± 6	230	78 ± 7	226
1 2 1	8 ± 15	86	12 ± 18	108	3 3 3	3 ± 6	316	16 ± 7	290
1 2 2	23 ± 12	162	72 ± 14	143	3 4 2	17 ± 5	135	38 ± 6	144
1 2 2	11 ± 12	184	7 ± 14	188	3 4 2	12 ± 5	223	7 ± 6	35
1 3 0	32 ± 17	113	26 ± 22	168	3 4 3	34 ± 6	55	61 ± 7	45
1 3 1	32 ± 13	297	43 ± 15	250	3 4 3	19 ± 6	91	15 ± 7	36
1 3 1	29 ± 13	8	11 ± 15	67	3 4 4	6 ± 6	196	34 ± 6	168
1 3 2	35 ± 12	222	25 ± 13	184	3 4 4	8 ± 6	347	7 ± 6	349
1 3 2	18 ± 12	334	11 ± 13	340	3 5 2	1 ± 4	342	18 ± 5	8
1 4 0	25 ± 14	220	50 ± 15	298	3 5 2	1 ± 4	255	9 ± 5	214
1 4 1	6 ± 9	197	34 ± 11	219	3 5 3	20 ± 5	245	26 ± 6	205
1 4 1	11 ± 9	299	3 ± 11	3	3 5 3	9 ± 5	293	5 ± 6	270
1 4 2	7 ± 9	126	40 ± 10	313	3 5 4	10 ± 5	161	7 ± 5	7
1 4 2	9 ± 9	138	13 ± 10	306	3 5 4	7 ± 4	192	13 ± 5	172
					3 6 3	7 ± 4	15	19 ± 5	268
2 1 1	39 ± 14	184	111 ± 19	106	3 6 3	4 ± 4	269	5 ± 5	152
2 1 1	22 ± 14	20	38 ± 18	195					
2 2 1	6 ± 13	97	95 ± 15	204	4 3 3	11 ± 3	134	25 ± 4	109
2 2 1	9 ± 13	324	34 ± 15	339	4 3 3	6 ± 3	175	2 ± 4	103
2 2 2	99 ± 11	19	151 ± 13	26	4 4 3	6 ± 3	321	4 ± 3	353
2 2 2	21 ± 11	84	35 ± 13	308	4 4 3	7 ± 3	324	4 ± 3	325
2 3 1	34 ± 10	282	59 ± 11	309	4 4 4	7 ± 3	94	5 ± 3	81
2 3 1	13 ± 10	152	15 ± 11	96	4 4 4	13 ± 3	9	0 ± 3	108
2 3 2	39 ± 10	211	73 ± 11	218	4 5 3	3 ± 2	335	9 ± 3	284
2 3 2	13 ± 10	346	21 ± 11	75	4 5 3	6 ± 2	136	1 ± 3	129
2 3 3	18 ± 9	22	57 ± 10	338	4 5 4	20 ± 3	247	32 ± 3	224
2 3 3	33 ± 9	217	30 ± 10	319	4 5 4	5 ± 3	161	4 ± 3	338
2 4 1	16 ± 7	239	36 ± 8	203	4 5 5	5 ± 2	333	9 ± 2	352
2 4 1	11 ± 7	60	13 ± 8	23	4 5 5	7 ± 2	359	5 ± 2	251
2 4 2	24 ± 8	40	54 ± 9	30	4 6 4	7 ± 2	55	9 ± 2	19
2 4 2	13 ± 8	178	7 ± 9	274	4 6 4	6 ± 2	213	5 ± 2	210
2 4 3	10 ± 7	44	22 ± 7	42					
2 4 3	19 ± 6	293	18 ± 7	210					
2 5 2	16 ± 6	81	29 ± 7	68					
2 5 2	14 ± 6	238	14 ± 7	278					

I, $A^k_{jmi}\cos(k\phi+mt+\alpha^k_{jmi})P^k_j$; II, $A^k_{jme}\cos(k\phi+mt+\alpha^k_{jme})P^k_j$;
I′, $B^k_{jmi}\cos(k\phi-mt+\beta^k_{jmi})P^k_j$; II′, $B^k_{jme}\cos(k\phi-mt+\beta^k_{jme})P^k_j$.

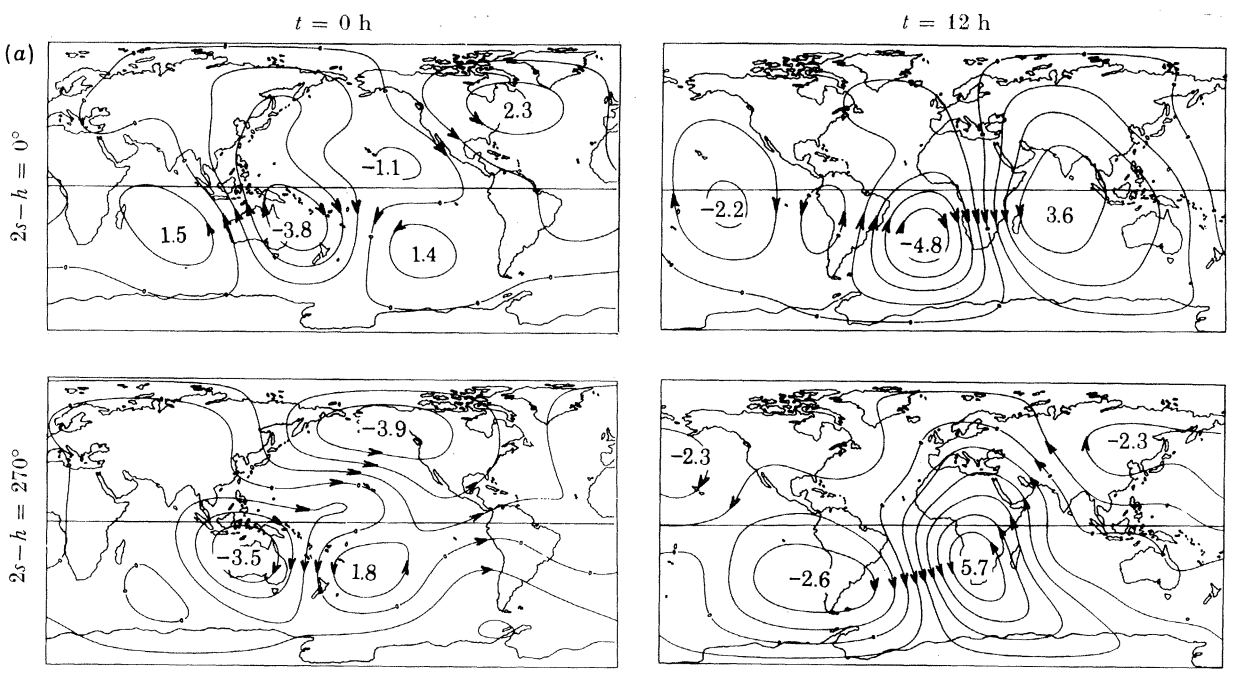

FIGURE 8.5 (*a*). $L(2s-h)$ phase-law tide current function; extrema in kiloamperes.

TABLE 8.5 (*b*). SPHERICAL HARMONIC ANALYSIS OF $L(2s-h)$ PARTIAL TIDES

(Amplitudes in picoteslas; phase angles in degrees.)

			internal		external	
n	j	k	III	$\alpha^k_{jm'i}$	IV	$\alpha^k_{jm'e}$
n	j	k	III′	$\beta^k_{jm'i}$	IV′	$\beta^k_{jm'e}$
1	1	0	30±16	108	49±32	28
1	1	1	34±11	211	144±16	191
1	1	1	14±11	122	19±16	179
1	2	0	47±14	62	112±22	18
1	2	1	28±11	268	101±14	296
1	2	1	18±11	278	30±14	298
1	2	2	5± 9	58	47±11	324
1	2	2	20± 9	295	25±11	226
1	3	0	22±12	295	34±19	165
1	3	1	26±10	66	66±11	91
1	3	1	2±10	37	24±11	293
1	3	2	4± 9	336	10±10	123
1	3	2	20± 9	96	12±10	48
1	4	0	11±12	164	55±12	307
1	4	1	17± 7	197	24± 8	295
1	4	1	19± 7	242	37± 8	336
1	4	2	17± 7	258	29± 8	223
1	4	2	12± 7	296	9± 8	150
2	1	1	22± 9	257	32±12	350
2	1	1	16± 9	80	7±12	271
2	2	1	35± 8	64	37± 9	79
2	2	1	13± 8	274	20± 9	326
2	2	2	8± 7	43	42± 9	97
2	2	2	11± 7	123	21± 9	312
2	3	1	17± 6	292	27± 7	290
2	3	1	16± 6	219	20± 7	227
2	3	2	10± 6	284	28± 7	263
2	3	2	11± 6	319	17± 7	138
2	3	3	9± 5	9	15± 6	110
2	3	3	14± 5	188	14± 6	25
2	4	1	15± 4	126	30± 5	105
2	4	1	14± 4	88	11± 5	174
2	4	2	4± 5	144	15± 6	319
2	4	2	3± 5	203	11± 6	6
2	4	3	9± 4	161	10± 5	73
2	4	3	8± 4	2	11± 5	194
2	5	2	2± 4	344	12± 5	333
2	5	2	1± 4	235	7± 5	47
3	2	2	6± 5	63	1± 6	35
3	2	2	13± 5	279	6± 6	217
3	3	2	7± 5	230	12± 6	328
3	3	2	9± 5	78	10± 6	357
3	3	3	7± 5	39	9± 6	352
3	3	3	7± 5	284	5± 6	212
3	4	2	7± 4	162	23± 5	142
3	4	2	9± 4	252	7± 5	222
3	4	3	8± 4	66	22± 5	33
3	4	3	6± 4	18	7± 5	11
3	4	4	11± 4	275	4± 5	239
3	4	4	7± 4	103	10± 5	323
3	5	2	5± 3	247	14± 4	283
3	5	2	3± 3	93	7± 4	140
3	5	3	5± 4	287	13± 4	149
3	5	3	3± 4	182	3± 4	15
3	5	4	9± 3	77	12± 4	5
3	5	4	5± 3	347	5± 4	131
3	6	3	4± 3	11	5± 3	307
3	6	3	1± 3	101	6± 3	45
4	3	3	5± 3	13	4± 4	240
4	3	3	7± 3	214	3± 4	126
4	4	3	3± 3	210	4± 3	46
4	4	3	3± 3	21	6± 4	167
4	4	4	8± 3	202	9± 3	205
4	4	4	5± 3	299	6± 3	32
4	5	3	5± 2	3	5± 3	303
4	5	3	3± 2	140	4± 3	24
4	5	4	10± 3	273	14± 3	219
4	5	4	5± 3	146	6± 3	173
4	5	5	2± 2	8	8± 3	26
4	5	5	4± 2	41	1± 2	82
4	6	4	4± 2	110	1± 2	262
4	6	4	5± 2	41	7± 2	23

III, $A^k_{jm'i}\cos(k\phi+m't+\alpha^k_{jm'i})P^k_j$; IV, $A^k_{jm'e}\cos(k\phi+m't+\alpha^k_{jm'e})P^k_j$;
III′, $B^k_{jm'i}\cos(k\phi-m't+\beta^k_{jm'i})P^k_j$; IV′, $B^k_{jm'e}\cos(k\phi-m't+\beta^k_{jm'e})P^k_j$.

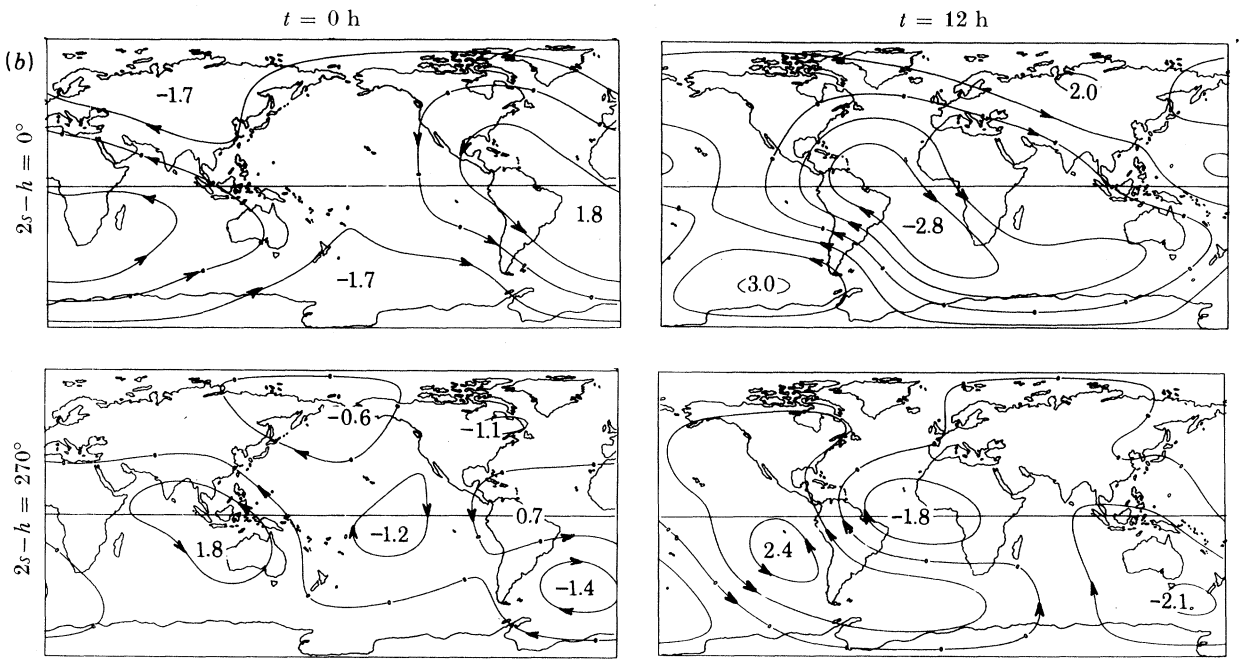

FIGURE 8.5 (*b*). $L(2s-h)$ partial tide current function; extrema in kiloamperes.

TABLE 8.6 (*a*). SPHERICAL HARMONIC ANALYSIS OF $L(2s)$ PHASE-LAW TIDES

(Amplitudes in picoteslas; phase angles in degrees.)

n n	j k	k	internal I / I′	α^k_{jmi} / β^k_{jmi}	external II / II′	α^k_{jme} / β^k_{jme}
1	1	0	64 ± 18	126	86 ± 28	149
1	1	1	38 ± 13	82	127 ± 18	62
1	1	1	23 ± 13	347	72 ± 18	324
1	2	0	12 ± 16	22	25 ± 21	88
1	2	1	52 ± 13	46	87 ± 15	32
1	2	1	19 ± 13	190	10 ± 15	271
1	2	2	28 ± 10	246	51 ± 13	213
1	2	2	12 ± 10	135	10 ± 13	290
1	3	0	18 ± 14	140	13 ± 16	184
1	3	1	15 ± 10	181	37 ± 12	26
1	3	1	26 ± 10	53	25 ± 12	304
1	3	2	10 ± 10	239	47 ± 12	219
1	3	2	2 ± 10	270	27 ± 12	132
1	4	0	11 ± 10	197	12 ± 12	29
1	4	1	7 ± 7	18	40 ± 8	257
1	4	1	17 ± 7	271	14 ± 8	301
1	4	2	2 ± 8	316	29 ± 9	27
1	4	2	13 ± 8	309	24 ± 9	19
2	1	1	19 ± 12	315	43 ± 15	171
2	1	1	15 ± 12	253	40 ± 16	119
2	2	1	9 ± 10	126	8 ± 12	319
2	2	1	16 ± 10	157	40 ± 12	287
2	2	2	43 ± 10	262	136 ± 11	259
2	2	2	23 ± 10	15	15 ± 11	230
2	3	1	14 ± 8	290	16 ± 9	283
2	3	1	5 ± 8	78	13 ± 9	153
2	3	2	33 ± 8	257	34 ± 9	238
2	3	2	16 ± 8	179	12 ± 9	182
2	3	3	20 ± 7	76	63 ± 8	21
2	3	3	15 ± 7	56	10 ± 8	314
2	4	1	7 ± 6	9	15 ± 7	227
2	4	1	11 ± 6	271	7 ± 7	214
2	4	2	11 ± 7	159	30 ± 7	209
2	4	2	5 ± 7	323	14 ± 7	232
2	4	3	4 ± 6	303	13 ± 6	135
2	4	3	19 ± 6	223	8 ± 6	173
2	5	2	16 ± 5	122	32 ± 6	62
2	5	2	9 ± 5	154	10 ± 6	137

n n	j k	k	internal I / I′	α^k_{jmi} / β^k_{jmi}	external II / II′	α^k_{jme} / β^k_{jme}
3	2	2	18 ± 6	131	24 ± 7	8
3	2	2	18 ± 6	223	17 ± 7	118
3	3	2	17 ± 5	278	28 ± 6	212
3	3	2	12 ± 5	70	14 ± 6	309
3	3	3	36 ± 5	125	88 ± 6	87
3	3	3	13 ± 5	293	20 ± 6	138
3	4	2	13 ± 4	101	5 ± 5	68
3	4	2	7 ± 4	359	5 ± 5	192
3	4	3	26 ± 5	60	31 ± 5	78
3	4	3	10 ± 5	142	13 ± 5	335
3	4	4	12 ± 5	307	33 ± 5	175
3	4	4	22 ± 5	52	14 ± 5	270
3	5	2	10 ± 3	323	12 ± 4	303
3	5	2	7 ± 3	149	7 ± 4	105
3	5	3	8 ± 4	108	19 ± 4	59
3	5	3	6 ± 4	276	13 ± 4	214
3	5	4	10 ± 4	198	17 ± 4	327
3	5	4	11 ± 4	226	11 ± 4	125
3	6	3	8 ± 3	287	22 ± 3	249
3	6	3	2 ± 3	243	12 ± 3	15
4	3	3	2 ± 3	232	7 ± 4	20
4	3	3	13 ± 3	203	8 ± 4	138
4	4	3	6 ± 3	24	9 ± 3	8
4	4	3	10 ± 3	20	10 ± 3	351
4	4	4	11 ± 3	338	22 ± 4	295
4	4	4	2 ± 3	67	2 ± 4	245
4	5	3	4 ± 2	335	7 ± 2	18
4	5	3	2 ± 2	60	5 ± 2	110
4	5	4	12 ± 3	248	16 ± 3	261
4	5	4	7 ± 3	184	4 ± 3	133
4	5	5	1 ± 2	134	13 ± 3	330
4	5	5	4 ± 2	14	2 ± 3	94
4	6	4	2 ± 2	21	3 ± 2	282
4	6	4	1 ± 2	319	2 ± 2	261

I, $A^k_{jmi} \cos(k\phi + mt + \alpha^k_{jmi}) P^k_j$; II, $A^k_{jme} \cos(k\phi + mt + \alpha^k_{jme}) P^k_j$;
I′, $B^k_{jmi} \cos(k\phi - mt + \beta^k_{jmi}) P^k_j$; II′, $B^k_{jme} \cos(k\phi - mt + \beta^k_{jme}) P^k_j$.

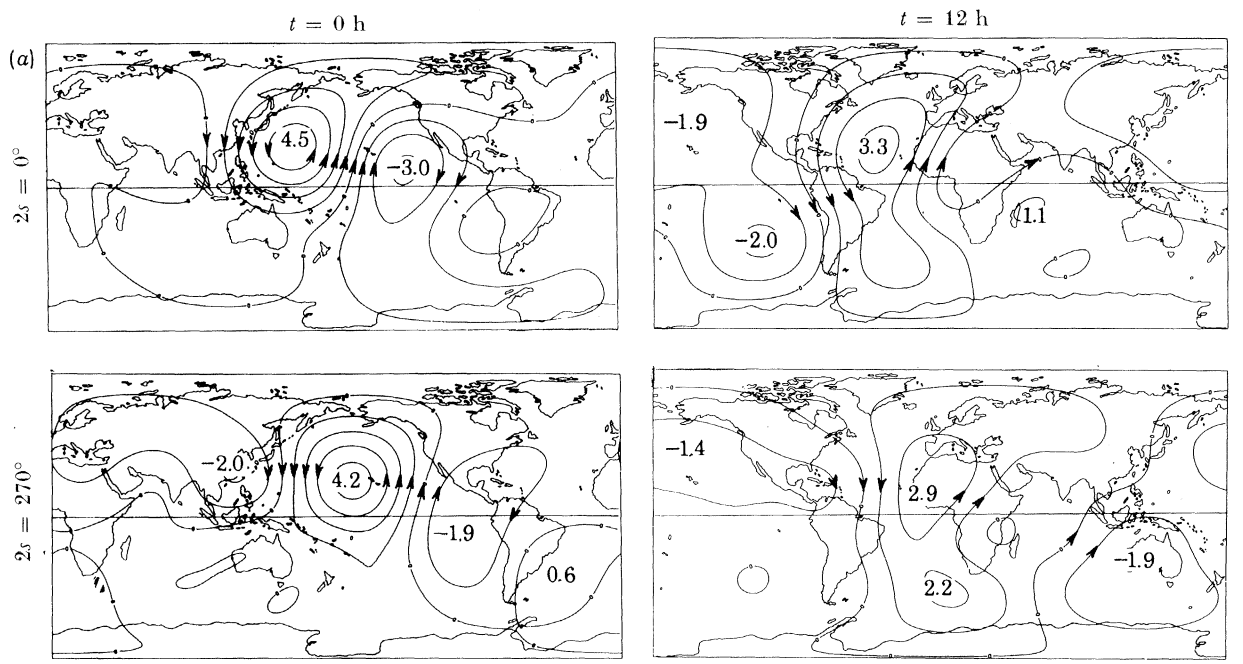

FIGURE 8.6 (*a*). $L(2s)$ phase-law tide current function; extrema in kiloamperes.

TABLE 8.6 (*b*). SPHERICAL HARMONIC ANALYSIS OF $L(2s)$ PARTIAL TIDES

(Amplitudes in picoteslas; phase angles in degrees.)

n j k	internal III / III′	$\alpha^k_{jm'i}$ / $\beta^k_{jm'i}$	external IV / IV′	$\alpha^k_{jm'e}$ / $\beta^k_{jm'e}$
1 1 0	56 ± 16	146	113 ± 25	166
1 1 1	39 ± 12	335	140 ± 17	333
1 1 1	33 ± 12	177	7 ± 17	109
1 2 0	16 ± 15	280	32 ± 18	353
1 2 1	52 ± 12	325	121 ± 14	286
1 2 1	10 ± 12	260	47 ± 14	201
1 2 2	10 ± 9	226	46 ± 11	8
1 2 2	37 ± 9	235	22 ± 11	283
1 3 0	43 ± 12	10	31 ± 15	331
1 3 1	3 ± 10	254	35 ± 11	323
1 3 1	20 ± 9	39	18 ± 11	1
1 3 2	37 ± 9	48	13 ± 11	215
1 3 2	38 ± 9	67	7 ± 11	213
1 4 0	29 ± 10	173	11 ± 11	322
1 4 1	6 ± 7	48	24 ± 8	293
1 4 1	18 ± 7	180	25 ± 8	85
1 4 2	23 ± 7	231	18 ± 8	313
1 4 2	17 ± 7	240	9 ± 8	231
2 1 1	56 ± 10	318	83 ± 13	299
2 1 1	13 ± 10	318	35 ± 13	157
2 2 1	12 ± 9	280	48 ± 10	303
2 2 1	17 ± 9	170	20 ± 10	258
2 2 2	15 ± 8	261	71 ± 10	249
2 2 2	12 ± 8	2	15 ± 10	226
2 3 1	7 ± 7	5	8 ± 7	260
2 3 1	5 ± 7	355	18 ± 7	97
2 3 2	16 ± 7	292	14 ± 8	326
2 3 2	16 ± 7	165	7 ± 8	183
2 3 3	2 ± 6	186	9 ± 7	15
2 3 3	7 ± 6	72	8 ± 7	278
2 4 1	18 ± 5	166	3 ± 6	128
2 4 1	11 ± 5	154	17 ± 6	225
2 4 2	11 ± 6	201	14 ± 6	157
2 4 2	6 ± 6	235	8 ± 6	246
2 4 3	14 ± 5	313	6 ± 5	284
2 4 3	7 ± 5	277	4 ± 5	305
2 5 2	7 ± 5	40	17 ± 5	4
2 5 2	4 ± 4	342	7 ± 5	274
3 2 2	20 ± 5	170	25 ± 7	176
3 2 2	19 ± 5	189	20 ± 7	111
3 3 2	12 ± 5	351	13 ± 6	327
3 3 2	9 ± 5	54	8 ± 6	200
3 3 3	18 ± 5	135	42 ± 6	85
3 3 3	7 ± 5	171	15 ± 6	137
3 4 2	8 ± 4	173	17 ± 5	149
3 4 2	4 ± 4	192	6 ± 5	49
3 4 3	9 ± 5	78	12 ± 5	63
3 4 3	8 ± 5	277	15 ± 5	338
3 4 4	8 ± 5	354	11 ± 5	157
3 4 4	10 ± 5	65	7 ± 5	264
3 5 2	9 ± 3	0	25 ± 4	354
3 5 2	5 ± 3	15	8 ± 4	341
3 5 3	6 ± 4	330	4 ± 4	182
3 5 3	1 ± 4	240	4 ± 4	175
3 5 4	11 ± 3	146	6 ± 4	87
3 5 4	3 ± 3	242	3 ± 4	90
3 6 3	1 ± 3	70	9 ± 3	302
3 6 3	3 ± 3	56	3 ± 3	100
4 3 3	2 ± 4	160	6 ± 4	137
4 3 3	3 ± 4	130	3 ± 4	347
4 4 3	3 ± 3	251	2 ± 4	117
4 4 3	1 ± 3	57	8 ± 4	109
4 4 4	7 ± 3	319	8 ± 4	312
4 4 4	7 ± 3	144	6 ± 4	155
4 5 3	4 ± 2	75	7 ± 3	275
4 5 3	4 ± 2	146	3 ± 3	305
4 5 4	4 ± 3	321	11 ± 3	296
4 5 4	5 ± 3	282	7 ± 3	248
4 5 5	3 ± 2	2	8 ± 3	298
4 5 5	3 ± 2	346	4 ± 3	38
4 6 4	5 ± 2	1	12 ± 2	8
4 6 4	2 ± 2	299	3 ± 2	9

III, $A^k_{jm'i}\cos(k\phi+m't+\alpha^k_{jm'i})P^k_j$; IV, $A^k_{jm'e}\cos(k\phi+m't+\alpha^k_{jm'e})P^k_j$;
III′, $B^k_{jm'i}\cos(k\phi-m't+\beta^k_{jm'i})P^k_j$; IV′, $B^k_{jm'e}\cos(k\phi-m't+\beta^k_{jm'e})P^k_j$.

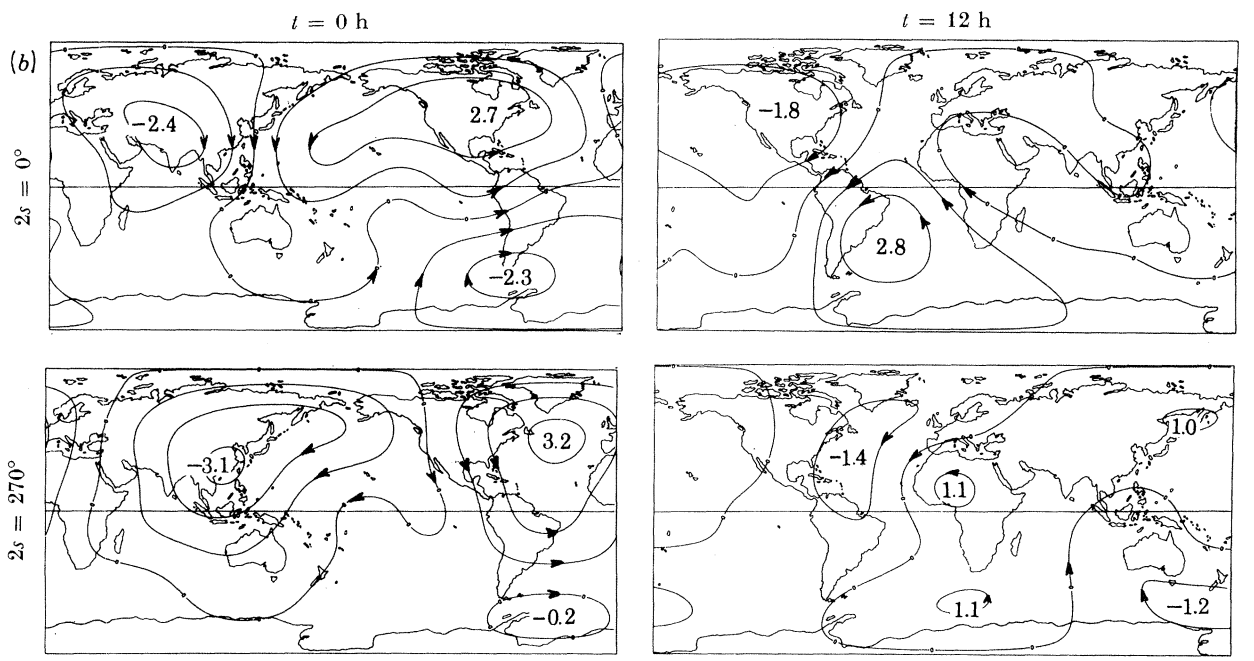

FIGURE 8.6 (*b*). $L(2s)$ partial tide current function; extrema in kiloamperes.

TABLE 8.7 (*a*). SPHERICAL HARMONIC ANALYSIS OF $L(3s-3h-p)$ PHASE-LAW TIDES

(Amplitudes in picoteslas; phase angles in degrees.)

			internal		external	
n	j	k	I	α^k_{jmi}	II	α^k_{jme}
n	j	k	I′	β^k_{jmi}	II′	β^k_{jme}
1	1	0	27 ± 14	270	57 ± 21	251
1	1	1	48 ± 9	320	123 ± 12	319
1	1	1	11 ± 9	150	12 ± 12	287
1	2	0	27 ± 11	274	68 ± 14	293
1	2	1	15 ± 9	336	51 ± 11	287
1	2	1	19 ± 9	264	17 ± 11	161
1	2	2	15 ± 7	138	23 ± 9	85
1	2	2	17 ± 7	234	21 ± 9	254
1	3	0	1 ± 10	10	3 ± 12	118
1	3	1	11 ± 8	139	21 ± 9	67
1	3	1	8 ± 8	183	14 ± 9	274
1	3	2	18 ± 7	47	12 ± 8	322
1	3	2	19 ± 7	47	6 ± 8	348
1	4	0	14 ± 8	232	28 ± 9	285
1	4	1	15 ± 6	276	26 ± 6	242
1	4	1	11 ± 6	62	20 ± 6	103
1	4	2	10 ± 6	259	12 ± 6	23
1	4	2	12 ± 6	246	20 ± 6	292
2	1	1	16 ± 8	342	62 ± 11	283
2	1	1	11 ± 8	14	8 ± 11	74
2	2	1	7 ± 7	322	66 ± 9	12
2	2	1	5 ± 7	83	11 ± 9	239
2	2	2	42 ± 7	156	97 ± 8	143
2	2	2	4 ± 7	84	3 ± 8	76
2	3	1	23 ± 6	46	11 ± 7	98
2	3	1	24 ± 6	278	10 ± 7	5
2	3	2	17 ± 6	277	4 ± 7	131
2	3	2	14 ± 6	173	26 ± 7	8
2	3	3	9 ± 5	306	17 ± 6	264
2	3	3	23 ± 5	64	20 ± 6	67
2	4	1	2 ± 4	171	18 ± 5	38
2	4	1	11 ± 4	57	12 ± 5	236
2	4	2	16 ± 5	154	26 ± 6	218
2	4	2	12 ± 5	22	19 ± 6	154
2	4	3	7 ± 4	209	14 ± 5	197
2	4	3	11 ± 4	223	10 ± 5	218
2	5	2	8 ± 4	333	3 ± 4	8
2	5	2	11 ± 4	68	19 ± 4	60
3	2	2	7 ± 5	169	33 ± 6	157
3	2	2	8 ± 5	257	16 ± 6	170
3	3	2	7 ± 4	213	13 ± 5	118
3	3	2	17 ± 4	78	14 ± 5	56
3	3	3	24 ± 4	353	52 ± 5	315
3	3	3	3 ± 4	21	6 ± 5	323
3	4	2	3 ± 4	158	6 ± 4	273
3	4	2	6 ± 4	163	8 ± 4	157
3	4	3	7 ± 4	217	3 ± 5	220
3	4	3	3 ± 4	167	7 ± 5	67
3	4	4	10 ± 4	125	11 ± 5	94
3	4	4	9 ± 4	181	4 ± 5	57
3	5	2	2 ± 3	299	1 ± 3	121
3	5	2	7 ± 3	88	10 ± 3	96
3	5	3	1 ± 3	326	7 ± 4	21
3	5	3	4 ± 3	85	2 ± 4	101
3	5	4	10 ± 3	38	8 ± 4	29
3	5	4	3 ± 3	350	2 ± 4	214
3	6	3	8 ± 3	5	10 ± 3	350
3	6	3	4 ± 3	221	10 ± 3	204
4	3	3	3 ± 3	347	6 ± 4	332
4	3	3	9 ± 3	35	5 ± 4	334
4	4	3	2 ± 3	38	7 ± 3	313
4	4	3	5 ± 3	255	2 ± 3	226
4	4	4	7 ± 3	145	17 ± 3	103
4	4	4	5 ± 3	226	6 ± 3	149
4	5	3	5 ± 2	285	4 ± 2	212
4	5	3	2 ± 2	337	4 ± 2	1
4	5	4	6 ± 3	20	8 ± 3	1
4	5	4	5 ± 3	116	7 ± 3	24
4	5	5	3 ± 2	165	8 ± 2	167
4	5	5	2 ± 2	223	2 ± 2	15
4	6	4	2 ± 2	174	9 ± 2	175
4	6	4	3 ± 2	28	7 ± 2	138

I, $A^k_{jmi}\cos(k\phi+mt+\alpha^k_{jmi})P^k_j$; II, $A^k_{jme}\cos(k\phi+mt+\alpha^k_{jme})P^k_j$;
I′, $B^k_{jmi}\cos(k\phi-mt+\beta^k_{jmi})P^k_j$; II′, $B^k_{jme}\cos(k\phi-mt+\beta^k_{jme})P^k_j$.

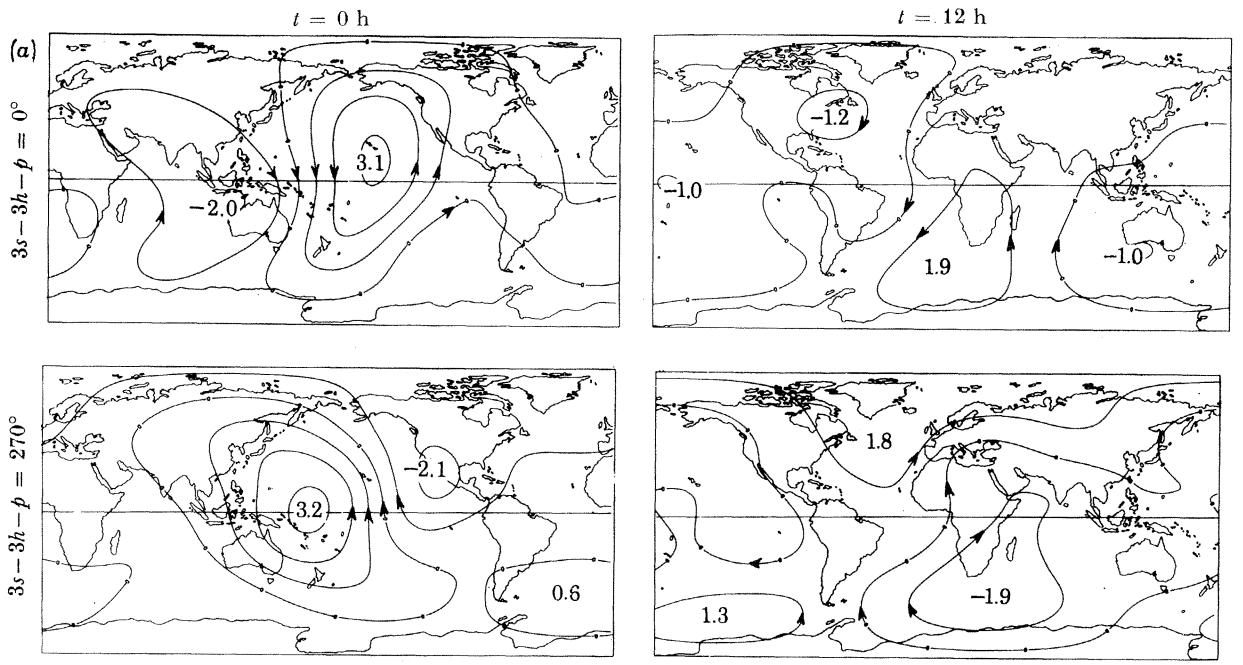

FIGURE 8.7 (*a*). $L(3s-3h-p)$ phase-law tide current function; extrema in kiloamperes.

TABLE 8.7 (*b*). SPHERICAL HARMONIC ANALYSIS OF $L(3s-3h-p)$ PARTIAL TIDES

(Amplitudes in picoteslas; phase angles in degrees.)

			internal		external	
n	j	k	III	$\alpha^k_{jm'i}$	IV	$\alpha^k_{jm'e}$
n	j	k	III′	$\beta^k_{jm'i}$	IV′	$\beta^k_{jm'e}$
1	1	0	102 ± 13	85	243 ± 20	97
1	1	1	42 ± 9	81	88 ± 12	45
1	1	1	6 ± 9	107	60 ± 12	303
1	2	0	30 ± 11	360	53 ± 14	262
1	2	1	20 ± 9	216	51 ± 10	150
1	2	1	13 ± 9	45	33 ± 10	144
1	2	2	24 ± 7	259	35 ± 8	250
1	2	2	16 ± 7	247	25 ± 8	292
1	3	0	16 ± 9	111	32 ± 11	137
1	3	1	8 ± 7	310	28 ± 8	307
1	3	1	13 ± 7	96	23 ± 8	51
1	3	2	1 ± 7	185	16 ± 8	156
1	3	2	4 ± 7	7	4 ± 8	302
1	4	0	10 ± 8	325	29 ± 9	177
1	4	1	3 ± 5	31	29 ± 6	170
1	4	1	9 ± 5	292	10 ± 6	57
1	4	2	5 ± 5	88	5 ± 6	164
1	4	2	10 ± 5	267	10 ± 6	253
2	1	1	19 ± 9	230	109 ± 12	177
2	1	1	11 ± 9	329	47 ± 12	126
2	2	1	33 ± 7	232	73 ± 9	261
2	2	1	21 ± 7	225	40 ± 9	298
2	2	2	11 ± 7	221	60 ± 9	223
2	2	2	13 ± 7	33	33 ± 9	251
2	3	1	2 ± 6	61	26 ± 7	154
2	3	1	19 ± 6	5	21 ± 7	2
2	3	2	6 ± 6	213	18 ± 7	90
2	3	2	8 ± 6	204	23 ± 7	50
2	3	3	21 ± 5	98	24 ± 6	60
2	3	3	8 ± 5	149	4 ± 6	97
2	4	1	12 ± 5	297	33 ± 5	277
2	4	1	10 ± 5	308	13 ± 5	320
2	4	2	8 ± 5	127	21 ± 6	166
2	4	2	10 ± 5	59	5 ± 6	288
2	4	3	8 ± 4	257	13 ± 5	247
2	4	3	10 ± 4	240	6 ± 5	178
2	5	2	5 ± 4	141	4 ± 5	106
2	5	2	3 ± 4	221	5 ± 5	200

			internal		external	
n	j	k	III	$\alpha^k_{jm'i}$	IV	$\alpha^k_{jm'e}$
n	j	k	III′	$\beta^k_{jm'i}$	IV′	$\beta^k_{jm'e}$
3	2	2	8 ± 5	23	7 ± 6	67
3	2	2	9 ± 5	17	23 ± 6	295
3	3	2	7 ± 5	180	2 ± 5	2
3	3	2	12 ± 5	263	3 ± 5	359
3	3	3	16 ± 5	59	23 ± 6	3
3	3	3	4 ± 5	34	4 ± 6	14
3	4	2	6 ± 4	314	6 ± 4	323
3	4	2	8 ± 4	29	7 ± 4	281
3	4	3	14 ± 4	242	3 ± 5	258
3	4	3	9 ± 4	274	7 ± 5	154
3	4	4	7 ± 4	244	5 ± 5	237
3	4	4	7 ± 4	133	5 ± 5	15
3	5	2	3 ± 3	108	11 ± 3	204
3	5	2	10 ± 3	289	7 ± 3	288
3	5	3	7 ± 4	59	9 ± 4	339
3	5	3	8 ± 4	80	7 ± 4	1
3	5	4	3 ± 3	344	8 ± 4	133
3	5	4	8 ± 3	14	3 ± 4	334
3	6	3	10 ± 3	183	8 ± 3	137
3	6	3	5 ± 3	195	8 ± 3	176
4	3	3	1 ± 3	312	5 ± 4	146
4	3	3	6 ± 3	273	7 ± 4	272
4	4	3	3 ± 3	290	2 ± 3	19
4	4	3	2 ± 3	111	2 ± 3	318
4	4	4	2 ± 3	86	3 ± 3	143
4	4	4	1 ± 3	329	2 ± 3	107
4	5	3	1 ± 2	133	5 ± 2	270
4	5	3	5 ± 2	233	5 ± 2	211
4	5	4	9 ± 2	106	10 ± 3	81
4	5	4	1 ± 2	104	3 ± 3	195
4	5	5	2 ± 2	33	4 ± 2	347
4	5	5	2 ± 2	315	3 ± 2	325
4	6	4	3 ± 2	257	6 ± 2	180
4	6	4	3 ± 2	310	3 ± 2	321

III, $A^k_{jm'i}\cos(k\phi+m't+\alpha^k_{jm'i})P^k_j$; IV, $A^k_{jm'e}\cos(k\phi+m't+\alpha^k_{jm'e})P^k_j$;
III′, $B^k_{jm'i}\cos(k\phi-m't+\beta^k_{jm'i})P^k_j$; IV′, $B^k_{jm'e}\cos(k\phi-m't+\beta^k_{jm'e})P^k_j$.

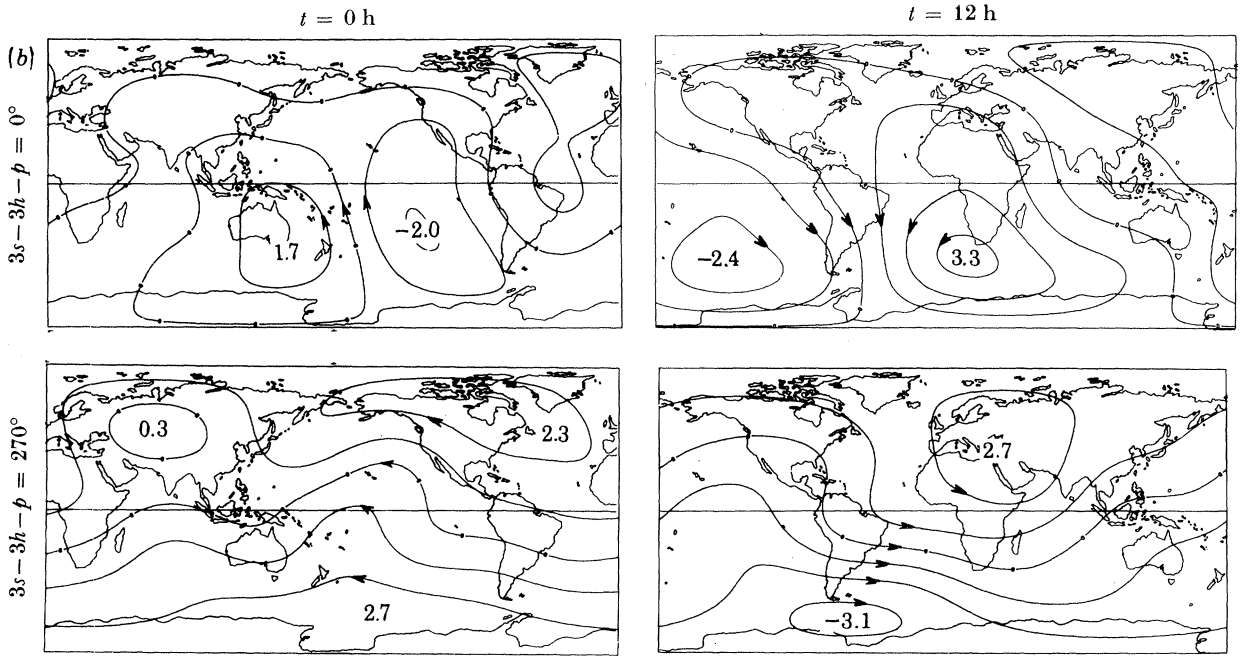

FIGURE 8.7 (*b*). $L(3s-3h-p)$ partial tide current function; extrema in kiloamperes.

TABLE 8.8 (*a*). SPHERICAL HARMONIC ANALYSIS OF $L(3s-2h-p)_{\text{iono.+oc.}}$ PHASE-LAW TIDES

(Amplitudes in picoteslas; phase angles in degrees.)

			internal		external	
n	j	k	I	α^k_{jmi}	II	α^k_{jme}
n	j	k	I′	β^k_{jmi}	II′	β^k_{jme}
1	1	0	31 ± 16	31	77 ± 23	47
1	1	1	47 ± 10	64	91 ± 13	37
1	1	1	27 ± 10	177	16 ± 13	42
1	2	0	19 ± 13	113	36 ± 17	195
1	2	1	23 ± 10	79	93 ± 12	93
1	2	1	14 ± 10	34	36 ± 12	129
1	2	2	16 ± 8	155	24 ± 10	86
1	2	2	15 ± 8	328	16 ± 10	332
1	3	0	12 ± 11	202	27 ± 13	332
1	3	1	21 ± 8	173	7 ± 10	240
1	3	1	15 ± 8	161	20 ± 10	8
1	3	2	4 ± 8	13	23 ± 9	194
1	3	2	6 ± 8	138	2 ± 9	31
1	4	0	11 ± 9	14	25 ± 10	78
1	4	1	26 ± 6	317	33 ± 7	274
1	4	1	19 ± 6	1	8 ± 7	130
1	4	2	6 ± 6	236	18 ± 7	7
1	4	2	5 ± 6	94	20 ± 7	199
2	1	1	4 ± 11	19	116 ± 14	202
2	1	1	40 ± 11	233	56 ± 14	88
2	2	1	13 ± 10	172	49 ± 11	18
2	2	1	32 ± 10	18	13 ± 11	286
2	2	2	24 ± 9	177	17 ± 10	285
2	2	2	14 ± 9	0	13 ± 10	200
2	3	1	5 ± 7	358	21 ± 8	5
2	3	1	11 ± 7	151	35 ± 8	51
2	3	2	52 ± 7	305	61 ± 8	250
2	3	2	19 ± 8	167	19 ± 8	299
2	3	3	8 ± 7	227	20 ± 8	14
2	3	3	11 ± 7	16	20 ± 8	220
2	4	1	6 ± 5	177	35 ± 6	219
2	4	1	14 ± 5	294	16 ± 6	136
2	4	2	14 ± 6	159	12 ± 7	10
2	4	2	7 ± 6	357	22 ± 7	135
2	4	3	18 ± 5	34	5 ± 6	335
2	4	3	9 ± 5	282	13 ± 6	327
2	5	2	1 ± 5	79	17 ± 5	97
2	5	2	6 ± 5	7	14 ± 5	257
3	2	2	5 ± 5	98	47 ± 6	26
3	2	2	10 ± 5	241	15 ± 6	16
3	3	2	5 ± 5	171	23 ± 5	183
3	3	2	7 ± 5	342	13 ± 5	57
3	3	3	8 ± 4	21	26 ± 5	80
3	3	3	11 ± 5	227	6 ± 5	172
3	4	2	6 ± 4	195	18 ± 4	194
3	4	2	11 ± 4	123	11 ± 4	242
3	4	3	20 ± 4	125	26 ± 5	89
3	4	3	10 ± 4	47	9 ± 5	302
3	4	4	6 ± 4	49	23 ± 5	226
3	4	4	13 ± 4	24	1 ± 5	283
3	5	2	3 ± 3	334	14 ± 3	38
3	5	2	7 ± 3	22	15 ± 3	67
3	5	3	9 ± 4	32	2 ± 4	265
3	5	3	6 ± 4	322	10 ± 4	119
3	5	4	13 ± 3	226	4 ± 4	18
3	5	4	13 ± 3	183	9 ± 4	20
3	6	3	3 ± 3	347	7 ± 3	31
3	6	3	3 ± 3	163	2 ± 3	163
4	3	3	4 ± 3	266	19 ± 3	203
4	3	3	6 ± 3	154	3 ± 3	124
4	4	3	2 ± 3	88	3 ± 3	38
4	4	3	6 ± 3	352	3 ± 3	277
4	4	4	7 ± 3	24	19 ± 3	333
4	4	4	5 ± 3	303	4 ± 3	129
4	5	3	11 ± 2	2	20 ± 2	345
4	5	3	4 ± 2	100	7 ± 2	80
4	5	4	4 ± 2	295	5 ± 3	261
4	5	4	3 ± 2	97	6 ± 3	341
4	5	5	4 ± 2	108	12 ± 2	51
4	5	5	3 ± 2	333	1 ± 2	298
4	6	4	4 ± 2	52	6 ± 2	358
4	6	4	3 ± 2	104	4 ± 2	136

I, $A^k_{jmi}\cos(k\phi+mt+\alpha^k_{jmi})P^k_j$; II, $A^k_{jme}\cos(k\phi+mt+\alpha^k_{jme})P^k_j$;

I′, $B^k_{jmi}\cos(k\phi-mt+\beta^k_{jmi})P^k_j$; II′, $B^k_{jme}\cos(k\phi-mt+\beta^k_{jme})P^k_j$.

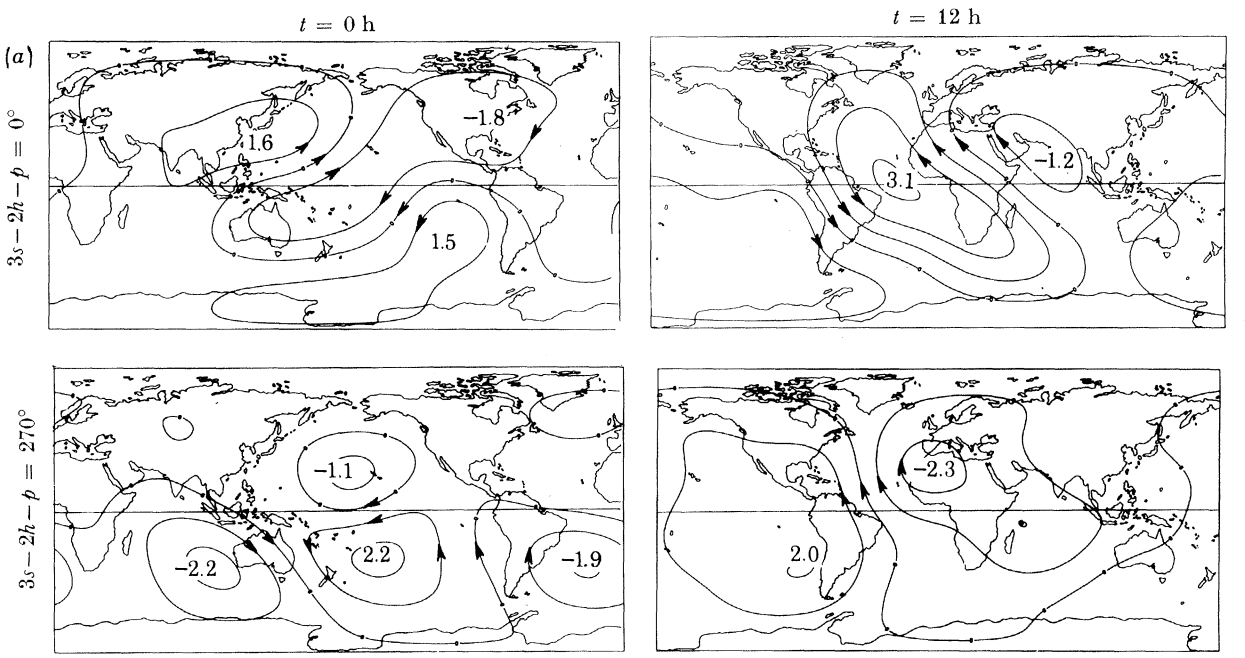

FIGURE 8.8 (*a*). $L(3s-2h-p)_{\text{iono.+oc.}}$ phase-law tide current function; extrema in kiloamperes.

TABLE 8.8 (*b*). SPHERICAL HARMONIC ANALYSIS OF $L(3s-2h-p)_{\text{iono.+oc.}}$ PARTIAL TIDES

(Amplitudes in picoteslas; phase angles in degrees.)

			internal		external	
n	j	k	III	$\alpha^k_{jm\text{i}}$	IV	$\alpha^k_{jm'\text{e}}$
n	j	k	III′	$\beta^k_{jm\text{i}}$	IV′	$\beta^k_{jm'\text{e}}$
1	1	0	40 ± 16	334	67 ± 24	3
1	1	1	12 ± 10	20	25 ± 13	355
1	1	1	14 ± 9	121	26 ± 13	76
1	2	0	52 ± 12	89	114 ± 15	68
1	2	1	25 ± 10	350	73 ± 12	353
1	2	1	15 ± 9	284	22 ± 12	341
1	2	2	16 ± 8	14	27 ± 9	112
1	2	2	17 ± 8	109	14 ± 9	162
1	3	0	25 ± 11	38	32 ± 13	27
1	3	1	7 ± 8	355	31 ± 9	268
1	3	1	10 ± 8	352	28 ± 9	322
1	3	2	5 ± 7	172	11 ± 9	355
1	3	2	15 ± 7	341	7 ± 9	31
1	4	0	11 ± 8	253	20 ± 10	211
1	4	1	5 ± 6	207	39 ± 7	67
1	4	1	5 ± 6	87	8 ± 7	327
1	4	2	6 ± 6	287	12 ± 7	122
1	4	2	8 ± 6	168	13 ± 7	72
2	1	1	68 ± 8	81	120 ± 11	60
2	1	1	14 ± 8	272	23 ± 11	3
2	2	1	5 ± 7	236	53 ± 9	93
2	2	1	14 ± 7	37	27 ± 9	248
2	2	2	26 ± 7	308	75 ± 8	306
2	2	2	11 ± 7	359	23 ± 8	56
2	3	1	2 ± 6	282	55 ± 6	231
2	3	1	14 ± 6	198	17 ± 6	68
2	3	2	17 ± 6	79	46 ± 7	104
2	3	2	12 ± 6	143	7 ± 7	282
2	3	3	14 ± 5	193	8 ± 6	195
2	3	3	13 ± 5	258	7 ± 6	175
2	4	1	12 ± 4	283	6 ± 5	194
2	4	1	13 ± 4	20	13 ± 5	112
2	4	2	4 ± 5	212	24 ± 5	346
2	4	2	12 ± 5	318	11 ± 6	117
2	4	3	9 ± 4	54	8 ± 5	91
2	4	3	3 ± 4	29	5 ± 5	0
2	5	2	6 ± 4	119	9 ± 4	94
2	5	2	9 ± 4	133	6 ± 4	320
3	2	2	30 ± 4	263	56 ± 5	235
3	2	2	15 ± 4	54	9 ± 5	4
3	3	2	9 ± 4	255	12 ± 4	269
3	3	2	14 ± 4	202	7 ± 4	292
3	3	3	15 ± 4	170	32 ± 4	166
3	3	3	13 ± 4	64	5 ± 4	101
3	4	2	3 ± 3	136	10 ± 4	14
3	4	2	6 ± 3	357	4 ± 4	144
3	4	3	8 ± 3	354	6 ± 4	350
3	4	3	3 ± 3	202	4 ± 4	330
3	4	4	4 ± 3	54	11 ± 4	5
3	4	4	9 ± 3	256	2 ± 4	74
3	5	2	2 ± 2	150	10 ± 3	133
3	5	2	6 ± 2	217	16 ± 3	280
3	5	3	4 ± 3	162	7 ± 3	213
3	5	3	5 ± 3	280	3 ± 3	135
3	5	4	9 ± 3	290	12 ± 3	265
3	5	4	2 ± 3	74	6 ± 3	233
3	6	3	3 ± 2	50	5 ± 3	169
3	6	3	2 ± 2	124	1 ± 3	128
4	3	3	0 ± 3	315	10 ± 3	352
4	3	3	2 ± 3	202	3 ± 3	46
4	4	3	1 ± 2	101	7 ± 3	148
4	4	3	2 ± 2	30	1 ± 3	127
4	4	4	12 ± 2	21	11 ± 3	9
4	4	4	1 ± 2	115	5 ± 3	293
4	5	3	4 ± 2	2	8 ± 2	294
4	5	3	4 ± 2	100	3 ± 2	23
4	5	4	5 ± 2	185	4 ± 3	154
4	5	4	2 ± 2	301	2 ± 3	91
4	5	5	7 ± 2	219	6 ± 2	175
4	5	5	1 ± 2	229	3 ± 2	49
4	6	4	2 ± 2	347	8 ± 2	345
4	6	4	3 ± 2	180	2 ± 2	166

III, $A^k_{jm'\text{i}} \cos(k\phi + m't + \alpha^k_{jm'\text{i}}) P^k_j$; IV, $A^k_{jm'\text{e}} \cos(k\phi + m't + \alpha^k_{jm'\text{e}}) P^k_j$;
III′, $B^k_{jm'\text{i}} \cos(k\phi - m't + \beta^k_{jm'\text{i}}) P^k_j$; IV′, $B^k_{jm'\text{e}} \cos(k\phi - m't + \beta^k_{jm'\text{e}}) P^k_j$.

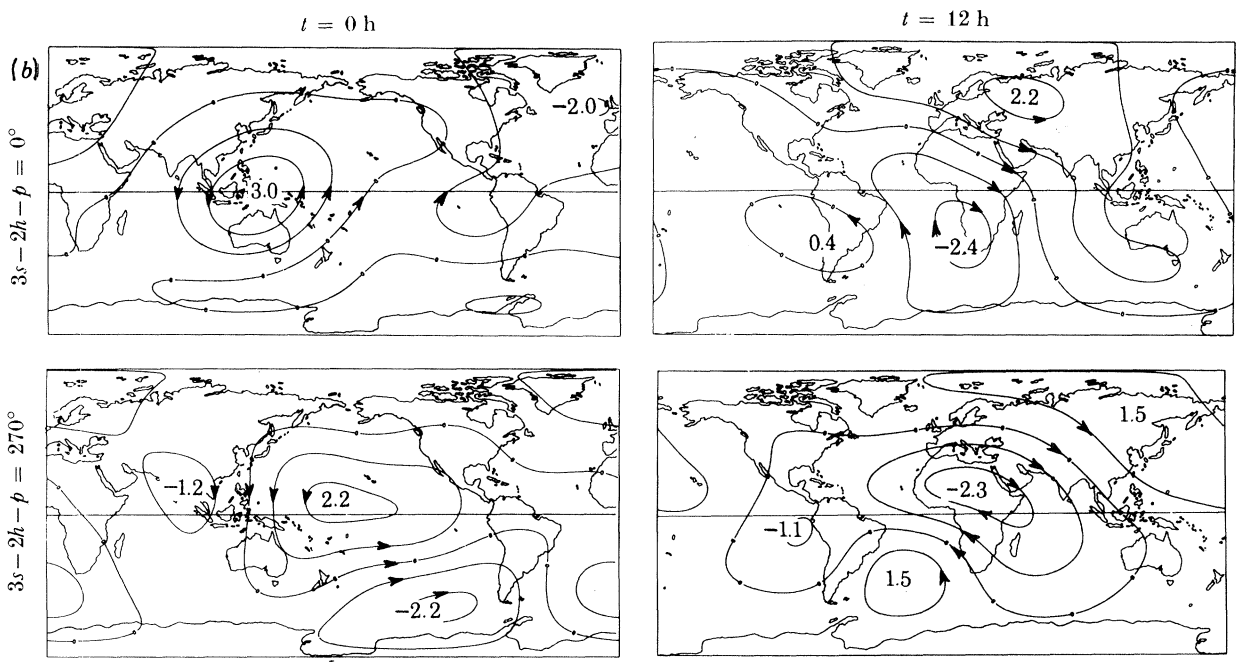

FIGURE 8.8 (*b*). $L(3s-2h-p)_{\text{iono+oc.}}$ partial tide current function; extrema in kiloamperes.

TABLE 8.9 (*a*). SPHERICAL HARMONIC ANALYSIS OF $L(3s-h-p)$ PHASE-LAW TIDES

(Amplitudes in picoteslas; phase angles in degrees.)

n j k	internal I	α^k_{jmi}	external II	α^k_{jme}
n j k	I′	β^k_{jmi}	II′	β^k_{jme}
1 1 0	82 ± 16	270	183 ± 23	288
1 1 1	14 ± 11	200	70 ± 14	175
1 1 1	32 ± 11	206	41 ± 14	121
1 2 0	27 ± 14	103	5 ± 17	279
1 2 1	50 ± 11	124	111 ± 13	104
1 2 1	25 ± 11	9	33 ± 12	335
1 2 2	18 ± 9	173	35 ± 10	217
1 2 2	9 ± 8	267	11 ± 10	123
1 3 0	43 ± 12	276	14 ± 14	72
1 3 1	3 ± 9	39	34 ± 10	74
1 3 1	9 ± 9	182	22 ± 10	230
1 3 2	6 ± 8	286	13 ± 9	183
1 3 2	15 ± 8	92	14 ± 9	55
1 4 0	8 ± 9	67	11 ± 11	207
1 4 1	17 ± 6	272	28 ± 7	254
1 4 1	8 ± 6	286	20 ± 7	76
1 4 2	7 ± 6	314	22 ± 7	184
1 4 2	13 ± 6	294	9 ± 7	9
2 1 1	31 ± 9	7	52 ± 12	42
2 1 1	6 ± 9	332	31 ± 12	153
2 2 1	10 ± 7	98	30 ± 9	5
2 2 1	9 ± 7	62	26 ± 9	330
2 2 2	30 ± 7	69	46 ± 9	68
2 2 2	7 ± 7	91	22 ± 9	259
2 3 1	21 ± 6	2	28 ± 6	300
2 3 1	20 ± 6	219	20 ± 6	135
2 3 2	36 ± 6	275	53 ± 7	278
2 3 2	12 ± 6	316	14 ± 7	58
2 3 3	6 ± 6	76	15 ± 6	1
2 3 3	9 ± 6	210	6 ± 6	268
2 4 1	5 ± 4	251	7 ± 5	72
2 4 1	21 ± 4	45	8 ± 5	163
2 4 2	13 ± 5	138	7 ± 5	316
2 4 2	7 ± 5	103	27 ± 5	142
2 4 3	3 ± 4	54	9 ± 5	147
2 4 3	5 ± 4	339	5 ± 5	294
2 5 2	4 ± 4	158	23 ± 4	120
2 5 2	8 ± 4	165	14 ± 4	237

n j k	internal I	α^k_{jmi}	external II	α^k_{jme}
n j k	I′	β^k_{jmi}	II′	β^k_{jme}
3 2 2	11 ± 5	221	22 ± 6	225
3 2 2	3 ± 5	80	26 ± 6	49
3 3 2	12 ± 5	102	31 ± 5	73
3 3 2	3 ± 5	55	1 ± 5	197
3 3 3	14 ± 4	269	26 ± 5	240
3 3 3	5 ± 4	348	10 ± 5	156
3 4 2	7 ± 4	136	14 ± 4	193
3 4 2	5 ± 4	78	2 ± 4	55
3 4 3	21 ± 4	134	42 ± 5	108
3 4 3	11 ± 4	180	3 ± 5	271
3 4 4	6 ± 4	307	6 ± 4	170
3 4 4	5 ± 4	98	8 ± 5	298
3 5 2	1 ± 3	326	11 ± 3	87
3 5 2	5 ± 3	15	12 ± 3	45
3 5 3	1 ± 4	298	14 ± 4	196
3 5 3	9 ± 4	14	5 ± 4	311
3 5 4	4 ± 3	121	16 ± 4	34
3 5 4	4 ± 3	148	7 ± 4	144
3 6 3	4 ± 3	84	9 ± 3	98
3 6 3	2 ± 3	215	4 ± 3	30
4 3 3	3 ± 3	351	12 ± 4	19
4 3 3	9 ± 3	344	2 ± 4	350
4 4 3	1 ± 3	212	8 ± 3	209
4 4 3	2 ± 3	336	11 ± 3	323
4 4 4	6 ± 3	75	19 ± 3	34
4 4 4	5 ± 3	158	5 ± 3	80
4 5 3	3 ± 2	58	12 ± 3	46
4 5 3	5 ± 2	315	10 ± 3	53
4 5 4	10 ± 3	356	22 ± 3	338
4 5 4	3 ± 3	87	4 ± 3	141
4 5 5	4 ± 2	119	10 ± 3	216
4 5 5	2 ± 2	338	3 ± 3	128
4 6 4	4 ± 2	122	2 ± 2	63
4 6 4	7 ± 2	42	3 ± 2	55

I, $A^k_{jmi}\cos(k\phi+mt+\alpha^k_{jmi})P^k_j$; II, $A^k_{jme}\cos(k\phi+mt+\alpha^k_{jme})P^k_j$;
I′, $B^k_{jmi}\cos(k\phi-mt+\beta^k_{jmi})P^k_j$; II′, $B^k_{jme}\cos(k\phi-mt+\beta^k_{jme})P^k_j$.

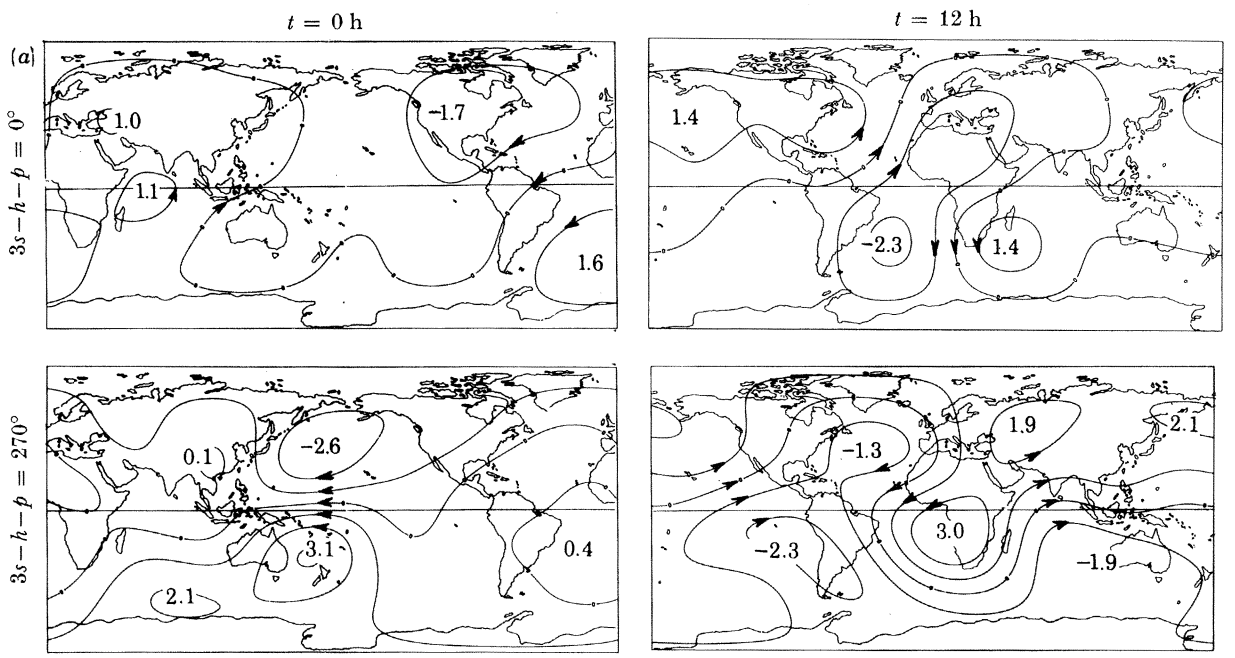

FIGURE 8.9 (*a*). $L(3s-h-p)$ phase-law tide current functions; extrema in kiloamperes.

TABLE 8.9 (*b*). SPHERICAL HARMONIC ANALYSIS OF $L(3s-3h-p)$ PARTIAL TIDES

(Amplitudes in picoteslas; phase angles in degrees.)

			internal		external	
n	j	k	III	$\alpha^k_{jm'i}$	IV	$\alpha^k_{jm'e}$
n	j	k	III′	$\beta^k_{jm'i}$	IV′	$\beta^k_{jm'e}$
1	1	0	68 ± 13	317	109 ± 18	303
1	1	1	31 ± 8	217	68 ± 12	209
1	1	1	30 ± 8	76	13 ± 12	51
1	2	0	29 ± 12	171	29 ± 13	81
1	2	1	30 ± 8	222	76 ± 10	188
1	2	1	14 ± 8	185	13 ± 10	140
1	2	2	11 ± 7	51	30 ± 8	158
1	2	2	10 ± 7	126	14 ± 8	335
1	3	0	34 ± 10	306	36 ± 11	283
1	3	1	9 ± 7	119	11 ± 8	148
1	3	1	5 ± 7	256	5 ± 8	69
1	3	2	21 ± 7	192	20 ± 8	202
1	3	2	21 ± 7	237	10 ± 8	183
1	4	0	11 ± 7	107	23 ± 9	36
1	4	1	12 ± 5	20	26 ± 6	113
1	4	1	5 ± 5	69	10 ± 6	203
1	4	2	7 ± 5	51	4 ± 6	181
1	4	2	12 ± 5	62	12 ± 6	64
2	1	1	30 ± 7	90	5 ± 10	44
2	1	1	16 ± 7	223	32 ± 10	28
2	2	1	20 ± 6	261	38 ± 7	114
2	2	1	29 ± 6	352	35 ± 7	238
2	2	2	2 ± 6	238	34 ± 7	347
2	2	2	3 ± 6	336	13 ± 7	73
2	3	1	12 ± 5	142	20 ± 6	303
2	3	1	20 ± 5	169	17 ± 6	46
2	3	2	8 ± 5	348	19 ± 6	213
2	3	2	18 ± 5	118	16 ± 6	222
2	3	3	6 ± 5	295	22 ± 6	327
2	3	3	4 ± 5	173	13 ± 6	197
2	4	1	4 ± 4	196	30 ± 4	125
2	4	1	4 ± 4	10	12 ± 4	211
2	4	2	5 ± 4	345	23 ± 5	336
2	4	2	11 ± 4	229	19 ± 5	86
2	4	3	17 ± 4	53	18 ± 4	10
2	4	3	6 ± 4	262	7 ± 4	224
2	5	2	4 ± 3	316	8 ± 4	214
2	5	2	5 ± 3	59	10 ± 4	220
3	2	2	9 ± 4	274	2 ± 5	142
3	2	2	9 ± 4	19	12 ± 5	50
3	3	2	12 ± 4	110	8 ± 4	89
3	3	2	7 ± 4	251	4 ± 4	3
3	3	3	7 ± 4	255	21 ± 4	214
3	3	3	8 ± 4	125	9 ± 4	78
3	4	2	3 ± 3	332	7 ± 4	62
3	4	2	4 ± 3	79	7 ± 4	337
3	4	3	5 ± 3	336	15 ± 4	341
3	4	3	10 ± 3	350	2 ± 4	325
3	4	4	7 ± 3	90	6 ± 4	70
3	4	4	6 ± 3	256	2 ± 4	214
3	5	2	9 ± 3	102	14 ± 3	85
3	5	2	7 ± 3	239	8 ± 3	213
3	5	3	4 ± 3	272	4 ± 3	208
3	5	3	2 ± 3	183	5 ± 3	90
3	5	4	6 ± 3	231	13 ± 3	162
3	5	4	2 ± 3	110	2 ± 3	288
3	6	3	5 ± 2	239	12 ± 3	231
3	6	3	4 ± 2	42	4 ± 3	244
4	3	3	1 ± 2	82	3 ± 3	21
4	3	3	4 ± 2	236	5 ± 3	270
4	4	3	5 ± 2	302	7 ± 3	228
4	4	3	3 ± 2	93	4 ± 3	87
4	4	4	1 ± 2	4	2 ± 3	46
4	4	4	6 ± 2	39	2 ± 3	256
4	5	3	5 ± 2	186	6 ± 2	155
4	5	3	2 ± 2	305	5 ± 2	305
4	5	4	6 ± 2	152	10 ± 2	138
4	5	4	3 ± 2	300	5 ± 2	86
4	5	5	4 ± 2	287	4 ± 2	293
4	5	5	6 ± 2	220	3 ± 2	327
4	6	4	1 ± 2	177	3 ± 2	65
4	6	4	1 ± 2	70	5 ± 2	285

III, $A^k_{jm'i}\cos(k\phi+m't+\alpha^k_{jm'i})P^k_j$; IV, $A^k_{jm'e}\cos(k\phi+m't+\alpha^k_{jm'e})P^k_j$;
III′, $B^k_{jm'i}\cos(k\phi-m't+\beta^k_{jmi})P^k_j$; IV′, $B^k_{jm'e}\cos(k\phi-m't+\beta^k_{jm'e})P^k_j$.

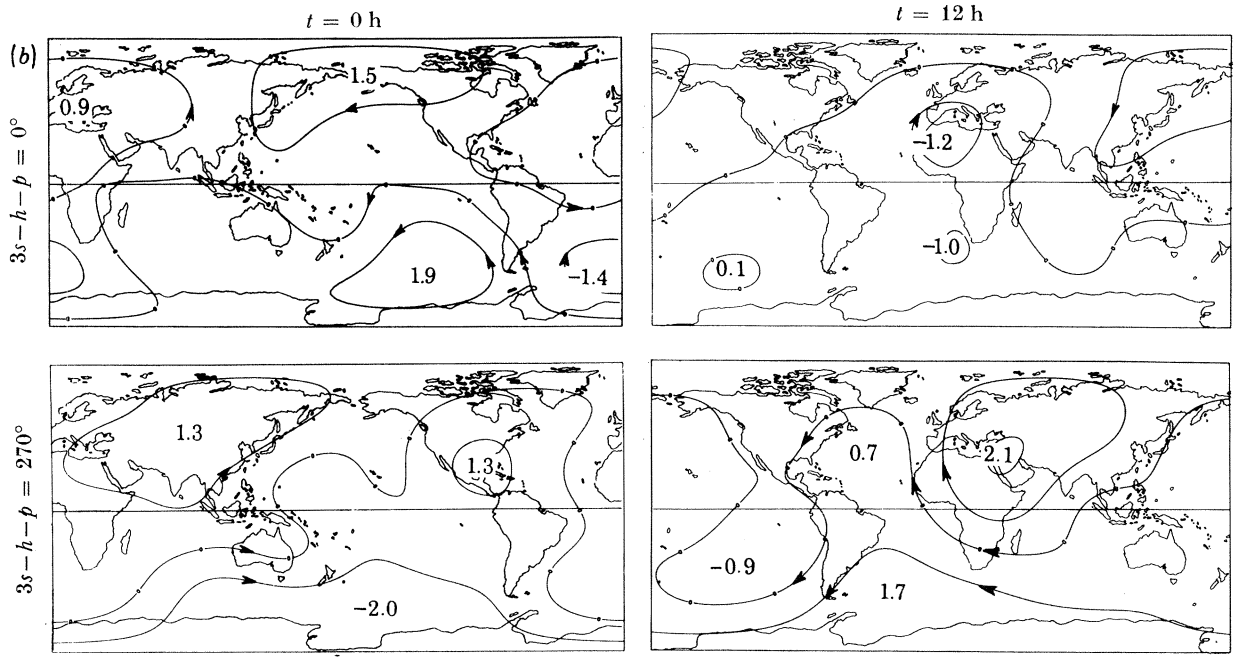

FIGURE 8.9 (*b*) $L(3s-h-p)$ partial tide current function; extrema in kiloamperes.

TABLE 8.10. SPHERICAL HARMONIC ANALYSIS OF S

(Amplitudes in picoteslas; phase angles in degrees.)

			internal		external	
n	j	k	I	α^k_{jni}	II	α^k_{jne}
n	j	k	I′	β^k_{jni}	II′	β^k_{jne}
1	1	0	539 ± 300	48	1405 ± 519	12
1	1	1	504 ± 223	82	1019 ± 314	81
1	1	1	136 ± 225	25	472 ± 314	80
1	2	0	647 ± 260	111	979 ± 334	106
1	2	1	2373 ± 202	17	6146 ± 249	19
1	2	1	74 ± 201	62	295 ± 250	192
1	2	2	587 ± 189	62	784 ± 232	95
1	2	2	224 ± 189	98	110 ± 232	101
1	3	0	283 ± 240	207	500 ± 275	248
1	3	1	162 ± 170	120	454 ± 200	202
1	3	1	213 ± 170	223	348 ± 200	324
1	3	2	214 ± 166	201	380 ± 193	163
1	3	2	200 ± 166	236	120 ± 193	263
1	4	0	313 ± 194	45	139 ± 231	197
1	4	1	558 ± 122	250	1100 ± 141	161
1	4	1	240 ± 122	20	203 ± 141	245
1	4	2	196 ± 129	31	435 ± 148	328
1	4	2	158 ± 129	2	377 ± 148	15
2	1	1	587 ± 152	83	1414 ± 198	99
2	1	1	181 ± 152	249	53 ± 200	319
2	2	1	307 ± 123	227	325 ± 145	183
2	2	1	337 ± 121	88	52 ± 144	325
2	2	2	416 ± 129	269	1102 ± 152	268
2	2	2	188 ± 126	1	74 ± 150	25
2	3	1	163 ± 93	285	394 ± 106	249
2	3	1	112 ± 95	187	314 ± 107	133
2	3	2	1329 ± 104	220	2922 ± 117	197
2	3	2	223 ± 104	219	93 ± 118	269
2	3	3	177 ± 97	220	397 ± 113	288
2	3	3	232 ± 97	137	270 ± 113	266
2	4	1	131 ± 69	1	113 ± 78	191
2	4	1	33 ± 69	342	8 ± 78	179
2	4	2	90 ± 84	84	371 ± 93	256
2	4	2	94 ± 84	107	195 ± 93	225
2	4	3	236 ± 71	12	263 ± 82	60
2	4	3	182 ± 72	276	71 ± 82	31
2	5	2	56 ± 64	45	281 ± 70	47
2	5	2	22 ± 64	236	119 ± 70	140
3	2	2	190 ± 47	144	214 ± 58	220
3	2	2	200 ± 47	298	243 ± 58	140
3	3	2	42 ± 42	62	95 ± 48	86
3	3	2	164 ± 42	93	84 ± 48	312
3	3	3	247 ± 45	143	457 ± 52	104
3	3	3	23 ± 45	354	71 ± 52	203
3	4	2	65 ± 34	80	120 ± 38	81
3	4	2	87 ± 34	236	45 ± 38	0
3	4	3	650 ± 39	48	1168 ± 44	33
3	4	3	70 ± 40	162	124 ± 44	4
3	4	4	89 ± 41	334	209 ± 45	125
3	4	4	73 ± 41	78	61 ± 45	331
3	5	2	12 ± 28	47	164 ± 30	0
3	5	2	23 ± 28	164	86 ± 30	225
3	5	3	65 ± 34	196	201 ± 36	69

TABLE 8.10 (*continued*)

			internal		external	
n	j	k	I	α^k_{jni}	II	α^k_{jne}
n	j	k	I′	β^k_{jni}	II′	β^k_{jne}
3	5	3	58 ± 33	316	89 ± 37	190
3	5	4	113 ± 30	163	198 ± 34	271
3	5	4	48 ± 30	290	61 ± 34	116
3	6	3	33 ± 26	323	67 ± 29	224
3	6	3	9 ± 26	42	81 ± 29	25
4	3	3	29 ± 21	309	30 ± 25	346
4	3	3	59 ± 21	208	11 ± 25	36
4	4	3	30 ± 19	282	9 ± 22	11
4	4	3	49 ± 19	37	31 ± 21	284
4	4	4	65 ± 21	324	174 ± 23	302
4	4	4	53 ± 21	339	8 ± 23	203
4	5	3	29 ± 13	252	103 ± 15	208
4	5	3	17 ± 13	221	29 ± 15	126
4	5	4	135 ± 18	244	238 ± 20	215
4	5	4	37 ± 18	127	18 ± 20	353
4	5	5	12 ± 16	284	40 ± 18	52
4	5	5	20 ± 16	36	20 ± 18	260
4	6	4	38 ± 13	309	102 ± 14	258
4	6	4	29 ± 13	283	19 ± 14	287

I, $A^k_{jni}\cos(k\phi+nt+\alpha^k_{jni})P^k_j$; II, $A^k_{jne}\cos(k\phi+nt+\alpha^k_{jne})P^k_j$.
I′, $B^k_{jni}\cos(k\phi-nt+\beta^k_{jni})P^k_j$; II′, $B^k_{jne}\cos(k\phi-nt+\beta^k_{jne})P^k_j$.

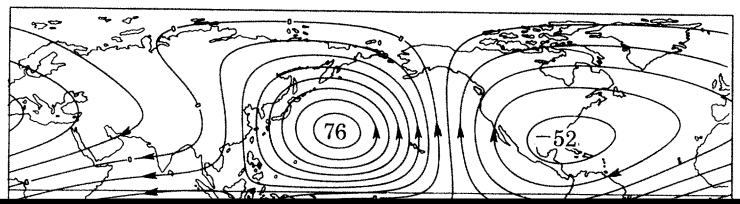

$t = 0$ h

TABLE 8.11 (*a*). SPHERICAL HARMONIC ANALYSIS OF $S^-(h)$

(Amplitudes in picoteslas; phase angles in degrees.)

n j k	internal I	α^k_{jmi}	external II	α^k_{jme}
n j k	I′	β^k_{jmi}	II′	β^k_{jme}
1 1 0	88 ± 70	108	278 ± 113	224
1 1 1	738 ± 48	126	2535 ± 69	117
1 1 1	136 ± 48	14	108 ± 70	270
1 2 0	102 ± 61	319	328 ± 79	16
1 2 1	76 ± 42	153	274 ± 52	237
1 2 1	60 ± 42	210	14 ± 52	150
1 2 2	153 ± 41	343	106 ± 51	318
1 2 2	111 ± 41	123	150 ± 51	297
1 3 0	171 ± 54	99	99 ± 64	52
1 3 1	340 ± 36	54	907 ± 42	74
1 3 1	70 ± 36	356	84 ± 42	333
1 3 2	108 ± 35	123	231 ± 41	39
1 3 2	131 ± 35	265	131 ± 41	112
1 4 0	112 ± 40	2	150 ± 50	264
1 4 1	35 ± 28	329	103 ± 33	293
1 4 1	15 ± 28	276	34 ± 33	194
1 4 2	21 ± 28	166	92 ± 32	203
1 4 2	106 ± 28	94	65 ± 32	253
2 1 1	121 ± 50	94	402 ± 68	36
2 1 1	86 ± 50	122	46 ± 69	72
2 2 1	54 ± 40	347	139 ± 48	209
2 2 1	94 ± 40	358	78 ± 48	64
2 2 2	376 ± 43	0	923 ± 54	11
2 2 2	76 ± 43	191	87 ± 54	349
2 3 1	96 ± 31	321	167 ± 36	235
2 3 1	38 ± 31	12	95 ± 35	7
2 3 2	64 ± 36	76	31 ± 41	305
2 3 2	58 ± 36	61	98 ± 41	174
2 3 3	39 ± 34	161	89 ± 42	166
2 3 3	57 ± 34	256	71 ± 42	65
2 4 1	96 ± 23	137	133 ± 26	83
2 4 1	6 ± 23	24	78 ± 26	44
2 4 2	154 ± 23	288	383 ± 32	269
2 4 2	21 ± 23	150	62 ± 32	94
2 4 3	43 ± 25	213	135 ± 29	236
2 4 3	23 ± 25	95	108 ± 29	191
2 5 2	19 ± 21	343	77 ± 24	300
2 5 2	28 ± 21	58	75 ± 24	57
3 2 2	93 ± 24	287	187 ± 32	253
3 2 2	72 ± 24	31	23 ± 32	204
3 3 2	64 ± 20	152	139 ± 24	59
3 3 2	40 ± 20	167	52 ± 24	9
3 3 3	207 ± 24	230	543 ± 29	224
3 3 3	36 ± 24	307	35 ± 29	339
3 4 2	34 ± 16	92	89 ± 19	118
3 4 2	41 ± 16	232	12 ± 19	19
3 4 3	65 ± 20	337	82 ± 23	338
3 4 3	16 ± 20	28	22 ± 23	45
3 4 4	29 ± 21	318	68 ± 25	26
3 4 4	62 ± 21	220	8 ± 25	282
3 5 2	40 ± 13	106	41 ± 15	116
3 5 2	31 ± 13	354	19 ± 15	207
3 5 3	38 ± 17	196	13 ± 19	132
3 5 3	34 ± 17	99	15 ± 19	250
3 5 4	24 ± 16	47	50 ± 19	44
3 5 4	25 ± 16	343	31 ± 19	255
3 6 3	24 ± 14	163	68 ± 15	102
3 6 3	21 ± 13	261	39 ± 15	142
4 3 3	21 ± 11	156	34 ± 13	129
4 3 3	50 ± 11	37	34 ± 13	97
4 4 3	22 ± 9	340	51 ± 11	288
4 4 3	22 ± 9	180	17 ± 11	229
4 4 4	116 ± 11	99	248 ± 12	95
4 4 4	13 ± 11	311	32 ± 12	209
4 5 3	11 ± 7	285	34 ± 8	261
4 5 3	4 ± 7	328	17 ± 8	8
4 5 4	75 ± 9	193	110 ± 10	174
4 5 4	19 ± 9	258	31 ± 10	336
4 5 5	22 ± 8	185	54 ± 9	214
4 5 5	30 ± 8	11	15 ± 9	327
4 6 4	51 ± 7	81	77 ± 8	82
4 6 4	12 ± 7	162	32 ± 8	134

I, $A^k_{jmi}\cos(k\phi+mt+\alpha^k_{jmi})P^k_j$; II, $A^k_{jme}\cos(k\phi+mt+\alpha^k_{jme})P^k_j$;
I′, $B^k_{jmi}\cos(k\phi-mt+\beta^k_{jmi})P^k_j$; II′, $B^k_{jme}\cos(k\phi-mt+\beta^k_{jme})P^k_j$.

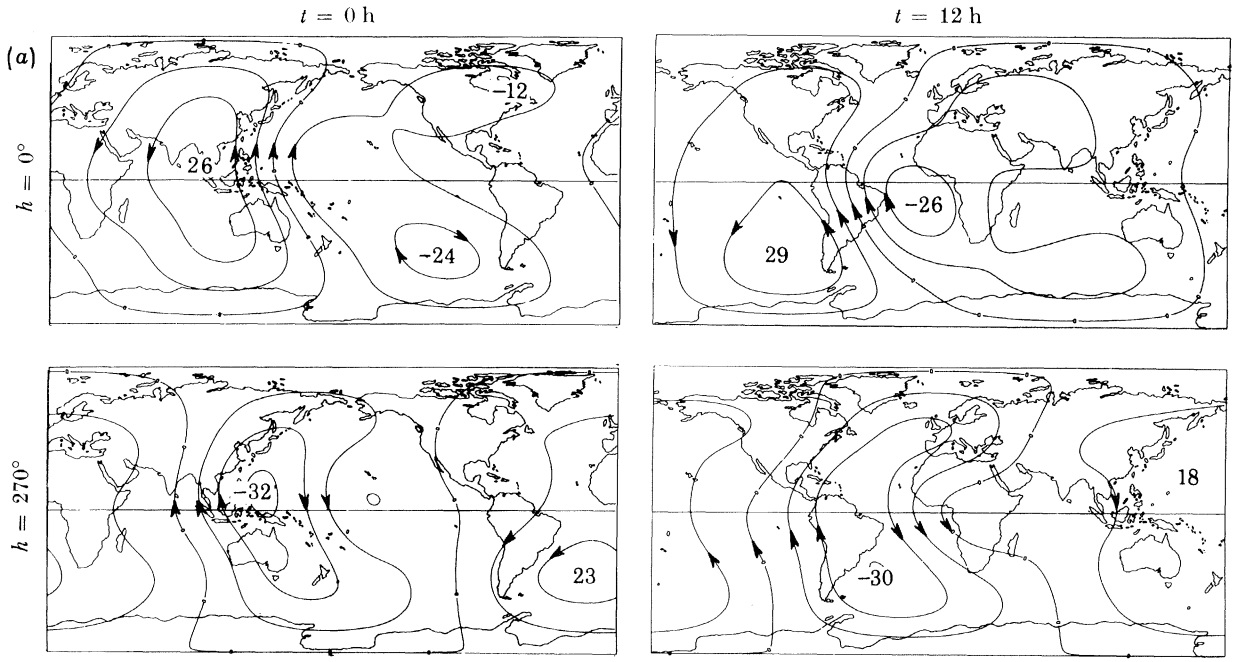

FIGURE 8.11 (*a*). $S^-(h)$ annual change of S current function; extrema in kiloamperes.

TABLE 8.11 (*b*). SPHERICAL HARMONIC ANALYSIS OF $S^+(h)$

(Amplitudes in picoteslas; phase angles in degrees.)

			internal		external	
n	j	k	III	$\alpha^k_{jm'i}$	IV	$\alpha^k_{jm'e}$
n	j	k	III′	$\beta^k_{jm'i}$	IV′	$\beta^k_{jm'e}$
1	1	0	107 ± 71	278	94 ± 115	210
1	1	1	924 ± 51	285	2394 ± 72	276
1	1	1	73 ± 51	233	111 ± 72	103
1	2	0	194 ± 64	139	314 ± 83	153
1	2	1	74 ± 44	282	328 ± 54	25
1	2	1	27 ± 44	242	93 ± 54	344
1	2	2	211 ± 42	146	294 ± 53	147
1	2	2	63 ± 42	332	122 ± 53	137
1	3	0	174 ± 55	285	222 ± 67	257
1	3	1	159 ± 38	233	585 ± 44	260
1	3	1	18 ± 38	140	105 ± 44	166
1	3	2	128 ± 37	292	160 ± 43	200
1	3	2	134 ± 37	115	121 ± 43	352
1	4	0	113 ± 43	168	50 ± 51	115
1	4	1	88 ± 30	190	124 ± 34	127
1	4	1	9 ± 30	151	104 ± 34	356
1	4	2	23 ± 29	44	56 ± 33	4
1	4	2	101 ± 29	306	55 ± 33	144
2	1	1	250 ± 45	254	314 ± 60	223
2	1	1	62 ± 46	9	127 ± 60	232
2	2	1	66 ± 37	59	283 ± 43	338
2	2	1	153 ± 37	209	29 ± 43	319
2	2	2	523 ± 38	150	1325 ± 47	147
2	2	2	65 ± 38	122	59 ± 47	225
2	3	1	36 ± 28	297	23 ± 31	119
2	3	1	34 ± 28	299	71 ± 31	226
2	3	2	92 ± 32	199	113 ± 37	150
2	3	2	44 ± 32	275	67 ± 36	355
2	3	3	18 ± 30	350	214 ± 36	328
2	3	3	16 ± 30	100	20 ± 36	278
2	4	1	62 ± 20	252	83 ± 23	248
2	4	1	26 ± 20	173	52 ± 23	238
2	4	2	176 ± 25	123	390 ± 28	107
2	4	2	29 ± 25	332	70 ± 28	266
2	4	3	37 ± 22	266	52 ± 25	330
2	4	3	23 ± 22	330	63 ± 25	43
2	5	2	13 ± 19	356	66 ± 21	150
2	5	2	29 ± 19	248	56 ± 21	263
3	2	2	103 ± 22	92	82 ± 28	82
3	2	2	60 ± 22	276	43 ± 28	98
3	3	2	64 ± 19	289	109 ± 22	177
3	3	2	45 ± 19	60	22 ± 22	284
3	3	3	295 ± 22	4	711 ± 26	354
3	3	3	32 ± 22	145	47 ± 26	181
3	4	2	37 ± 15	130	35 ± 17	197
3	4	2	29 ± 15	98	17 ± 17	205
3	4	3	34 ± 18	116	41 ± 20	55
3	4	3	49 ± 18	205	15 ± 20	27
3	4	4	61 ± 19	173	163 ± 22	161
3	4	4	58 ± 19	116	17 ± 22	290
3	5	2	20 ± 12	258	45 ± 13	311
3	5	2	18 ± 12	218	30 ± 13	61
3	5	3	55 ± 16	330	71 ± 17	306
3	5	3	28 ± 16	12	18 ± 17	224
3	5	4	42 ± 15	99	31 ± 16	138
3	5	4	17 ± 15	315	18 ± 16	74
3	6	3	24 ± 12	300	41 ± 13	254
3	6	3	12 ± 12	300	25 ± 14	19
4	3	3	10 ± 9	20	14 ± 11	12
4	3	3	26 ± 9	297	10 ± 11	305
4	4	3	27 ± 8	115	36 ± 9	60
4	4	3	10 ± 8	36	29 ± 9	70
4	4	4	103 ± 9	219	206 ± 10	214
4	4	4	11 ± 9	126	30 ± 10	62
4	5	3	17 ± 6	339	25 ± 7	6
4	5	3	4 ± 6	118	20 ± 7	199
4	5	4	60 ± 7	324	91 ± 8	311
4	5	4	27 ± 7	150	20 ± 8	199
4	5	5	30 ± 7	9	67 ± 8	352
4	5	5	15 ± 7	267	17 ± 8	151
4	6	4	17 ± 6	199	18 ± 6	232
4	6	4	19 ± 6	360	20 ± 6	340

III, $A^k_{jm'i}\cos(k\phi+m't+\alpha^k_{jm'i})P^k_j$; IV, $A^k_{jm'e}\cos(k\phi+m't+\alpha^k_{jm'e})P^k_j$;
III′, $B^k_{jm'i}\cos(k\phi-m't+\beta^k_{jm'i})P^k_j$; IV′, $B^k_{jm'e}\cos(k\phi-m't+\beta^k_{jm'e})P^k_j$.

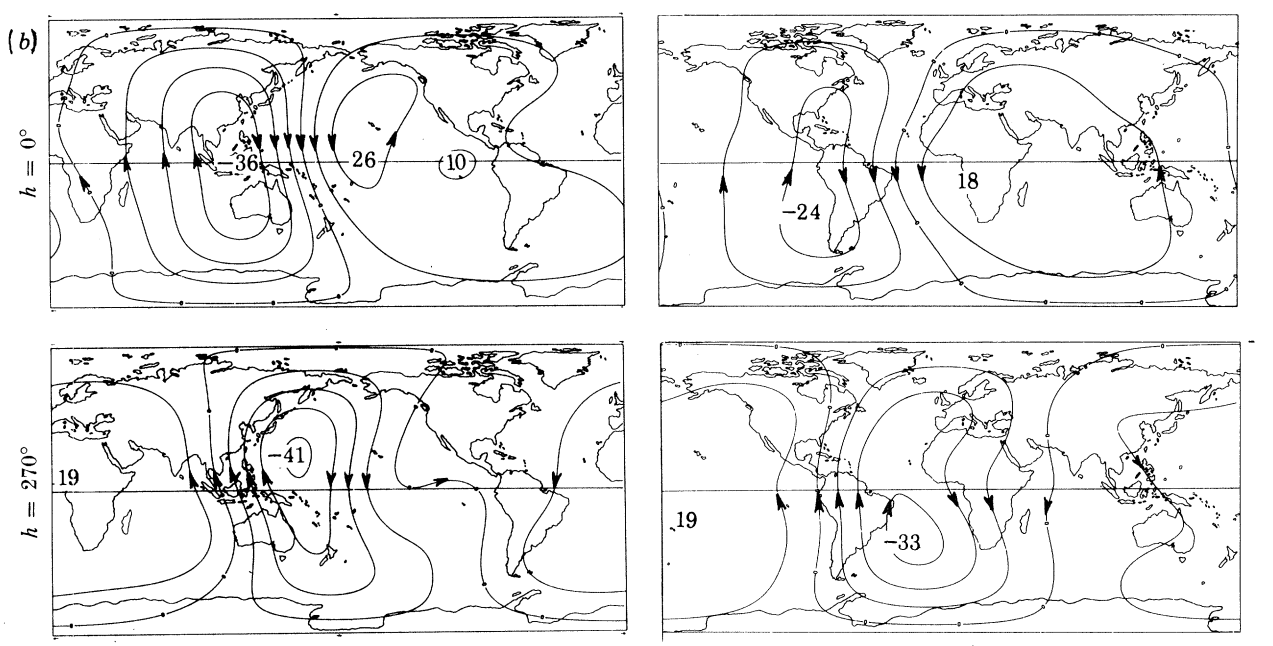

FIGURE 8.11 (*b*). $S^+(h)$ annual change of S current function; extrema in kiloamperes.

TABLE 8.12 (*a*). SPHERICAL HARMONIC ANALYSIS OF $S^-(2h)$

(Amplitudes in picoteslas; phase angles in degrees.)

n j k	internal I	α^k_{jmi}	external II	α^k_{jme}
n j k	I′	β^k_{jmi}	II′	β^k_{jme}
1 1 0	81±23	258	114±44	225
1 1 1	46±21	118	39±28	172
1 1 1	52±21	155	52±23	193
1 2 0	120±24	158	40±31	190
1 2 1	33±19	23	164±23	45
1 2 1	5±19	152	110±23	220
1 2 2	37±18	177	38±21	243
1 2 2	32±18	240	16±21	224
1 3 0	35±21	48	81±25	52
1 3 1	30±16	60	81±18	55
1 3 1	25±16	247	66±18	11
1 3 2	23±15	41	76±18	73
1 3 2	21±15	86	23±18	116
1 4 0	34±18	230	113±20	231
1 4 1	59±11	185	203±13	154
1 4 1	23±11	14	55±13	270
1 4 2	8±12	15	23±13	227
1 4 2	5±12	103	45±13	32
2 1 1	106±21	259	455±27	256
2 1 1	19±21	230	60±27	4
2 2 1	14±17	313	77±19	62
2 2 1	16±17	224	81±19	2.9
2 2 2	57±17	23	154±20	3
2 2 2	29±17	344	29±20	168
2 3 1	37±13	319	134±14	279
2 3 1	19±13	311	23±14	61
2 3 2	17±14	143	122±16	155
2 3 2	23±14	207	31±16	257
2 3 3	22±13	194	72±15	125
2 3 3	27±13	47	34±15	35
2 4 1	22± 9	243	58±10	216
2 4 1	5± 9	309	8±10	201
2 4 2	10±11	153	76±12	339
2 4 2	37±11	57	23±12	81
2 4 3	20±10	223	51±11	207
2 4 3	15±10	210	9±11	30
2 5 2	19± 9	118	82± 9	110
2 5 2	4± 9	352	29± 9	314

n j k	internal I	α^k_{jmi}	external II	α^k_{jme}
n j k	I′	β^k_{jmi}	II′	β^k_{jme}
3 2 2	14±10	29	94±13	63
3 2 2	37±10	199	22±13	179
3 3 2	5± 9	200	38±11	253
3 3 2	26± 9	20	20±11	259
3 3 3	26±10	208	38±12	195
3 3 3	11±10	312	2±12	99
3 4 2	18± 8	186	65± 9	136
3 4 2	20± 8	223	23± 9	129
3 4 3	38± 9	77	91±10	40
3 4 3	8± 9	76	23±10	222
3 4 4	24± 9	341	42±10	301
3 4 4	12± 9	7	18±10	337
3 5 2	6± 6	156	22± 7	321
3 5 2	7± 6	135	12± 7	125
3 5 3	12± 7	356	47± 8	117
3 5 3	16± 7	215	14± 8	56
3 5 4	12± 7	47	49± 8	355
3 5 4	14± 7	264	17± 8	318
3 6 3	25± 6	16	86± 7	341
3 6 3	12± 6	62	9± 7	175
4 3 3	19± 7	244	37± 8	235
4 3 3	19± 7	129	10± 8	56
4 4 3	14± 6	10	14± 7	318
4 4 3	12± 6	280	9± 7	173
4 4 4	30± 6	89	49± 7	62
4 4 4	31± 6	267	20± 7	213
4 5 3	8± 4	356	29± 5	314
4 5 3	13± 4	50	5± 5	19
4 5 4	34± 6	293	88± 6	255
4 5 4	10± 6	87	11± 6	334
4 5 5	23± 5	208	59± 5	154
4 5 5	3± 5	169	7± 5	173
4 6 4	8± 4	276	14± 4	271
4 6 4	12± 4	143	10± 4	125

I, $A^k_{jmi}\cos(k\phi+mt+\alpha^k_{jmi})P^k_j$; II, $A^k_{jme}\cos(k\phi+mt+\alpha^k_{jme})P^k_j$;
I′, $B^k_{jmi}\cos(k\phi-mt+\beta^k_{jmi})P^k_j$; II′, $B^k_{jme}\cos(k\phi-mt+\beta^k_{jme})P^k_j$.

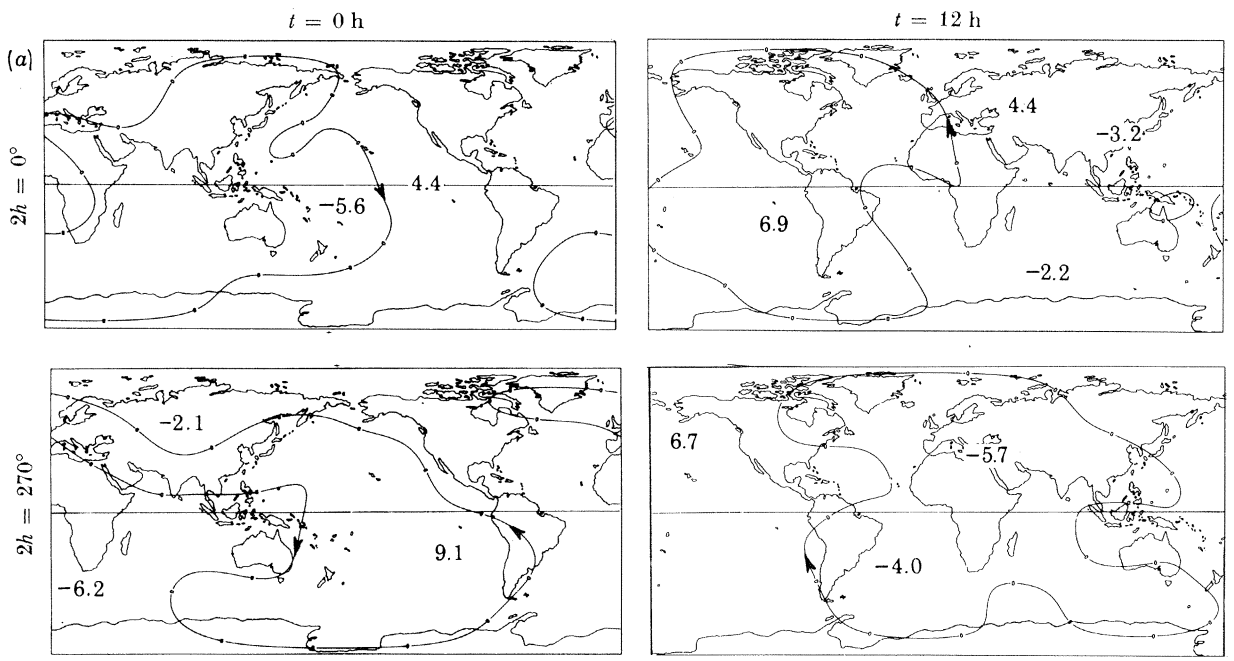

FIGURE 8.12 (*a*). $S^-(2h)$ semi-annual change of S current function; extrema in kiloamperes.

TABLE 8.12 (*b*). SPHERICAL HARMONIC ANALYSIS OF $S^+(2h)$

(Amplitudes in picoteslas; phase angles in degrees.)

			internal		external	
n	j	k	III	$\alpha^k_{jm'i}$	IV	$\alpha^k_{jm'e}$
n	j	k	III′	$\beta^k_{jm'i}$	IV′	$\beta^k_{jm'e}$
1	1	0	84 ± 43	79	208 ± 71	354
1	1	1	130 ± 33	89	358 ± 45	94
1	1	1	18 ± 33	105	127 ± 45	44
1	2	0	67 ± 39	77	81 ± 48	76
1	2	1	148 ± 29	346	273 ± 35	345
1	2	1	34 ± 29	349	148 ± 35	183
1	2	2	43 ± 23	134	100 ± 33	197
1	2	2	20 ± 23	76	22 ± 33	201
1	3	0	22 ± 33	169	129 ± 39	91
1	3	1	27 ± 25	120	106 ± 29	271
1	3	1	37 ± 25	180	92 ± 23	353
1	3	2	19 ± 24	335	40 ± 28	264
1	3	2	22 ± 24	262	20 ± 23	203
1	4	0	70 ± 28	173	147 ± 32	208
1	4	1	46 ± 17	203	243 ± 20	166
1	4	1	53 ± 17	7	23 ± 20	211
1	4	2	42 ± 19	153	22 ± 21	50
1	4	2	27 ± 19	53	73 ± 21	33
2	1	1	68 ± 32	23	156 ± 39	220
2	1	1	128 ± 33	250	42 ± 39	59
2	2	1	133 ± 26	212	181 ± 28	148
2	2	1	101 ± 26	90	94 ± 28	223
2	2	2	93 ± 26	235	446 ± 30	296
2	3	2	99 ± 26	0	42 ± 30	62
2	3	1	29 ± 19	245	144 ± 21	266
2	2	1	31 ± 19	235	33 ± 21	124
2	3	2	83 ± 21	188	363 ± 23	150
2	3	2	26 ± 21	206	22 ± 23	270
2	3	3	25 ± 19	175	114 ± 22	34
2	3	3	40 ± 19	110	32 ± 22	263
2	4	1	14 ± 14	51	49 ± 15	186
2	4	1	16 ± 14	256	18 ± 15	226
2	4	2	12 ± 17	123	76 ± 18	302
2	4	2	33 ± 17	200	52 ± 18	247
2	4	3	41 ± 14	41	94 ± 15	106
2	4	3	43 ± 14	272	32 ± 15	324
2	5	2	38 ± 12	75	144 ± 13	59
2	5	2	9 ± 12	45	26 ± 14	139
3	2	2	60 ± 14	124	80 ± 18	11
3	2	2	62 ± 14	280	65 ± 18	147
3	3	2	68 ± 13	37	67 ± 15	41
3	3	2	53 ± 13	89	15 ± 15	321
3	3	3	91 ± 14	154	192 ± 16	116
3	3	3	35 ± 14	279	10 ± 16	225
3	4	2	29 ± 10	152	47 ± 12	106
3	4	2	41 ± 10	259	6 ± 12	46
3	4	3	139 ± 12	31	190 ± 13	4
3	4	3	35 ± 12	138	36 ± 13	317
3	4	4	41 ± 13	306	77 ± 14	210
3	4	4	44 ± 13	58	14 ± 14	37
3	5	2	18 ± 8	320	59 ± 9	328
3	5	2	3 ± 8	119	40 ± 9	239
3	5	3	25 ± 10	189	68 ± 11	64
3	5	3	28 ± 10	338	26 ± 11	166
3	5	4	4 ± 9	188	109 ± 10	301
3	5	4	35 ± 9	234	25 ± 10	149
3	6	3	28 ± 8	316	47 ± 9	255
3	6	3	15 ± 8	116	27 ± 9	14
4	3	3	21 ± 8	227	54 ± 10	209
4	3	3	29 ± 8	205	13 ± 10	25
4	4	3	31 ± 7	281	29 ± 8	247
4	4	3	23 ± 7	13	7 ± 8	290
4	4	4	24 ± 8	356	58 ± 9	312
4	4	4	28 ± 8	345	7 ± 9	163
4	5	3	9 ± 5	254	37 ± 6	241
4	5	3	4 ± 5	72	4 ± 6	146
4	5	4	64 ± 7	244	117 ± 8	211
4	5	4	15 ± 7	140	10 ± 8	348
4	5	5	3 ± 6	168	39 ± 7	68
4	5	5	9 ± 6	3	16 ± 7	244
4	6	4	8 ± 5	260	42 ± 5	227
4	6	4	8 ± 5	173	6 ± 5	309

III, $A^k_{jm'i}\cos(k\phi + m't + \alpha^k_{jm'i})P^k_j$; IV, $A^k_{jm'e}\cos(k\phi + m't + \alpha^k_{jm'e})P^k_j$;
III′, $B^k_{jm'i}\cos(k\phi - m't + \beta^k_{jm'i})P^k_j$; IV′, $B^k_{jm'e}\cos(k\phi - m't + \beta^k_{jm'e})P^k_j$.

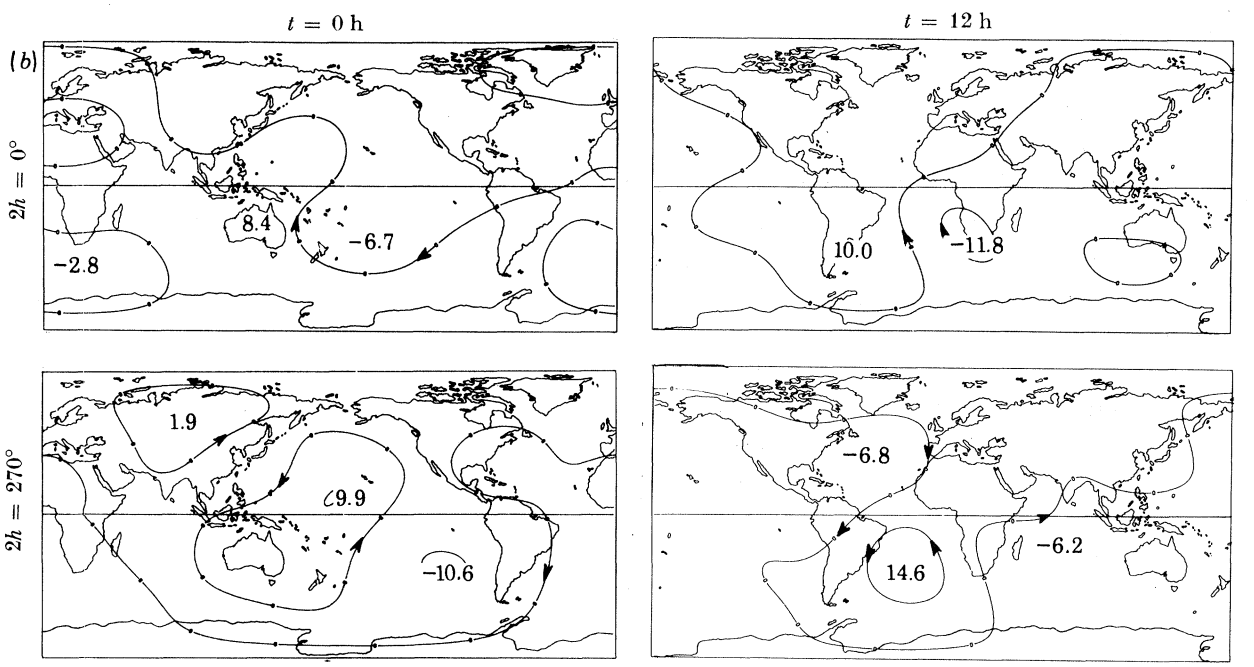

FIGURE 8.12 (*b*). $S^+(2h)$ semi-annual change of S current function; extrema in kiloamperes.

TABLE 8.13. SPHERICAL HARMONIC ANALYSIS OF LONG-PERIOD TIDES

(Amplitudes in picoteslas; phase angles in degrees.)

	n	j	k	internal I	α^k_{jmi}	external II	α^k_{jme}
	n	j	k	I′	β^k_{jmi}	II′	β^k_{jme}
$2s-4h$	0	1	0	231±45	348	597±68	331
	0	1	1	54±23	76	137±30	102
	0	1	1	95±23	77	102±30	69
	0	2	0	109±40	166	201±46	106
	0	2	1	31±22	132	50±26	25
	0	2	1	23±22	226	58±27	61
	0	3	0	23±29	312	70±34	219
	0	3	1	19±22	193	70±24	217
	0	3	1	15±22	337	24±24	122
	0	4	0	69±22	105	72±26	332
	0	4	1	33±16	49	49±18	34
	0	4	1	22±16	119	48±18	89
$2s-3h$	0	1	0	146±44	56	387±77	9
	0	1	1	45±24	140	114±32	141
	0	1	1	44±24	352	48±32	115
	0	2	0	47±43	349	55±46	81
	0	2	1	51±23	199	54±23	69
	0	2	1	22±23	300	9±23	85
	0	3	0	33±30	235	51±34	95
	0	3	1	65±22	34	48±25	335
	0	3	1	36±22	119	18±25	321
	0	4	0	54±25	42	45±26	296
	0	4	1	22±16	283	50±18	133
	0	4	1	31±16	74	28±18	90
$2s-2h$	0	1	0	124±44	276	652±103	189
	0	1	1	14±30	49	231±41	309
	0	1	1	42±30	212	83±41	343
	0	2	0	237±52	143	111±75	176
	0	2	1	59±31	100	134±37	152
	0	2	1	27±30	160	77±37	143

	n	j	k	internal I	α^k_{jmi}	external II	α^k_{jme}
	n	j	k	I′	β^k_{jmi}	II′	β^k_{jme}
$2s-2h$	0	3	0	55±46	188	179±42	300
	0	3	1	57±23	180	67±33	49
	0	3	1	47±23	153	76±33	57
	0	4	0	41±34	157	34±38	206
	0	4	1	22±20	307	39±23	245
	0	4	1	74±20	335	49±23	257
$2s-h$	0	1	0	318±48	158	905±76	164
	0	1	1	39±25	239	83±33	272
	0	1	1	63±25	286	144±33	292
	0	2	0	123±42	263	66±52	237
	0	2	1	34±25	157	74±30	115
	0	2	1	7±25	38	36±30	323
	0	3	0	61±33	319	87±39	336
	0	3	1	18±24	302	13±27	305
	0	3	1	24±24	34	79±27	125
	0	4	0	24±25	205	120±28	68
	0	4	1	28±17	352	18±19	8
	0	4	1	39±17	184	48±19	306
$2s$	0	1	0	641±60	173	1135±89	164
	0	1	1	86±29	275	165±38	182
	0	1	1	131±29	303	193±38	232
	0	2	0	355±55	11	134±68	349
	0	2	1	91±29	323	85±35	297
	0	2	1	73±29	298	58±35	237
	0	3	0	69±33	77	32±41	243
	0	3	1	29±27	80	128±31	76
	0	3	1	20±23	7	34±31	335
	0	4	0	34±31	338	76±36	175
	0	4	1	14±20	103	67±22	297
	0	4	1	50±20	98	63±22	256

Sectorial terms in the semi-annual variation of the lunar magnetic tide are shown to come into phase at certain times of the year and to dominate the principal lunar magnetic tide $L(2s-2h)$.

Non-local time terms that are sectorial in form and westward-drifting are found in all types of magnetic tide. They occur in groups for which the 1, 2, 3, 4, c/d terms come into phase at local-noon and also in tidal groups that come into phase at certain times of the year.

All long-period tides are found to be of external origin with the exception of the annual and six-monthly tides which are of internal origin.

Inclusion of the dynamical equation of motion in ionospheric dynamo theory is shown to resolve the lack of uniqueness in the determination of the wind velocity from the magnetic tide. Hough functions are introduced and their relation to scalar functions Φ, Ψ, derived. For the generation of the solar diurnal tide, the (1, 1) mode is found to be the dominant mode, although the (1, −2) mode is shown to be a more efficient generator of the P_2^1 magnetic tide. For S, $L(2s-2h)$ and $L(3s-2h-p)$ semi-diurnal magnetic tides, the (2, 2) mode is the dominant mode. It is found that this mode is directly able to produce the 180° phase angle difference found between the P_3^2 and P_5^2 lunar and lunar elliptic tidal parameters.

TABLE 8.13 (*continued*)

	n	j	k	internal I	internal α^k_{jmi}	external II	external α^k_{jme}
	n	j	k	I′	β^k_{jmi}	II′	β^k_{jme}
$3s-3h-p$	0	1	0	186±39	322	325±56	27
	0	1	1	39±23	12	65±30	69
	0	1	1	62±23	131	73±30	100
	0	2	0	169±35	133	20±46	160
	0	2	1	15±20	261	36±24	109
	0	2	1	38±21	189	67±25	200
	0	3	0	28±27	300	62±35	331
	0	3	1	56±18	104	39±21	267
	0	3	1	10±18	274	35±21	137
	0	4	0	10±19	101	23±22	298
	0	4	1	35±15	245	15±16	343
	0	4	1	24±15	75	12±16	258
$3s-2h-p$	0	1	0	179±40	352	176±59	330
	0	1	1	17±21	237	41±28	187
	0	1	1	58±21	348	112±28	228
	0	2	0	93±35	185	57±43	174
	0	2	1	82±21	136	60±25	342
	0	2	1	55±21	43	12±25	46
	0	3	0	74±26	247	12±32	339
	0	3	1	5±19	205	35±22	201
	0	3	1	68±19	173	84±22	71
	0	4	0	52±20	89	47±22	250
	0	4	1	23±14	267	29±16	214
	0	4	1	30±14	223	52±16	238
$3s-h-p$	0	1	0	384± 47	17	854± 67	24
	0	1	1	90± 24	64	46± 32	99
	0	1	1	49± 24	66	134± 32	49
	0	2	0	171± 42	159	152± 52	174
	0	2	1	18± 23	124	215± 27	58
	0	2	1	78± 23	57	46± 27	18
$3s-h-p$	0	3	0	19± 29	272	42± 35	234
	0	3	1	26± 23	94	46± 25	257
	0	3	1	100± 22	219	28± 25	177
	0	4	0	30± 25	174	22± 27	212
	0	4	1	45± 16	245	31± 18	33
	0	4	1	35± 16	68	24± 18	344
h	0	1	0	4417±461	174	653±539	309
	0	1	1	290±193	174	254±240	206
	0	1	1	157±192	210	477±240	156
	0	2	0	3969±371	356	2007±342	68
	0	2	1	1473±199	291	880±223	138
	0	2	1	1122±200	289	766±226	253
	0	3	0	602±266	10	767±308	178
	0	3	1	682±166	48	487±183	311
	0	3	1	919±164	71	464±181	84
	0	4	0	229±224	5	580±204	51
	0	4	1	160±117	111	320±128	156
	0	4	1	133±116	24	209±128	324
$2h$	0	1	0	1694±308	251	1732±404	301
	0	1	1	190±141	306	451±172	227
	0	1	1	233±140	141	235±170	9
	0	2	0	1808±223	58	1290±290	82
	0	2	1	721±138	10	340±153	316
	0	2	1	440±137	241	699±154	191
	0	3	0	594±188	111	879±169	327
	0	3	1	308±116	134	453±128	97
	0	3	1	191±114	330	343±123	7
	0	4	0	197±104	354	167±171	99
	0	4	1	104± 81	174	273± 89	260
	0	4	1	219± 81	9	242± 89	172

I, $A^k_{jmi}\cos(k\phi+wt+\alpha^k_{jmi})P^k_j$; II, $A^k_{jme}\cos(k\phi+wt+\alpha^k_{jme})P^k_j$.
I′, $B^k_{jmi}\cos(k\phi-wt+\beta^k_{jmi})P^k_j$; II′, $B^k_{jme}\cos(k\phi-wt+\beta^k_{jme})P^k_j$.

8. NUMERICAL RESULTS

Results of calculations for the magnetic tides and their elliptic and seasonal components are given in tables 8.1–8.13. Amplitudes and their standard deviations are given in picoteslas (1 pT = 10^{-3} nT), phase angles are given in degrees. Standard deviations have not been given for phase angles. The analysis by Malin (1973) of the solar and lunar magnetic tide for the I.G.Y. years is given in table 8.14 in a form directly comparable with the preceding tables, i.e. as coefficients of eastward- and westward-moving waves.

Within each column of the tables, the amplitudes and phase angles are given in the order

$$n\quad j\quad k\quad A^k_{jme}\cos(k\phi+mt+\alpha^k_{jme})P^k_j \quad \text{(westward-moving)},$$

$$n\quad j\quad k\quad B^k_{jme}\cos(k\phi-mt+\beta^k_{jme})P^k_j \quad \text{(eastward-moving)},$$

where the subscript e refers to terms of external origin, often originating in the ionosphere. A subscript i is used to refer to terms of internal origin, induced in the electrically conducting Earth

TABLE 8.14(*a*). SPHERICAL HARMONIC ANALYSIS OF $L(2s-2h)$ BY MALIN (1973)

(Amplitudes in picoteslas; phase angles in degrees.)

n	j	k	internal I	α^k_{jmi}	external II	α^k_{jme}
n	j	k	I′	β^k_{jmi}	II′	β^k_{jme}
1	1	0	84±45	266	85±65	356
1	1	1	54±24	232	91±34	159
1	1	1	42±24	333	72±34	300
1	2	0	24±34	154	132±44	191
1	2	1	139±25	103	338±31	94
1	2	1	20±25	254	103±31	347
1	2	2	73±19	50	120±23	127
1	2	2	107±19	53	37±23	152
1	3	0	60±31	219	102±36	347
1	3	1	74±21	107	14±25	87
1	3	1	28±21	154	5±25	122
1	3	2	45±16	242	27±19	297
1	3	2	40±16	248	30±19	344
1	4	1	97±17	285	151±19	270
1	4	1	38±17	299	40±19	69
2	1	1	70±40	123	123±57	135
2	1	1	151±41	199	86±57	60
2	2	1	38±42	43	78±51	260
2	2	1	55±42	343	16±51	239
2	2	2	55±30	121	103±37	338
2	2	2	123±30	286	32±37	60
2	3	1	58±34	307	198±39	40
2	3	1	74±34	77	87±39	154
2	3	2	220±29	291	497±34	273
2	3	2	86±29	51	22±34	71
2	3	3	80±24	240	132±28	300
2	3	3	85±23	356	64±28	130
2	4	1	68±25	74	88±27	175
2	4	1	37±24	169	40±27	160
2	4	2	22±23	7	90±26	95
2	4	2	46±23	180	30±27	227
2	4	3	45±19	41	10±22	93
2	4	3	32±19	116	72±22	36
3	2	2	92±16	320	144±20	303
3	2	2	33±16	134	39±20	306
3	3	2	30±14	156	59±17	106
3	3	2	21±14	163	37±17	195
3	3	3	16±13	54	45±16	112
3	3	3	55±13	196	31±16	165
3	4	2	20±12	151	31±13	295
3	4	2	35±12	319	12±13	344
3	4	3	96±13	112	189±15	101
3	4	3	28±13	59	28±15	57
3	4	4	22±12	155	54±13	119
3	4	4	22±11	276	34±13	83
3	5	3	19±10	253	42±11	261
3	5	3	8±10	117	9±11	201
4	3	3	20± 6	129	24± 7	111
4	3	3	9± 6	21	25± 7	245
4	4	3	8± 6	178	25± 7	211
4	4	3	5± 6	238	10± 7	93
4	4	4	3± 5	248	2± 6	278
4	4	4	16± 5	150	2± 6	337
4	5	3	14± 5	238	10± 5	184
4	5	3	8± 5	146	12± 5	144
4	5	4	22± 5	281	39± 6	266
4	5	4	10± 5	271	14± 6	291
4	5	5	17± 5	26	20± 5	316
4	5	5	12± 5	260	11± 5	337
4	6	4	4± 4	348	15± 5	71
4	6	4	3± 4	344	8± 5	174

I, $A^k_{jmi}\cos(k\phi+mt+\alpha^k_{jmi})P^k_j$; II, $A^k_{jme}\cos(k\phi+mt+\alpha^k_{jme})P^k_j$
I′, $B^k_{jmi}\cos(k\phi-mt+\beta^k_{jmi})P^k_j$; II′, $B^k_{jme}\cos(k\phi-mt+\beta^k_{jme})P$

or oceans by the external terms. For phase-law tides $m = n-w$ and for partial tides m is replaced by m', where $m' = n+w$. Values of the parameter w for the various magnetic tides are given in equation (6). For solar magnetic tides in table 8.10, the parameter w is zero, and the parameter n is used in place of both m and m'.

When the parameter k is zero, only the westward-moving form with coefficient A^k_{jme}, etc. is used. When the parameter n is zero the tide is a long-period tide, and all such results are collected together in table 8.13.

Schmidt quasinormalized spherical harmonic functions have been used throughout in the calculations, as defined in Chapman & Bartels (1940, ch. 17, §4). See Table 4.1.

Table 8.1 contains the results for the phase-law tides of the principal lunar and lunar elliptic magnetic tides, $L(2s-2h)$ and $L(3s-2h-p)$ respectively. The semi-diurnal $n = 2$ harmonic in both cases has been derived from the harmonics $n = 1, 3, 4$ by using the ocean dynamo calculation of Malin (1970). Hence the results of table 8.1 are for magnetic tides of purely

TABLE 8.14 (*b*). SPHERICAL HARMONIC ANALYSIS OF *S* BY MALIN (1973)

(Amplitudes in picoteslas; phase angles in degrees.)

			internal		external	
n	*j*	*k*	III	$\alpha^k_{jn'i}$	IV	$\alpha^k_{jn'e}$
n	*j*	*k*	III′	$\beta^k_{jn'i}$	IV′	$\beta^k_{jn'e}$
1	1	0	1618±655	127	1904±954	288
1	1	1	1210±336	107	1359±506	55
1	1	1	725±330	182	756±504	12
1	2	0	669±493	95	3443±665	85
1	2	1	4497±368	7	12213±479	7
1	2	1	380±368	17	1104±479	178
1	2	2	880±266	79	2939±344	65
1	2	2	221±266	157	348±344	93
1	3	0	1141±454	78	2154±539	277
1	3	1	437±319	333	1071±388	171
1	3	1	562±319	266	855±388	352
1	3	2	177±234	61	882±282	232
1	3	2	223±234	339	453±282	349
1	4	1	1721±258	207	2928±296	160
1	4	1	712±258	31	738±296	233
2	1	1	204±254	61	2499±351	58
2	1	1	544±256	272	166±347	161
2	2	1	541±254	18	553±302	179
2	2	1	757±255	93	373±303	101
2	2	2	539±182	295	1307±228	254
2	2	2	473±185	34	610±232	333
2	3	1	474±198	247	999±228	301
2	3	1	277±198	175	211±223	199
2	3	2	2500±181	198	5953±210	182
2	3	2	138±181	342	408±209	196
2	3	3	482±143	206	1050±166	238
2	3	3	622±143	151	443±166	240
2	4	1	255±141	280	687±156	150
2	4	1	269±142	301	147±156	29
2	4	2	262±142	32	696±160	347
2	4	2	402±143	196	121±159	144
2	4	3	346±124	342	391±139	88
2	4	3	188±122	282	87±139	78
3	2	2	187± 86	228	700±107	196
3	2	2	77± 86	18	153±107	54
3	3	2	287± 78	182	167± 92	225
3	3	2	83± 78	204	74± 92	129
3	3	3	154± 74	104	521± 87	93
3	3	3	96± 74	284	210± 87	295
3	4	2	333± 62	59	326± 71	43
3	4	2	40± 62	55	153± 71	264
3	4	3	955± 69	34	2144± 79	16
3	4	3	144± 69	175	133± 79	99
3	4	4	189± 62	89	166± 70	45
3	4	4	102± 62	21	178± 70	125
3	5	3	95± 54	172	146± 60	119
3	5	3	80± 54	22	29± 60	74
4	3	3	86± 34	34	182± 41	12
4	3	3	74± 34	140	90± 41	311
4	4	3	31± 33	50	119± 38	85
4	4	3	66± 33	302	66± 38	104
4	4	4	63± 32	332	171± 37	237
4	4	4	71± 32	203	58± 37	245
4	5	3	86± 26	235	105± 30	219
4	5	3	15± 26	237	39± 29	257
4	5	4	195± 30	232	420± 34	209
4	5	4	42± 30	329	48± 34	56
4	5	5	37± 27	30	38± 30	307
4	5	5	47± 27	338	30± 30	5
4	6	4	77± 24	292	143± 26	276
4	6	4	33± 24	47	34± 26	333

III, $A^k_{jni}\cos(k\phi+nt+\alpha^k_{jni})P^k_j$; IV, $A^k_{jne}\cos(k\phi+nt+\alpha^k_{jne})P^k_j$;
III′, $B^k_{jni}\cos(k\phi-nt+\beta^k_{jni})P^k_j$; IV′, $B^k_{jne}\cos(k\phi-nt+\beta^k_{jne})P^k_j$.

ionospheric origin with no direct contribution from ocean dynamos associated with the tides M_2 and N_2.

Tables 8.2–8.6 contain spherical harmonic coefficients for phase-law tides and partial tides of $L(2s-4h)$, $L(2s-3h)$, $L(2s-2h)$, $L(2s-h)$ and $L(2s)$ respectively. The $n = 2$ coefficients in table 8.4 are computed directly from observatory Fourier coefficients, and include ocean dynamo M_2 contributions.

Tables 8.7–8.9 contain spherical harmonic coefficients for phase-law tides and partial tides of $L(3s-3h-p)$, $L(3s-2h-p)$ and $L(3s-h-p)$. The $n = 2$ coefficients in table 8.8 have been computed directly from observatory Fourier coefficients, and include ocean dynamo N_2 contributions.

Table 5.10 contains spherical harmonic coefficients for the solar magnetic tide *S*, while tables 5.11 and 5.12 contain coefficients of the annual and semi-annual change of *S*, denoted

$S(h)$ and $S(2h)$, respectively. The nomenclature 'phase-law tide' and 'partial tide', based on the physical mechanism for the generation of lunar magnetic tides does not apply to the seasonal variation of the solar magnetic tide, even though the mathematical form is essentially the same. A new nomenclature has been introduced, e.g. $S^{-}(h)$ for what might otherwise have been referred to as a phase-law tide associated with $S(h)$ and $S^{+}(h)$ in place of partial tide.

Table 8.13 contains results for the analysis of long-period tides which were obtained as a by-product of the analyses of magnetic tides given in the preceding tables. The periods and corresponding frequencies of the long-period tides are given in equation (6).

I am indebted to World Data Center A, Boulder, Colorado for providing geomagnetic hourly mean values for 1964–1965 in yearbook or machine-readable form. Mr W. Paulishak of World Data Center A answered all of the many queries about the data that arose during the analysis. Mr P. A. Rickards and Mrs M. Garwood of the Agricultural Business Research Institute at the University of New England, Armidale, New South Wales, organized the punching and verification of approximately 350000 punch cards containing geomagnetic hourly mean values. Dr S. R. C. Malin of the Institute of Geological Sciences, Edinburgh, kindly provided solar and lunar geomagnetic Fourier coefficients for the I.G.Y. years on punch cards. The research project was supported by a grant (B65/15071) from the Australian Research Grants Committee.

References

Anderssen, R. S., Gustafson, S. Å. & Winch, D. E. 1979 Estimating the phase of the response of the Earth to long-period geomagnetic fluctuations. *Earth. planet. Sci. Lett.* **44**, 1–6.

Appleton, E. V. & Weekes, K. 1939 On lunar tides in the upper atmosphere. *Proc. R. Soc. Lond.* A **171**, 171–187.

Arora, B. R. & Rao, D. R. K. 1975 Modulation of geomagnetic lunar daily variation in H at Alibag with lunar distance. *Geophys. Jl R. astr. Soc.* **43**, 627–633.

Ashour, A. A. & Price, A. T. 1948 The induction of electric currents in a non-uniform ionosphere. *Proc. R. Soc. Lond.* A **195**, 198–224.

Ayamenc, P. 1974 Tidal oscillations of the meridional neutral wind at mid-latitudes. *Radio Sci.* **9**, 281–293.

Baker, W. G. & Martyn, D. F. 1952 Conductivity of the ionosphere. *Nature, Lond.* **170**, 1090–1093.

Baker, W. G. & Martyn, D. F. 1953 Electric currents in the ionosphere. I. The conductivity. *Phil. Trans. R. Soc. Lond.* A **246**, 231–294.

Bartels, J. 1957 Gezeitenkräfte. *Handb. Phys.* **48**, 746–774.

Bartels, J., Chapman, S., Elvey, C. T. & Cain, J. C. 1954 A table of daily integers, 1902–1952, seasonal, solar, lunar and geomagnetic. *Scient. Rep. geophys. Inst. Univ. Alaska* no. 2, AF 19(6047–503).

Bartels, J. & Fanselau, G. 1938 Geophysikalische Mond-Tafeln 1850–1975. *Abh. geophysikalisches Inst., Potsdam* no. 2.

Beer, T. 1974 *Atmospheric waves.* London: Adam Hilger.

Belmont, A. D., Nastrom, G. D. & Mayr, H. G. 1974 Significance of semi-annual waves in the mesospheric zonal wind and evidence of the influence by the geomagnetic field. *J. geophys. Res.* **79**, 5049–5051.

Benkova, N. P. 1940 Spherical harmonic analysis of the S_q variations, May–August 1933. *Terr. Magn. atmos. Elect.* **45**, 425–432.

Berdichevskiy, M. N. & Faynberg, E. B. 1972 Possibility of experimental separation of the variable geomagnetic field into a poloidal and toroidal part. *Geomagn. Aeron.* **12**, 826–830.

Berdichevskiy, M. N. & Faynberg, E. V. 1974 Separation of the field of S_q variations into poloidal and toroidal parts. *Geomagn. Aeron.* **14**, 315–318.

Bhargava, B. N. 1972*a* Semiannual component of the Earth's magnetic field and its generating mechanism. *Indian J. Radio Space Phys.* (1) **1**, 9–11.

Bhargava, B. N. 1972*b* A two component model of the annual line in the spectrum of the geomagnetic field. *Annals géophys.* **28**, 357–361.

Bhargava, B. N. 1972*c* Semi-annual and annual modulation of the magnetic field. *Planet. Space Sci.* **20**, 423–427.

Boller, B. R. & Stolov, H. L. 1970 Kelvin–Helmholtz instability and the semiannual variation of geomagnetic activity. *J. geophys. Res. Space Phys.* **75**, 6073–6084.

Brown, G. M. 1975 S_q variability and aeronomic structure. *J. atmos. terr. Phys.* **37**, 107–117.

Brown, G. M. & Williams, W. R. 1969 Some properties of the day-to-day variability of S_q(H). *Planet. Space Sci.* **17**, 455–470.

Bullard, E. & Gellman, H. 1954 Homogeneous dynamos and terrestrial magnetism. *Proc. R. Soc. Lond.* A **247** 213–278.

Burrows, D. & Hall, S. H. 1964 In situ detection of an ionospheric electric current. *Nature, Lond.* **204**, 721–722.

Callis, L. B., Natarajan, M. & Nealy, J. E. 1979 Ozone and temperature trends associated with the 11-year solar cycle. *Science, Wash.* **204**, 1303–1306.

Campbell, W. H. 1980 Annual and semi-annual variations of the lunar semi-diurnal geomagnetic field components at North American locations. *J. Geomagn. Geoelect., Kyoto* **32**, 105–128.

Chakrabarty, S. K. & Pratap, R. 1954 On the dynamo theory of geomagnetic field variations. *J. geophys. Res.* **59**, 1–15.

Chapman, S. 1913 On the diurnal variations of the Earth's magnetism produced by the Moon and Sun. *Phil. Trans. R. Soc. Lond.* A **213**, 279–321.

Chapman, S. 1915 The lunar diurnal magnetic variation, and its change with lunar distance. *Phil. Trans. R. Soc. Lond.* A **215**, 161–176.

Chapman, S. 1918 The influence of changes in lunar distance upon the lunar diurnal magnetic variations. *Terr. Magn. atmos. Elect.* **23**, 25–28.

Chapman, S. 1919 The solar and lunar diurnal variations of terrestrial magnetism. *Phil. Trans. R. Soc. Lond.* A **218**, 1–118.

Chapman, S. 1951 Atmospheric tides and oscillations. *Compendium of Meteorology*, pp. 510–530. Boston: American Meteorological Society.

Chapman, S. & Bartels, J. 1940 *Geomagnetism.* Oxford University Press.

Chapman, S., Gupta, J. C. & Malin, S. R. C. 1971 The sunspot cycle influence on the solar and lunar daily geomagnetic variations. *Proc. R. Soc. Lond.* A **324**, 1–15.

Chapman, S. & Lindzen, R. S. 1970 *Atmospheric tides: thermal and gravitational.* Dordrecht, Holland: D. Reidel Publishing Co.

Chapman, S. & Malin, S. R. C. 1970 Atmospheric tides, thermal and gravitational: Nomenclature, notation and new results. *J. atmos. Sci*, **27**, 707–710.

Chapman, S. & Miller, J. C. P. 1940 The statistical determination of lunar daily variations in geomagnetic and meteorological elements. *Mon. Not. R. astr. Soc. geophys. Suppl.* **4**, 649–659.

Chen, Zhe-Ming 1979 Numerical calculations of the eigenvalue–eigenfunction problem for the diurnal mode of the atmospheric tide. *Acta geophys. sin.* **22**, 242–253.

Chree, C. 1912 *Studies in terrestrial magnetism*, pp. 80–85. London: Macmillan.

Davis, T. N., Stolarik, J. D. & Heppner, J. P. 1965 Rocket measurements of S_q currents at midlatitude. *J. geophys. Res.* **70**, 5883–5894.

Davis, T. N., Stolarik, J. D. & Heppner, J. P. 1966 Rocket measurements of mid-latitude S_q currents. *J. Geomagn. Geoleect., Kyoto* **18**, 183–188.

Doodson, A. T. 1921 The harmonic development of the tide-generating potential. *Proc. R. Soc. Lond.* A **100**, 305–329.

Explanatory supplement to the astronomical ephemeris and the American ephemeris and the nautical almanac, p. 107. 1961 London: H.M.S.O.

Evans, J. V. 1978 A note on lunar tides in the ionosphere. *J. geophys. Res.* **83**, 1647–1652.

Ferris, G. A. J. & Price, A. T. 1964 Electric currents induced in an anisotropic ionosphere. *Geophys. Jl R. astr. Soc.* **9**, 285–308.

Flattery, T. W. 1967 Hough Functions. University of Chicago, Department of Geophysical Sciences, Ph.D. thesis.

Forbes, J. M. & Garrett, H. B. 1979 Solar tidal wind structures and the *E*-region dynamo. *J. Geomagn. Geoelect., Kyoto* **31**, 173–182.

Forbes, J. M. & Lindzen, R. S. 1976 Atmospheric solar tides and their electrodynamic effects. I. The global S_q current system. *J. atmos. terr. Phys.* **38**, 879–910.

Fritsche, H. 1902 Die tagliche periode der erdmagnetischen elemente. St. Petersburg.

Fritsche, H. 1905 Die jahrliche und tagliche periode der erdmagnetischen elemente. Riga.

Fukushima, N. 1968 Three dimensional electric current and toroidal magnetic field in the ionosphere. *Rep. Ionosph. Space Res. Japan* **22**, 173–195.

Geller, M. A. 1970 An investigation of the lunar semidiurnal tide in the atmosphere. *J. atmos. Sci.* **27**, 202–218.

Gupta, J. C. & Malin, S. R. C. 1972 Seasonal variations in the solar and lunar daily geomagnetic variations. *Geophys. Jl R. astr. Soc.* **30**, 11–18.

Hasegawa, M. 1950 A suggestion for the electric conductivity of the upper atmosphere from an analysis of the diurnal variations of terrestrial magnetism. In *Transactions of Oslo Meeting, August* 19–28, 1948 (ed. J. W. Joyce), *I.A.T.M.E. Bulletin* 13, pp. 507–509. Washington D.C.: Association of Terrestrial Magnetism and Electricity, I.U.G.G.

Hasegawa, M. 1960 On the position of the focus of the geomagnetic S_q current system. *J. geophys. Res.* **65**, 1437–1447.

Hasegawa, M. & Maeda, H. 1951 A suggestion for the electric conductivity of the upper atmosphere from an analysis of the diurnal variations of terrestrial magnetism (II). *Rep. Ionosph. Res. Japan* **5**, 167–178.

Hasegawa, M. & Ota, M. 1950*a* On the magnetic field of S_q in the middle and lower latitudes during the II Polar Year. In *Transactions of the Oslo Meeting, August* 19–28, 1948 (ed. J. W. Joyce) *I.A.T.M.E. Bulletin* 13, pp. 426–430. Washington D.C.: Association of Terrestrial Magnetism and Electricity, I.U.G.G.

Hasegawa, M. & Ota, M. 1950*b* The representation of magnetic field of S_q with potential calculated through a method of graphical integration. In *Transactions of Oslo Meeting, August* 19–28 (ed. J. W. Joyce), *I.A.T.M.E. Bulletin* 13, pp. 431–434. Washington D.C.: Association of Terrestrial Magnetism and Electricity, I.U.G.G.

Hines, C. O. 1966 Diurnal tide in the upper atmosphere. *J. geophys. Res.* **71**, 1453–1459.

Hough, S. S. 1898 On the application of harmonic analysis to the dynamical theory of tides. II. On the general integration of Laplace's dynamical equations. *Phil. Trans. R. Soc. Lond.* A **191**, 139–185.

I.A.G.A. News 1977 Three-letter symbols of magnetic stations (with remarks to permanent magnetic observatories), vol. 16, pp. 129–144.

Jones, M. N. 1970 Atmospheric Oscillations. I. *Planet. Space Sci.* **18**, 1393–1416.

Jones, M. N. 1973 On the ionospheric dynamo and its two-dimensional representation. *Beitr. Geophys.* **82**, 427–432.

Kato, S. 1966*a* Diurnal and semi-diurnal atmospheric tidal oscillations, eigenvalues and Hough functions. *Rep. Ionosph. Space Res. Japan* **20**, 448–463.

Kato, S. 1966*b* Diurnal atmospheric oscillation: 1. Eigenvalues and Hough functions. *J. geophys. Res.* **71**, 3201–3214.

Kitamura, T. 1979 On an origin of ultra long-period (several days) of geomagnetic fluctuations. *J. Geomagn. Geoelect., Kyoto* **31**, 211–223.

Kolesnik, A. G. 1976 Semiannual variations in the ionosphere and upper atmosphere at heights of 120–150 km. *Geomagn. Aeron.* (English edn) **16**, 256–259.

Lewis, R. P. W., McIntosh, D. H. & Watson, R. A. 1955 Annual variation of the magnetic elements. *J. geophys. Res.* **60**, 71–74.

Lindzen, R. S. 1966 On the theory of the diurnal tide. *Month. Weath. Rev. U.S. Dep. Agric.* **94**, 295–301.

Longuet-Higgins, M. S. 1968 The eigenfunctions of Laplace's tidal equations over a sphere. *Phil. Trans. R. Soc. Lond.* A **262**, 511–607.

Love, A. E. H. 1913 Notes on the dynamical theory of tides. *Proc. Lond. math. Soc.* **12**, 309–314.

Maeda, H. 1952 A suggestion for the electric conductivity of the upper atmosphere from an analysis of diurnal variations of terrestrial magnetism. II. (supplement). *Rep. Ionosph. Space Res. Japan* **6**, 155–158.

Maeda, H. 1953 On the residual part of the geomagnetic S_q-field in the middle and lower latitudes during the International Polar Year 1932–1933. *J. Geomagn. Geoelect., Kyoto* **5**, 39–59.

Maeda, H. 1955 Daily variations of the electrical conductivity of the upper atmosphere as deduced from the daily variations of geomagnetism. I. Equatorial zone. *Rep. Ionosph. Space Res. Japan* **9**, 148–165.

Maeda, H. 1956 Daily variations of the electrical conductivity of the upper atmosphere as deduced from the daily variations of geomagnetism. II. *Rep. Ionosph. Space Res. Japan* **10**, 49–68.

Maeda, H., Araki, T., Suzuki, A. & Takeda, M. 1979 Electric fields and neutral winds in the ionospheric dynamo region as deduced from the daily geomagnetic variations in December 1964. *Data book no.* 2, *World Data Center C2 for Geomagnetism*, pp. 1–194.

Maeda, H. & Suzuki, A. 1967 Preliminary report on a practical method of analysis of the daily geomagnetic variations. *Special contributions, Geophysical Institute, Kyoto University* **7**, 23–27.

Maeda, K. & Murata, H. 1965 Ionospheric dynamo theory with consideration of magnetospheric current along the geomagnetic lines of force. *Rep. Ionosph. Space Res. Japan* **19**, 272–285.

Malin, S. R. C. 1969 The effect of the sea on lunar variations of the vertical component of the geomagnetic field *Planet. Space Sci.* **17**, 487–490.

Malin, S. R. C. 1970 Separation of lunar daily geomagnetic variations into parts of ionospheric and oceanic origin *Geophys. Jl R. astr. Soc.* **21**, 447–455.

Malin, S. R. C. 1971 Morphology of the lunar daily geomagnetic variation and its relation to *S*. *Beitr. Geophys* **80**, 151–154.

Malin, S. R. C. 1973 Worldwide distribution of geomagnetic tides. *Phil. Trans. R. Soc. Lond.* A **274**, 551–594.

Malin, S. R. C. 1974 Revision of Chapman's spherical harmonic model of L. *Geophys. Jl R. astr. Soc.* **39**, 565–569

Malin, S. R. C. 1977 Ocean effects in geomagnetic tides. *Annls géophys.* **33**, 109–114.

Malin, S. R. C., Ceccre, A. & Palumbo, A. 1975 The sunspot cycle influence on lunar and solar daily geomagnetic variations. *Geophys. Jl R. astr. Soc.* **41**, 115–126.

Malin, S. R. C. & Gupta, J. C. 1977 The S_q current system during the International Geophysical Year. *Geophys Jl R. astr. Soc.* **49**, 515–529.

Malin, S. R. C. & Mete Isikara, A. 1976 Annual variations of the geomagnetic field. *Geophys. Jl R. astr. Soc.* **47** 445–457.

Matsushita, S. 1960 Seasonal and day-to-day changes of the central position of the S_q overhead current system *J. geophys. Res.* **65**, 3835–3839.

Matsushita, S. 1966 Lunar geomagnetic variations. *J. Geomagn. Geoelect., Kyoto* **18**, 163–172.

Matsushita, S. 1967 Solar and lunar daily variation fields. In *Physics of geomagnetic phenomena* (ed. S. Matsushita & W. H. Campbell), pp. 301–424. London, New York: Academic Press.

Matsushita, S. 1969 Dynamical currents, winds and electric fields. *Radio Sci.* **4**, 771–781.
Matsushita, S. 1971 Interactions between the ionosphere and the magnetosphere for solar regular daily geomagnetic variations. *Beitr. Geophys.* **80**, 91–110.
Matsushita, S. 1973 Solar and lunar tidal effects on the low-latitude ionosphere – A review. *J. atmos. terr. Phys.* **35**, 1027–1034.
Matsushita, S. 1975 IMF polarity effects on the S_q current location. *J. geophys. Res.* **80**, 4751–4754.
Matsushita, S. & Maeda, H. 1965*a* On the geomagnetic solar quiet daily variation field during the IGY. *J. geophys. Res.* **70**, 2535–2558.
Matsushita, S. & Maeda, H. 1965*b* On the geomagnetic lunar daily variation field. *J. geophys. Res.* **70**, 2559–2578.
Maxwell, J. C. 1881 *A treatise on electricity and magnetism.* Oxford: Clarendon Press.
McNish, A. G. 1937 Progress of research in magnetic diurnal variations at the Department of Terrestrial Magnetism, Carnegie Institution of Washington. *Transactions of Edinburgh Meeting, September* 17–24, 1936 (ed. D. La Cour in collaboration with J. Bartels and M. Bruun de Neergaard), *Bulletin no. 10*, pp. 271–280. Copenhagen: Association of Terrestrial Magnetism and Electricity, I.U.G.G.
Mishin, V. M., Basarzhapov, A. D., Matveev, M. I., Popov, G. V., Tubalova, V. M. & Nemtsova, E. I. 1971 On the dynamo theory of S_q variations. *Beitr. Geophys.* **80**, 171–184.
Möhlmann, D. 1971*a* Derivation of the dynamo equations. *Beitr. Geophys.* **80**, 185–194.
Möhlmann, D. 1971*b* Special solutions of the dynamo equations. *Beitr. Geophys.* **80**, 195–198.
Möhlmann, D. 1973 A possible origin of the geomagnetic S_q-variations. *Beitr. Geophys.* **82**, 248–249.
Möhlmann, D. 1974*a* Non-uniqueness of ionospheric winds and electric fields, deduced from geomagnetic S_q-variations. *Beitr. Geophys.* **83**, 16–18.
Möhlmann, D. 1974*b* Ionospheric dynamo-electric fields. *Beitr. Geophys.* **83**, 101–112.
Möhlmann, D. 1975 Power series solutions of Laplace's tidal equations. *Beitr. Geophys.* **84**, 463–472.
Möhlmann, D. 1976*a* Ionospheric winds not contributing to the ionospheric currents. *Beitr. Geophys.* **85**, 249–250.
Möhlmann, D. 1976*b* Two wind systems causing the global ionospheric dynamo electric field. *Beitr. Geophys.* **85**, 343–345.
Möhlmann, D. 1977*a* Separation of the ionospheric potential equation. *Beitr. Geophys.* **86**, 23–27.
Möhlmann, D. 1977*b* Is there a zonal electrostatic potential at ionospheric heights? *Beitr. Geophys.* **86**, 338–339.
Möhlmann, D. 1977*c* Ionospheric electrostatic fields. *J. atmos. terr. Phys.* **39**, 1325–1332.
Parkinson, W. D. 1971 An analysis of the geomagnetic diurnal variation during the International Geophysical Year. *Beitr. Geophys.* **80**, 199–232.
Pogrebnoy, V. N. 1969 Semiannual $S_q(H)$ variations. *Geomagn. Aeron.* (English edn) **9**, 625–627.
Price, A. T. 1968 Ionospheric conductivity and S_q variations. *Geophys. Jl R. astr. Soc.* **15**, 93–102.
Price, A. T. 1969 Recent work on S_q variations. *Solar terrestrial physics: terrestrial aspects, annals of the IQSY*, vol. 5, pp. 369–395. Massachusetts: M.I.T. Press.
Price, A. T. & Cocks, A. C. 1969 The air motions in the dynamo theory of S_q. *Beitr. Geophys.* **78**, 131–140.
Price, A. T. & Wilkins, G. A. 1963 New methods for the analysis of geomagnetic fields and their application to the S_q field of 1932–33. *Phil. Trans. R. Soc. Lond.* A **256**, 31–98.
Rao, D. R. K. & Sastri, N. S. 1971 Lunar partial tides in H at Alibag. *J. Geomagn. Geoelect., Kyoto* **23**, 417–418.
Rao, D. R. K. & Sastri, N. S. 1972 Geomagnetic lunar partial tides in the Indian equatorial region. *J. atmos. terr. Phys.* **34**, 1859–1864.
Richmond, A. D. 1971 Tidal winds at ionospheric heights. *Radio Sci.* **6**, 175–189.
Richmond, A. D. 1979 Ionospheric wind dynamo theory: A review. *J. geomagn. Geoelect., Kyoto* **31**, 287–310.
Richmond, A. D., Matsushita, S. & Tarpley, J. D. 1976 On the production mechanism of electric currents and fields in the ionosphere. *J. geophys. Res.* **81**, 547–555.
Rikitake, T. 1961 S_q and Ocean. *J. geophys. Res.* **66**, 3245–3254.
Roberts, P. H. & Lowes, F. J. 1961 Earth currents of deep internal origin. *J. geophys. Res.* **66**, 1243–1254.
Roden, R. B. 1964 The effect of an ocean on magnetic diurnal variations. *Geophys. Jl R. astr. Soc.* **8**, 375–388.
Rodgers, T. A. 1980 Seasonal variations in the La Cour baseline values at Scott Base, Antarctica. *I.A.G.A. News*, no. 18, 108–112.
Roper, R. 1966 The semi-diurnal tide in the lower thermosphere. *J. geophys. Res.* **71**, 5745–5748.
Salah, H. E. 1974 Daily oscillations of the mid-latitude thermosphere studied by incoherent scatter at Millstone Hill. *J. atmos. terr. Phys.* **36**, 1891–1909.
Salah, J. E. & Wand, R. H. 1974 Tides in temperature of the lower thermosphere at mid-latitudes. *J. geophys. Res.* **79**, 4295–4304.
Salah, J. E., Wand, R. H. & Evans, J. V. 1975 Tidal effects in the *E*-region from incoherent scatter observations. *Radio Sci.* **10**, 347–355.
Sastri, N. S. & Rao, D. R. K. 1971 Separation of lunar daily geomagnetic variations into parts of oceanic and ionospheric origin in the Indian region. *Geophys. Jl R. astr. Soc.* **23**, 269–272.
Sawyer, C. 1974 Semi-annual and solar-cycle variation of sector structure. *Geophys. Res. Lett.* **1**, 295–297.
Schieldge, J. P., Venkateswaran, S. V. & Richmond, A. D. 1973 The ionospheric dynamo and equatorial magnetic variations. *J. atmos. terr. Phys.* **35**, 1045–1061.

Schlapp, D. M. 1977 Lunar geomagnetic tides and the ocean dynamo. *J. atmos. terr. Phys.* **39**, 1453–1457.
Schlapp, D. M. & Malin, S. R. C. 1976 On the width of tidal lines in the geomagnetic spectrum. *J. atmos. terr. Phys.* **38**, 1351–1355.
Schlapp, D. M. & Malin, S. R. C. 1979 Some features of the seasonal variation of geomagnetic lunar tides. *Geophys. Jl R. astr. Soc.* **59**, 161–170.
Schlapp, D. M. & Weekes, K. 1973 The determination of lunar tides. I. Methods of analysis. *J. atmos. terr. Phys.* **35**, 1811–1831.
Schneider, O. 1963 A generalization of the phase-law of lunar geomagnetic tides. *Nature, Lond.* **199**, 548–550.
Schuster, A. 1889 The diurnal variation of terrestrial magnetism. *Phil. Trans. R. Soc. Lond.* A **180**, 467–518.
Schuster, A. 1908 The diurnal variation of terrestrial magnetism. *Phil. Trans. R. Soc. Lond.* A **208**, 163–204.
Sharma, R. P. & Rastogi, R. G. 1971 Lunar–solar tides in electron density at fixed heights of the ionosphere. *Planet. Space Sci.* **19**, 1349–1357.
Shiraki, M. 1974 Variations of focus latitude and intensity of equivalent current system of geomagnetic solar daily variation with a period from about ten to thirty days. *Mem. Kakioka magn. Obs.* **16**, 29–43.
Siebert, M. 1961 Atmospheric Tides. *Adv. Geophys.* **7**, 105–187.
Steiner, L. 1914 Über die tägliche Variation der erdmagnetischen Kraft. *Met. Z.* **31**, 417–428.
Stening, R. J. 1968 Calculation of electric currents in the ionosphere by an equivalent circuit method. *Planet. Space Sci.* **16**, 717–728.
Stening, R. J. 1969 An assessment of the contributions of various tidal winds to the S_q current system. *Planet. Space Sci.* **17**, 889–908.
Stening, R. J. 1977*a* Ionospheric dynamo calculations with semi-diurnal winds. *Planet. Space Sci.* **25**, 1075–1080.
Stening, R. J. 1977*b* Field aligned currents driven by the ionospheric dynamo. *J. atmos. terr. Phys.* **39**, 933–937.
Stening, R. J. & Winch, D. E. 1979 Seasonal changes in the global lunar geomagnetic variation. *J. atmos. terr. Phys.* **41**, 311–323.
Stewartson, K. & Walton, I. C. 1976 On waves in a thin shell of stratified rotating fluid. *Proc. R. Soc. Lond.* A **349**, 141–156.
Sugiura, M. & Fanselau, G. 1966 Lunar phase numbers ν and ν' for the years 1850 to 2050. *Goddard Space Flight Center NASA* X-612-66-401.
Suzuki, A. 1973 A new analysis of the geomagnetic S_q field. *J. Geomagn. Geoelect., Kyoto* **25**, 259–280.
Suzuki, A. 1979 UT and day-to-day variations in equivalent current systems for world geomagnetic variations. *J. Geomagn. Geoelect., Kyoto* **31**, 21–46.
Suzuki, A. & Maeda, H. 1978 Equivalent systems of the daily geomagnetic variations. *Data Book no.* 1, *Data Analysis Center for Geomagnetism and Spacemagnetism, Faculty of Science, Kyoto University.*
Swift, D. W. 1972 Effective height-integrated conductivity of the ionosphere. *J. geophys. Res.* **77**, 1279–1285.
Tarpley, J. D. 1970*a* The ionospheric wind dynamo: I. Lunar tide. *Planet. Space Sci.* **18**, 1075–1090.
Tarpley, J. D. 1970*b* The ionospheric wind dynamo: II. Solar tides. *Planet. Space Sci.* **18**, 1091–1103.
van Bemmelen, von. W. 1912 Die lunare Variation des Erdmagnetismus. *Met. Z.* **29**, 218–230.
van Bemmelen, von W. 1913 Berichtigung zu meiner Abhandlung über die lunare Variation des Erdmagnetismus. *Met. Z.* **30**, 589–594.
van Sabben, D. 1970 Solstitial S_q-currents through the magnetosphere. *J. atmos. terr. Phys.* **32**, 1331–1336.
van Sabben, D. 1971 Remark on the determination of ionospheric winds and field-aligned magnetospheric currents from surface observations of S_R. *Beitr. Geophys.* **80**, 268–269.
van Vleuten, A. 1917*a* Dagelijksche Variatie. *Proc. Sect. Sci. K. ned. Akad. Wet.* SER. 1, **26**, 293–299.
van Vleuten, A. 1917*b* Over de dagelijksche variatie van het Aardmagnetisme. *Meded. Verh. K. ned. met.In st.* **102**, 1–107.
Volland, H. 1971 A note on the height of the geomagnetic S_q current. *J. Geomagn. Geoelect., Kyoto* **23**, 117–121.
Volland, H. 1974 Solutions of Laplace's tidal equation for complex frequencies. II. Zonal wave numbers $s = 2$ and 3. *J. atmos. terr. Phys.* **36**, 1975–1986.
Wagner, C. U. 1968*a* About a 'semi-annual' variation of the amplitude of the geomagnetic S_q-variations in median latitudes. *J. atmos. terr. Phys.* **30**, 579–589.
Wagner, C. U. 1968*b* Das Modell des symmetrischen atmosphärischen Dynamos und seine Anwendung zur Bestimmung der Leitfähigkeit des Ionospharenplasmas aus den geomagnetischen S_q-Variation. *Abh. geomagn. Inst. Obs. Potsdam-Niemegk* no. 37.
Wagner, C. U. 1968*c* The electrical conductivity in the region from 105 to 125 km. *Planet. Space Sci.* **16**, 353–362.
Wagner, C. U. 1971 The atmospheric dynamo – Theoretical investigations of different models (A review). *Beitr. Geophys.* **80**, 129–140.
Walker, G. W. 1913 The diurnal variation of terrestrial magnetism. *Proc. R. Soc. Lond.* A **89**, 379–392.
White, M. L. 1960 Atmospheric tides and ionospheric electrodynamics. *J. geophys. Res.* **65**, 153–171.
Winch, D. E. 1970 Geomagnetic Lunar Partial Tides. *J. Geomagn Geoelect., Kyoto* **22**, 291–318.
Winch, D. E. & Cunningham, R. A. 1972 Lunar magnetic tides at Watheroo: Seasonal, elliptic, evectional, variational and nodal components. *J. Geomagn. Geoelect., Kyoto* **24**, 381–414.
Yaramenko, L. N. 1978 Spherical analysis of magnetic quiet-day solar daily variation in the equatorial zone of the Earth. *Geomagn. Aeron.* (English edn) **15**, 646–649.